NASA Technical Memorandum 86852

RESEARCH AND TECHNOLOGY

ANNUAL REPORT 1985

Ames Research Center
Moffett Field, California

Introduction

This annual report illustrates selected achievements at the Ames-Moffett and Ames-Dryden sites of Ames Research Center. The contents illustrate the challenging work that has been accomplished in the past year in the areas of Engineering and Technical Services, Aerospace Systems, Flight Operations and Research, Aerophysics, and Space Research. The contents clearly demonstrate the diversity of the research activities at Ames and provide an indication of the stimulating challenges that will be met in the future.

If you desire further information on any of the Ames research and technology programs, please write to the Chief Scientist, Dr. Jack Nielsen, MS 200-1A, NASA Ames Research Center, Moffett Field, CA 94035, or call the investigator listed in the report.

William F. Ballhaus, Jr.
Director

Table of Contents

NOTE: For additional information on any item, the Ames Staff member(s) named at the end of each item may be contacted. To call Ames Moffett staff (where a four-digit extension number is indicated), commercial telephone users should dial 415-694- followed by the extension number (users with access to the Federal Telecommunications System (FTS) should dial 464- followed by the extension number). To call Ames Dryden staff (where a four-digit extension number is indicated), commercial telephone users should dial 805-258-3311 and ask for the extension (dial directly on FTS, 961- followed by the extension number).

Index

Title	Author	Ames Moffett/ Ames Dryden	Organizational Division	Headquarters Program Office
Objective Assessment of Pilot Performance	C. Billings	Ames Moffett	Aerospace Human Factors Research	OAST-FL
Development of Workload and Performance	S. Hart	Ames Moffett	Aerospace Human Factors Research	OAST-FL
Intelligent-Perspective Display Systems	S. Ellis	Ames Moffett	Aerospace Human Factors Research	OAST-FL
Advanced Wide Field-of-View Stereo Displays	M. McGreevy J. Humphries	Ames Moffett	Aerospace Human Factors Research	OAST-FL
Intelligent-Operator Aids: Operator Task Models	E. Palmer	Ames Moffett	Aerospace Human Factors Research	OAST-FL
Intelligent-Operator Aids: An Expert System for the Orbital Refueling System	E. Palmer	Ames Moffett	Aerospace Human Factors Research	OAST-FL
Models of Color Constancy and Color Perception	A. Watson	Ames Moffett	Aerospace Human Factors Research	OAST-FL
NASA Fatigue and Jet-Lag Study: A Short-Haul Crew Performance	H. Foushee J. Lauber	Ames Moffett	Aerospace Human Factors Research	OAST-FL
Pilot Performance Factors in Short-Haul Flight Operations: A Field Study	J. Lauber	Ames Moffett	Aerospace Human Factors Research	OAST-FL
Aircraft Automation: Field Studies and Guidelines	J. Lauber	Ames Moffett	Aerospace Human Factors Research	OAST-FL
Advanced Space Suit Technology	H. Vykukal	Ames Moffett	Aerospace Human Factors Research	OAST-FL
Effects of High-Order Dynamics on Helicopter Flight Control System Bandwidth	R. Chin	Ames Moffett	Flight Systems and Simulation Research	OAST-FS
Dual-Life Control System	L. Cicolani G. Kanning	Ames Moffett	Flight Systems and Simulation Research	OAST-FS
Helicopter Engine-Out Studies	W. Decker	Ames Moffett	Flight Systems and Simulation Research	OAST-FS
The YAV-8B and VTOL Research	J. Foster V. Merrick	Ames Moffett	Flight Systems and Simulation Research	OAST-FS
Development of Model-Following Control Systems Concepts for Rotorcraft	K. Hilbert	Ames Moffett	Flight Systems and Simulation Research	OAST-FS
Helicopter Air Combat II (HAC II) Simulation	M. Lewis	Ames Moffett	Flight Systems and Simulation Research	OAST-FS
Quiet Short Haul Research Aircraft (QSRA)	D. Watson	Ames Moffett	Flight Systems and Simulation Research	OAST-FS
Space Shuttle Simulations - 1985	D. Astill	Ames Moffett	Flight Systems and Simulation Research	OAST-FS
V-22 Simulation on the NASA-Ames Vertical Motion Simulator	B. Parris	Ames Moffett	Flight Systems and Simulation Research	OAST-FS
X-Band Portable Precision Approach Concept	T. Davis	Ames Moffett	Flight Systems and Simulation Research	OAST-FS
Digital Flight Control System Verification Laboratory (DFCSVL)	D. Doane J. Saito	Ames Moffett	Flight Systems and Simulation Research	OAST-FS
Helicopter Satellite-Based Guidance Differential Global Positioning System (GPS)	F. Edwards	Ames Moffett	Flight Systems and Simulation Research	OAST-FS
Air Traffic Control Automation	H. Erzberger	Ames Moffett	Flight Systems and Simulation Research	OAST-FS
Automated Low-Altitude/Nap-of-the-Earth Rotorcraft Flight	L. McGee	Ames Moffett	Flight Systems and Simulation Research	OAST-FS
Applications of State Estimation in Aircraft Flight-Data Analysis	R. Wingrove R. Bach	Ames Moffett	Flight Systems and Simulation Research	OAST-FS
Rotorcraft Systems Integration Simulator (RSIS)	A. Deel	Ames Moffett	Flight Systems and Simulation Research	OAST-FS

Title	Author	Ames Moffett/ Ames Dryden	Organizational Division	Headquarters Program Office
Flight Operations				
X-29 Wing Canard Aerodynamic Studies	L. Jennett	Ames Dryden	Research Engineering	OAST-OF
F-104 Skin-Friction Balance Development	R. Meyer, Jr.	Ames Dryden	Research Engineering	OAST-OF
In-Flight Shuttle Tile Moisture Impact Tests	R. Meyer, Jr.	Ames Dryden	Research Engineering	OAST-OF
F-100 Engine Model Derivative Augmentor Performance Evaluation	L. Meyer	Ames Dryden	Research Engineering	OAST-OF
Flow Visualization of Trapped Vortices Using Trailing Disks	T. Moes J. Del Frate	Ames Dryden	Research Engineering	OAST-OF
F-15 Supersonic Laminar Flow Experiment	J. Johnson	Ames Dryden	Research Engineering	OAST-OF
In-Flight Thrust Calculation Accuracy	D. Hughes	Ames Dryden	Research Engineering	OAST-OF
HiMAT Wing Test	A. Vano	Ames Dryden	Research Engineering	OAST-OF
Buckling Characterization of Hypersonic Aircraft Wing Tubular Panels	W. Ko	Ames Dryden	Research Engineering	OAST-OF
Hot Structures Research	W. Ko	Ames Dryden	Research Engineering	OAST-OF
Fatigue Life Prediction of Airborne Launch System	W. Ko	Ames Dryden	Research Engineering	OAST-OF
X-29A Flight Loads and Deflection Measurements	L. Schuster W. Lokos	Ames Dryden	Research Engineering	OAST-OF
Flow Separation in an Advanced Turbofan Engine	F. Burcham	Ames Dryden	Research Engineering	OAST-OF
Three-Dimensional Optimal Intercept Experiment	F. Jones E. Duke	Ames Dryden	Research Engineering	OAST-OF
X-29 Flight Controls Testing	T. Maine	Ames Dryden	Research Engineering	OAST-OF
Expert System Flight Status Monitor	V. Regenie E. Duke	Ames Dryden	Research Engineering	OAST-OF
Flying Qualities Study Through In-Flight Simulation	S. Sarrafian	Ames Dryden	Research Engineering	OAST-OF
Aerophysics				
Optical Information Processing	D. Ennis	Ames Moffett	Information Sciences	OAST-RC
Advanced Distributed System Networks	T. Grant	Ames Moffett	Information Sciences	OAST-RC
Automated Airborne Astronomical Flight Planning Tool	P. Nachtsheim	Ames Moffett	Information Sciences	OAST-RC
Generalized Leading-Edge Modifications for Increased Cl Max of NACA-6-Series Airfoils	S. Cliff	Ames Moffett	Aerodynamics	OAST-RA
V/STOL Fighter Configuration Aerodynamics	D. Durston	Ames Moffett	Aerodynamics	OAST-RA
Transonic PAN AIR Development	A. Woo	Ames Moffett	Aerodynamics	OAST-RA
Turbulence Model Improvements for Application to Transonic Airfoils	M. Rubesin J. Viegas D. Johnson	Ames Moffett	Fluid Dynamics	OAST-RF
Transonic Separated Solutions for the Augmentor Wing	J. Flores W. Van Dalsem	Ames Moffett	Fluid Dynamics	OAST-RF
Transonic Aeroelastic Analysis of the B-1 Aircraft	G. Guruswamy P. Goorjian	Ames Moffett	Fluid Dynamics	OAST-RF
Computation of Transonic Separated Wing Flows Using an Euler/Navier-Stokes Zonal Approach	U. Kaynak T. Holst	Ames Moffett	Fluid Dynamics	OAST-RF
Space Shuttle Main Engine Power Head Flow Analysis	D. Kwak	Ames Moffett	Fluid Dynamics	OAST-RF
A Simulation of Rotor-Stator Interaction Using Patched and Overlaid Grids	M. Rai	Ames Moffett	Fluid Dynamics	OAST-RF
Fast Simulation of Separated Three-Dimensional Flows	W. Van Dalsem	Ames Moffett	Fluid Dynamics	OAST-RF
Large Eddies in a Supersonic Turbulent Boundary Layer	S. Robinson	Ames Moffett	Fluid Dynamics	OAST-RF
Development of a New Laser Doppler System for the High Reynolds Number Facility (HAC-II)	H. Seegmiller	Ames Moffett	Fluid Dynamics	OAST-RF
Swept Circulation-Control Research Wing	E. Keener	Ames Moffett	Fluid Dynamics	OAST-RF

Title	Author	Ames Moffett/ Ames Dryden	Organizational Division	Headquarters Program Office
High-Speed Aerodynamic Prediction for Rotor Flow	I-C. Chang	Ames Moffett	Fluid Dynamics	OAST-RF
Turbulent Boundary Layer Control for Drag Reduction	R. Westphal	Ames Moffett	Fluid Dynamics	OAST-RF
Computer-Aided Visualization of Fluid Flow	P. Buning V. Watson	Ames Moffett	Fluid Dynamics	OAST-RF
Oblique Wing Aerodynamics Determined from the Navier-Stokes Equations	U. Mehta	Ames Moffett	Fluid Dynamics	OAST-RF
Circulation Control Airfoil Calculation	T. Pulliam	Ames Moffett	Thermosciences	OAST-RT
Properties of Molecules and Clusters	D. Cooper R. Jaffee	Ames Moffett	Thermosciences	OAST-RT
Properties of Nonequilibrium Air in the Shock Layer Surrounding Aero-Assisted Orbital Transfer Vehicles	R. Jaffee D. Cooper	Ames Moffett	Thermosciences	OAST-RT
Use of Computer Modeling to Increase Performance of Arc-Jet Wind Tunnels	W. Winovich	Ames Moffett	Thermosciences	OAST-RT
Advanced Low-Density Heat-Shield Materials	D. Leiser H. Goldstein	Ames Moffett	Thermosciences	OAST-RT
Thermal Protection Materials Applications	H. Goldstein	Ames Moffett	Thermosciences	OAST-RT
Lightweight and Heat Resistant Composite Panels	D. Kourtides	Ames Moffett	Thermosciences	OAST-RT
Tailorable Advanced Blanket Insulation (TABI)	P. Sawko H. Goldstein	Ames Moffett	Thermosciences	OAST-RT

Space Research

Space Research				
Ames Research Center Life Sciences Payload on Spacelab Mission 3: A Spaceflight of 24 Rats and 2 Monkeys (UPN 805)	J. Ferandin	Ames Moffett	Life Science Flight Experiment	OSSA-SP
Joint US/USSR Cosmos Spaceflight Experiment	J. Hines	Ames Moffett	Life Science Flight Experiment	OSSA-SP
Space Lab-3 Data Analysis	C. Schatte	Ames Moffett	Life Science Flight Experiment	OSSA-SP
Large Primate Facility	C. Schatte	Ames Moffett	Life Science Flight Experiment	OSSA-SP
Evaluation of a Mounting System for a Silica Mirror	J. Mansfield	Ames Moffett	SIRTF Study Office	OSSA-SR
Design Studies for a Life Science Research Facility on a Space Station	R. Arno	Ames Moffett	Life Sciences	OSSA-SL
Ground-Based Vestibular Research Facility (VRF)	R. Mah	Ames Moffett	Life Sciences	OSSA-SL
Multicrop Area Estimation and Mapping	J. Lawless E. Sheffner	Ames Moffett	Life Sciences	OSSA-SL
Permafrost Modeling from Satellite Data	J. Lawless L. Morrissey	Ames Moffett	Life Sciences	OSSA-SL
Pilot Land Data System-System Access Capabilities	W. Likens	Ames Moffett	Life Sciences	OSSA-SL
Nitrous Oxide Flux from Tropical Forest Ecosystems in the Amazon	G. Livingston P. Matson P. Vitousek	Ames Moffett	Life Sciences	OSSA-SL
Pathways of Nitrogen Loss Following Land Clearing in a Humid Tropical Forest in Central America	P. Matson P. Vitousek	Ames Moffett	Life Sciences	OSSA-SL
Remote Sensing Prediction of Deciduous Forest Nutrient Condition	D. Peterson	Ames Moffett	Life Sciences	OSSA-SL
Building a Geographic Information System for Water Management in Oregon	J. Lawless G. Thelin	Ames Moffett	Life Sciences	OSSA-SL
Instrumentation Used in the Search for Extraterrestrial Intelligence	B. Oliver	Ames Moffett	Life Sciences	OSSA-SL
Flight Trials on Space Shuttle of Autogenic Feedback Training as a Motion-Sickness Countermeasure	P. Cowings	Ames Moffett	Life Sciences	OSSA-SL
Exercise Training and Orthostatic Intolerance	J. Greenleaf	Ames Moffett	Life Sciences	OSSA-SL
Muscle Atrophy in Simulated Weightlessness on Earth and on Spacelab 3	R. Grindeland	Ames Moffett	Life Sciences	OSSA-SL

Title	Author	Ames Moffett/ Ames Dryden	Organizational Division	Headquarters Program Office
Mechanism of Rapid Bone Loss	D. Young	Ames Moffett	Life Sciences	OSSA-SL
Trace Contaminant Gases in a Space Cabin	M. Schwartz	Ames Moffett	Life Sciences	OSSA-SL
Multiplex Gas Chromatography for Future Planetary Studies	J. Valentin	Ames Moffett	Life Sciences	OSSA-SL
Superoxide Mixtures as Air Revitalization Chemicals	T. Wydeven P. Wood (USN)	Ames Moffett	Life Sciences	OSSA-SL
Ion Mobility Drift Spectrometry (IMDS) as a Flight Analytical Instrument Technique	D. Kojiro	Ames Moffett	Life Sciences	OSSA-SL
Modulated Voltage Metastable Ionization Detector (MVMID)	D. Kojiro G. Carle	Ames Moffett	Life Sciences	OSSA-SL
Investigations of Porous Polymer Gas Chromatography Packings for Atmospheric Analysis of Extraterrestrial Bodies	G. Pollock	Ames Moffett	Life Sciences	OSSA-SL
Production of Hydrocarbon Gases by Lightning in the Atmospheres of the Outer Planets	C. McKay T. Scattergood	Ames Moffett	Life Sciences	OSSA-SL
Possible Evolution of RNA Polynucleotides in the Absence of Enzymes	S. Chang A. Kanavarioti	Ames Moffett	Life Sciences	OSSA-SL
Mineral Energetics in Prebiotic Chemistry	L. Coyne	Ames Moffett	Life Sciences	OSSA-SL
Controlled Ecological Life Support Systems (CELSS)	R. MacElroy	Ames Moffett	Life Sciences	OSSA-SL
Cooperation of Primitive Genes	D. White S. Chang	Ames Moffett	Life Sciences	OSSA-SL
Molecular Microenvironments and the Origin of Life	R. MacElroy A. Pohorille	Ames Moffett	Life Sciences	OSSA-SL
A Model for Stray Radiation in Infrared Telescopes	A. Dinger	Ames Moffett	Space Sciences	OSSA-SS
Opaque Coatings Developed for the Submillimeter Region of the Electromagnetic Spectrum	S. Smith	Ames Moffett	Space Sciences	OSSA-SS
Antireflection Overcoat Found for the Submillimeter Region of the Electromagnetic Spectrum	S. Smith	Ames Moffett	Space Sciences	OSSA-SS
Early Results from the Stratosphere-Troposphere Exchange Project	P. Russell	Ames Moffett	Space Sciences	OSSA-SS
Cyrogenic Testing of Secondary Mirror Chopping Mechanisms	M. Dix	Ames Moffett	Space Sciences	OSSA-SS
Development of a Sensitive Infrared Array Camera	J. Goebel	Ames Moffett	Space Sciences	OSSA-SS
Dewar Simulator for PODS Testing	P. Kittel	Ames Moffett	Space Sciences	OSSA-SS
Aperature Shade Design Trade-Off Study for SIRTF in a Low Inclination Orbit	J. Lee W. Brooks S. Maa	Ames Moffett	Space Sciences	OSSA-SS
Development of Antimony-Doped Silicon Integrated IR Arrays	C. McCreight	Ames Moffett	Space Sciences	OSSA-SS
Development of Beryllium Mirrors for Cryogenically-Cooled Infrared Telescopes	R. Melugin	Ames Moffett	Space Sciences	OSSA-SS
Lightning in Planetary Atmospheres	W. Borucki C. McKay	Ames Moffett	Space Sciences	OSSA-SS
Atmospheric Evolution Studies	J. Kasting	Ames Moffett	Space Sciences	OSSA-SS
Nonmethane Hydrocarbon Chemistry in the Troposphere	J. Kasting	Ames Moffett	Space Sciences	OSSA-SS
Dynamics and Energetics of the Venus Ionosphere	R. Whitten	Ames Moffett	Space Sciences	OSSA-SS

Engineering and Technical Services

Fatigue Cracking of Aluminum Under Spectrum Loading at Various Humidities

The effect of moisture on Stage I fatigue (initiation and initial growth of a crack) in aluminum was studied in an effort to develop a new and more realistic cumulative damage methodology for fatigue-life prediction of engineering components under spectrum loading. Stage I fatigue was monitored using accurate specimen-compliance measurements statistically generated using computer-aided data acquisition and analysis. Fatigue strength in aluminum at 50 Hz was found to be greatly reduced by humidity under both constant amplitude and log-normal spectrum loading. Use of Miner's theory of cumulative damage was evaluated to predict the outcome of spectrum tests given the results of constant amplitude tests. A systematic pattern of deviation from Miner's theory was found with Miner's theory being reasonably accurate in the typical helicopter regime above $N = 10^6$ cycles and conservative for shorter lifetimes.

(H. Nelson and D. Chappel, Ext. 6137/5578)

Aerospace Systems

Design Synthesis Program Enhancements

A design synthesis program (ACSYNT) was developed at Ames Research Center for the conceptual/preliminary design and analysis of civil, commercial, and military aircraft. It is characterized by the close coupling between the numerical optimization, configuration, definition, and design analysis algorithms; and by methods that represent the compromise between accuracy and execution speed. The Advanced Plans and Programs Office has used ACSYNT to evaluate technological alternatives and proposed configurations. To augment the analytical capabilities of the code, and to make it applicable to more aircraft types, several new capabilities have been added.

One major addition is a takeoff analysis, a time-step integration method that can handle vertical/short, ski jump, and conventional takeoffs, and allows the user to specify control to a number of devices, such as flaps, thrust vectoring nozzles, and lift engines. This capability enables the design of powered lift aircraft or the study of takeoff performance sensitivities. Another added feature is the automatic determination of the maneuvering flight envelope for an aircraft with specified load factor and specific excess power values. Also, a fast table-lookup code for use with typical engine data has been developed to supplement the original cycle analysis propulsion module. ACSYNT development is an ongoing activity, with work oriented toward increasing its accuracy and applicability to new aircraft types and technologies of current research interest.

(G. Kidwell, Ext. 5886)

U.S./Canada Ejector Technology Program

NASA and the Canadian Department of Regional Industrial Expansion are generating a Letter of Agreement to conduct an ejector technology program.

The primary focus of this program will be to fabricate a 0.9 scale model of the General Dynamic Design E-7 STOVL Aircraft. The model will be fabricated by de Havilland Aircraft of Canada, Ltd., and will be powered by a Rolls Royce Spey 801-SF engine. The aircraft thrust in hover will be generated by chordwise ejector on either side of the fuselage in the wing-root area fed by the engine fan air at a pressure ratio of approximately 3.0 and aft engine core thrust which is vectored vertically. In the cruise mode, the fan air is directed aft through a second nozzle and the ejector areas are closed by fairing doors. The core thrust is vectored horizontally. The aircraft is designed to have a supersonic dash capability.

The aircraft model propulsion systems is scheduled to be calibrated and tested on the Powered Lift Test Rig at Lewis Research Center in mid-1988. At a later date, the fully assembled model will be tested on the Outdoor Aerodynamic Research Facility and in the 40- by 80-Foot Wind Tunnel at Ames Research Center. Simulation investigations of the aircraft concept will be conducted at Ames Research Center following

generation of the mathematical model which will be predicated on the results of the wind tunnel investigation.

(B. Lampkin, Ext. 6039)

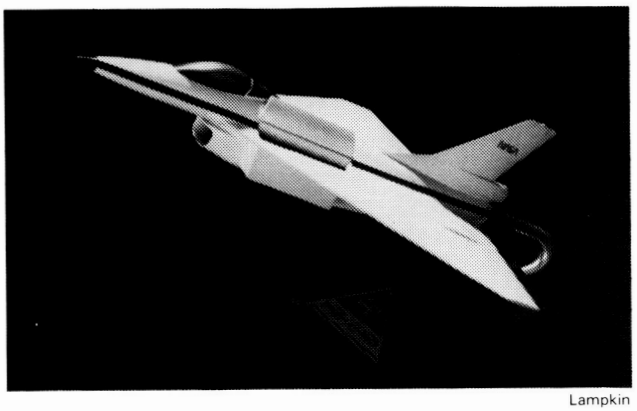

Lampkin

Small-scale model of General Dynamics Design E-7 STOVL aircraft

Applications of Optimization Methods to Helicopter Conceptual Design and Flight-Trajectory Planning

Two studies on applications of numerical-optimization methods to helicopter design and operational problems were completed by Bell Helicopter Textron under a NASA contract awarded by the Advanced Plans and Programs Office. In the first study, a single-rotor helicopter design and performance estimation program was integrated with a numerical-optimization program. Four rotor parameters (radius, chord, linear twist, and tip speed) are considered as the independent design variables. Optimization objectives may be selected out of eight possible alternatives, including minimum production cost, minimum gross weight, or maximum dash speed, while satisfying various performance criteria.

One of the most significant findings of this study was that important sensitivity information can be obtained using this type of program. For example, the effect of longer range requirements on gross weight can be readily estimated by this program. Since all the design points are optimized by adjusting all design variables, complex coupling effects are automatically taken into account. These effects would be difficult to incorporate without the use of automated optimization. Helicopter manufacturers may be able to use this type of approach to identify technology areas where research investment is expected to yield the highest possible payoff (e.g., research areas which would contribute to reduce production cost) of optimization methods.

The second study is an application of optimization methods to helicopter flight-trajectory planning. Based on the relatively simple (but practical) model drawn from the operator's handbook and manufacturer's test data, this program can provide assistance in planning flight trajectory by selecting climb/descent rates and indicated air speed in each of 10 equally spaced range segments. The optimization objective may be chosen from one of the following: minimum fuel, minimum flight time, minimum total operating cost, and maximum range for given payload. For example, the minimum fuel flight path to make a round trip between two points 180 miles apart is shown in the figure. This program is small enough to be installed on a portable personal computer, thus can easily be used onboard an aircraft. The model may also be tailored to include individual aircraft or engine characteristics.

(H. Miura, Ext. 5888)

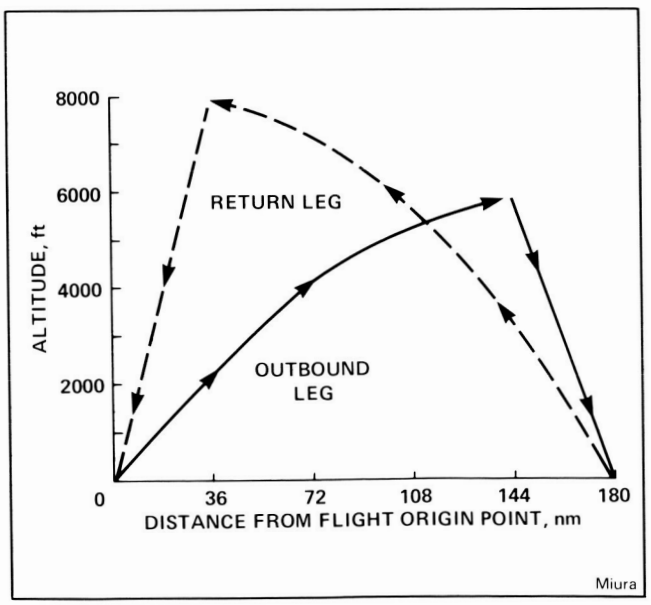

Flight profile for minimum fuel cost

40- by 80- by 120-Foot Wind Tunnel

Ames Research Center is about to have the 40X80X120-Foot Wind Tunnel operational following an extensive upgrade. The 40X80-Foot Wind Tunnel was increased in test-section speed from 200 to 300 knots, and a nonreturn wind-tunnel leg with a test section 80X120 ft in size and a speed of 100 knots was added. To accomplish this, a new fan drive was installed which increased the available power from 27 to 100 megawatts (see figures). This tunnel design activity has been supported by a major effort in aerodynamic design and analysis of the turning vanes, 80X120 inlet, air-exchange system, and the fan drive. The theoretical part of this activity was accomplished, primarily with the use of singularity-type panel computer codes. Testing of the vane sets was done in an especially built 1/10-scale two-dimensional wind tunnel. A 1/50-scale three-dimensional model of the entire 40X80 circuit was used to develop the air exchange system. Finally, the 80X120 inlet was developed in the 1/10-scale facility, the 7X10-Foot Wind Tunnel, and an especially built 1/15-scale three-dimensional powered model of the inlet.

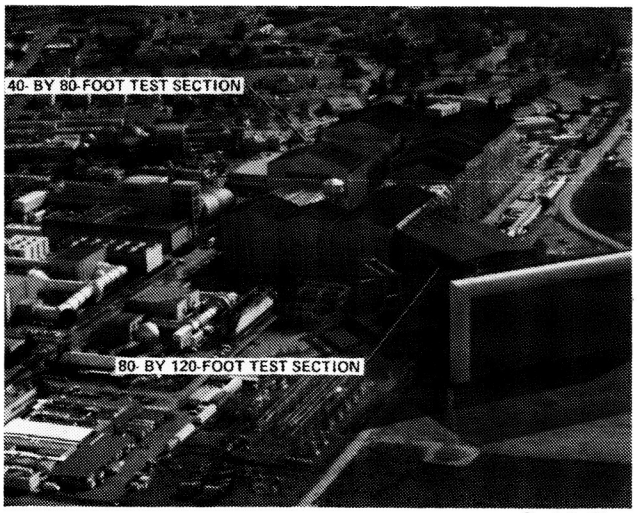

Corsiglia/Olson

Aerial view of the 40X80/80X120-Foot Wind Tunnel

The design of the 80X120-Foot Wind Tunnel inlet has required a major effort to achieve acceptable flow quality in the test section. The conflicting requirements were: to have a large test section, low construction cost, low use of land, low community noise from the fan drive and powered models, and to have acceptable flow quality in the test section. The selected inlet design is relatively short and has an area ratio five with an acoustically treated muffler followed by a screen. It was shown, theoretically and experimentally, that the test-section distribution of dynamic pressure was sensitive to the distribution of drag of the inlet muffler and screen. By adjusting this drag, acceptable test-section flow quality was obtained (i.e., dynamic pressure variation within 0.5%, flow inclination within 0.5°, turbulence intensity under 0.5%). Extensive tests were conducted with the 1/15-scale model outdoors and exposed to a variety of atmospheric wind conditions. It was shown that the 80X120 inlet performs well in the presence of winds.

(V. Corsiglia and L. Olson, Ext. 6677/6681)

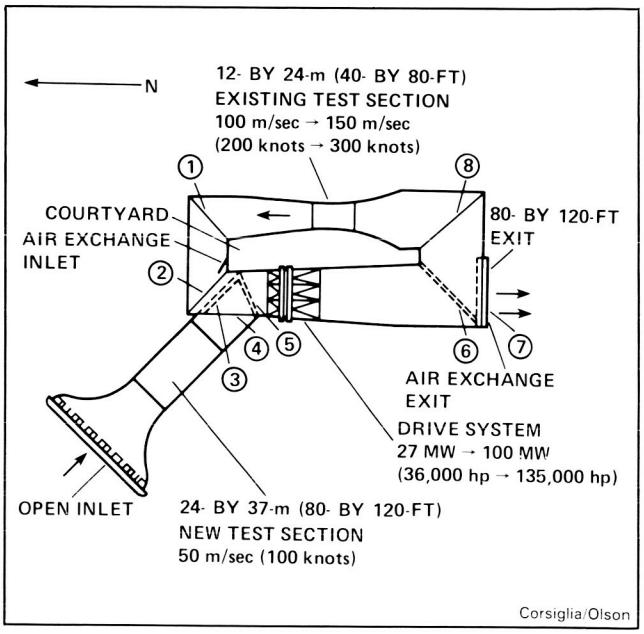

Schematic of 40X80/80X120-Foot Wind Tunnel at NASA Ames Research Center

Full-Scale Tilt-Rotor Hover Performance

Correlation of the measured hover performance of three full-scale tilt rotors with theoretical predictions has been performed. The correlation study included the following rotors: the original XV-15 rotor; a new, advanced technology rotor for the XV-15; and a 2/3-scale model of the proposed V-22A (JVX) rotor. This correlation effort was made possible by the acquisition of high-quality hover performance data for these rotors at the Ames Outdoor Aerodynamic Research Facility.

Analysis of the test data has provided insight into the performance characteristics of these rotors. All rotors had exceptionally high performance, with peak figures of merit of approximately 0.8. The XV-15 rotor performance was not affected by tip Mach number variations up to 0.73. The advanced technology XV-15 rotor and V-22A rotor performances were slightly reduced as the tip Mach number was increased from 0.69 to 0.73. Blade-tip taper and sweep improved the performance of the advanced technology XV-15 rotor. However, blade-tip sweep caused a significant increase in steady control system loads.

Comparisons of the test data with the expectations of current, state-of-the-art rotor performance prediction methods show that the measured rotor performance is consistently higher than the predictions at high rotor thrusts. This is true for all rotors tested. A sensitivity study was performed that demonstrated that these errors are not due to incorrect assumptions in the wake geometry model, and that further research is required.

(F. Felker, Ext. 6096)

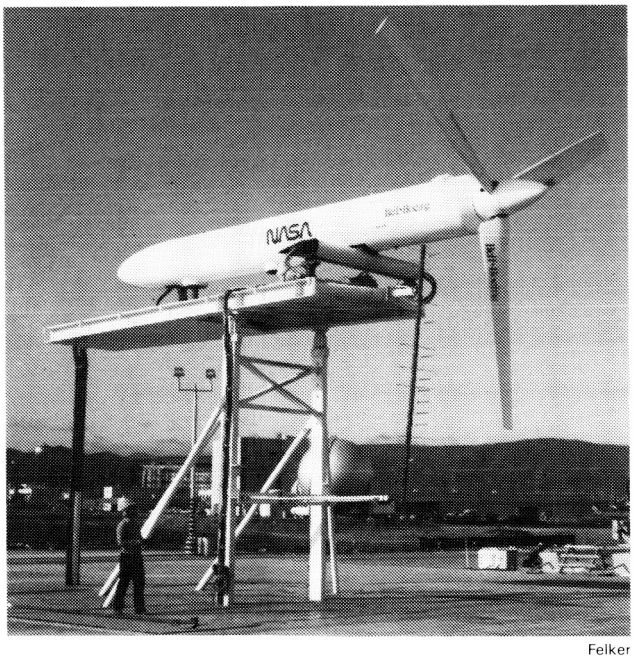

Felker

V-22A (JVX) 2/3-scale model rotor

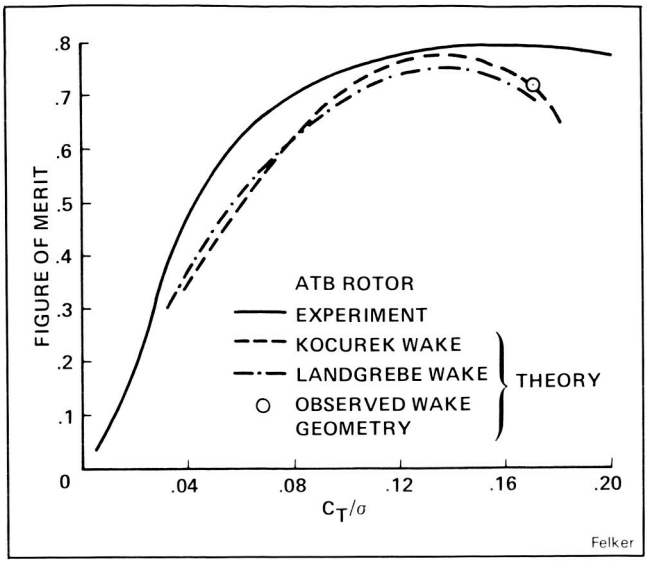

Comparison of predicted rotor performance with test data

Rotor/Wing Aerodynamic Interactions in Hover

Rotor/wing aerodynamic interactions have a large effect on the hover performance of tilt-rotor aircraft and compound helicopters. An experimental program has been initiated to investigate these interactions, and to evaluate the effect of changes in rotor/wing geometry.

A preliminary investigation was performed with a 2/3-scale model of a V-22A (JVX) rotor and wing. Rotor thrust and wing flap angle were varied during this test. The wing download was about 10% of the rotor thrust for the optimum flap angle. Tufts placed on the wing and smoke flow visualization revealed that the rotor/wing flow field is complex and three-dimensional. Consequently, a more fundamental research program has been initiated.

The effect of rotor/wing geometry variations is being investigated in a model-scale test. Geometry variations that are being tested include: vertical distance between the rotor and wing; rotor center at wing tip (tilt rotor); and rotor center at center

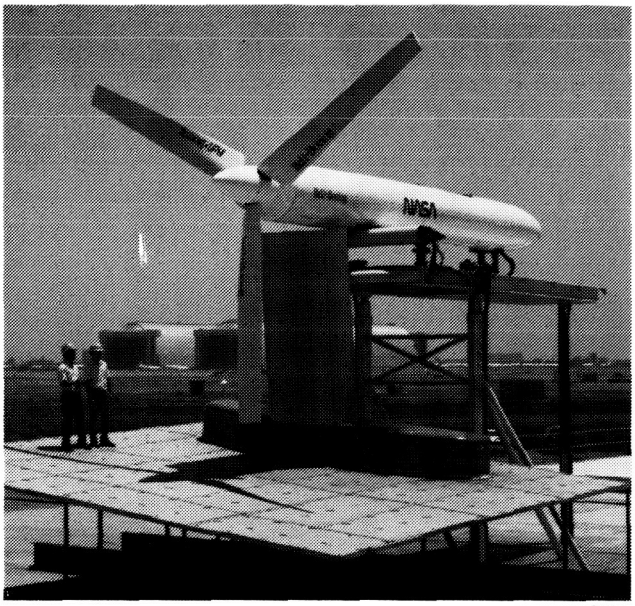

Felker

V-22A (JVX) 2/3-scale model rotor and wing

of wing (compound helicopter); wing flap angle; wing angle of attack; and wing dihedral angle. The effect on wing download of an advanced boundary-layer control technique is also being tested. Future tests will evaluate the effect on download of wing airfoil section geometry and various wing leading- and trailing-edge devices.

(F. Felker, Ext. 6096)

Active Control of Rotorcraft Dynamics

Many dynamic phenomena associated with rotorcraft can be modified or eliminated by the use of high-speed active control or rotor blade pitch. Investigations of several promising active control concepts have been initiated.

Rotorcraft vibration and loads can be reduced by multicyclic control of rotor blade pitch. A comprehensive model-scale and full-scale experimental investigation is under way using an advanced multicyclic control computer system. The design concepts used for this high-performance, real-time control system were presented at the 1985 American Control Conference. A model-scale hover test demonstrating multicyclic control is currently in progress. A full-scale hover test, model-scale wind tunnel test, and a full-scale wind tunnel test are also planned.

(S. Jacklin and J. Leyland, Ext. 6668)

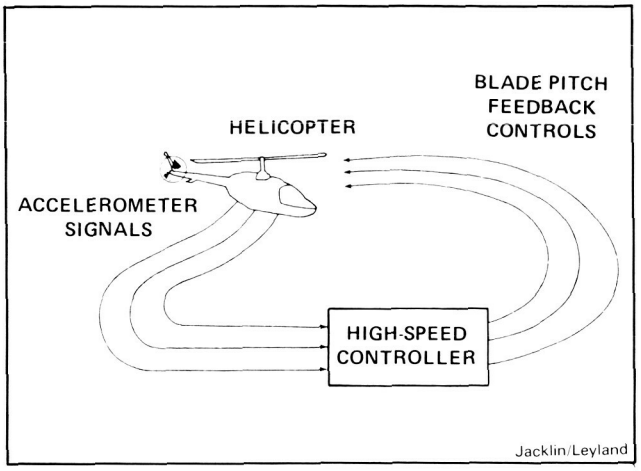

Modification of rotorcraft dynamics

Scale Effects on Rotor Noise

There are recognized advantages in using model-scale rotors in research. This practice necessitates, however, the development of accurate methods to extrapolate the results to full-scale rotors. To develop such methodology, a 2.1-m diam, four-bladed scale model helicopter rotor was tested in hover in the Ames 40- by 80-Foot Wind Tunnel. Subsequently, it was tested in the 7- by 10-Foot Wind Tunnel in forward flight. The primary objective of the tests was to

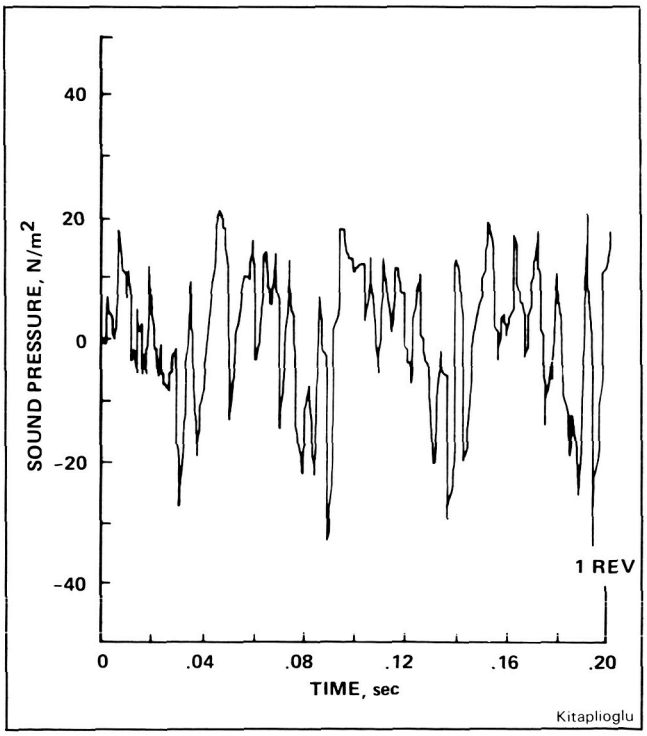

Full-scale aircraft hover acoustic waveform

obtain performance and acoustic data at various thrust conditions, tip Mach numbers; and, in the forward flight test, various advance ratios. These data were then compared with similar existing data on full-scale helicopter rotors.

This comparison yielded a preliminary evaluation of the scaling of helicopter rotor performance and acoustic radiation in hover and in forward flight. Correlation in hover between model-scale and full-scale performance and acoustics was quite good. In forward flight, significant Reynolds number effects were found in the lift-to-drag ratio for the two cases. The acoustic spectra exhibited similar trends but the overall sound levels differed by 5 to 10 dB.

(C. Kitaplioglu, Ext. 6679)

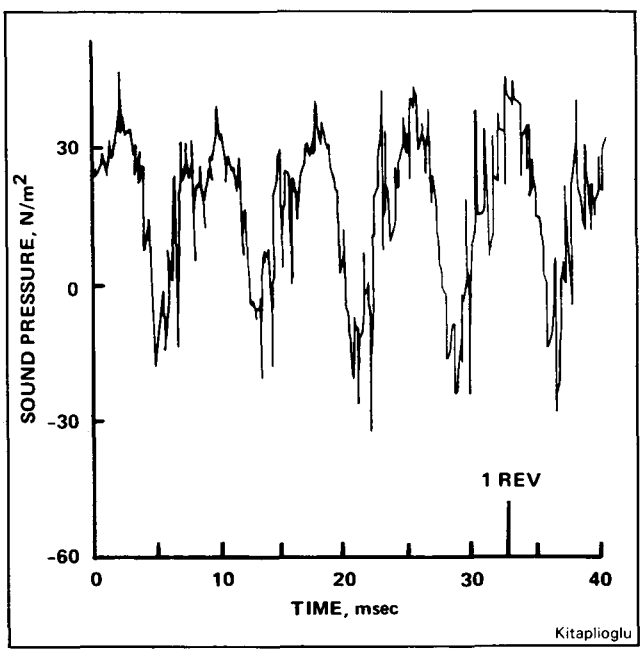

Small-scale model rotor hover noise data

Prediction of the Influence of Wind-Tunnel Walls on Discrete Frequency Noise

Ideally, measurements of rotor noise would be made in an anechoic environment. Unfortunately, most wind tunnels cannot provide this type of environment. Measurements of rotor noise in most wind tunnels are influenced by flow turbulence, tunnel geometry, tunnel background noise, and, most importantly, reflection from the tunnel walls. The walls produce a complicated, semi-reverberant sound field in which it is difficult to extract the noise due only to the rotor.

A method has been developed that can be used to examine the effects of wind-tunnel walls on discrete frequency noise, such as the rotational noise produced by a helicopter rotor. The current model consists of a known harmonic acoustic source of finite dimension inside an infinite duct of constant cross-sectional area with uniform subsonic flow. The convected wave equation for a periodic source is transformed to an integral relation using the free-field Green's function. The boundary condition at the wall is represented by an acoustic impedance relation. This integral relation is then solved on the surface of the duct by conventional panel methods. This method has been compared with an analytical solution for the case of a low-frequency monopole in a rectangular duct with flow and shown to have excellent agreement. Extensions to include more complex sources and more complex duct geometries are now being developed.

(M. Mosher, Ext. 6719)

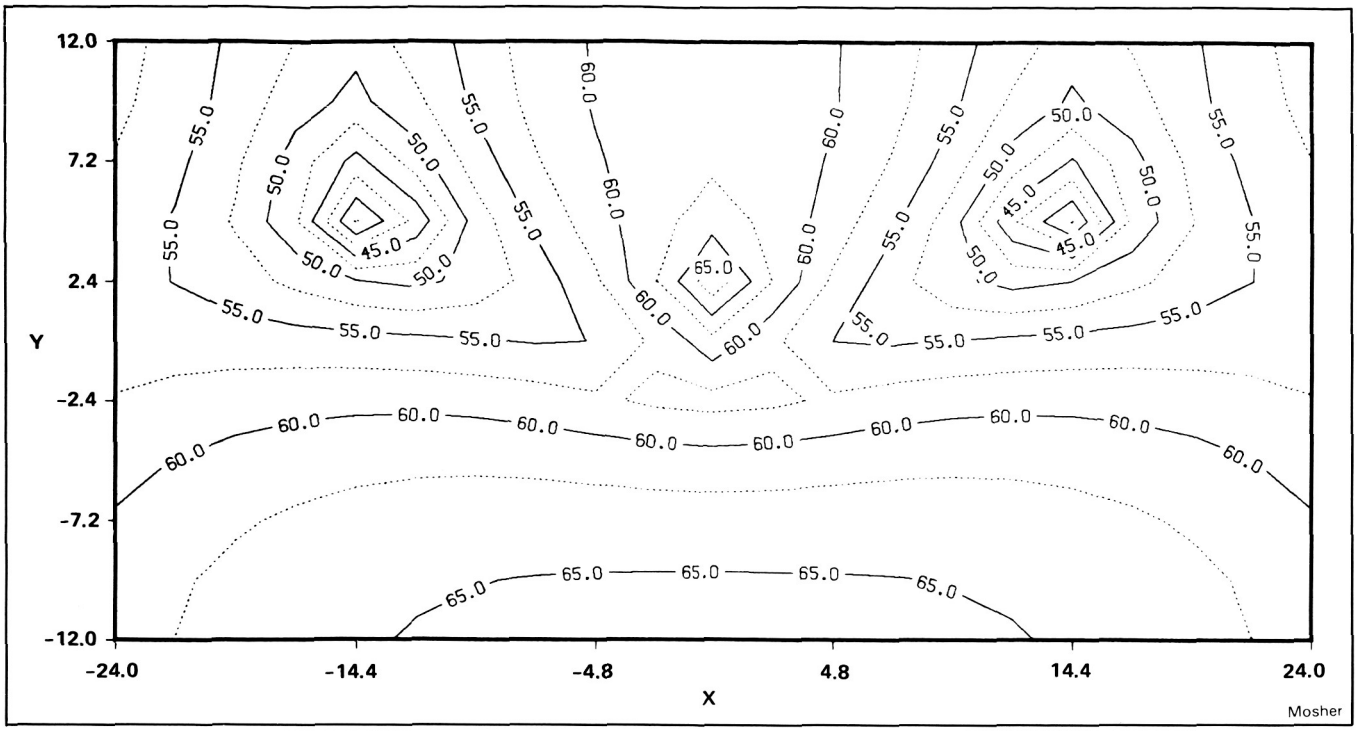

Plan view of sound pressure level of a monopole in an infinitely long duct. M = 0.1, k = 0.12, absorption coefficient = 0.18

Visualization of Rotor Wakes Using Shadowgraphy

In a joint study of rotorcraft flow fields by the Jet Propulsion Laboratory (JPL) and Ames Research Center, the vortex wake generated by a helicopter tail rotor was visualized using a wide-field shadowgraph technique. Tip vortex trajectories were visible in shadowgraphs for tip Mach numbers ranging from 0.38 to 0.60. The effect of angle-of-attack on the visibility of the vortices was substantial. At an angle-of-attack greater than 8°, the visibility of the vortex core was significant even at relatively low tip Mach numbers.

A theoretical analysis of the visibility of a rotor wake was carried out. This analysis demonstrated that the visibility increases with increasing tip Mach number. Based on this investigation, it is concluded that the wide-field shadowgraph flow visualization technique should be feasible to study the flow field generated by a large main rotor in a wind tunnel, and in an outdoor full-scale test stand.

In conjunction with the JPL efforts, Ames will conduct a flow visualization experiment on a model scale helicopter main rotor using the shadowgraph technique. This experiment has three main objectives: the first is to confirm the shadowgraph technique as a viable way to visualize the wake of a hovering model rotor; the second is to provide sets of two simultaneous orthogonal shadowgraphs to be used to determine the 3-D tip vortex geometry; the final objective is to determine the sensitivity of the shadowgraph technique and/or the rotor wake to varying thrust coefficients.

(T. Norman, Ext. 6653)

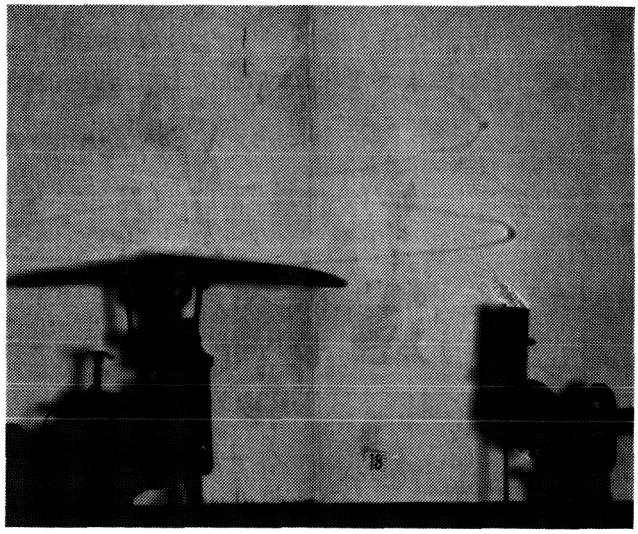

Shadowgraph of tail rotor flow field

Tunnel Utilization Trainer with Operating Rotor

Safe operation of a full-scale helicopter rotor in the 40- by 80-Foot Wind Tunnel requires the coordinated efforts of many test personnel including engineers, and the tunnel and rotor operators. Hence, a means of training personnel, both in the safe operation of the rotor and in reacting to emergency situations, is required. Such a system can also provide a way to study unusual or potentially unsafe test situations in a safe and controlled manner.

A simulator has been developed that combines a real-time model of a modern four-bladed rotor with the equations governing the controls of the Ames Rotor Test Apparatus (RTA), and the operation of the 40- by 80-Foot Wind Tunnel. The simulator hardware consists of consoles with the same appearance and function as those in the wind-tunnel control room. It operates in real time, and provides immediate and realistic feedback information to the operators. Operating procedures can be practiced and evaluated, and the response to emergencies (such as wind-tunnel drive failure) can be developed.

The simulation incorporates equations which model the wind tunnel, rotor controls, and rotor motions. The rotor model is an existing blade-element model of the UH-60 Blackhawk rotor. Each rigid blade has flapping and lead-lag degrees of freedom. The elements of the wind tunnel that were modeled were restricted to the main features relevant to a rotor test. These include tunnel motor frequency/voltage ratio, fan blade pitch and rpm, and tunnel velocity. Additional software is included to simulate failures and drive the displays.

Operating results have been obtained for some failure modes, three of which have been investigated thus far: rotor-drive motor failure, wind-tunnel drive-system failure, and rotor-control system failure. For the rotor and tunnel drive-system failures, both controlled rotor and uncontrolled rotor shutdowns were investigated. With initial rotor speed at full operating rpm, two sets of cases were run at tunnel speeds of 60 and 80 knots. Additional parameters varied by the rotor and tunnel operators were collective pitch and model angle of attack. Rotor response was found to be acceptable for the range of conditions tested.

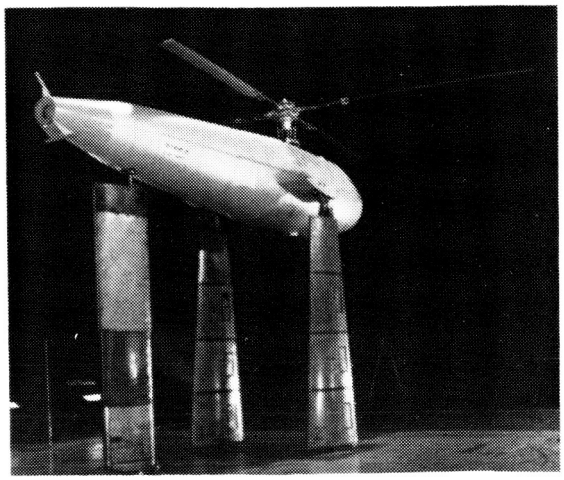

40- BY 80-FOOT HELICOPTER ROTOR TEST
- SIMULATE HELICOPTER ROTOR IN 40- BY 80-FOOT WIND TUNNEL
- MODELS ROTOR, WIND TUNNEL AND THEIR CONTROLS
- REAL-TIME OPERATION

SIMULATOR CONTROL CONSOLES
- ESTABLISH SAFE TEST PROCEDURES DURING NORMAL OPERATION AND EMERGENCIES
- TRAIN TEST PERSONNEL

Peterson/Stroub/Graham

Modern four-bladed rotor and console hardware used in training

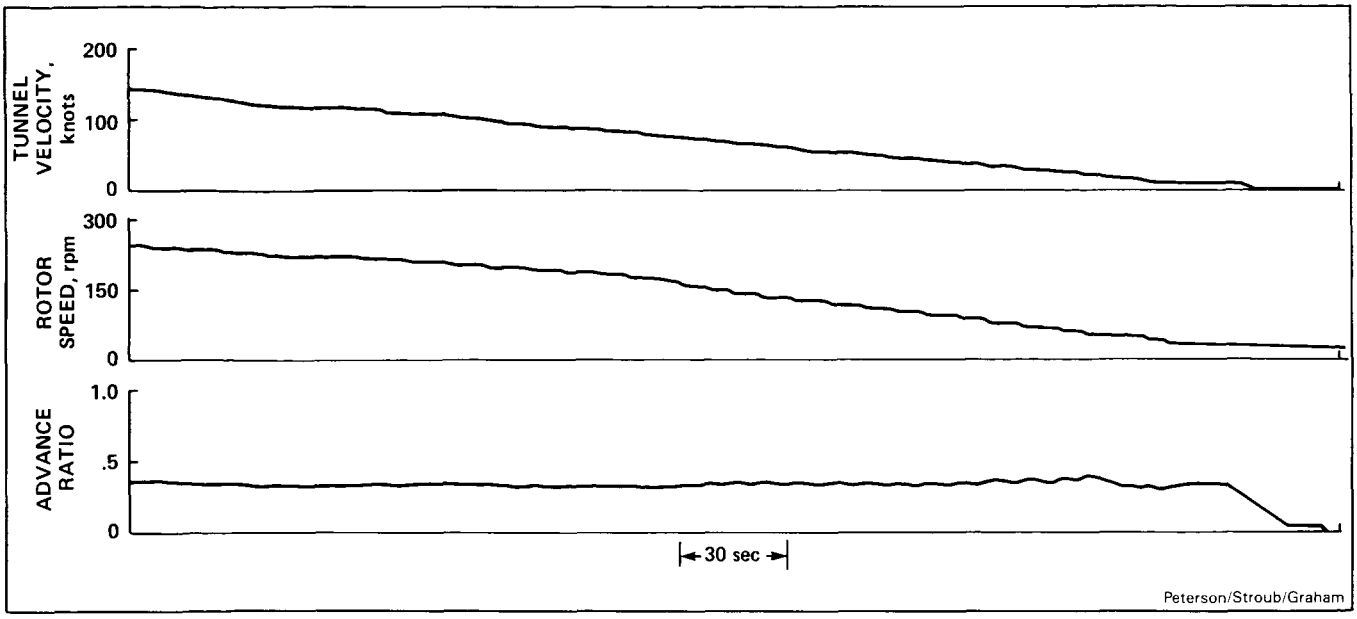

TUTOR simulation – loss of rotor control input, constant advance ratio shutdown

A limited investigation was conducted of the third failure mode: failure of rotor-control system. The emergency procedural response to this failure is a constant advance ratio shutdown. The time history shown is with the initial rotor speed at 245 rpm, and a tunnel speed of 140 knots. Reduction of both rotor speed and tunnel speed to zero was executed by the respective operators under the direction of the test engineer. The advance ratio is shown to have been maintained at a relatively constant level as the emergency shutdown was executed.

(R. Peterson, R. Stroub, and D. Graham, Ext. 5044/6732/6976)

Advanced Bearingless Rotor System

Current generation helicopter rotors are sophisticated mechanical systems which operate with high loads in an adverse aerodynamic environment. To relieve high rotor-blade root moments and maintain dynamic stability, helicopter rotor blades typically have several hinges, bearings, and/or dampers at the blade root. These mechanical devices operate in the rotating system and experience large oscillatory loads. They require frequent maintenance and can drastically reduce reliability of the rotor system. Consequently, the need exists to develop advanced helicopter rotor systems with a minimum of hinges and bearings in order to reduce maintenance and to improve reliability characteristics without degrading the aerodynamic performance or stability.

Previous full-scale wind-tunnel test programs, as well as some flight tests, have verified the feasibility of such designs, and the structural and operational integrity of the rotor systems. However, several important areas of bearingless rotor technology have not been adequately investigated to date. For example, the dynamic and aerodynamic characteristics of these rotors in forward flight have not been fully determined. Also, tests have shown that state-of-the-art analytical modeling techniques are incapable of predicting aeroelastic stability of bearingless rotors at moderate and high forward-flight speeds. Finally, previous testing has not sufficiently investigated parametric changes to the rotor configuration which might have significant effects on rotor stability, aerodynamic performance, transient behavior, and reducing system vibratory loads. Therefore, additional full-scale wind-tunnel testing should be performed if the full advantages of bearingless rotor technology are to be realized.

A new, advanced, bearingless rotor system is being acquired to address some of these technical concerns. It will be used to support a full-scale wind-tunnel investigation of the dynamic and aerodynamic characteristics of bearingless rotors. These characteristics can then be compared with analytical results, small-scale data, and flight-test data for the purpose of predicting the aeroelastic stability of such rotors at forward speeds up to

200 knots. The rotor system consists of two beams, incorporating a simplified rectangular flexure, each passing through a hub block and attaching to two opposite blades. A cuff, attached at a blade-to-beam clevis, will surround each beam. Its inboard end will be supported at a shear pivot attached to the hub block, and a pitch link attachment point will be provided on the trailing-edge side. This rotor system is being designed to operate on the Rotor Test Apparatus (RTA). Quantitative data will be obtained as to the rotor's control power, blade loads, transmitted vibration, performance, and acoustic characteristics and the influence of configuration changes on these properties.

(R. Peterson, Ext. 5044)

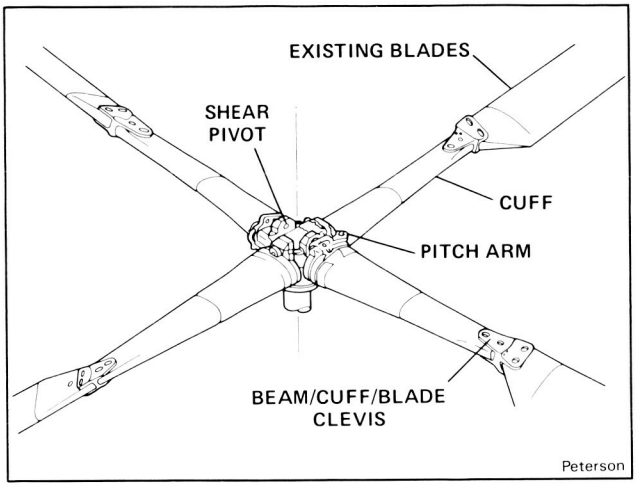

Advanced bearingless rotor system

Tail-Rotor Noise Mechanisms

The tail rotor can be the predominant noise source of single rotor helicopters. The interaction of the tail rotor with the complex flow around it is the cause of this noise. The principal sources of the complex flow environment are: (1) mean downwash from the main rotor; (2) rolled-up ground vortex from the main rotor; (3) the main rotor tip vortices; (4) the separated flow from the fuselage; (5) turbulence in the main rotor wake, and (6) atmospheric turbulence.

A series of tests has begun to investigate the effect of each of the above contributions to the complex flow around a tail rotor. A Lynx tail rotor mounted on a horizontal and vertical traversing mechanism will be used throughout the tests. Instrumented blades and a calibrated balance will measure rotor loads.

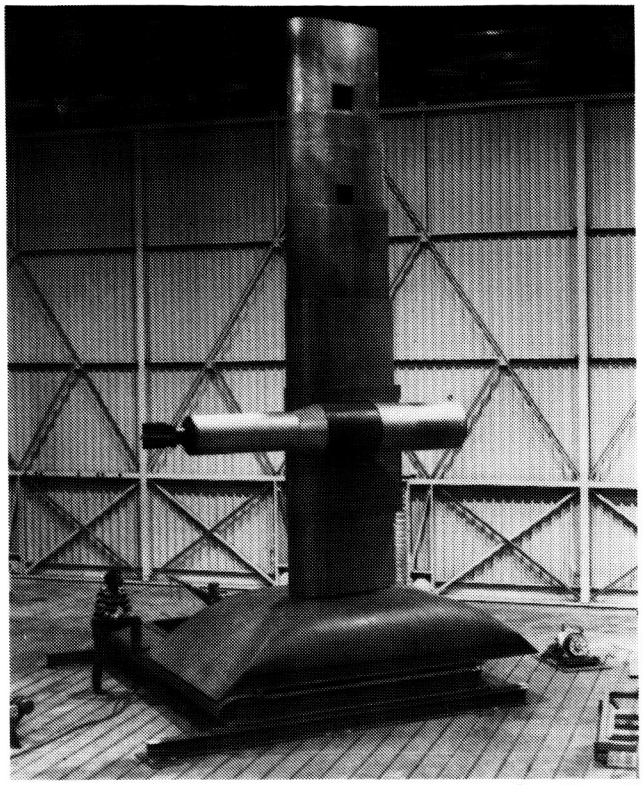

Signor/Yamauchi

Lynx T/R positioning stand

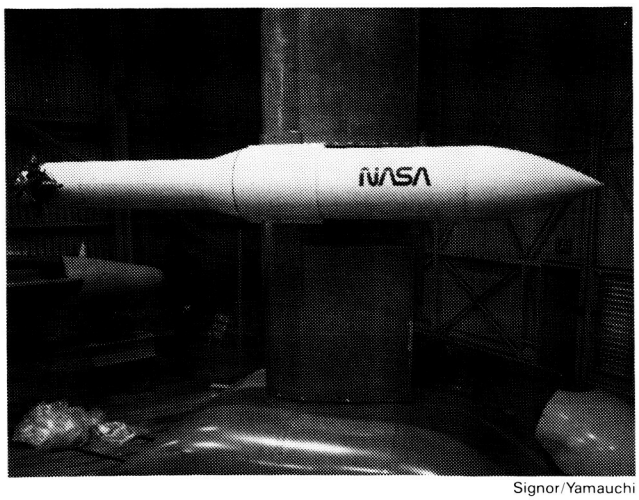

Signor/Yamauchi

Lynx T/R hub assembly

The effect of atmospheric turbulence on the tail rotor will be investigated in the initial test. The near-field and far-field turbulence will be measured and correlated with noise measurements.

Subsequent testing will investigate the effect of main rotor and fuselage on noise generated by the tail rotor.

(D. Signor and G. Yamauchi, Ext. 5044/6719)

Laser Speckle Velocimetry

One of the most difficult problems in experimental fluid dynamics has been the measurement of the vorticity field in fluid flows. This difficulty arises from the fact that vorticity is a quantity defined in terms of local velocity gradients. In contrast, the currently available velocity-measurement techniques (e.g., hot-wire or LV) are sensitive only to the local velocity.

Recently, a novel flow-velocity measurement technique (laser speckle velocimetry) has been developed. This technique provides both the visualization of the two-dimensional streamline pattern in an unsteady flow as well as the quantification of the instantaneous velocity field. The main advantage of this new technique is that the entire two-dimensional velocity field can be recorded in a single measurement, with great accuracy and spatial resolution. From this measurement the instantaneous vorticity field can be easily and directly obtained. This constitutes a great asset for the study of a variety of flows that evolve stochastically in time and space, such as the unsteady vortical flows in rotorcraft aerodynamics.

The experiment set-up itself is simple. A plane of interest in the fluid, seeded with microparticles as scatterers, is illuminated by a coherent light source, usually a pulsed laser. When the plane is imaged through a lens onto a photographic film or plate, the statistically scattered light gives rise to a speckle pattern. In usual speckle photography, two or more such speckle patterns are superposed on the same photographic plate. The result is called a specklegram. Through the appropriate choice of the time interval between exposures information on the local particle velocities is stored on the specklegram and may be transformed to a fluid-flow pattern through microscopic inspection. Elegant but simple coherent optical methods are used to extract this information.

(C. Smith, Ext. 6714)

Smith

Specklegram of a NACA 0012 wing at 45° angle of attack

Aerodynamic Interaction Program

The flow around any single helicopter component, such as the main rotor or the fuselage, is extremely complex. When isolated aerodynamically, each component has its own unique flow field and resultant aerodynamic characteristics. Nevertheless, present analytical techniques can predict reasonably well the flow around such isolated components. However, when in close proximity to one another, as in the helicopter, each component encounters a nonuniform and unsteady flow induced by all the other components. Hence, the total flow field is influenced, not only by the flow around each component, but also by the mutual interactions between the components.

A series of experimental and theoretical investigations are planned to provide detailed quantitative information on the aerodynamic and acoustic interactions that occur between various helicopter components. Two experimental investigations and a theoretical study have been completed to date. Future tests include studies of rotor/wing, rotor/

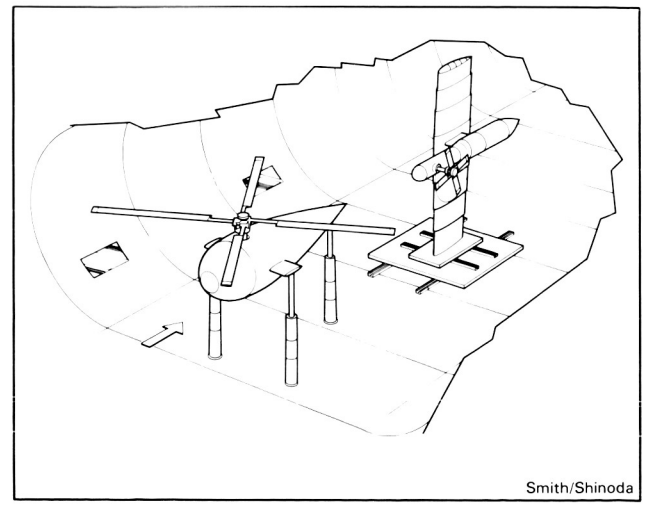

Smith/Shinoda

Interactional aerodynamics and acoustics test configuration

fuselage, rotor/fuselage/tail rotor, rotor/turbulence, and rotor/vortex interaction. Additional theoretical work in each of these areas is also planned.

Present experimental results indicate that body loads, normalized by rotor thrust, scale proportionally to a velocity ratio based on the free-stream velocity and the induced velocity or the rotor wake. Calculated oscillatory blade bending moments were always increased by the presence of the body for the cases considered thus far.

C. Smith and P. Shinoda, Ext. 6714/6679)

Numerical Methods for Vortical Flow Fields

A numerical method for computing the two-dimensional aerodynamic interaction between external vortical wakes and the viscous flow about a circular cylinder is presented. External vortical wakes refer to wakes generated by lifting surfaces or bodies other than the vortex wake generated at the cylinder surface caused by viscous forces. The method solves for the flow-field velocities on a body-fitted computational mesh using finite-difference techniques. The flow field is not constrained to steady or symmetric flow. The external vortical wake is represented by an array of discrete vortices, which, in turn, are represented by a finite-core model. The evolution of the external vortical wake is calculated by Lagrangian techniques. The viscous flow field of the circular cylinder is calculated on an Eulerian grid. The influence of the external vortical wake is represented directly through the governing equations for the viscous flow field. Results for the time-dependent viscous flow about a circular cylinder in the absence of external vortical wakes have been calculated for Reynolds numbers 40 and 100. The calculated drag coefficient, separated wake length, and point flow separation are in good agreement with other numerical and experimental results.

Computations modeling the interaction between the viscous flow field about a helicopter tail boom and the wake shed from a rotating wing above the tail boom have been made. This interaction was calculated for Reynolds number 100. The dependence of the shed wake around the tail boom, the point of separation on the tail boom,

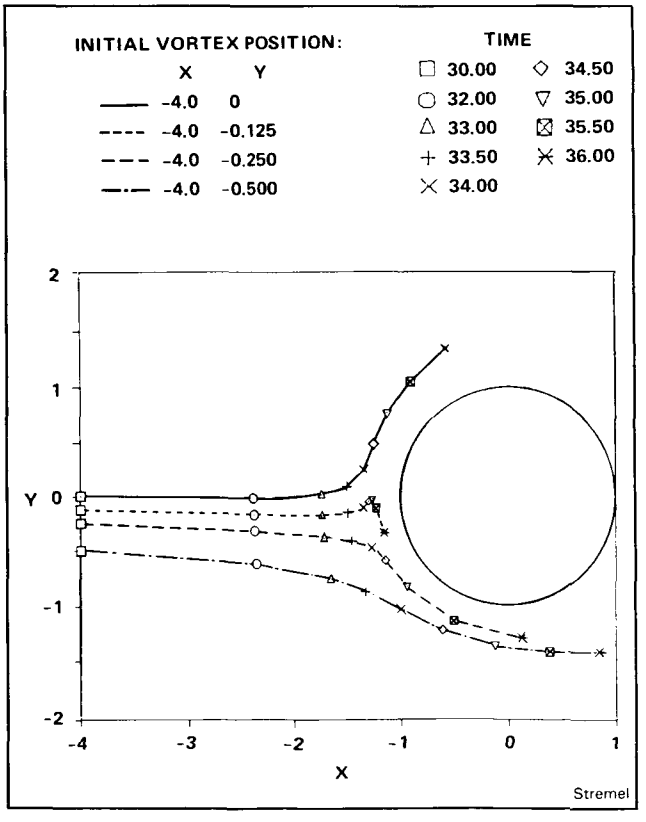

Vortex trajectory

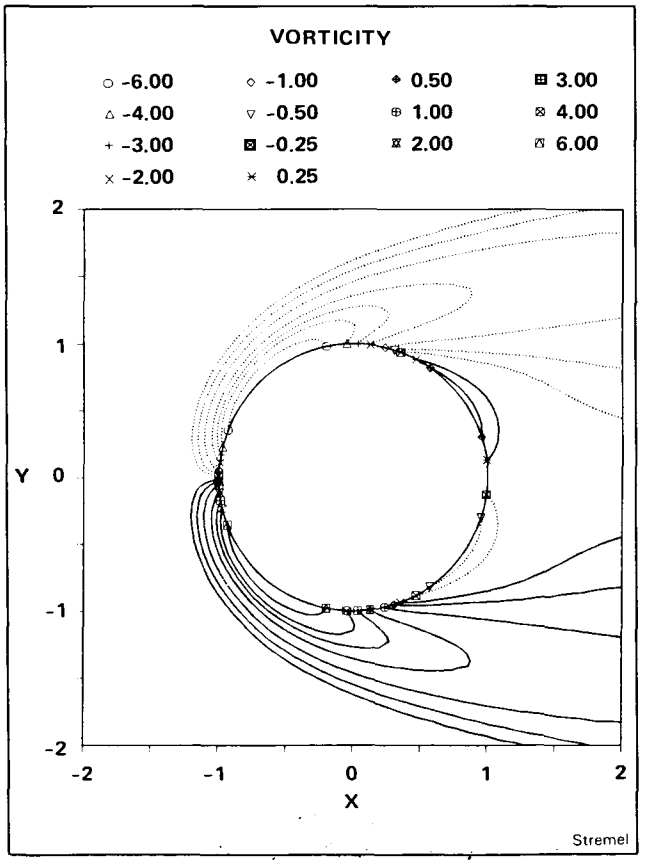

Vorticity contour

and the aerodynamic characteristics of the flow field owing to the presence of the rotor wake were evaluated. The flow field about the helicopter tail boom was found to be highly dependent on the location of the rotor wake relative to the tail boom.

(P. Stremel, Ext. 6714)

The Free Tip for Increased Helicopter Performance and Reduced Oscillatory Loads

A new tip concept in helicopter rotors called the free tip has been developed by NASA. This tip is self-driven and free to change its pitch angle independent of the rest of the rotor blade. This new degree of freedom causes two effects: smoothening of the tip's oscillatory lift, and more power efficient lift loading on the blade and the tip. The benefits of this concept compared to a conventional fixed tip were demonstrated in a wind-tunnel test of the free-tip configuration. The attached figure presents a description of the free-tip concept, the wind-tunnel test configuration, and the test results. The wind-tunnel test data show the benefits to be: (a) 12% less power required at cruise speeds, and even more power savings at higher speeds owing to lessened compressibility penalties, (b) 16% greater rotor lift capability at the same power level as with conventional fixed tip. This increased lift capability translates into 45% increase in payload for a 200 n. mi. range mission at the same cruise speed, (c) peak vibratory blade loads reduced by 48%.

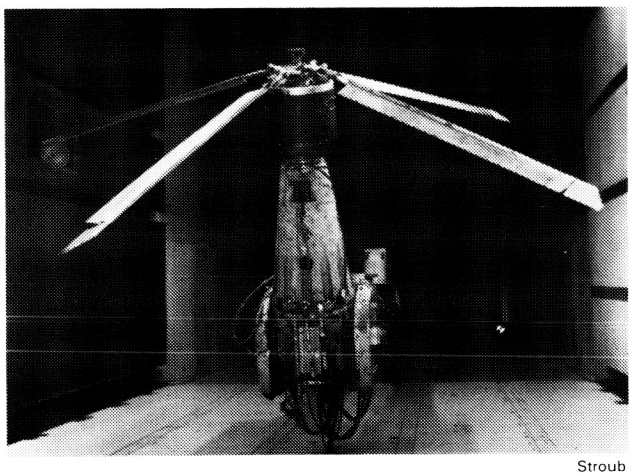

Stroub

Free-tip rotor

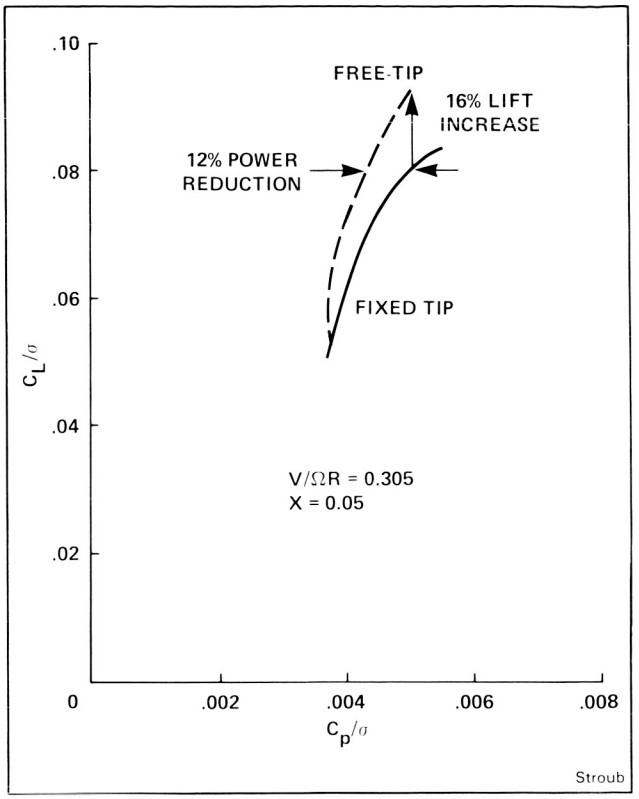

Free tip reduces power requirements

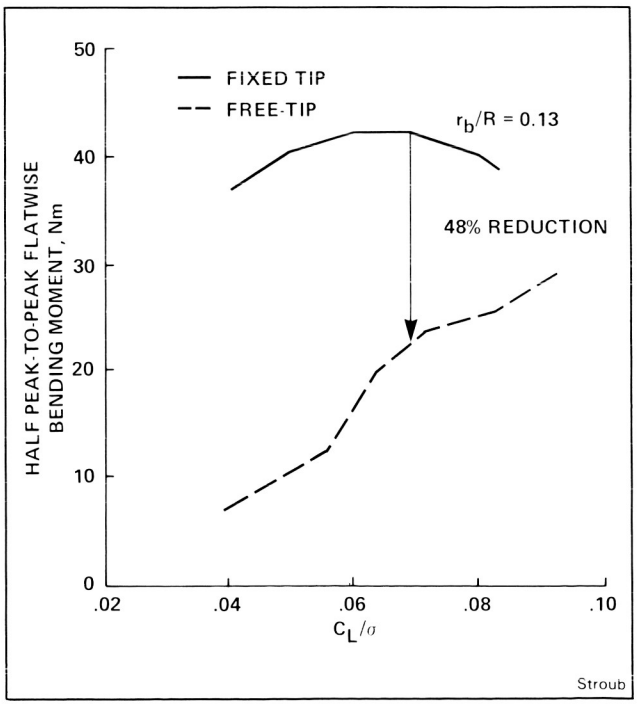

Free tip reduces flatwise bending moments

In addition to the performance improvements and the reduced vibratory blade loads, the free-tip concept caused a 70% reduction in oscillatory loads going into control system.

To implement the concept for the wind-tunnel test, the required additional hardware was simple and the parts were relatively few in number. It is expected that when implemented on a full size rotor, fewer parts will be required.

Because of the favorable wind-tunnel test results and the simple hardware requirements, development of the free tip is continuing. The concept will be further developed to exploit the unique opportunity offered. New tip configurations are being developed that tailor the tip design to the aerodynamic environment and further improve rotor lift and power efficiencies. The new tip configurations will be evaluated in both small-scale and full-scale wind-tunnel tests. In addition, the free-tip rotor data base will be greatly enlarged to aid development of computational capabilities.

(R. Stroub, Ext. 6653)

Hub-Drag Reduction

Hub/shaft drag contributes significantly to total helicopter drag (approximately 20-50%). Substantial rotorcraft fuel consumption improvements could be attained if this high drag contribution was reduced. A 7×10 wind-tunnel test was recently conducted to obtain data on various proposed drag reduction methods. Model loads, flow visualization photographs, and wake pressure measurements were acquired. Both coaxial and standard single-rotor hub configurations were tested. The modeling of both types of rotor assemblies was kept simple: nonrotating hubs and no blade shanks.

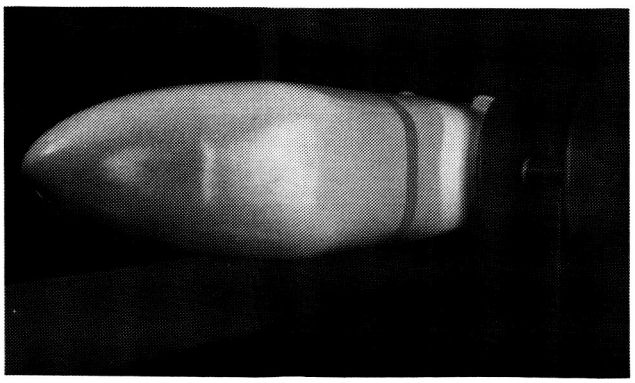

Young

Coaxial helicopter hub fairing configuration

Preliminary evaluation of test data suggests at least three important results. First, shaft fairings/pylons can result in substantial drag improvements over nonfaired shaft assemblies (a 40-50% drag reduction was obtained during the test). Second, a cambered, elliptical, hub fairing demonstrated a 10-20% drag reduction over a single-rotor hub elliptical fairing baseline. Third, a coaxial, cambered, elliptical hub-fairing configuration had approximately 50% less drag than an elliptical hub-fairing baseline.

(L. Young, Ext. 6732)

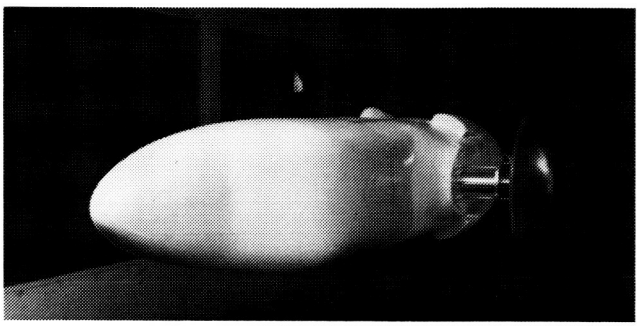

Young

Single main rotor helicopter with faired hub

Modern Airship Flight Test and Hybrid Vehicle Computer Program Validation

A nonreal-time simulation program capable of modeling various hybrid aircraft has been compared to flight test data. The program, called HYBRDS, can be used to model a variety of vehicle concepts including multirotor, multipropeller, and buoyant hull vehicles, either singly or in various combinations. The program models each of the components with an equal amount of technical complexity, so that the simulation is both efficient and meaningful.

Flight-test data was obtained on a modern airship (the Airship Industries Skyship 500) during a joint NASA, Navy, and Coast Guard flight evaluation called the Patrol Airship Concept Evaluation (PACE). An Ames research pilot and several Ames test engineers participated directly in the tests. The airship's response to various inputs, including frequency response and step inputs to both the rudder and the elevator, was measured. Engine-thrust data was also obtained. The flight-data results were of such a high quality so as to easily allow the recognition of both vehicle- and structural-vibration modes and frequencies.

Some selected data generated by the HYBRDS program are compared with the flight-test data in the figure. The particular response is that of vehicle roll rate to rudder input. The model matches the data very well for the mid-range frequencies. The higher frequencies show the onset of the vibration mode of the cab-on-hull mode. At the low frequency, the flight-data is not representative of a linear function anymore because of the nonlinear pendulum effects.

Other data comparisons showed a similar high degree of correlation which adds to the confidence of the fidelity of the HYBRDS program. The program will be made available for applications such as the Navy's ongoing effort to reexamine airship concepts for long endurance/long range surveillance support of the battle ship fleets.

(P. Gelhausen, Ext. 6276)

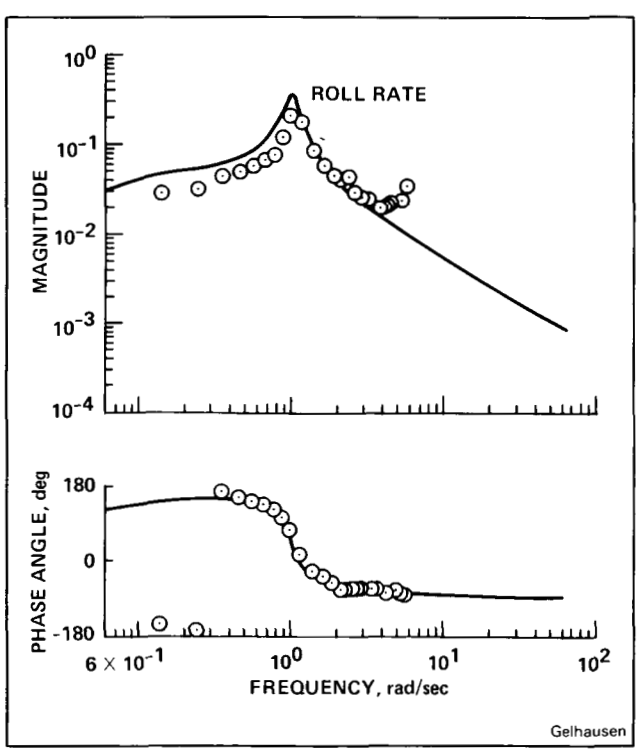

Comparison of simulation data versus flight-test data, roll response to rudder input

Electro-Expulsive Deicers for Rotorcraft

A major technological impediment to extending helicopter operations into the all-weather flight regime is the lack of rotor blade ice protection. The sensitivity of the blades to ice accumulation is well recognized. Anticipated weight and power penalties for existing helicopters have been cited as a major reason users have been reluctant to incorporate ice protection on existing helicopters.

A low-cost, low-power and light-weight solution to the problem of icing protection for helicopter rotor blades appears available from efforts of NASA Ames research personnel. The newly disclosed next generation deicing system is described in a recent patent application. The electro-expulsive deicer boot is readily bondable onto almost any substrate, and requires no mechanical moving parts or pneumatic inflation to effectively shed ice from aircraft surfaces. The new deicer takes the form of an elastomeric boot that cyclically, expulsively, expands and throws off any accreted ice.

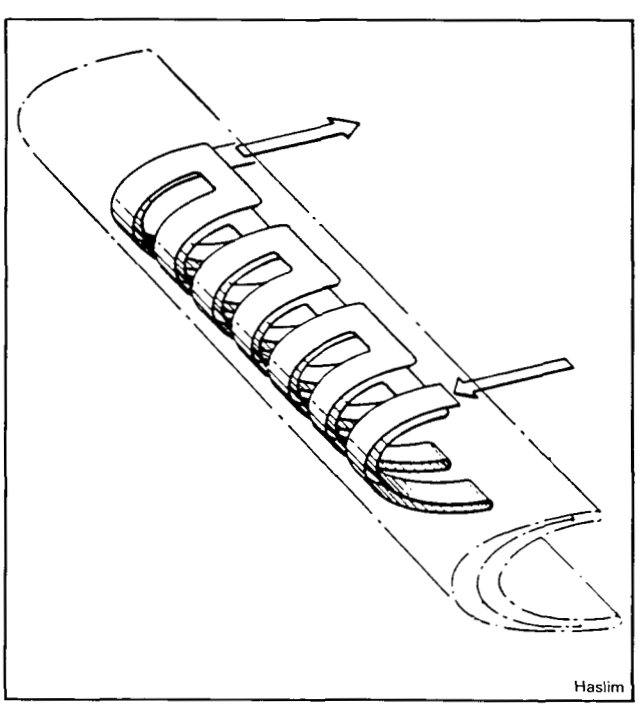

Perspective view of an overlapped serpentine ribbon conductor of the electro-expulsive deicing system, embedded in a flexible elastomer sheet

The operation could be described as the snapping of a small rug to shake the dust out. In the relaxed state, the thin deicer boot is flat against the airfoil surface with no significant voids in its interior. During fabrication of the low-temperature rubber boot, however, there are enclosed unbonded sections included (resembling knife slits) which are completely surrounded by the elastomer. These slits are in between and in parallel with a series of high-voltage ribbon conductors embedded in the rubber.

When a bank of capacitors in the power supply is discharged into the conductors in a zoned-sequence pattern, the large pulse of electricity (about 3000 amperes discharged in less than a few milliseconds) suddenly inducing these conductor pairs to repel one another with a powerful force. This force causes the slit-voids to expand vigorously (as in the rug-snapping simile) to throw off any ice buildup. The voids immediately collapse again owing to the elastic rebound of the boot material, and thus the operation cycle has virtually no adverse effect on aerodynamic performance because of the rapidity of its action.

The concept has been prototype tested at Ames and planning is under way for an icing tunnel testing when the facility reopens.

(L. Haslim, Ext. 6575)

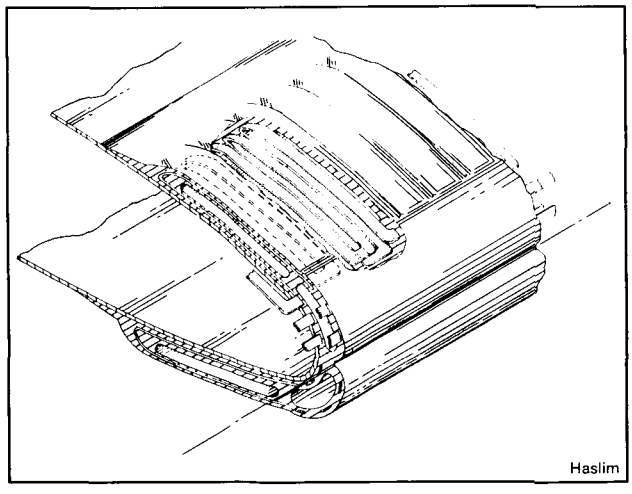

Sectional perspective illustration of a version of the electro-expulsive boot with the conductors electrified and portions of the elastimer vigorously distended to shed ice

Rotor Airloads Program

The Rotor Airloads Program is a key element of the NASA-Army program to advance the state-of-the-art in helicopters by providing appropriate, detailed, rotor systems flight-research data and analysis. This flight research is necessary in order to improve and validate the analytical capability to predict the performance and vibratory airload characteristics of current and projected advanced rotor systems. Implementation of the improved theoretical analysis is a prerequisite to substantially improved performance, dynamics, acoustics, handling qualities, and cost of new rotorcraft. The objective of this program is to obtain extensive in-flight data on an advanced high-speed rotor and to make this data available to the domestic helicopter industry.

The need to develop an extensive data base on rotor aerodynamic loads and related acoustic signature is well recognized throughout industry and government. One advanced helicopter rotor that is of particular interest to NASA is the Boeing Vertol 360 rotor, a design which evolved from Boeing IR&D and the NASA AFRR program. The 360 rotor is a unique high speed, composite rotor design incorporating advanced airfoils and an advanced planform. The intent of the initial effort is to acquire 360 rotor blades for ultimate testing on the RSRA; to complete the qualification and ground testing of the blades; and to acquire flight-test data generated by Model 360 flight-test program. This approach permits NASA to acquire an initial data base early in the program on a Boeing test aircraft, and in the second stage (where the RSRA is utilized as the test vehicle) to undertake a thorough and complete flight investigation using the unique RSRA capabilities.

The complexity of the flow environment over helicopter blades in forward flight, the exact nature of the phenomena at the source of the vibratory airloading and noise is poorly understood, and therefore is poorly modeled by analysis. This inadequacy of the analytical tools, in turn, makes the definition of advanced rotor systems a costly task requiring extensive iterations between analysis and test. In order to help resolve this problem and to improve the research utility of the overall program, the scope has been

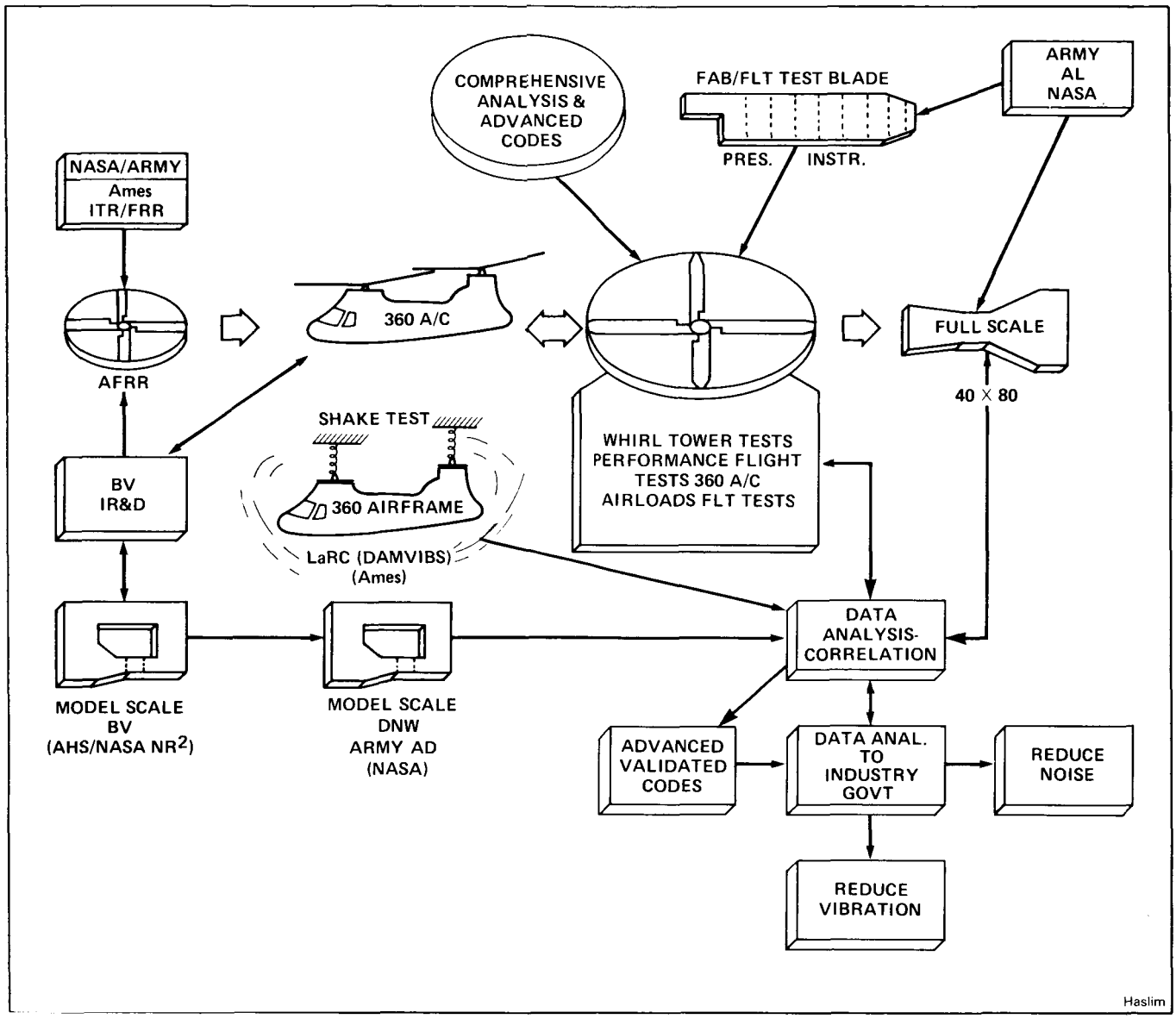

Rotor airloads NASA/Army/Boeing model 360; advanced high speed rotor (tandem configuration flight tests)

expanded to include: the acquisition of a pressure instrumented 360 main rotor blade, flight testing of the blade on the Model 360 helicopter, and wind tunnel testing of the rotor.

In addition to the hardware development, the rotor is also being modeled utilizing CAMRAD as the basic methodology. The full-scale 360 rotor program is part of an integrated model scale, full-scale, ground, and flight test and analysis program as illustrated on the attached figure.

(L. Haslim, Ext. 6575)

Tilt-Rotor Advanced Technology Blades

The advanced technology rotor blades (ATB) for the XV-15 Tilt Rotor Research Aircraft were delivered to Ames in September 1985. The ATB are the first flightworthy rotor blades which incorporate a recently developed high-strain graphite. The new blade design will offer a significant improvement in fatigue life over the current blades and should enable expansion of the XV-15 flight envelope.

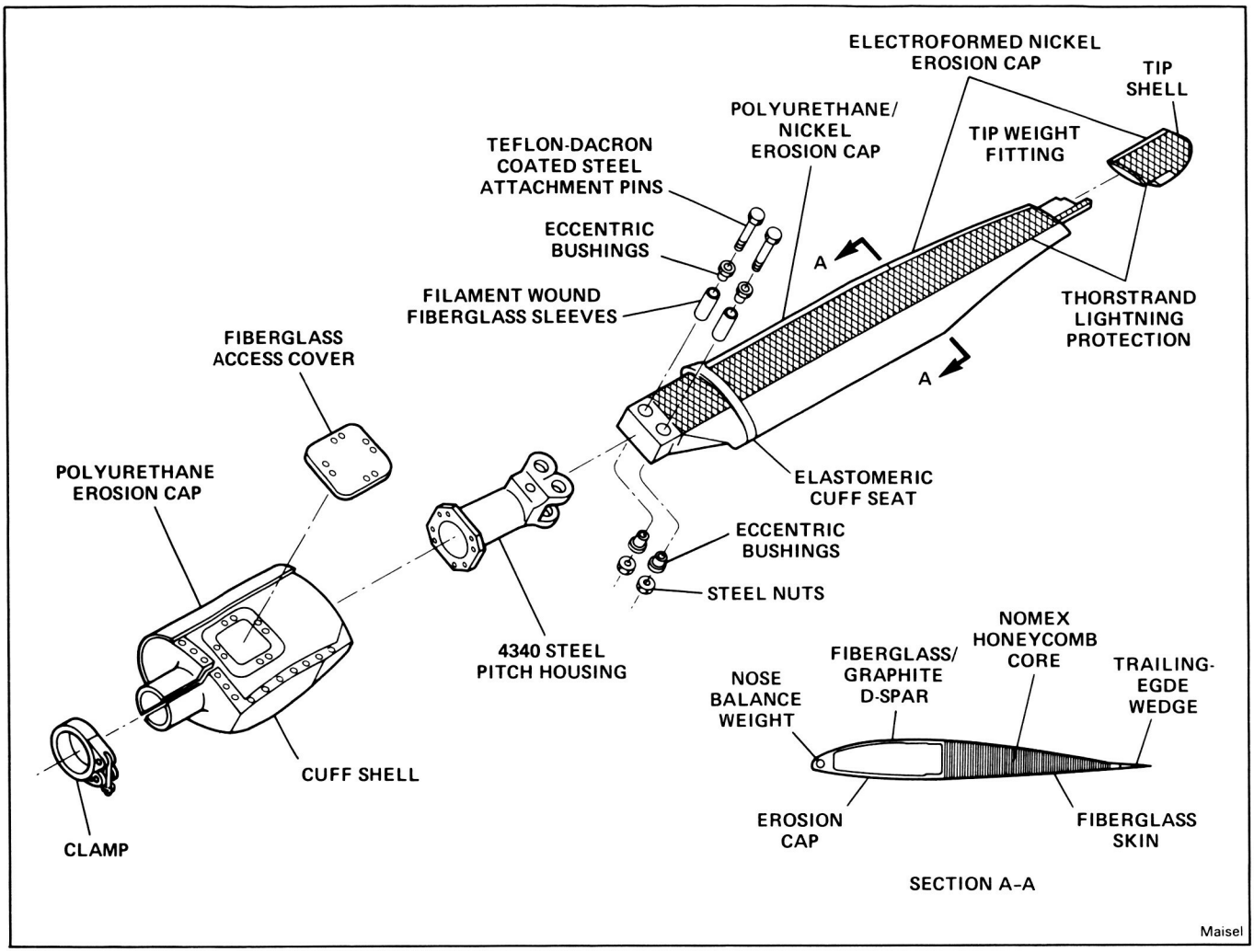

Components of the ATP rotor blades

The blades were designed to increase the hover-mode thrust capability without degrading the high-speed airplane mode performance of the XV-15. Boeing Vertol used a combination of state-of-the-art (VR-7 and VR-8) airfoil sections, a high twist, and a nonlinear tapered planform to achieve the aerodynamic trade-off between the conflicting high-speed and hover-mode requirements.

An additional research feature of the ATB is the ability to alter the geometry by replacing the removable tip and cuff sections to investigate planform and twist variations, and to change the blade sweep (which influences loads and aeroelastic stability) by changing eccentric bushings at the twin retention pins.

Flight testing and evaluations of the baseline ATB on the XV-15 will begin in the Fall of 1985.

(M. Maisel, Ext. 6372)

Rotor Airloads of Modern Single Rotor NASA/Army UH-60 Black Hawk

The NASA-Rotorcraft Flight Investigations Branch, in cooperation with the Aeroflightdynamics Directorate—AVSCOM, has initiated programs to investigate the aerodynamics performance limitations of modern rotors at high speed, in maneuvers, and at low speeds. These investigations are being undertaken to promote a better understanding of basic rotor aerodynamic and dynamic phenomena, and to support near-term developments, such as experimental light helicopters (LHX). Tasks include systematic flight research to investigate blade airloads for noise and vibration.

The initial flight phase, which will support LHX, will use an Army UH-60. The later phases

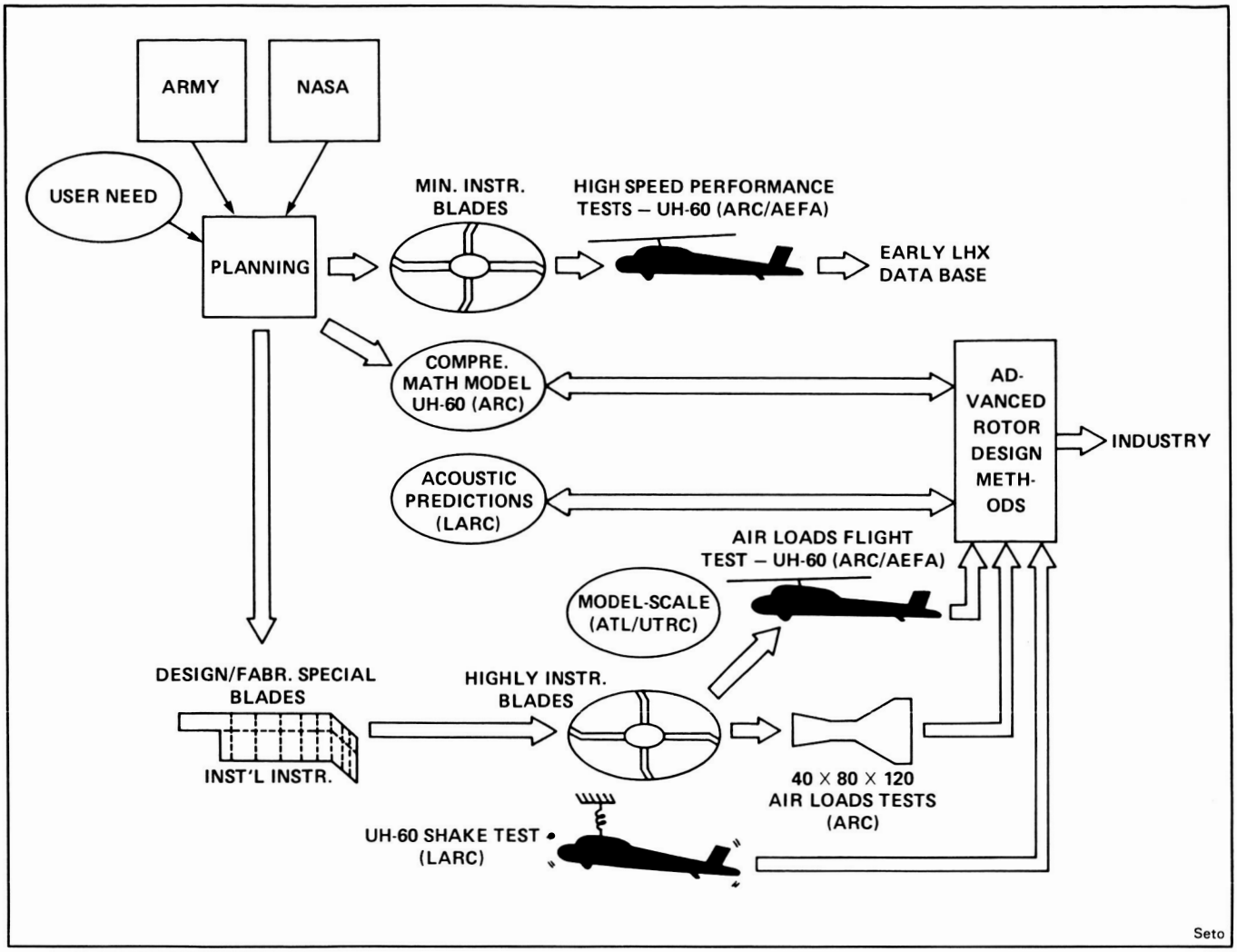

Rotor air loads near term modern single rotor NASA/Army UH-60 Black Hawk

of the program are focused on obtaining comprehensive in-flight rotor airloads measurements for providing a national rotor data base using a special set of highly instrumented UH-60 blades.

In this last year, the U.S. Army Aviation Engineering Flight Activity has agreed to provide the UH-60 and to conduct the flight investigation with NASA's active participation. Theoretical predictions are being obtained from several rotorcraft analytical computer programs, including the Comprehensive Analytical Model of Rotorcraft Aerodynamics and Dynamics (CAMRAD). The predictions are being compared with each other for preliminary verification purposes. These predictions will be used to assist in the planning and will figure prominently in post-flight analysis. The compilation and correlation of the CAMRAD input data with other developed rotorcraft prediction programs are almost completed. Preparation for the flight investigation is well under way with plans to conduct the initial flight phase early in 1986. The design of the highly instrumented blades is complete. The blade set will consist of two blades: one blade will house 242 miniature pressure transducers, while the other blade will house an assortment of 70 strain gages and accelerometers.

(E. Seto, Ext. 5664)

Rotor Systems Research Aircraft Experiments

The Rotor Systems Research Aircraft (RSRA) offers a unique opportunity for flight experiments of the rotor system which are of general interest. The rotor-load measuring system measurs the resultant forces and moments within an accuracy of 2%. The aircraft is also equipped with a complete set of conventional fixed-wing surfaces and controls enabling the aircraft to fly in three different configurations: helicopter, compound, and fixed-wing airplane. The flight investigation programs have been developed for initial testing on the RSRA using these unique capabilities. The first two (hover-download experiment and fixed-wing test) have been completed during the past several years, while preparations are currently under way for the third (rotor performance mapping).

The RSRA rotor load measuring system was used to conduct an experiment to determine vertical drag, and main rotor-thrust augmentation as affected by ground clearance and flight velocity. The RSRA was flown in the helicopter configuration at speeds near hover from wheel heights of 5 ft to out-of-ground effect. The vertical drag decreases rapidly as wheel height is reduced, and is zero at the low wheel heights. Vertical drag was also found to decrease with forward speed and approaches zero at 60 knots. The test data showed the effect of wheel height and forward speed on thrust, and gross weight capability and power. It provided the relationships for power and collective pitch at constant gross weight which are required for the simulation of helicopter takeoffs and landings.

The RSRA flew 11 flights in the fixed-wing configuration. Main rotor hub drag and airplane configuration acoustics data were acquired, along with parameter identification, control sensitivity, and aircraft stability data. The control power and aircraft stability data were obtained principally to satisfy RSRA/X-wing design support requirements. Certain test maneuvers were performed to provide data for definition of the aircraft flight characteristics by parameter identification methods. Two types of maneuvers were performed in each axis: sine-wave inputs of increasing frequency over 90 sec, and alternating control step inputs using time-duration sequences of 3-2-1-1 and 2-3-1-1. These sequences excited different response frequencies of the aircraft while keeping the aircraft close to trim.

The capability to fly as a fixed-wing aircraft allowed measurements of various helicopter components without main-rotor interference; in particular, hub drag and aircraft acoustics. The RSRA force-and-moment balance system provided drag data for the main rotor shaft, and the main rotor shaft with rotor hub installed. Shown are hub data versus the fuselage angle of attack at constant dynamic pressure. The data were taken at 167 KCAS, and obtained by variation of wing incidence from 0 to 10°. Acoustic data were obtained during low level flybys over a ground-based microphone array. The data set provides the acoustic signature of the RSRA engines, airframe, and tail rotor. Planned acoustic tests in the compound configuration can now be used to provide isolated main rotor acoustic data.

The rotor performance mapping has the following goals: obtain a detailed mapping of the rotor performance characteristics over a wide operating range; define the high-speed rotor lift boundary of the rotor system; gather a data set in the compound mode to complete parameter identification work in all three aircraft configurations of the RSRA. This test, to be conducted in the compound configuration, will provide an accurate map of rotor system performance. The

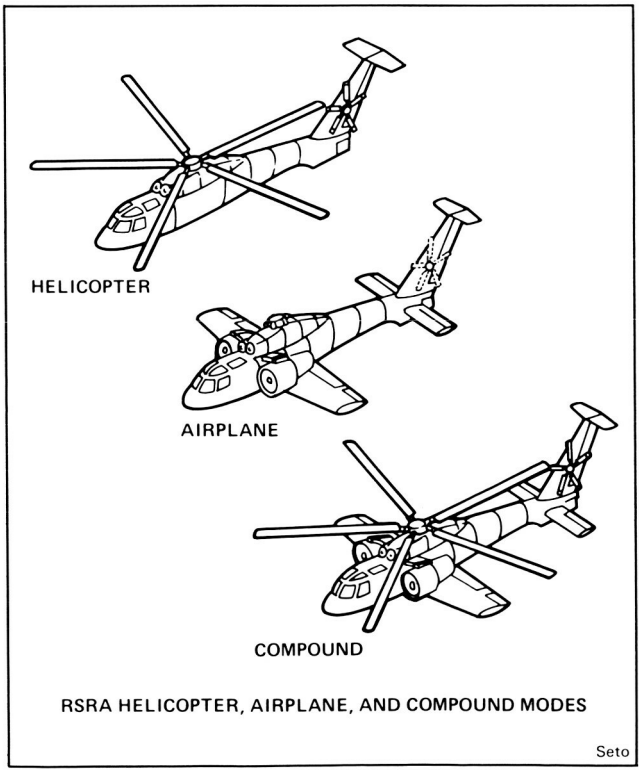

RSRA flight configurations

test points consist of a four-dimensional matrix of nondimensional coefficients, which extend beyond the operational envelope of modern helicopters. The parameter identification data will consist of dynamic maneuvers from specified steady state conditions. The test points will all be conducted in level flight and will be calculated by a ground-based computer in real time. Computed test data will be telemetered to the pilot in the aircraft, where four parameters will be graphically displayed.

Upon conclusion of the current flight investigation program, the RSRA will have completed research programs in each of its three aircraft configurations. The following experiments/programs/studies are expected to provide information on:

(a) Hover download experiment: unequalled, accurate database to verify tool designs.

(b) Hub-drag: unique data for correlation with performance predictions.

(c) Fixed-wing acoustic: baseline data set to allow for derivation of rotor-only acoustic data sets from compound testing.

(d) Rotor performance mapping and high-speed limits: inflight data set comparable to extensive full-scale tunnel tests conducted on the H-34 rotor system in 1960 (which are still being used as standard references).

(E. Seto, Ext. 5664)

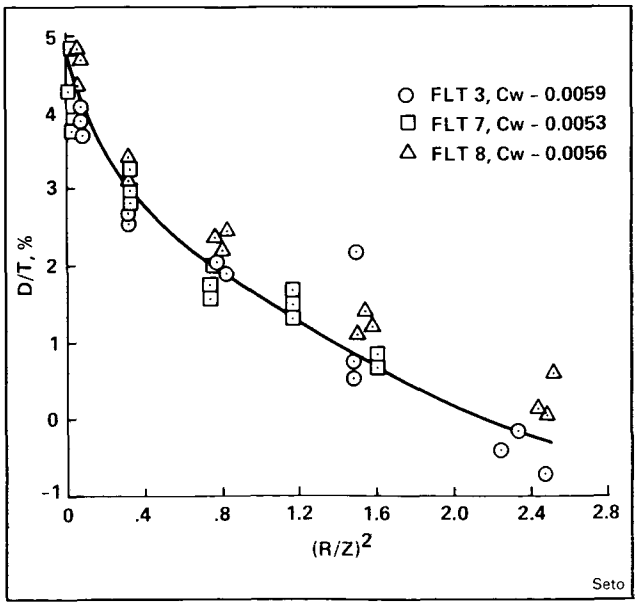

Download/thrust versus rotor height

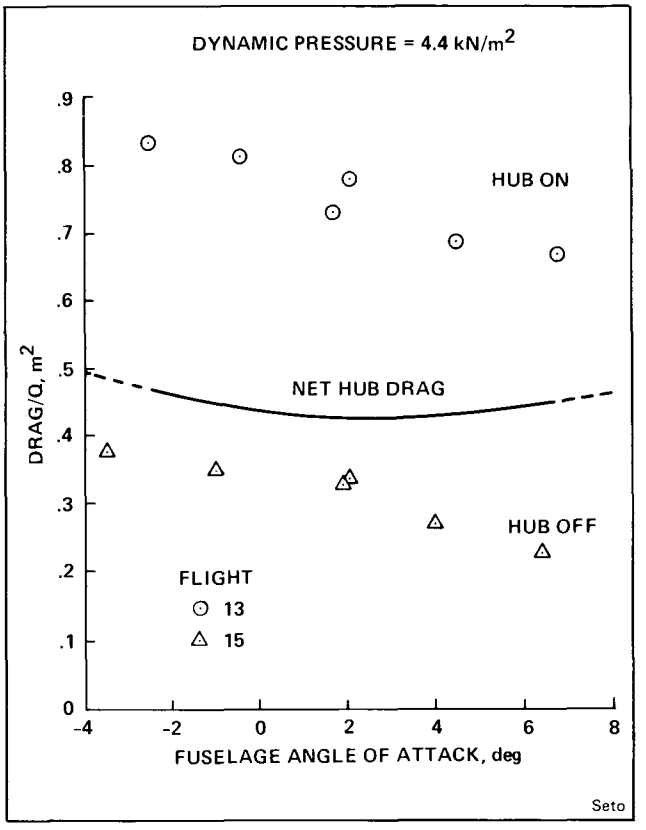

Hub drag versus angle of attack at constant Q

Rotor Systems Research Aircraft/X-Wing Program

One of two Rotor Systems Research Aircraft (RSRA) (Sikorsky Aircraft) is being modified to incorporate a four-bladed, extremely stiff rotor that can be stopped in flight. For takeoff, hovering, and low-speed flight, the rotor will function as a helicopter rotary wing. At a speed of about 200 mph, the rotor will be stopped and locked in place, making the aircraft a fixed-wing airplane with two forward-swept wings and two aft-swept wings in an "X" configuration. In the latter mode, it is expected that the RSRA will have a speed potential approaching 500 miles per hour.

The goal of this research program (sponsored by NASA and the Defense Advanced Projects Research Agency (DARPA)) is to demonstrate adequately conversion from the rotor-turning mode to stopped, and back again. This demonstration, coupled with the successful completion of the NASA/DARPA Convertible Engine Program and the DARPA/Army NOTAR Program, would provide the necessary technology base to initiate an X-wing prototype vehicle.

During this past year, the various components of the circulation-controlled composite blade have been fabricated and successfully bonded for the first propulsion system test bed (PSTB) blade. Also during tis year, the compressor which will blow compressed air out of the blade edges to provide circulation control was successfully manufactured and accepted for use on the PSTB. This will provide transmission and drive-train integrity tests prior to first flight.

This past year, the extremely complex wind-tunnel model, one 5/7th the size of the actual RSRA/X-Wing aircraft, has been fabricated and will be tested in the United Technologies Research Center wind tunnel next year.

The most challenging aspect of the program to date has been the flight control computer, which is comparable in sophistication to that of the Space Shuttle owing to the quadraplex system with four digital processors per channel needed to manage circulation control blowing with higher harmonic control and hub-moment feedback. The detail design of the hardware for this system has been completed this past year and the brassboard is being tested in Sikorsky's Vehicle Systems Management Laboratory (VMSL), a simulator for validation and verification of all of the flight software and hardware to be used in the aircraft.

(J. Burks, Ext. 6576)

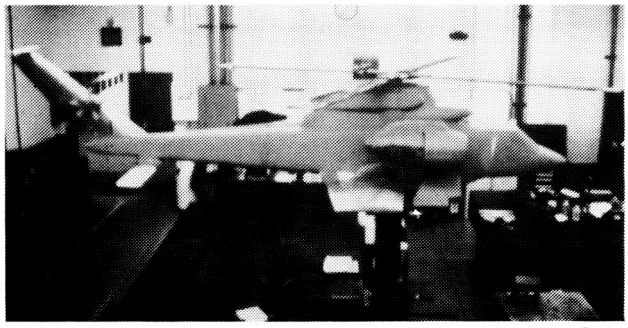

Burks

RSRA/X-Wing wind-tunnel model

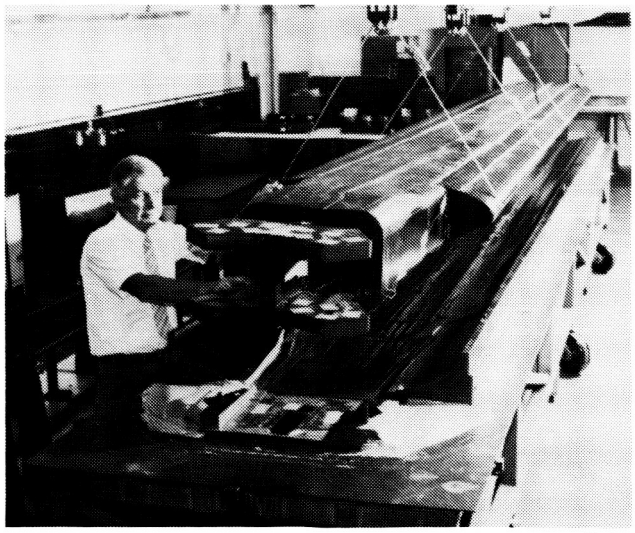

Burks

Composite blade for RSRA/X-Wing

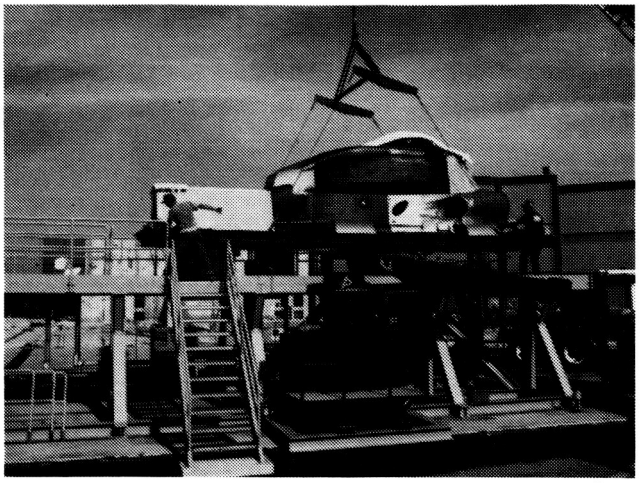

Burks

Propulsion system test bed for RSRA/X-Wing

Objective Assessment of Pilot Performance

The objective of this program is to develop a series of short, full-crew, full-mission flight scenarios for use by researchers in the Man-Vehicle Systems Research Facility; to evaluate the scenarios during flight by experienced pilots temporarily placed at reduced levels of proficiency by means of ethyl alcohol; to collect a database of objective performance data that can be used to evaluate various measures of pilot performance in existence, or proposed, for use in subsequent investigations. Many measures of pilot performance have been used during the past three decades to assess the effect of a great variety of stresses on aircrew effectiveness; these measures range from very simple to very complex; many appear to be highly correlated. Most of these measures have been designed and applied under conditions where investigators had full knowledge of the experiment; however, there has been little or no systematic comparative study of the measures themselves.

The Man-Vehicle Systems Research Facility provides investigators with the opportunity to collect large amounts of data in highly structured

studies of aircrew behavior under tightly controlled experimental conditions. The Facility is capable of producing far more data than can be effectively used unless automated, efficient methods of data compression and reduction are applied. This study represents an attempt to develop and evaluate such measures, as well as to develop a library of standard scenarios which can be called upon by other investigators wishing to utilize the Facility's unique capabilities.

Eight scenarios (four transport flights in each direction between San Francisco and Los Angeles) have been constructed. The weather, routings, air-traffic control complexity, anomalies, and distractions have been chosen so as to produce approximately equal workload in the various scenarios. An experiment has been designed to present eight experienced air-carrier pilots with each of the scenarios. Four levels of proficiency, influenced by graded doses of ethyl alcohol, are utilized in the experiment which is patterned on an earlier study conducted in general aviation aircraft in actual flight. Preliminary results indicate that the variability previously seen in flight is also present in the performance of these pilots, notwithstanding their high experience and their currency in the aircraft being simulated, a Boeing 727. To date, major errors by these pilots have been less than would have been anticipated based on the earlier studies.

Data collection and compression techniques have been designed, coded and tested; they have also been found useful in other studies within the Facility. Study of the data collected in this experiment may make it possible to characterize pilot and other aircrew performance automatically, in near-real time. Such a characterization will, in turn, permit experimental conditions to be varied in real time in such a way that maximum experimental yield is gained more quickly and with substantially decreased expense to the investigators. It is also hoped that these data will lead to better insights into the reasons for pilot and aircrew errors in the operational environment.

(C. Billings, Ext. 5718)

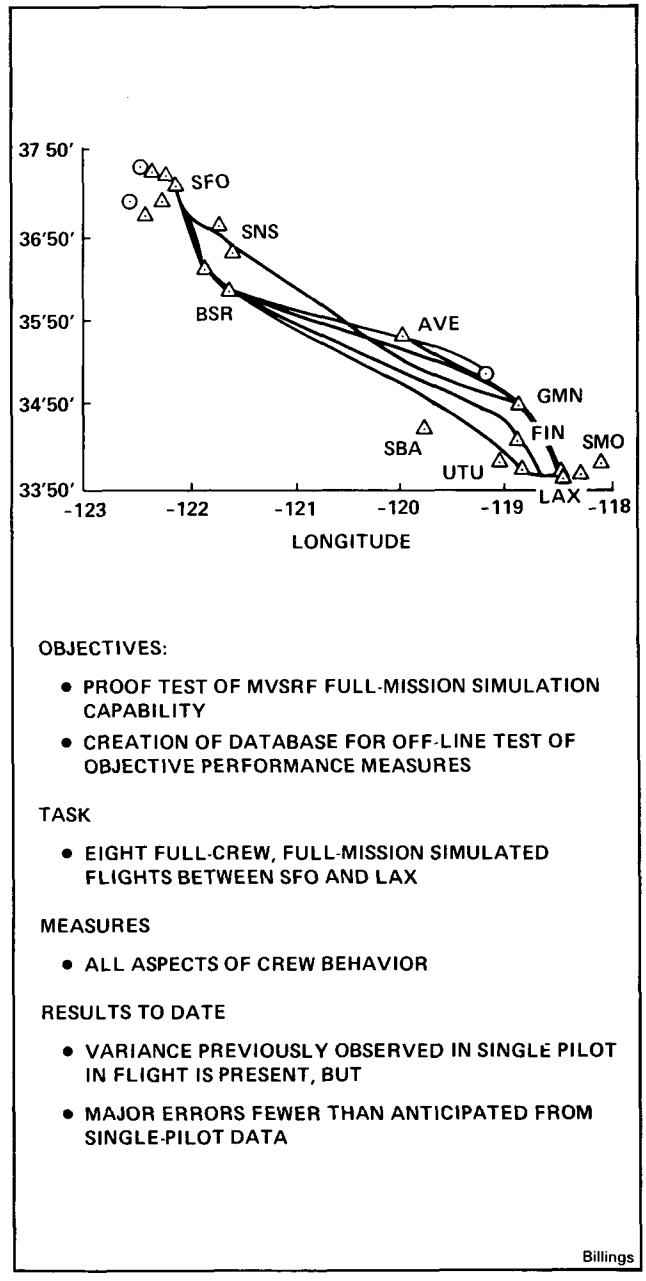

Simulation scenario

Development of Workload and Performance Assessment Methods

In order to evaluate pilot workload and performance, reliable valid measures are required. The search for such measures was the initial focus of research for the Human Performance Assessment Research Group at Ames. Considerable progress has been made in this area through both in-house and the sponsored research of university collaborators. Five categories of workload assessment techniques have been investigated: primary task performance measures, secondary-task performance measures, physiological measures, subjective ratings, and task analyses. Within each category several promising measures were developed and evaluated. For each of these measures, the types of workload questions for which they are particularly appropriate and the environments in which they can be applied have been identified. A summary of this research is being compiled in a NASA Technical Paper and coded into an "expert system" for workload assessment on a microprocessor for general distribution.

Many of these measures have been applied in operational environments at the request of organizations outside Ames (e.g., the U.S. Army). One example of such an experiment is the measurement of pilot workload, inflight, during training with the pilot night-vision system (PNVS). This research is being conducted in the Cobra Surrogate Trainer at Crow's Landing, California, in collaboration with the U.S. Army. The workload measures that have been developed and applied to this test include: inflight and retrospective pilot ratings, communications analysis, time estimation, heart rate, and heart rate variability.

(S. Hart, Ext. 6072)

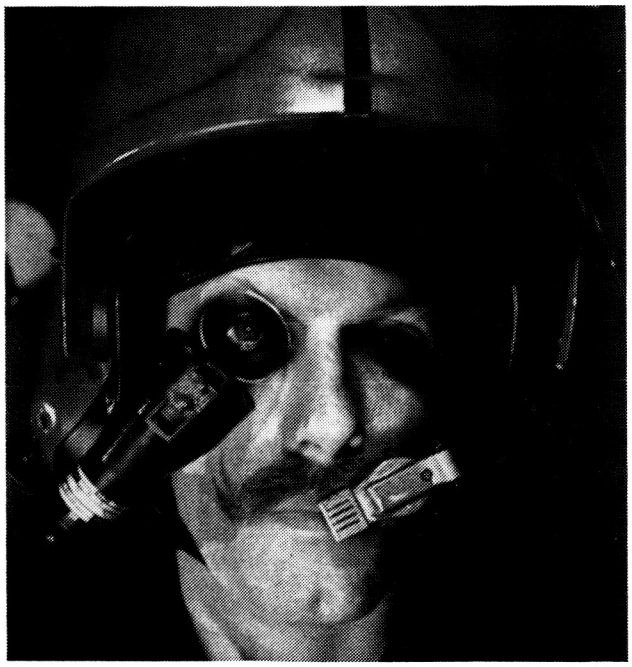

Hart

Workload assessment in operational settings

Intelligent Perspective Display Systems

Previous fundamental and applied research in spatial perception, manual control, and air traffic displays has provided background for current and future work concerning display concepts for proximity operation and teleoperations displays.

The following have been the major accomplishments of research on intelligent perspective display systems:

(a) A report has been published which describes the design and implementation of a perspective display intended to be used as a spatial instrument by commercial airline pilots. The design incorporates the opinion of airline pilots who served as expert consultants, and illustrates that such expert opinion may assist in the design of display systems.

(b) A report has been completed which describes how the major geometric parameters defining a perspective display influence a user's direction judgments while using it. The empirical results and theoretical models resulting from this and subsequent investigation will allow objective optimization of the design of spatial instruments using perspective displays.

(c) An experiment has been completed and a preliminary report has been written describing an experiment which confirmed a theoretical model of errors in direction judgments made by users of a perspective display.

(d) Several experiments have been conducted and preliminary reports have been completed describing users' abilities to perform three-dimensional tracking of a target which is presented on a perspective display. The empirical results of these studies and of the theoretical models derived from them will provide a basis for the design of perspective instruments for proximity operation and teleoperations displays.

Papers have been presented at the Rendezvous, a Proximity Operations Workshop at JSC, describing how perspective displays may be applied to rendezvous and proximity operations activities.

(S. Ellis, Ext. 6147)

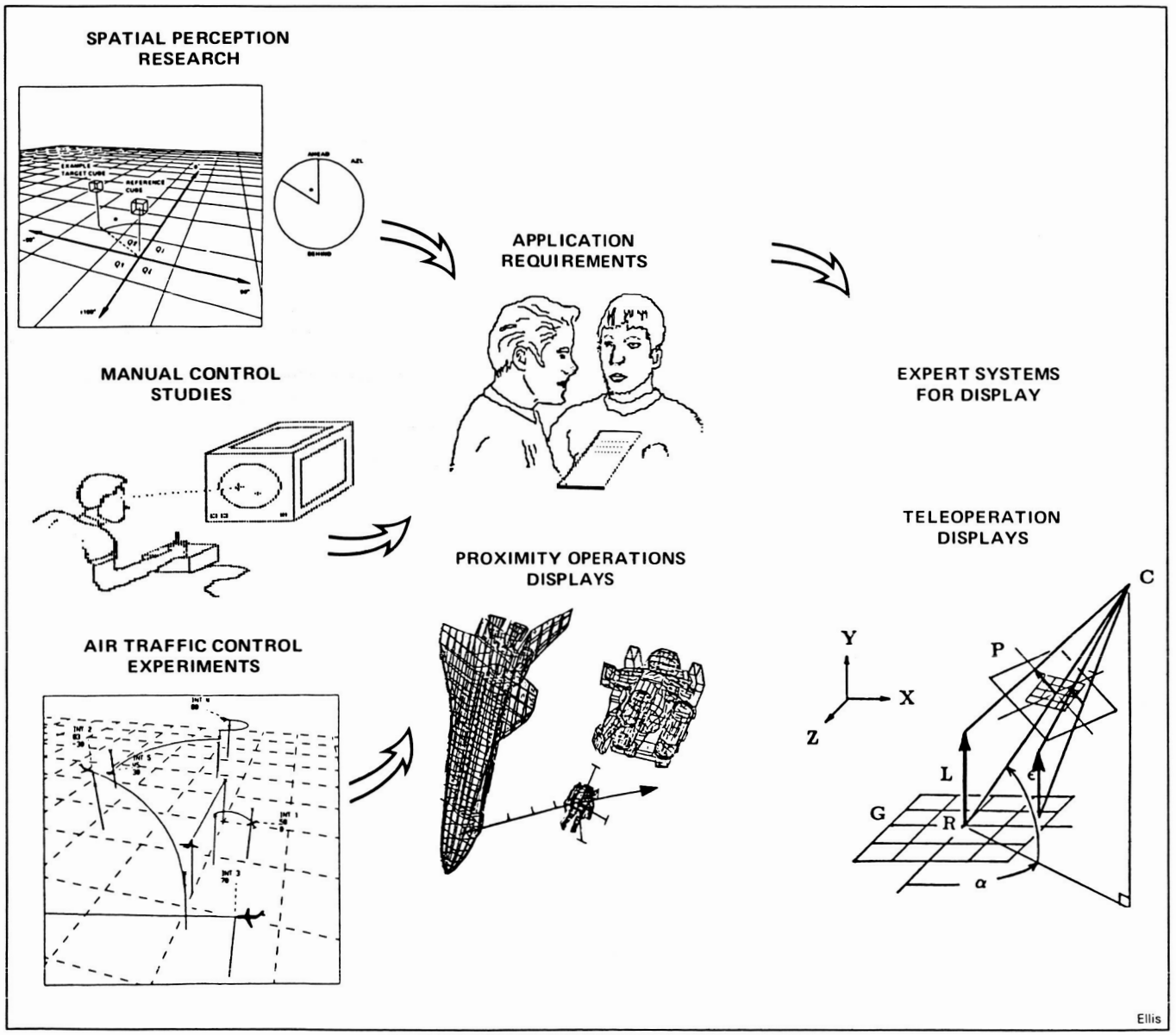

Intelligent perspective displays: enhanced situation awareness and control

Advanced Wide Field-of-View Stereo Displays

Over the past few years, interest in developing advanced helmet-mounted display systems has grown both within the DOD and for EVA use. For the most part, the systems thus far developed can be characterized by high cost and restricted performance relative to the human visual system. Wide field-of-view display systems capable of full- or near-full-field stereo offer several potential advantages over conventional display technologies. First, stereo provides an enhancement in the ability of the display to represent visual depth. Thus, a third spatial dimension becomes available within which to encode additional information; greater information flux is thus theoretically possible. Second, such a display provides a better spatial representation of three dimensional space. Here displays intended to provide such a representation for telerobotics, teleoperation, proximity operations and the like, may be expected to provide the operator with an improved display "presence."

At Ames, a low-cost, high-performance display system has been developed, largely with off-the-shelf components. The system provides a wide-field, full-stereo display capability that currently uses relatively low resolution LCD display elements. It has been integrated with a head tracking system and high-performance calligraphic display generator; the total system is thus capable of displaying images which are adjusted dynamically to point of regard.

(M. McGreevy and J. Humphries,
Ext. 6147/6433)

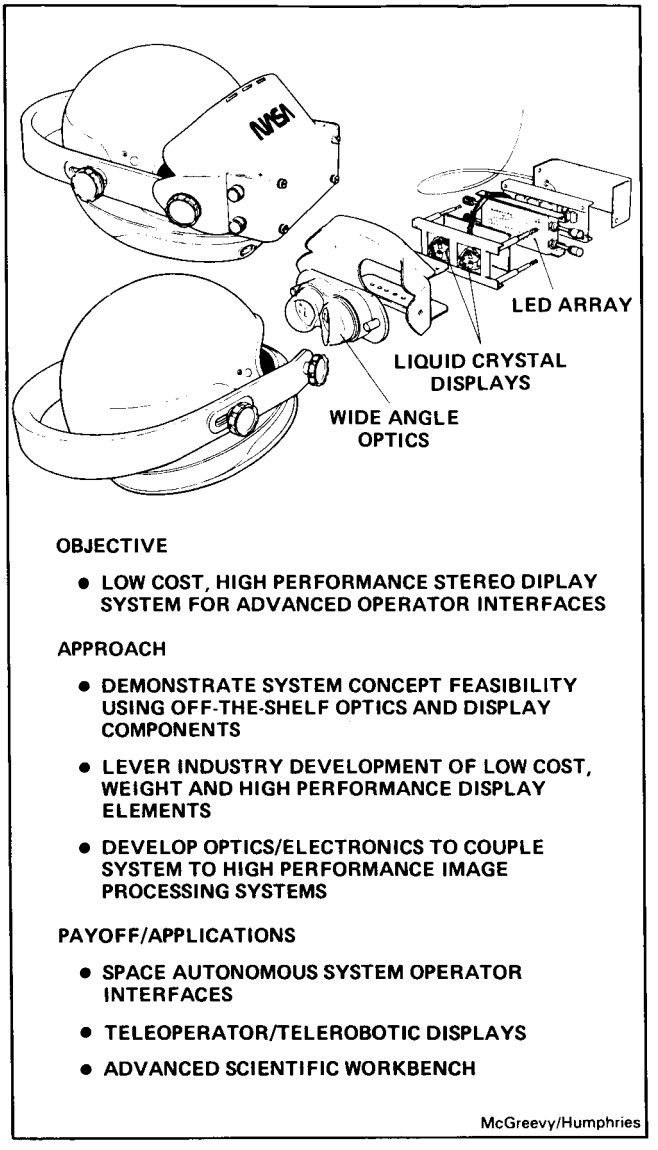

Virtual Visual Environment Display

Intelligent-Operator Aids: Operator Task Models

A discrete control model represents how an operator decomposes a complex system into simpler control tasks. The model contains states, and conditional transfers between states. It describes operator-knowledge representation, information-flow requirements, and decision making. The model is equivalent to a hierarchic/heterarchic network of finite-state machines.

The utility of the model is twofold. It can be used to understand operator decisions and actions through its representation of operator goals. Second, it can be used to design adaptive information displays which modify displayed information based on system state and operator goals. Currently, this modeling effort has been completed.

(E. Palmer, Ext. 6073)

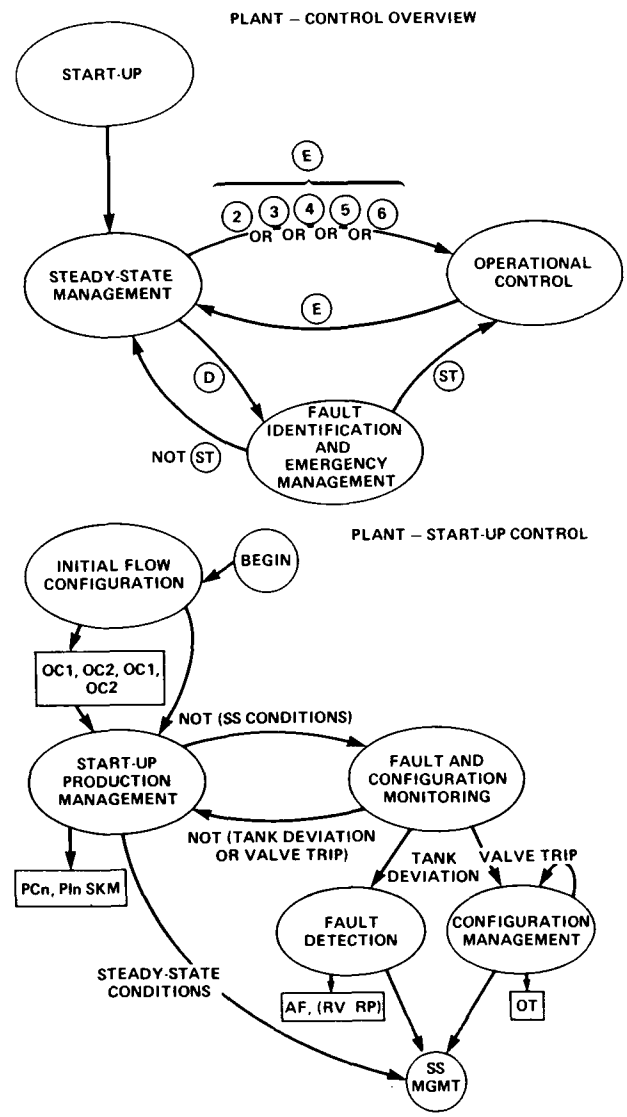

OBJECTIVE

- DEVELOP OPERATOR TASK MODELS FOR USE IN INTELLIGENT AIDS FOR SPACE SYSTEM OPERATORS

APPROACH

- TASK NETWORK MODEL ENCOMPASSING: TASK DECOMPOSITION; SYSTEM KNOWLEDGE; GOALS, PLANS AND ACTIONS; INFORMATION FLOW; DECISION MAKING
- APPLY MODEL TO GENERIC PROCESS CONTROL PLANT
- MODEL THE OPERATOR OF A SPACE SHUTTLE PAYLOAD (ORS)
- MODEL A SPACE SHUTTLE GROUND CONTROLLER (INCO)

APPLICATION/PAYOFF

- ADAPTIVE INFORMATION DISPLAY MANAGER
- OPERATOR ERROR TOLERANT SYSTEMS
- TASK AUTOMATION KERNELS

Palmer

Space automation: intelligent operator aids, operator task models

Intelligent-Operator Aids: An Expert System for the Orbital Refueling System

Expert systems, training, and checklists all share a common flaw: to diagnose an equipment failure, it must have been anticipated by the designer, and since designers cannot anticipate every failure, the operator will at times be faced with an unforeseen problem.

To assist the human faced with a novel failure, the following approach is proposed. First, the aiding program will contain an internal, qualitative model of the failed system. This model will allow the aid to reason about the system. Second, the aid will detect human decision-making biases that occur during fault diagnosis.

An example of such a bias is cognitive tunnel vision. In this bias, the operator stays with first hypothesis long after the data have refuted it. The solution is for the aid, through its internal

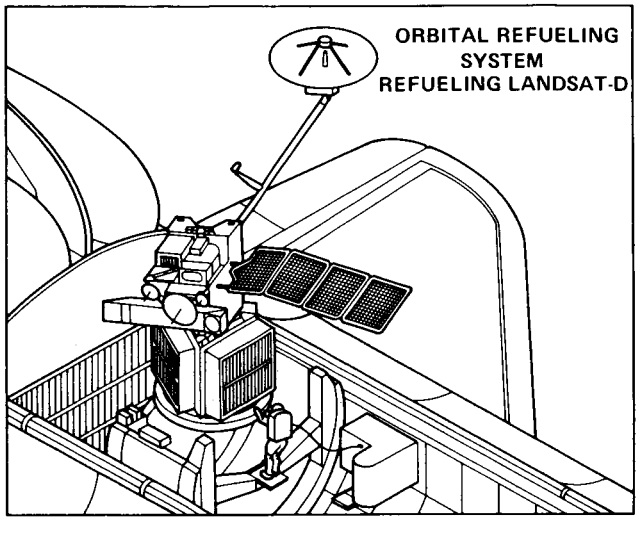

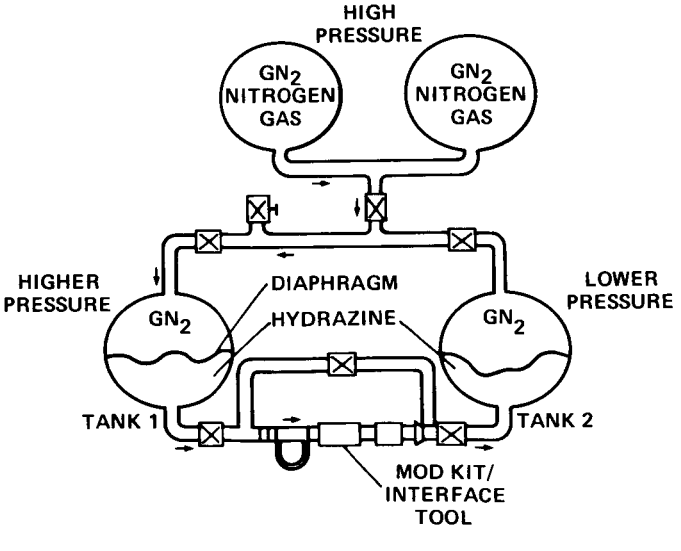

ORS SCHEMATIC

OBJECTIVE

- FAULT DIAGNOSIS AID FOR ORS OPERATORS
- EMPIRICAL METHODS FOR EVALUATING INTERACTIVE SYSTEM PERFORMANCE

FEATURES

- EXPLAINS REASONING
- DYNAMIC DATA SOURCE
- TOLERANCE FUNCTIONS – FUZZY LOGIC
- GRAPHIC INTERFACE
- BASED ON KNOWN MALFUNCTION PROCEDURES

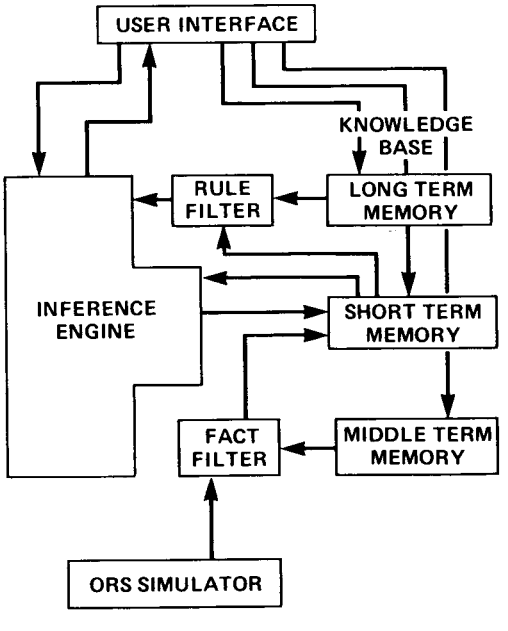

HUMAN ORBITAL REFUELING SYSTEM EXPERT SYSTEM

Palmer

Space automation: intelligent operator aids, HORSES: an expert system for the ORS

model, to detect that the hypothesis is invalid and that the information requested by the human is irrelevant. The aid can then suggest that the human try another hypothesis. It is believed that this approach should offer substantial improvements in human diagnosis of novel failures.

The orbital refueling system (ORS) on the Shuttle is being modeled. A qualitative model equation solver has been coded. Future plans are: the qualitative equations for the ORS must be entered to complete the model. An interface to the model must be created to allow the operator and the aid to test hypotheses about the equipment failure. Methods must be coded for detecting and compensating for human decision-making biases. Finally, the aid must be evaluated.

(E. Palmer, Ext. 6073)

Models of Color Constancy and Color Perception

Ambient lighting conditions affect our perceptions. The images on the left show the same set of objects which were photographed under two different ambient lighting conditions. The camera images are quite different because of the difference in the ambient light. The particular lights used in this demonstration were chosen to appear identical to the human eye, although they are physically different. (The ambient lights are metameric.)

Variations in the color of the ambient light occur frequently. As we pass from early morning sun to high noon, from cloudy days to sunny days, from natural light to artificial light, the color of the ambient lighting changes significantly. Film images record such changes, but we do not perceive large changes. Instead, the visual system performs an automatic correction (a neural adjustment) that compensates for the change in the color of the ambient light. In the middle picture an apparatus is shown with which the human ability to adjust for changing ambient light conditions is measured. As anyone who has tried to find his car in a parking lot illuminated by inexpensive sodium vapor lights knows, the ability to correct for changes in the ambient light is limited. In order to model human performance, we must first measure it.

Until recently, the human ability to correct for changes in the ambient light has been better than the ability of computer visions systems. This year, a new algorithm has been designed which — under noise-free circumstances — outperforms the

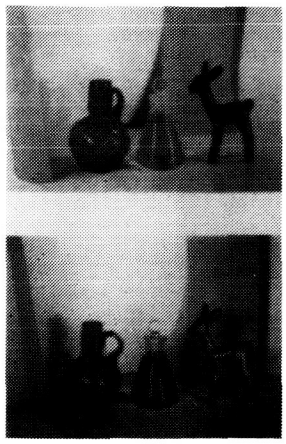

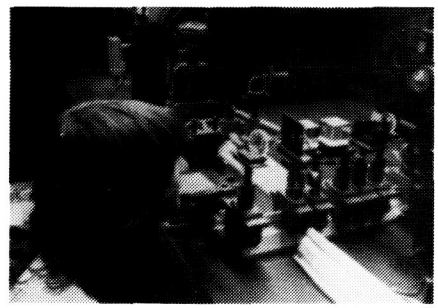

FAILURES OF COLOR CONSTANCY
- SAME OBJECTS, DIFFERENT ILLUMINANTS
- CAMERAS, SENSORS RECORD SURFACE COLORS AS DIFFERENT
- HUMANS CORRECT FOR COLOR DIFFERENCES OVER BROAD RANGE OF CONDITIONS

ACCOMPLISHMENTS
- NEW MEASURES OF HUMAN COLOR SENSITIVITY
- COMPUTATIONAL MODELS FOR COLOR APPEARANCE
- ALGORITHMS FOR MACHINE COLOR CORRECTION

APPLICATIONS
- USAGE STANDARDS FOR COLOR CODING IN DISPLAYS
- COLOR CORRECTION FOR REMOTE SENSING
- COLOR-BASED OBJECT RECOGNITION FOR MACHINE VISION SYSTEMS

Watson

Color perception experiments

human visual system. The algorithm has been implemented on a UNIX 4.2BSD machine using the C-programming language. Presently, ways are being studied for reducing the algorithm's performance to bring it into line with human performance. It is planned to use the adjusted version of instrumentation display.

The optimal algorithm has applications to several areas beyond human vision: first, the ability to accurately recognize surface reflectance independent of the ambient light should be helpful in processing remote sensing data in land survey research; and second, the ability to estimate surface reflectance is a useful tool in the development of machine-vision algorithms for inspection of parts.

(A. Watson, Ext. 6290)

NASA Fatigue and Jet-Lag Study: Short-Haul Crew Performance

Excessive flight-crew fatigue as a result of trip exposure has long been cited as a factor with potentially serious safety consequences. Various laboratory studies have implicated fatigue as a causal factor associated with varying levels of performance deterioration, depending on the amount of fatigue and the type of measure utilized in assessing performance. From an operational standpoint, these studies have been of limited use because of the difficulty of generalizing laboratory task performance to the demands associated with the operation of a complex multipilot aircraft. Moreover, there are few, if any, controlled experimental studies of operational performance as a function of fatigue.

This study examined the performance of 20 volunteer twin-jet transport crews in a full-mission simulator scenario that included all aspects of an actual line operation (see figure). The scenario included both routine flight operations and an unexpected mechanical abnormality which created a high level of crew workload. Half of the crews flew the simulation within two to three hours after completing a three-day, high-density, short-haul duty cycle (postduty condition). The other half of the crews flew the scenario after a minimum of three days off duty (preduty condition). The target trips in this study averaged eight hours of on-duty time per day and five takeoffs and landings, with at least one day (usually the last) averaging close to thirteen hours of duty and eight takeoffs and landings.

The results of this study revealed that, not surprisingly, postduty crews were significantly more fatigued than preduty crews. The former averaged

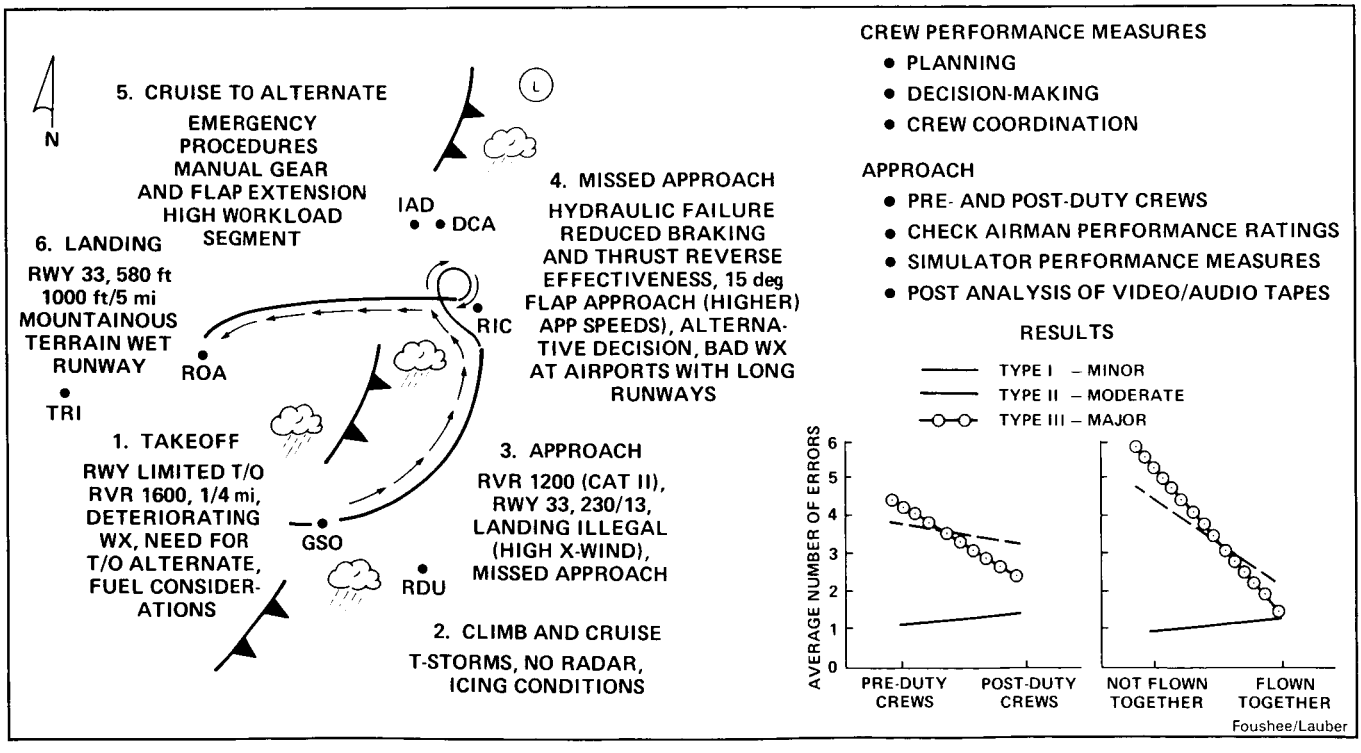

Simulation scenario for NASA fatigue and jetlag study

less sleep during the trip and reported higher levels of fatigue than the latter. However, a fascinating and somewhat counter-intuitive pattern of results emerged on the crew performance measures: in general, the performance of postduty crews was significantly better than the performance of preduty crews. Postduty crews were rated as performing better by an expert observer on a number of dimensions relevant to flight safety; they flew more stable approaches, and they made substantially fewer significant operational errors than did preduty crews. Analysis of the flightcrew communication patter revealed that postduty crews communicated significantly more overall, although preduty crews exhibited more nontask related communication, suggesting as in previous research, that communication is a good predictor of overall crew performance. Other analyses suggested that the primary cause of this pattern of results is the fact that crewmembers usually have more operating experience together at the end of a trip, and that this recent operating experience serves to facilitate crew coordination, which can be an effective countermeasure to the fatigue present at or near the end of duty cycle. These results have important aircrew training and aviation safety implications.

(H. Foushee and J. Lauber, Ext. 6114/5717)

Pilot Performance Factors in Short-Haul Flight Operations: A Field Study

In-flight field studies were designed to document the psychological and physiological impact of fatigue and circadian factors on crews flying domestic short-haul and international long-haul trips. In addition, efforts are being made to identify those individual factors and behaviors which may exacerbate or moderate such effects in order to develop countermeasure recommendations for the aviation community.

Miniaturized solid-state technology is used to continuously record participating pilot's heart rate, body temperature, and limb activity before, during, and after flying line trips. Trip selections are based on the number of flights per day, trip and layover length, unusual flight times, high-density airspace, multiple time-zone crossings, etc. The physiological record is supplemented with time-linked cockpit observer logs of operational events per flight segment. Individual factors are documented by combining background, personality, and lifestyle information with daily logbooks in which each pilot's sleep, activities, diet, and mood are recorded.

Short-haul data collection has been completed with two east coast carriers on 91 crewmembers on 46 trips (821 flights). Briefings on preliminary results have been presented to industry, pilot, and government (NASA, FAA, NTSB) representatives. The data analysis for final report is in progress. Long-haul data collection was initiated July 1985. The study will consist of four crews on each of six or seven representative trips in eastward, westward, and north-south directions. One eastward and three westward crews completed this part of the study with 100% volunteer participation by all crewmembers contacted. The anticipated completion of the data collection is about July 1986.

(J. Lauber, Ext. 5717)

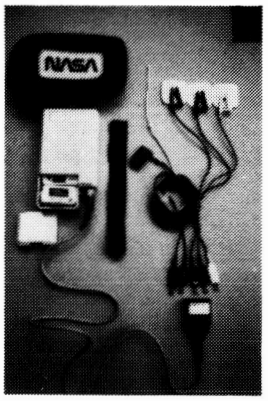

Pilot performance factors

Aircraft Automation: Field Studies and Guidelines

Automation and the wide-spread application of microprocessor technology to aircraft cockpits is proceeding at a rapid pace because of several technical, economic, and safety benefits offered by its use. However, experience thus far with highly automated man-machine systems suggests that these benefits are not achieved without significant cost, and may, under some circumstances, be unattainable. The purpose of the present field studies was to evaluate two recent approaches to flight-deck automation to determine desirable and undesirable features and characteristics thereof, and to gain insight into related issues, including training requirements, and factors determining flight-crew acceptance of advanced technology.

Studies were conducted during the early period of line operations of the McDonnell Douglas DC-9-80 (MD-80) and the B-767. The investigators attended ground school, observed line operations, administered questionnaires and rating scales, and interviewed pilots, check airmen, and instructors. A total of four airlines and their pilots participated in these studies. The results indicate widespread acceptance of the new cockpit technology by flight crews (although some specific design features are neither like nor used). Significant improvements in training in the operation of the advanced cockpit systems is possible, and in some cases, certain design features and operating characteristics of these systems are not being adequately conveyed to the operators or their pilots. Improvements are possible in the way operational modes of certain systems are displayed to the flight crew, and in displays which indicate the status of separate but related sys-

PILOT-MATCHED CDU MENU ORGANIZATION

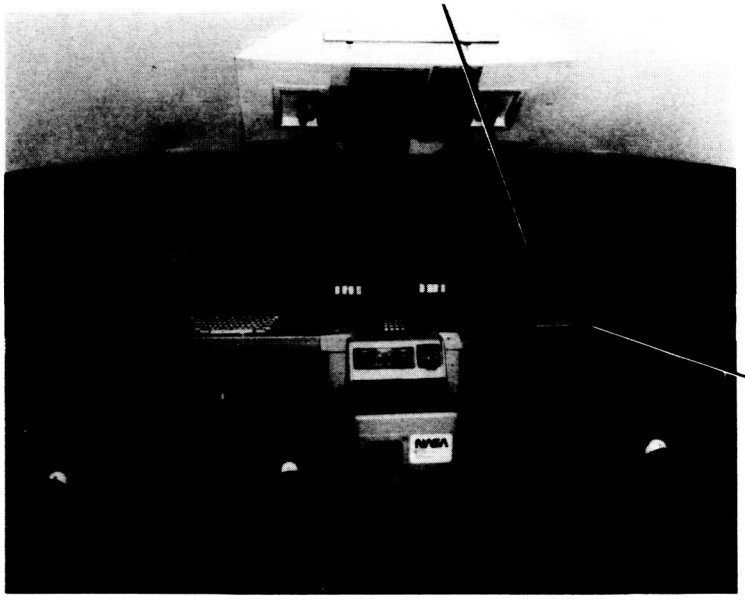

OBJECTIVE

- DEVELOP PRINCIPLES FOR MENU ORGANIZATION TO REDUCE SEARCH TIMES AND ENTRY ERRORS

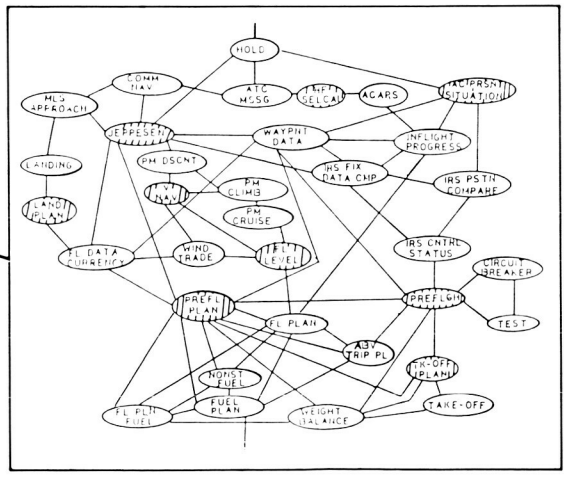

COGNITIVE NETWORK FOR PILOTS' CDU ORGANIZATION

APPROACH

- NASA/UNIVERSITY COLLABORATION
- MEASURE COGNITIVE ORGANIZATION/ REPRESENTATION OF CDU KNOWLEDGE FOR PILOTS USING COGNITIVE ENGINEERING TOOLS
- STRUCTURE CDU PAGE ORGANIZATION TO REFLECT PILOT ORGANIZATION
- COMPARATIVELY EVALUATE CDU USE IN MUSRF

Lauber

Intelligent cockpits: pilot-matched CDU menu organization

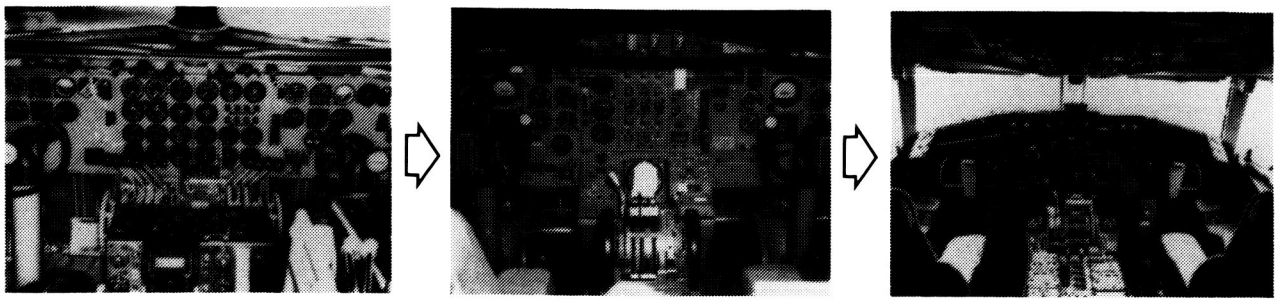

OBJECTIVES
- DETERMINE PILOT ACCEPTANCE OF NEW COCKPIT TECHNOLOGY
- IDENTIFY UNIQUE TRAINING REQUIREMENTS
- IDENTIFY DESIGN ISSUES AND GUIDELINES
- PROVIDE FEEDBACK TO OPERATORS AND MANUFACTURERS

APPROACH
- SURVEYS AND QUESTIONNAIRES
- INTERVIEWS
- COCKPIT OBSERVATION
- GROUND SCHOOL

OBSERVATIONS AND CONCLUSIONS
- PILOTS ENTHUSIASTIC ABOUT ADVANCED COCKPIT TECHNOLOGY
- POTENTIAL SKILL LOSS CAN BE AVERTED
- THERE ARE UNIQUE TRAINING REQUIREMENTS
- IMPROVED DESIGN GUIDELINES ARE SUGGESTED

Lauber

Field studies of flight crew transition to advanced technology cockpits

tems, especially autothrottles and the pitch channels of the autopilot. Certain design principles or guidelines are proposed in the reports of these studies.

Two other reports were completed during the reporting year and were published or are in press. Both of these review the development of aircraft automation, its effect or potential effects on reducing or changing pilot error, and suggest design philosophies for future automation systems to reduce the incidence or effects of pilot error.

(J. Lauber, Ext. 5717)

Advanced Space Suit Technology

Extravehicular activity (EVA) has been identified as a major element of space station operations. Historically, the role of EVA has been one of extreme conservatism, in that EVA was (and is) either planned as a short-duration activity or is used for contingency operations of minimal duration. The EVA hardware was subsequently designed to meet these requirements, but with the luxury of ample time between missions for refurbishment, resizing, and routine maintenance.

The current baseline (STS) EVA system will not meet the requirements of routine space station EVA operations. Due to the extensive number of EVA hours being projected for space station, issues that have not been of concern in the past will become drivers in the selection and development of technologies required to meet routine space station EVA requirements.

The Ames Research Center has an ongoing development program to address EVA suit technology issues for a space station. The program emphasis is being placed on technology areas that provide: no prebreathing requirement; improved suit and glove performance; increased hardware and system life; hazard protection (radiation, mechanical); minimal maintenance; quick change-sizing capability; and reduced manufacturing and operations costs. These technologies will be demonstrated, tested and evaluated in a fully functional space suit configuration (Ames AX-5 Hard Space Suit Demonstrator). This suit is being designed to operate at one atmosphere internal pressure. Completion of two suits is projected for November 1985.

(H. Vykukal, Ext. 5386)

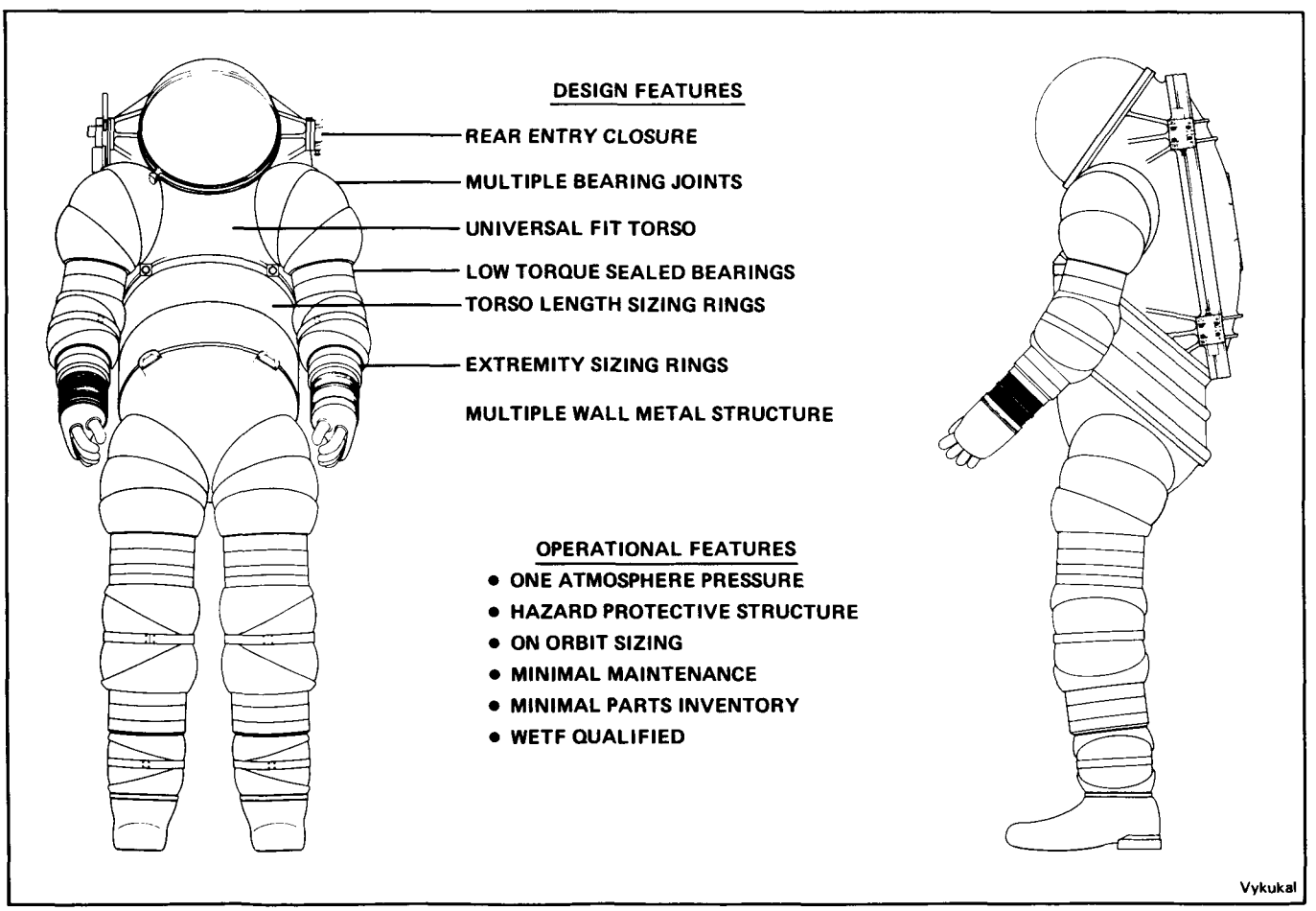

Ames AX-5 hard space suit

Effects of High-Order Dynamics on Helicopter Flight Control System Bandwidth

The increasing use of highly augmented digital flight-control systems in modern military helicopters has prompted an examination of the influence of rotor dynamics and other higher-order dynamics (such as sensor filters, servo actuators, and on-board computational delays) on control-system performance. A study has been conducted at Ames Research Center to correlate theoretical predictions of feedback-gain limits in the roll axis with experimental test data obtained from the variable stability CH-47B helicopter. Feedback gains, the break frequency of the presampling sensor filter, and the computational frame time of the flight computer on board the CH-47B were systematically varied. The results, which showed excellent theoretical and experimental correlation, indicate that the rotor dynamics, sensor filter, and digital-data processing delays can severely limit the usable value of the roll-rate and roll-attitude feedback gains.

(R. Chen, Ext. 5008)

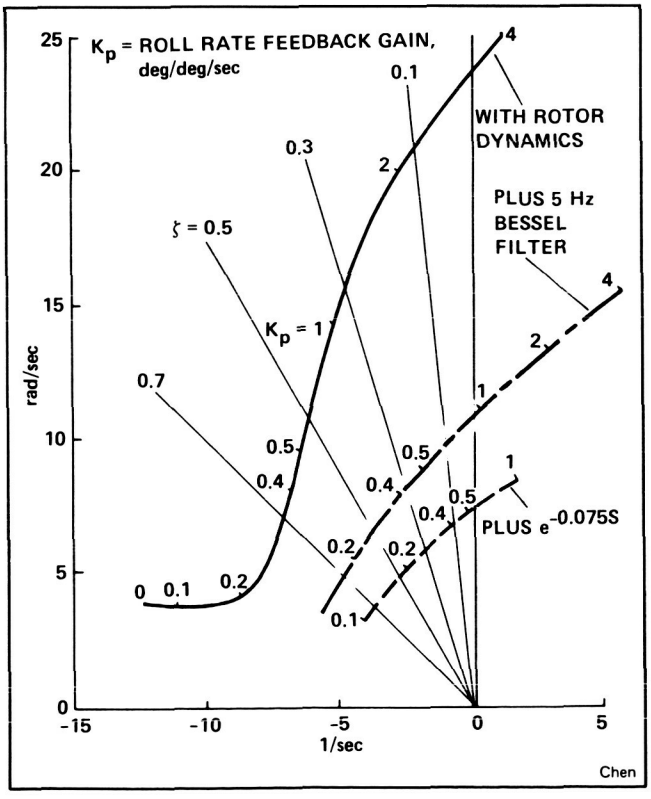

Predicted roll oscillation for the variable stability CH-47B

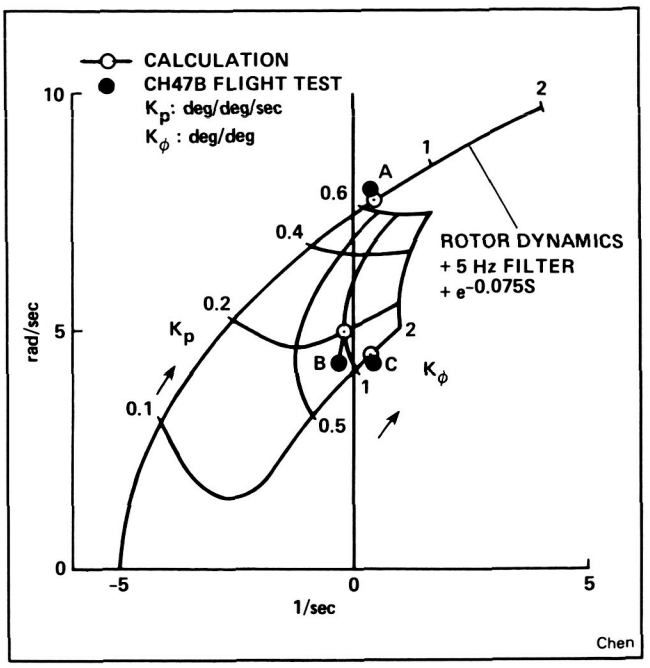

Analytical prediction

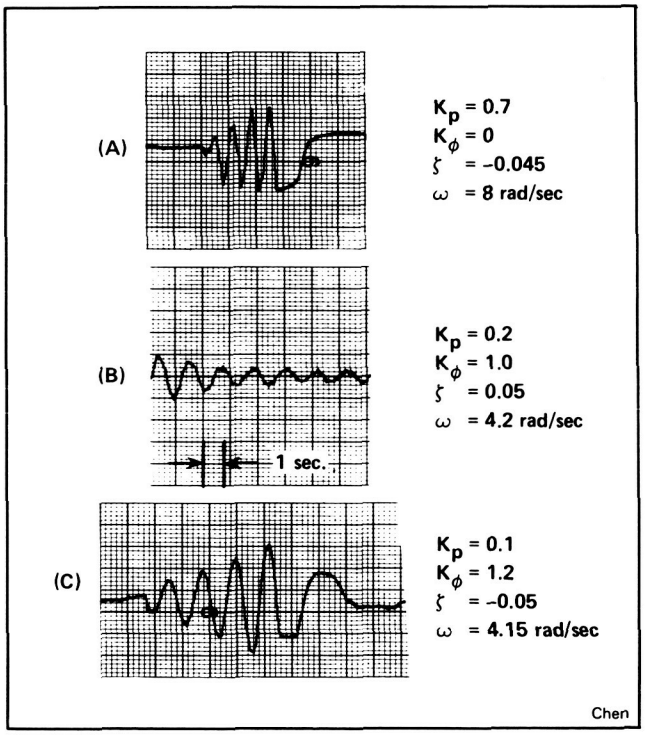

CH-47B flight test results

Dual-Lift Control System

The system to be controlled consists of two helicopters carrying a load suspended on cables separated by a spreader bar. Such a system has been considered periodically since the initial success of single helicopter slung-load operations, but has yet to be developed. A significant obstacle has been the complexity and workload of the system coordination and control task. Current digital flight-control systems and new Ames-developed methodology for the design of automatic flight control laws for nonlinear systems now offer a basis for the control of the dual-lift system.

The steady-state characteristics of the dual-lift configuration at any static equilibrium or maneuvering flight condition have been studied and results have been obtained for: (a) the suspension-system geometry and forces; (b) the thrust vector requirements for any helicopter pair; (c) load-sharing ratio; and (d) formation angle relative to the groundtrack. It is found that the tether angles can be selected for minimum thrust, the spreader bar tilt-controls load sharing, and the variation in system geometry with maneuvering depends strongly on the selected formation angle. These results provide a basis for coordinating the helicopters in automatic or manual control along any reference trajectory.

Linearized equations of motion, system simulation, and analysis of the natural modes, parameter effects, and stabilization and control are under study under a grant to Princeton University. Results for 2-dimensional motion near hover have been reported at the annual AHS meeting, and are being extended to 3-dimensional motion. A nonlinear dynamic model is also under development from D'Alembert's principle and aided by the MACSYMA symbol manipulation software.

(L. Cicolani and G. Kanning, Ext. 5446/6037)

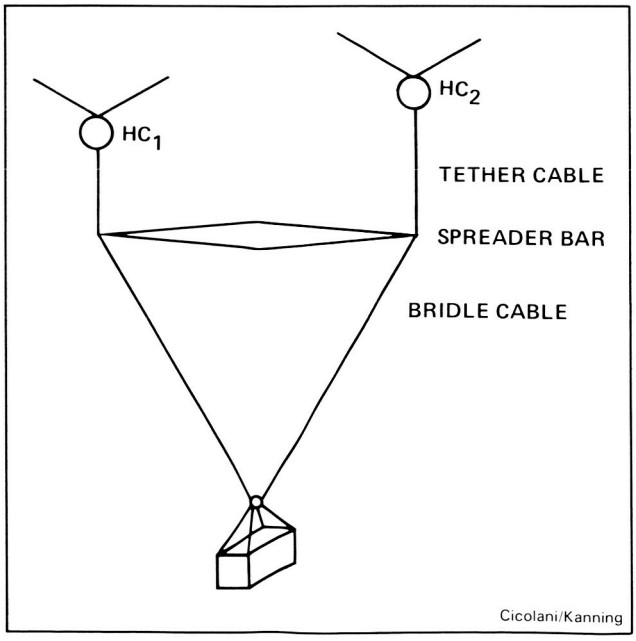

Dual-lift helicopter system

Helicopter Engine-Out Studies

A basic helicopter emergency maneuver involves an autorotation; however, autorotations are involved in a significant portion of all helicopter accidents. A primary objective of the helicopter engine-out study is to determine if significant safety improvements are possible owing to control technique or equipment changes. The high accident rate during practice autorotations emphasizes the desire of both military and civilian operators to conduct autorotation training in ground-based simulators. A second objective of this study is to determine the simulator elements necessary for autorotation simulation. Information gained from this objective will feed into the FAA program developing helicopter simulator certification criteria.

The first autorotation simulation experiment was conducted on the NASA/Ames Vertical Motion Simulator in January 1984. This experiment investigated the influence of rotor and control-system variations on autorotation landing success. The experiment successfully identified

Decker

An airfield scene with gray-hatched landing zone, human scaling (vehicles) and height-reference pylons

those factors influencing the definition of the height-velocity restriction curve. The reproduction of rotor inertia effects expected from flight results confirmed the usefulness of the simulator for autorotation research.

A second simulation experiment was conducted on the VMS in June-July 1985. Systematic variation of motion cues showed degraded collective-control technique during the landing flare with reduced motion. Visual scene variations showed that the acceptable pilot performance was possible with careful selection of scene content, but pilot perception of height above ground was very difficult with a computer-generated scene. Simulation of the helicopter sound model was important to the autorotation task where the pilot attention is concentrated external to the cockpit. A head-up display of aircraft situation, including rotor rpm, was usable during the approach, but could be a distraction during the landing flare.

(W. Decker, Ext. 5362)

The YAV-8B and VTOL Research Aircraft

Ames Research Center is conducting a flight research program using the unique YAV-8B Harrier aircraft. This program is aimed primarily at verifying the results of many years of piloted simulation directed toward extending the capabilities of this class of aircraft to include flight operations aboard small ships in adverse weather.

Additional objectives of the YAV-8B program are to improve our understanding of aerodynamic and propulsion interaction and to investigate possible benefits from integrating the propulsion and aircraft controls. Currently, VTOL aircraft operate in less severe weather and visibility conditions than do conventional fixed-wing aircraft. V/STOL aircraft are currently limited to operation with visibility greater than 1 n. m. visibility and 300 ft ceiling and sea states less than 2-3. The key to improved operational capability lies in improved control systems and pilot displays. Advanced control systems envisioned for the aircraft have been evaluated using flight simulators and have received preliminary acceptance. These advanced control systems and displays are expected to provide operations with zero visibility and zero ceiling in sea states as great as 6.

(J. Foster and V. Merrick, Ext. 5453/6194)

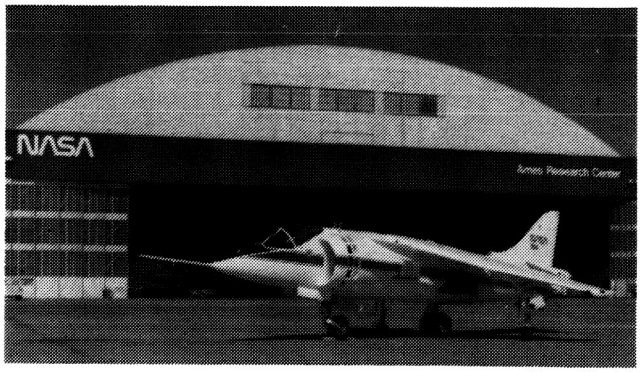

Foster/Merrick

NASA V/STOL flight research program aircraft

Development of Model-Following Control System Concepts for Rotorcraft

A new explicit, model-following control system for advanced rotorcraft has been developed, and implemented on two fly-by-wire helicopters (NASA's CH-47B variable-stability helicopter, and the German DFVLR's BO-105 helicopter), and evaluated in a series of flight-test experiments. A model-following control system consists of two dynamic systems: the "plant" and the "model." The objective of this control technique is to develop control laws that enable the plant to follow the model whose equations of motion represent the desired (or ideal) dynamical behavior for the vehicle. The advantage of using a model-following control system on a fly-by-wire helicopter is that the characteristics of the model to be followed can be varied in flight quickly and easily depending on the desired application.

The development of high bandwidth model-following control systems for helicopters is a challenging and difficult task because of the high degree of nonlinearities, aerodynamic and control cross-couplings, and vibrations associated with rotorcraft. The system that has been developed (in a joint research program with the German DFVLR Institute for Flight Mechanics) attempts to decouple the motions of the basic helicopter, and to systematically deal with "real-world" problems such as actuator rate and position limits, rotor dynamics, and time delays. The design methodology was initially validated in a series of ground simulation experiments for the UH-1H, BO-105, and CH-47 helicopters.

The results of the initial flight-validation tests on the CH-47 and BO-105 research helicopters are very encouraging. Excellent model-following performance in all four axes has been achieved in

hover on the CH-47. Presented in the figure is actual CH-47 flight-test data showing the response of the augmented CH-47 to a step input in the pilot's lateral cyclic stick. The CH-47 is able to follow the desired model with less than 0.5 degree of error in roll angle. Further analytical and computer simulation studies are currently being performed to guide in the understanding and improvement of the model-following control system. In addition, existing helicopter model-following control systems are being analysed and compared with this new approach.

(K. Hilbert, Ext. 5272)

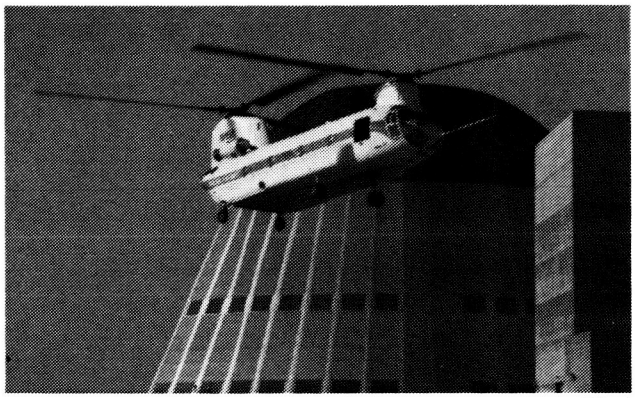

Hilbert

NASA/Army CH-47B helicopter

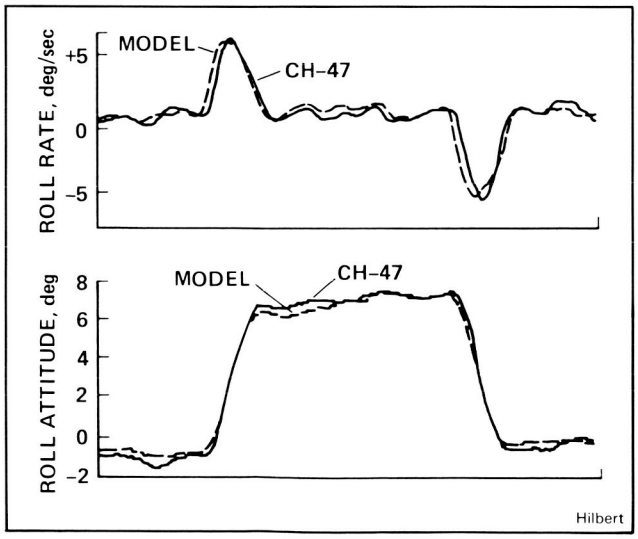

Roll axis response to the 1-inch cyclic stick in hover

Helicopter Air Combat II (HAC II) Simulation

A major simulation to further probe the handling qualities and flight characteristics required for helicopter air-to-air combat was conducted. The Vertical Motion Simulator (VMS) system at Ames, the only facility capable of conducting the low-level air combat research, was used to investigate this important new role for Army rotorcraft.

Experimental variables for this test were the maneuver envelope size (load factor and sideslip), directional axis handling qualities, and control response type. Over 450 simulated engagements were conducted with personnel from the Army, NASA, and industry serving as evaluation pilots.

Preliminary results from the experiment show a relatively highly damped directional response, low sideforce owing to sideslip, and some effective dihedral which are all desirable. The rate-command system was favored over the attitude type pitch-and-roll responses for most applications, and an enhanced maneuver envelope size over current generation aircraft is advantageous. Pilot technique, background, and experience all play a role in adaptability and success in the air-combat task.

These simulation studies provide a more thorough understanding of the requirements of the air-combat task on rotorcraft and will allow the development of systems and standards to enhance their performance. The MIL-H-8501 and LHX design criteria will be influenced by these experiments, and further work is planned.

(M. Lewis, Ext. 6115)

Lewis

Cockpit view — Air Combat II simulation

Quiet Short Haul Research Aircraft

Flight experiments were conducted with Ames Research Center's Quiet Short-Haul Research Aircraft (QSRA) to evaluate the influence of highly augmented control modes and electronic displays on the ability of pilots to execute precision instrument flight operations in the terminal area, particularly approaches to and landings on a short runway.

The aircraft used is a powered-lift, short-takeoff and landing configuration that is equipped with a modern digital fly-by-wire flight-control system, a head-up display, and a color head-down display that make it possible to investigate control concepts and display format and content for full envelope, powered-lift operations. Considerable attention has been devoted in this flight program to assessing flightpath and airspeed command and stabilization modes developed using nonlinear, inverse model-following methods. Flightpath-oriented display presentations that provide status and command information in a format with minimal clutter were also investigated.

The pilot can fly the aircraft with the precision associated with flight-director guidance and with a high degree of situation awareness. The primary benefits of these control and display concepts were realized when the pilot was required to execute a complex transition and approach under instrument conditions and in the presence of a wide range of wind and turbulence conditions. These concepts and their design criteria have been defined to the point that they are ready for applications in aircraft design when warranted by mission requirements or complex control configurations.

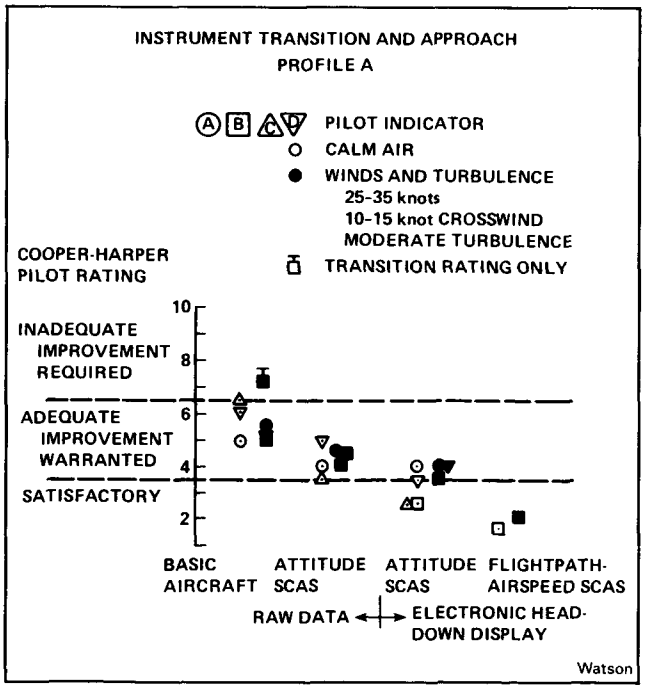

QSRA flying qualities evaluation

(D. Watson, Ext. 5826)

Space Shuttle Simulations — 1985

Twice in 1985 the Space Shuttle program used the Vertical Motion Simulator (VMS) in support of enhancements to the orbiter. Each project was primarily concerned with the behavior of the orbiter vehicle on touchdown and rollout.

Difficulties have been experienced with braking and nose-wheel steering on the vehicle on recent flights. Modifications to the braking system were proposed, but before installation on the vehicle an evaluation using the extensive motion and visual capabilities of the VMS was considered necessary. The first series of tests were conducted in February 1985.

Based on the results of various configurations of brake-pedal-spring forces installed in the VMS Shuttle cab, a final system was selected for installation on the Shuttle Orbiter.

For the evaluation, 10 brake-spring configurations were developed and installed in the VMS Shuttle cab; the simulation landing-gear model was improved and verified; various runway scenes were provided on the computer generated out-the-window visual display; different wind and turbulence conditions were imposed on the aircraft; runway conditions were varied, including the slope and crown. Finally, failures of nose and main wheel tires were simulated at various stages of rollout. In all, more than 1,000 motion flights were made to evaluate the proposed options.

The second simulation, run in July/August 1985, concentrated on evaluating nose-wheel steering-control system modifications. In the past, steering on rollout has been accomplished using asymmetrical braking. This technique has limitations during adverse conditions such as crosswinds. An initial engineering session verified the nose-wheel control-law configuration which was then evaluated by five astronauts to obtain a final design. A training session was then conducted to familiarize as many astronauts as possi-

ble with the new configuration. In all, more than 2,500 flights were made during the total simulation session, including 1,500 motion runs. Thirty-five astronauts took part in the session. The modifications decided on during this simulation will be installed and flown on a Shuttle flight before the end of 1985.

The VMS is utilized for these types of studies because of its unique motion capabilities, advanced visual system, and its flexible "engineering" configuration which allows many options to be installed and evaluated in a short period of time. It has contributed significantly to the Space Shuttle program.

(D. Astill, Ext. 6171)

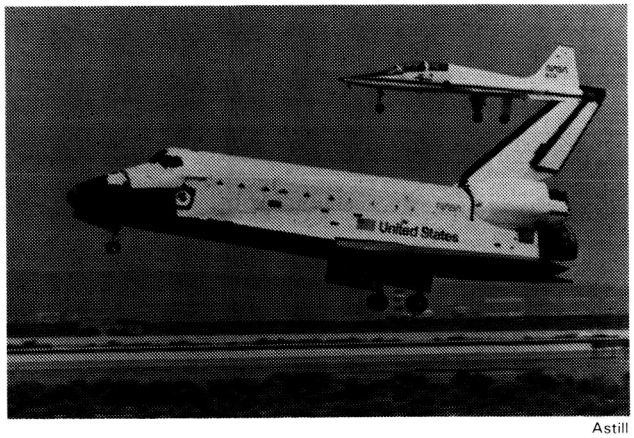

Astill

Space Shuttle landing accompanied by chase plane

V-22 Simulation on the NASA Ames Vertical Motion Simulator

The Navy and Bell-Boeing conducted a series of three piloted simulations of the Osprey (formerly JVX) on the Vertical Motion Simulator (VMS) at NASA Ames.

The benefits derived from these simulations are: (1) establishment of the effects of design characteristics and identification of areas requiring improvement at the early design phase; (2) confirmation of predicted handling qualities; (3) development of the Primary Flight Control System (PFCS) and Automatic Flight Control System (AFCS); and (4) pilot input to the design process by first-hand experience of the aircraft flight characteristics.

These simulations allowed a general and specific handling-qualities evaluation of the V-22 aircraft concept for selected points within the flight envelope with all operable flight-control modes. A result of these evaluations was the aircraft being judged to have Level 1 handling qualities with the AFCS operating, and Level 2 with only the PFCS operating.

The major control-law concepts evaluated during these simulations were the model-following approach in the AFCS, and the forward loop shaping in the PFCS. The approach for the AFCS was extensively modified to incorporate attitude and rate command, and stabilization. The forward-loop shaping was found to be desirable in the PFCS. The shape and levels of control author-

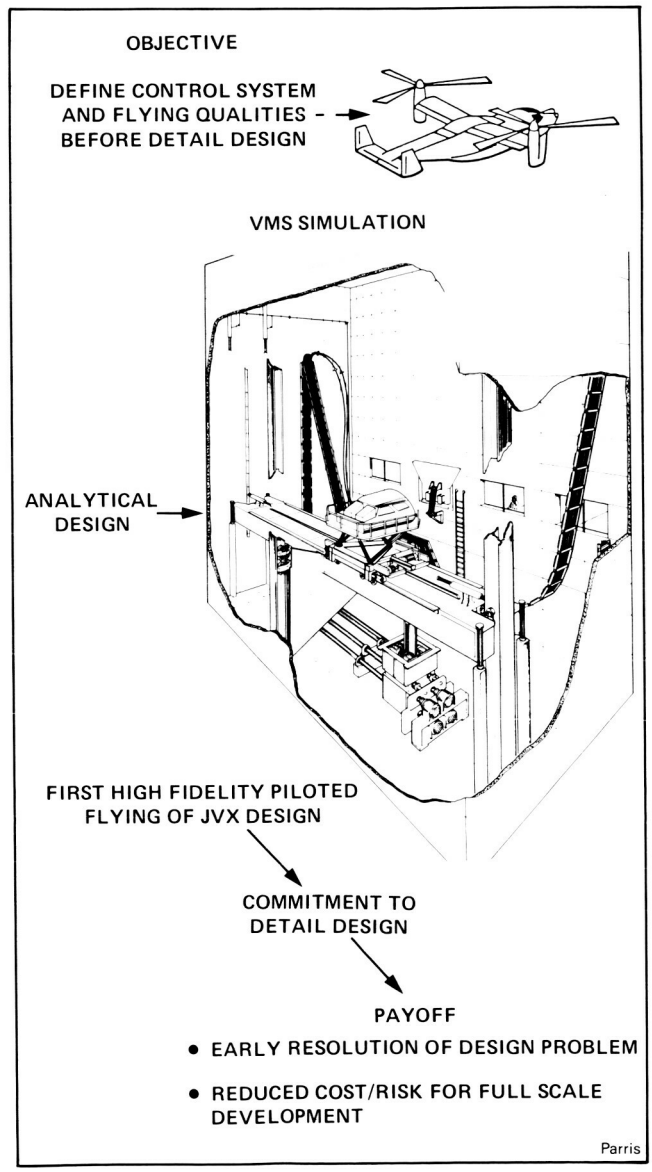

V-22 (JVX) simulation on NASA Ames VMS

ity for phasing from helicopter to airplane mode were examined in depth. Improvements were also achieved in the Thrust/Power Management System, Auto Flap control, Auto RPM control, and the Lateral Translation Mode control.

Some of the design problems that surfaced were an undesirable pitch/power coupling, a consistent over-torque of the transmission for the higher gross weights, adverse effects of the intentional roll-and-pitch coupling to the vertical AFCS, and an undesirable short period mode in pitch.

The main benefit of conducting these simulations was the early isolation of design problems and errors. This significantly reduced risk and cost of the overall design and development effort.

(B. Parris, Ext. 6171)

X-Band Portable Precision Approach Concept

A beacon landing system (BLS) based on a novel, X-band, precision approach concept has been developed and flight tested as a part of NASA's Rotorcraft All-Weather Operations Research Program. In conjunction with this program, NASA has been working with the Airbase Survivability Group at Eglin Air Force Base to apply the BLS technology in the development and flight test of a portable tactical approach-guidance system (PTAG). The systems are based on state-of-the-art X-band radar technology and digital processing techniques. The BLS and PTAG airborne hardware consists of an X-band receiver and a small microprocessor, installed in conjunction with the aircraft instrument landing system (ILS) receiver. The microprocessor analyzes the X-band, BLS or PTAG pulses and outputs ILS-compatible localizer and glide slope signals. The BLS ground station combines both localizer and glide slope into a single inexpensive, portable unit; it weighs less than 70 lb and can be quickly deployed in less than 10 min at a landing site. PTAG has separate ground stations for localizer and glide slope which allows for a more conventional ILS-type split-site installation. The PTAG ground stations each weigh less than 85 lb. Results from the flight-test program show that the BLS has a significant potential for providing rotorcraft with low-cost, precision instrument-approach capability in remote areas. Approach cross-track errors were shown to be comparable to those achieved on MLS approaches. PTAG has also shown great promise for use in a battle-damaged-airfield mission scenario and as a complement to the Tactical MLS for both fixed-wing and rotorcraft operations. In addition, both Military Airlift Command (MAC) and Communications Command within the Air Force have shown a great amount of interest in PTAG.

(T. Davis, Ext. 5452)

Davis

Helicopter on final approach to Beacon Landing System ground station

Digital Flight Control System Verification Laboratory (DFCSVL)

The DFCSVL, developed under a joint NASA/FAA program, is being used to assess specific verification techniques at the software and system levels of DFCS. Current investigations are focused on the development and assessment of software tools, including assertions and stress testing, for flight software verification and hardware fault insertion as a key step in systems-level testing.

During 1985 in-house research, augmented by the Boeing Commercial Airplane Company, has been investigating the effectiveness of a sample set of software verification tools accessed through the environment of the DFCSVL. Preliminary findings indicate that to achieve maximum effectiveness, software verification tools for a high-level language must be designed coincident with the compiler in order to achieve a similar level of

maturity in the syntax and constructs of the target language. It was also found that an environment which is tailored to the needs of a flight controls engineer is important to the effective use of those tools. Research activities will now focus on more actual testing of those tools showing the greatest potential in the verification environment.

University-based research at Stanford has resulted in the development of a specification language, DIVERS, to describe generic flight software functions. During the next phase of research, DIVERS will be used to automatically generate the alternate flight software necessary for the comparison of outputs during dynamic software testing, a fundamental feature of the previously developed stress testing technique. Stanford also found that the use of executable assertions are effective in testing flight software. Recent findings showed that a minimum set of assertions could detect a maximum of errors, especially if variables are asserted which offer the greatest collateral testing.

Current systems level verification research has included FAA sponsored activities with Lockheed-Georgia Company aimed at the verification of advanced DFCS redundancy levels. Reliability estimation, failure effects analysis, and system simulator methods were combined into an integrated approach. The next phase will investigate the role of hardware fault insertion combined with an instrumented simulation environment for system level testing.

(D. Doane and J. Saito, Ext. 5048)

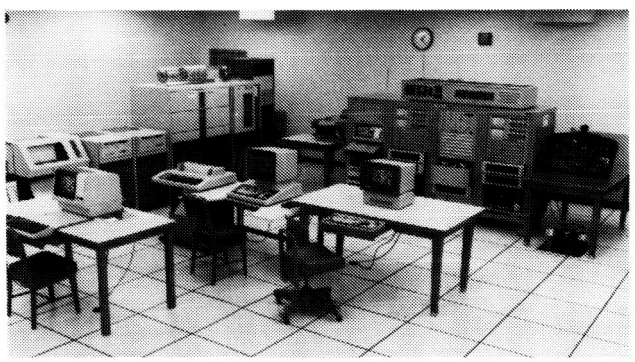

Doane/Saito

Verification laboratory

Helicopter Satellite-Based Guidance Differential Global Positioning System (GPS)

The NASA Ames Research Center is conducting a research program to evaluate the use of the conventional NAVSTAR Global Positioning System (GPS) and differential GPS (DGPS) to support civil helicopter precision approach and landing guidance. For the conventional system, a single channel GPS navigator has been installed in a NASA helicopter and is being evaluated for several types of missions. Flight tests have shown that even with poor satellite geometry, the system provides navigation accuracies much better than any other navigation system currently available. Results of these tests and other limited flight tests reaffirmed that the position accuracies of a single channel sequential GPS navigator are sufficient to support area navigation and nonprecision approaches, but are not sufficient to meet the requirements for a precision approach.

For the differential system, NASA-sponsored analytical studies have shown that differential GPS (DGPS) can provide significant improvement when compared to conventional GPS. Lateral performance appears adequate to support precision approaches. Vertical axis performance is also considerably improved but requires some further enhancement. Additional studies are under way to investigate alternative techniques to improve the vertical axis performance of differential GPS.

One of three candidate differential GPS concepts will be evaluated at Ames. The concept requires both an airborne and a ground-based component. The airborne research system has been developed in-house and is being installed in a NASA SH-3G helicopter. The system is built around a PDP-11/34m digital computer, uses a GPS Z-Set as the airborne navigation receiver, and a telemetry receiver to acquire the uplinked differential corrections. The ground-based component of the differential system is being developed under contract by Ohio University. This system will be installed in a mobil van and delivered to Ames during the fall of 1985. Flight evaluation of the concept is scheduled for the following winter and spring.

Nonreal-time differential flight tests were conducted during the late spring (1984) using the partially completed airborne system and a leased ground reference receiver. Analysis of these data confirmed the results of the analytical studies for typical satellite geometries and showed significantly better performance than expected under conditions of poor satellite geometry. Test results also indicate that because of the slow variation of the ground computed differential corrections, differential update corrections as low as once per minute are acceptable.

(F. Edwards, Ext. 5437)

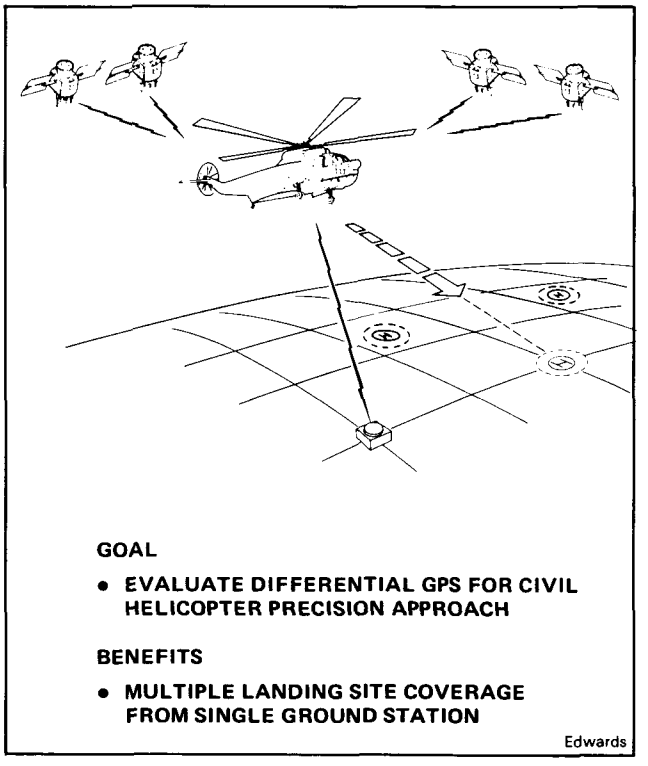

Satellite-based guidance differential GPS terminal experiments

Air Traffic Control Automation

A concept for automating terminal area traffic management based on time control of both 4-D equipped and conventionally equipped aircraft is being investigated in piloted and air traffic control simulations at Ames Research Center. The objective of this work is to increase airport landing rates, improve fuel efficiency, and reduce delays through greater automation of the air traffic control process. This work is done under a cooperative program with the FAA.

A major issue affecting the feasibility of the concept is the requirement to achieve accurate time control of conventionally equipped aircraft. The Ames 727 Full Mission Simulator was used to evaluate the effectiveness of a four-dimensional descent advisor for predicting and controlling descent times of conventionally equipped aircraft. The advisor is a ground-computer based algorithm that includes accurate models of airline descent procedures, aircraft performance, and wind profiles. Advisories specify the top-of-descent point and the descent speed profile and are issued to the pilot by an air traffic controller at approximately 120 n. m. from touchdown.

The piloted simulations flown with the advisories showed a striking reduction in descent time variability as well as fuel consumption when compared to those flown without them. The time variability of the descents without the advisories was an unacceptable 200 sec at 30 n. m. from touchdown. With the advisories, the time variability was reduced to less than 30 sec at that point. Airline pilots participating in the simulation also reacted favorably toward the concept. The high time accuracy demonstrated in the simulation removes a critical obstacle in the path toward implementing a time-based traffic-management system in the near future. On the basis of these favorable results, NASA and FAA plan to evaluate the descent advisor concept under live traffic conditions at an Enroute Air Traffic Control Facility.

(H. Erzberger and L. Tobias, Ext. 5425/5451)

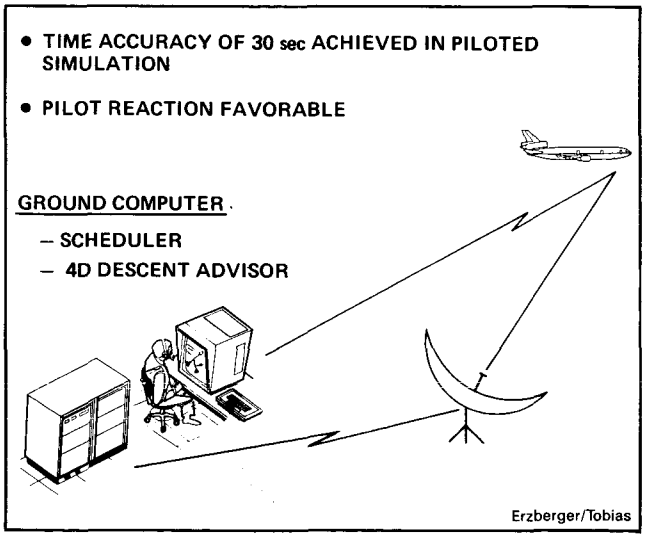

Ground-based four-dimensional descent advisor

Automated Low-Altitude/NOE Rotorcraft Flight

Automated Low-Altitude/Nap-of-the-Earth rotorcraft flight has been identified as a major technology void by both military and civil agencies. Technical advances in this area would significantly reduce rotorcraft impacts with terrain and obstacles (such as wires). Terrain Following/Terrain Avoidance Nap-of-the-Earth (TF/TA/NOE) technology is also needed for the military's new single pilot scout/attack helicopter.

The near-term objective of this research is to develop TF/TA guidance and to apply expert systems with heuristic reasoning to flightpath management concepts for automated NOE flight with the long-term objective of simulation/flight demonstrations of automated NOE flight.

A joint NASA/AIR FORCE/IBM simulation has been completed to investigate the control/display requirements for terrain following using flight-director guidance superimposed on forward looking infrared (FLIR) imagery. The tests were conducted on the Vertical Motion Simulator using both NASA and Air Force pilots. Results showed that the guidance algorithms are effective and that the integration of the command symbology and attitude information with a limited field-of-view FLIR image requires a nonconformal superposition. These results are being incorporated in the Air Force HH-60D Night Hawk display definition.

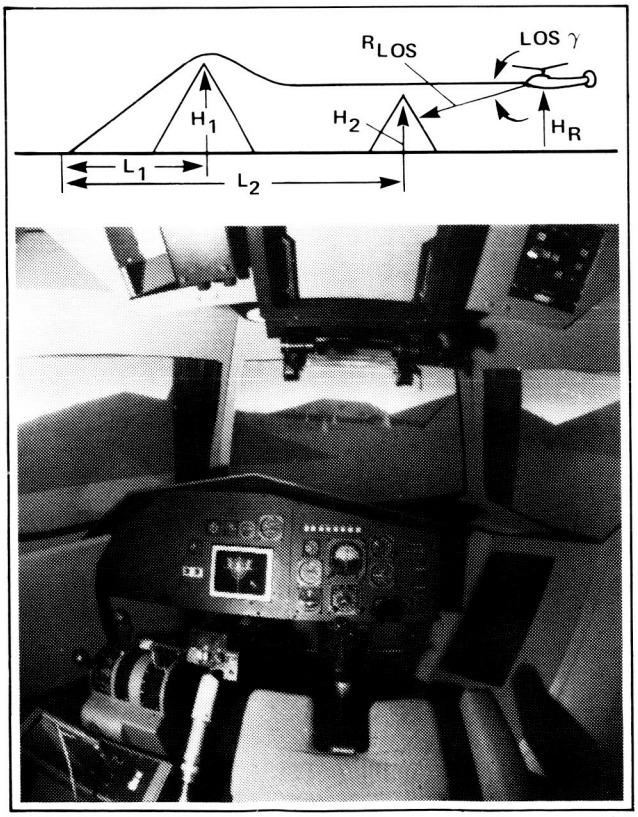

McGee

Terrain following – joint NASA/Air Force/IBM program

(L. McGee, Ext. 5443)

Applications of State Estimation in Aircraft Flight-Data Analysis

Accurate determination of aircraft motions from noisy or incomplete measurements is an important problem in the analysis of flight-test experiments. The measurements may contain significant errors which must be identified before the data are used in performance calculations. Furthermore, direct measurements of certain important dynamic variables may be unreliable or impractical to perform.

A similar problem occurs in the analysis of aircraft accidents, where the actual motions may have to be determined from a very limited data set. These problems are being solved by the analytical method known as state estimation. An advanced state-estimation program called SMACK (smoothing for aircraft kinematics) has been developed at NASA Ames Research Center.

This state estimation technique is being applied at Ames to determine severe winds and turbulence encountered in flight using data from the digital flight data recorders onboard wide-body airliners along with ATC surveillance radar data. A list of recent and ongoing applications follows:

Case	Aircraft	Location	Date
1	DC-10	Hannibal, MO	April 1981
2	DC-10	Morton, WY	July 1982
3	DC-10	Atlantic near Bermuda	Oct. 1983
4	L-1011	Offshore So. Carolina	Nov. 1983
5	DC-10	Calgary, Canada	Nov. 1975
6	B-747	Over Greenland	Jan. 1985
7	B-747	Over Greenland	Feb. 1985
8	B-747SP	Offshore California	Feb. 1985
9	L-1011	Dallas/Ft. Worth	Aug. 1985

The first 7 cases involved severe turbulence encounters at cruise altitude. Case 8 involved atmospheric disturbances and engine failure at

cruise altitude. Case 9 involved a microburst encounter during landing approach.

Analysis of the data from those flights involving severe turbulence at cruise altitudes indicates that the aircraft encountered vortex arrays caused by a breakdown of wind shear layers (Kelvin-Helmholtz instability). The analysis indicates that the vortices can be up to 1,200 ft in diam, at spacings of about 3,000 ft, with whorls of wind above 80 fps. These vortex parameters obtained from airline flight data provide a way to simulate and investigate the operational problems for the other types of aircraft that may unexpectedly encounter this severe turbulence.

(R. Wingrove and R. Bach, Ext. 5429)

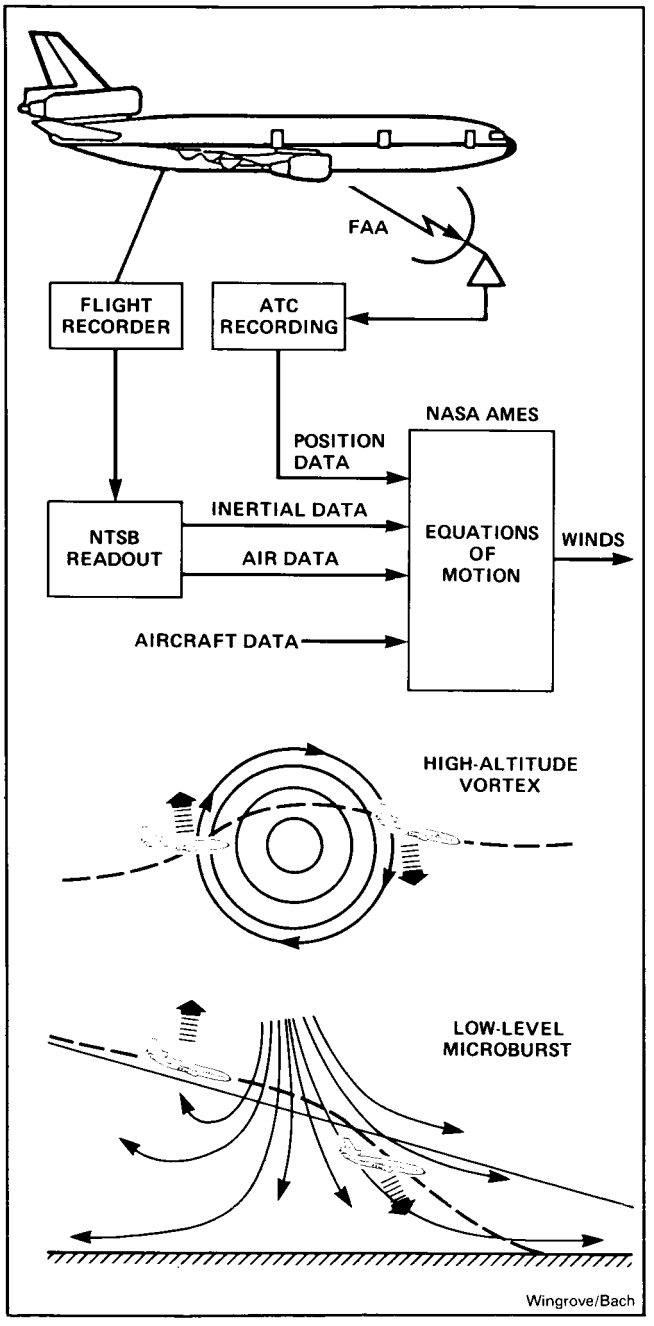

Determination of severe winds and turbulence from wide-body airline data

Rotorcraft Systems Integration Simulator (RSIS)

The Rotorcraft Systems Integration Simulator (RSIS) (see figure), will be an advanced simulator for research and development. The RSIS, developed by NASA in joint participation with the Army, will provide NASA with an advanced R&D simulation capability that supports:

(a) A systems approach to rotorcraft design (i.e., LHX)

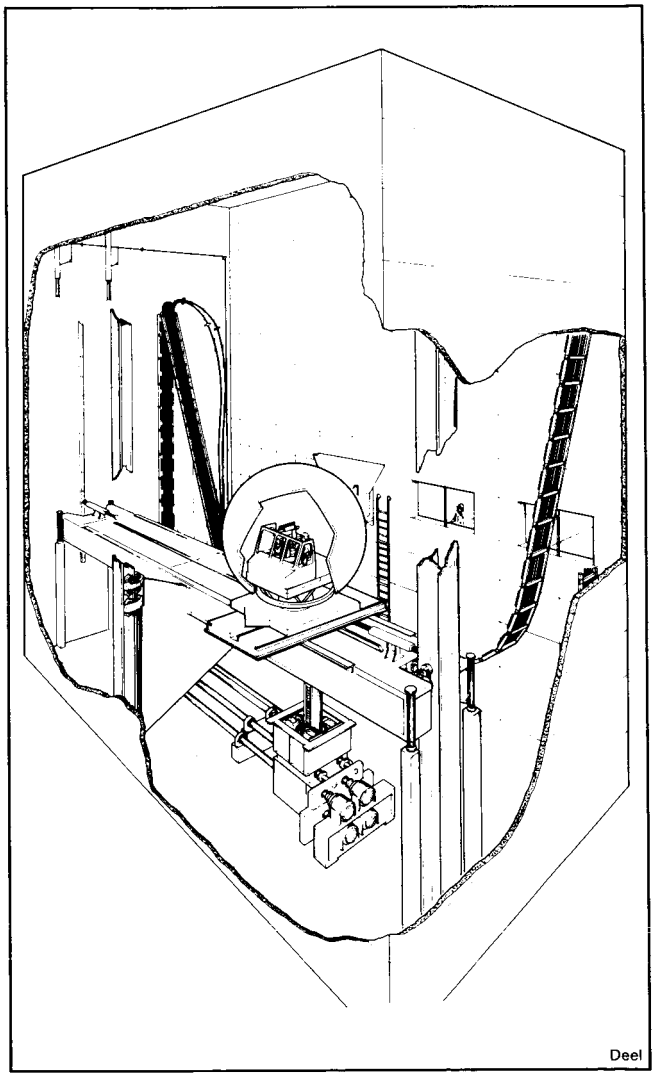

Advanced simulator

(b) Flight tests, safety analysis, and product improvement evaluations

(c) Research in basic rotorcraft technology.

The RSIS will include a simulator cab and cockpit, a motion-base system, a wide field-of-view computer generated imagery (CGI) visual system, and a computer facility. It will also include its own development station where the cab can be reconfigured for the next simulation and operationally checked before being placed on the motion base.

The jointly approved project plan calls for modification of the existing Vertical Motion Simulator (VMS) to accept the new 4 DOF motion generator and the new cab and visual system as shown (see figure). The motion generator, known as the Rotorcraft Simulator Motion Generator (RSMG) was built by Franklin Research Center, Philadelphia, PA and delivered to Ames in 1983. The cab and visual system, known as the Advanced Cab and Visual System (ACAVS), is being built by American Airlines Training Corporation, Ft. Worth, TX and will be delivered to Ames in January 1986. Integration will take place in 1986 and 1987 and RSIS will become operational in early FY 88.

(A. Deel, Ext. 5168)

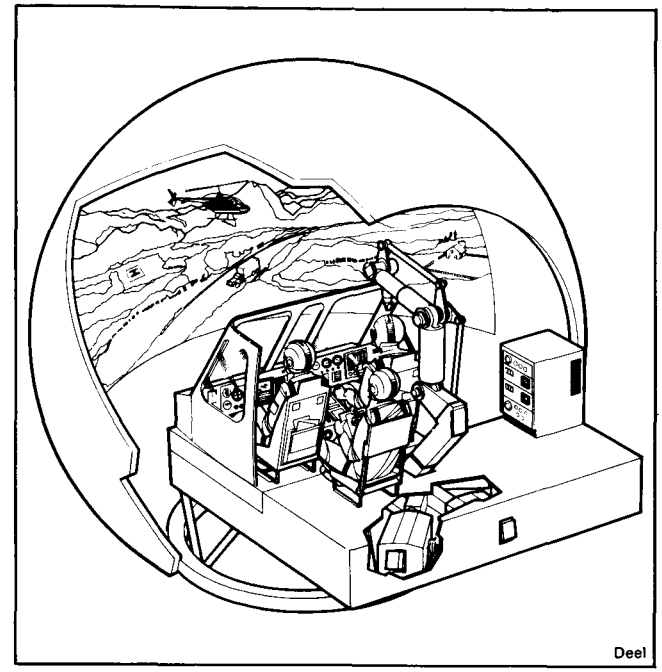

Advanced Cab and Visual System (ACAVS)

Flight Operations

X-29 Wing/Canard Aerodynamics Studies

During the limited-envelope flight testing of the X-29, pressure-distribution studies were made. The purpose of these studies was to determine flow characteristics of a forward swept wing in the presence of a close-coupled canard; to determine the effect of an automatic camber control system; and to provide a data base in order that flight-to-wind tunnel and/or flight-to-analytical code comparisons can be made.

Pressure measurements were obtained from five flush static-pressure orifice rows on the left wing and two rows on the left canard (see first figure). The right wing is instrumented with a deflection measurement system (DMS) from which wing deflections and twist can be determined. This information will complement the pressure measurements. In addition, initial flow-visualization studies have been conducted using tufts and flow cones (see second figure). The results from these studies used with the pressure distributions illustrate the regions of separated flow on the wing. Typical results are shown in the third figure. Actual scales are omitted because data are restricted to the U.S. government agencies and their contractors.

Future plans have been made for more flow-visualization studies which will include both in-flight tests with flow cones and a water-tunnel study. In addition, wing canard molds will be made. From these molds, the exact manufactured airfoil coordinates can be determined. The coordinates along with wing twist determined from the DMS will be made available to analytical code users.

(L. Jennett, Dryden Ext. 3716)

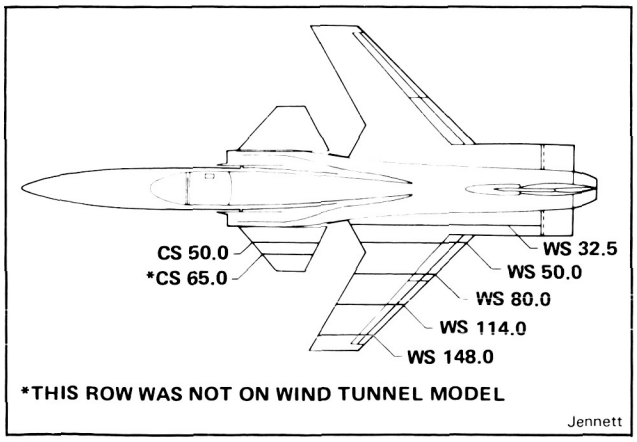

X-29A static pressure orifice row locations

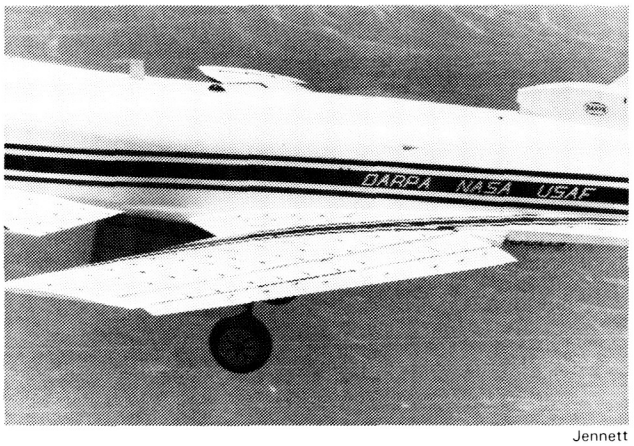

In-flight flow cone visualization

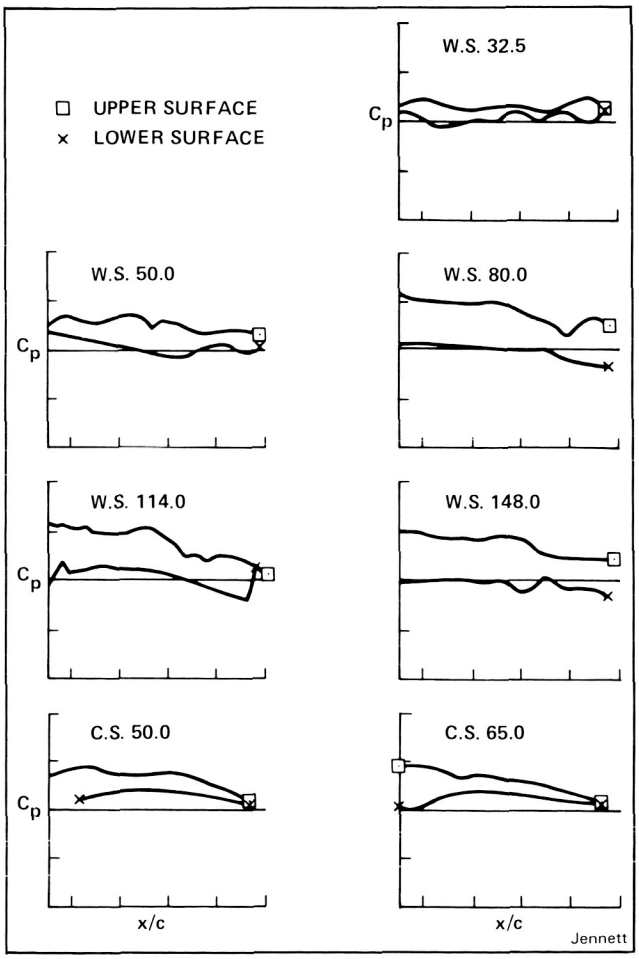

Typical in-flight pressure distribution at $M = 0.6$, $\alpha = 4°$

F-104 Skin-Friction Balance Development

NASA Ames-Dryden is testing, in flight, a large force balance capable of measuring skin friction on a 1-ft square plate. The objective of the effort is to develop a rugged skin-friction measurement system for flight-research applications. The balance panel is intended to be capable of detecting small changes in skin friction, through the use of excrescences directly attached to the plate.

The large force balance units are installed in a flight-test fixture (FTF) mounted on the lower fuselage centerline of a NASA F-104G. One balance panel is installed flush on the left side of the FTF, while the other balance is installed in the same location, on the right side of the FTF. The balance plates are exposed to the same environment (Mach and Reynolds number) simultaneously, providing the capability to use one side as a "control" and the other as the "experiment." The NASA F-104G carrier aircraft provides a Mach number envelope of 0.4 to 1.8, and a Reynolds number capability of 1.5 million/ft to 6 million/ft.

Calibration and check-out flights of the large force balance have been conducted. Currently, the results are encouraging and flight testing of the Langley Research Center riblets are expected to occur in early winter 1985.

(R. Meyer, Jr., Dryden Ext. 3707)

Meyer

Large force balance unit, shown in-flight on F-104G

In-Flight Shuttle Tile Moisture Impact Tests

At the present time, Space Shuttle launch and landing operations are severely limited because of weather constraints. One of the constraints is potential damage to the orbiter's thermal protection system (TPS) tiles while flying through rain, mist, or ice particles. NASA Johnson Space Center is currently engaged in a program to define the TPS tile-damage threshold owing to moisture particle impact, and to technically characterize the weather-related environment.

NASA Ames-Dryden will perform a major portion of the TPS tile flight-test program on an instrumented F-104G in both a USAF KC-135 water spray-tanker-generated environment and actual cloud/rain conditions. Shuttle TPS tile coupons will be mounted on the leading edge of a flight test fixture (FTF) which is mounted on the lower fuselage centerline of the F-104G carrier aircraft. The TPS test coupons will consist of 2- by 6-in. pieces of TPS tile mounted at 90°, 60°, 30°, and 15° to the freestream flow, as well as a 6- by 8-in. tile mounted at 0° to the freestream flow.

Damage to the tile coupons will be documented as functions of tile angle, moisture particle size, and particle speed. Particle size will be measured by a particle measurement sensor mounted on the right wing pylon and inferred from a liquid water content probe mounted on the FTF. Impact intensity will be measured by sensors mounted in the tile test fixture.

Flights are expected to begin in October 1985. Flight conditions will vary from about 200 knots indicated airspeed (KIAS) to 1.5 Mach number. Approximately 12 flights will take place behind the spray tanker, and about 6 flights in natural rain/cloud conditions. Results will feedback into the shuttle program.

(R. Meyer, Jr., Dryden Ext. 3707)

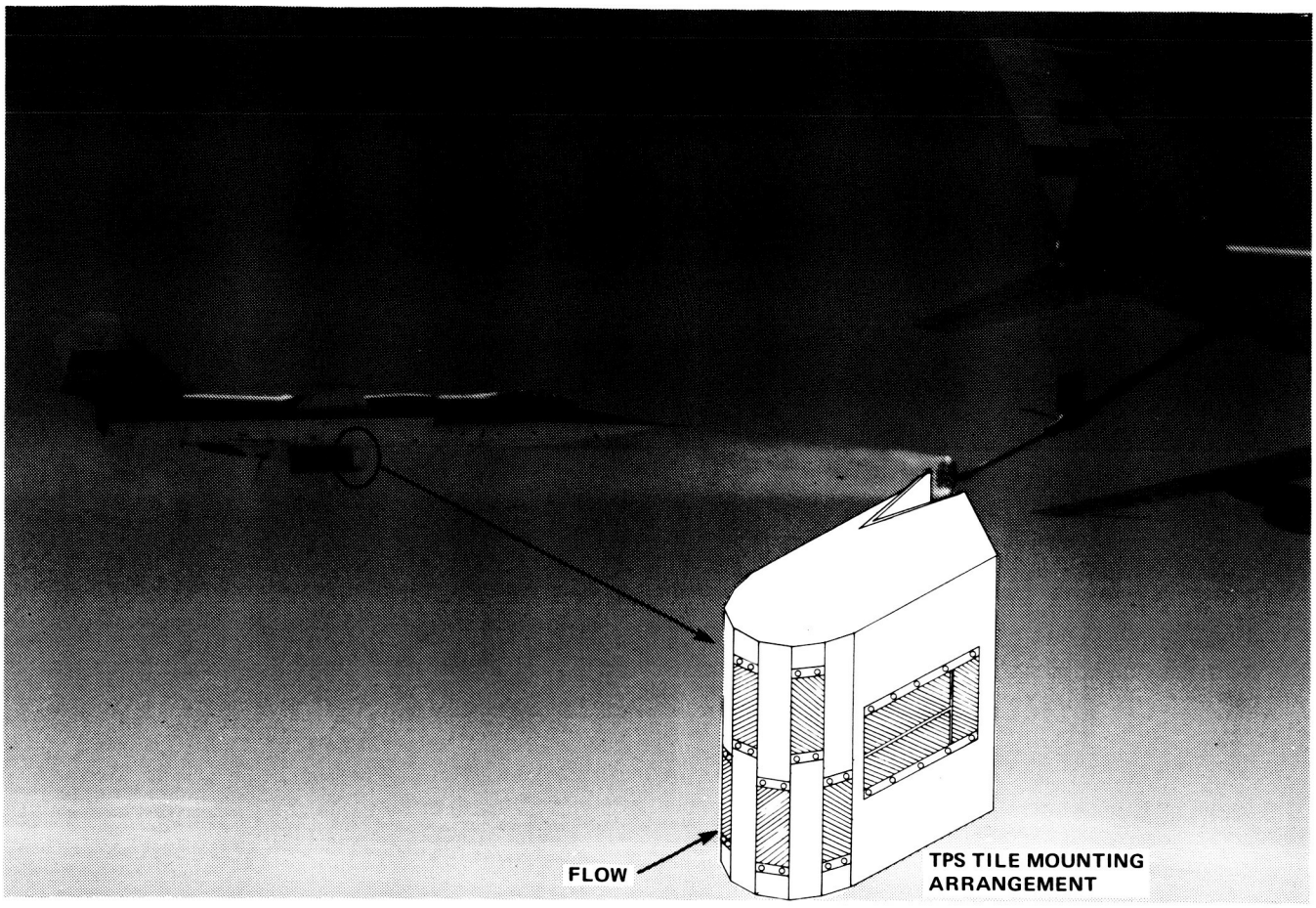

Meyer

In-flight photograph of NASA F-104G behind USAF KC-135 water spray tanker

F100 Engine Model Derivative Augmentor Performance Evaluation

The transient performance of the augmentor of the F100 engine model derivative (EMD) was evaluated in the NASA Ames-Dryden F-15 airplane. One of the objectives of the F100 EMD was to improve the augmentor performance. The augmentor must exhibit good transient capability, including the ability to light reliably and rapidly throughout the F-15 flight envelope. Previous F100 engine augmentors experienced operational problems in the high-altitude and low-airspeed flight regime, including stalls, blowouts, rumble, and failure to light.

The augmentor of the F100 EMD had 16 segments (discrete burning regions), compared to 5 in the standard F100 engine. Because the segment volumes are relatively small, the fuel-pressure surges during segment sequencing were small, thereby reducing the tendency for stalls and

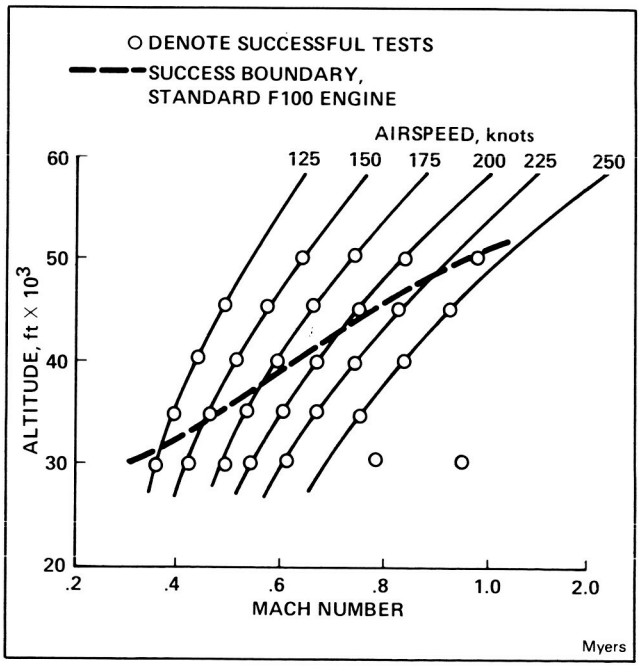

F-15/F100 EMD idle to maximum transients

blowouts. Augmentor transient performance was evaluated with a series of rapid throttle transients, the most severe being the idle-to-maximum power transient. All augmentor throttle transients were successful as shown in the first figure. Throttle transients were evaluated up to 50,000 ft and at a minimum flying speed as indicated by the slowest airspeed for level flight at a particular altitude. This augmentor performance was significantly better than the standard F100 engine success boundary also shown in the figure.

One of the causes of augmentor instability is rumble; this is a combustion-acoustic dynamic coupling phenomenon related to locally overrich fuel-air ratios. Rumble typically exhibits a frequency in the 50- to 100-Hz range, and can cause blowouts and stalls. Flight clearance testing in ground facilities had shown that the F100 EMD augmentor was free of rumble over the flight envelope. However, flight tests at 20,000 ft and 150 knots indicated mild rumble. A time history of an idle-to-maximum-to-idle throttle transient is shown in the second figure. Just as the last segment turns on, the random characteristics of the fan discharge pressure are replaced by a larger amplitude pressure with a discrete 70-Hz frequency. In this case, the amplitude was small enough that no problems occurred; however, the occurrence of even mild rumble was unexpected. Further augmentor testing is planned. Overall, the performance of the F100 EMD augmentor in its first flight tests was impressive.

(L. Myers, Dryden Ext. 3698)

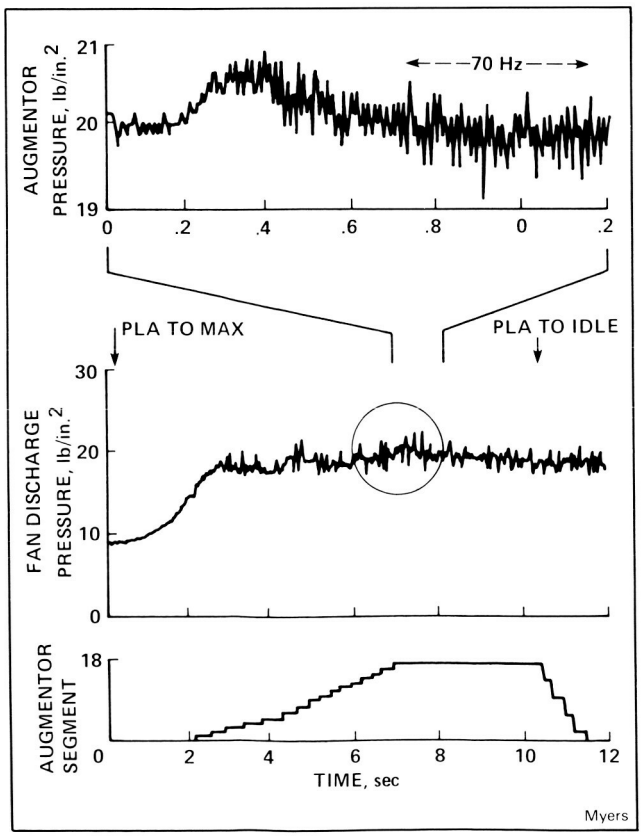

Verge of rumble during idle-to-maximum-to-idle transient at 20,000 ft/150 knots

Flow Visualization of Trapped Vortices Using Trailing Disks

The possibility of decreasing drag on blunt based vehicles has generated interest in a technique that utilizes trailing disks. The effect of the trailing-disk concept is basically to cause the flow to taper behind the disk similar to that of a streamlined boat-tail fairing which would have the least base drag. This is accomplished by trapping a vortex between the body base and the trailing disk which, in turn, pulls the flow in behind the trailing disk base. The trailing disk concept is also desirable since it would eliminate the weight and size disadvantage associated with a faired afterbody.

Wind-tunnel and flight experiments have shown the benefits in drag reduction from mounting a trailing disk behind a circular body of revolution. A single disk could reduce base drag by 35% and with two disks a reduction of 55% could be obtained. This would typically represent a 10% to 20% reduction in total drag. The lower drag occurred when a "smooth and stable" vortex

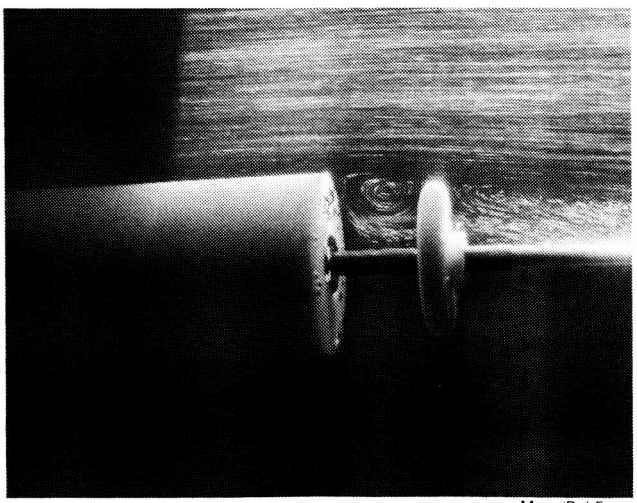

Moes/Del Frate

Trapped vortex on the base of a blunt cylinder with a trailing disk

filled the gap completely. Some smoke-flow visualization research has been done using a trailing disk configuration, but in general, there is little flow visualization data. Therefore, a limited water-tunnel study was conducted to photographically document the vortex and wake-flow interactions behind the blunt bases of a cylinder and square model with trailing disks. The results of this limited study have quantitatively demonstrated that a disk behind a cylinder can be effective in creating a slowly rotating stable vortex; however, trailing a disk behind a square base did not appear as effective.

(T. Moes and J. Del Frate, Dryden Ext. 3704)

F-15 Supersonic Laminar Flow Experiment

Recently, there has been a renewed interest in the efficiency of supersonic aircraft. A specific area of interest is the feasibility of obtaining significant amounts of laminar flow in this flight regime. Consequently, NASA Ames-Dryden will conduct a preliminary flight experiment with an F-15 to generate a limited full-scale data base for assessing computational tools, defining follow-on experiments, and improving instrumentation for measuring boundary-layer transition at supersonic speeds. The F-15 was chosen because it provides 45° of leading-edge sweep, and a Mach envelope to 2.0 M. (Also, previous tests showed that the wing has a favorable pressure gradient.)

A 3/16-in. foam and fiberglass "clean-up" glove will be applied to the right wing. The glove will have two rows of flush pressure orifices. In addition, hot-film anemometers and subliming chemicals will be used to identify transition location.

The tests are expected to occur in the early part of 1986. Approximately seven flights are planned at several Mach numbers up to 2.0 M and at several Reynolds numbers.

(J. Johnson, Dryden Ext. 3706)

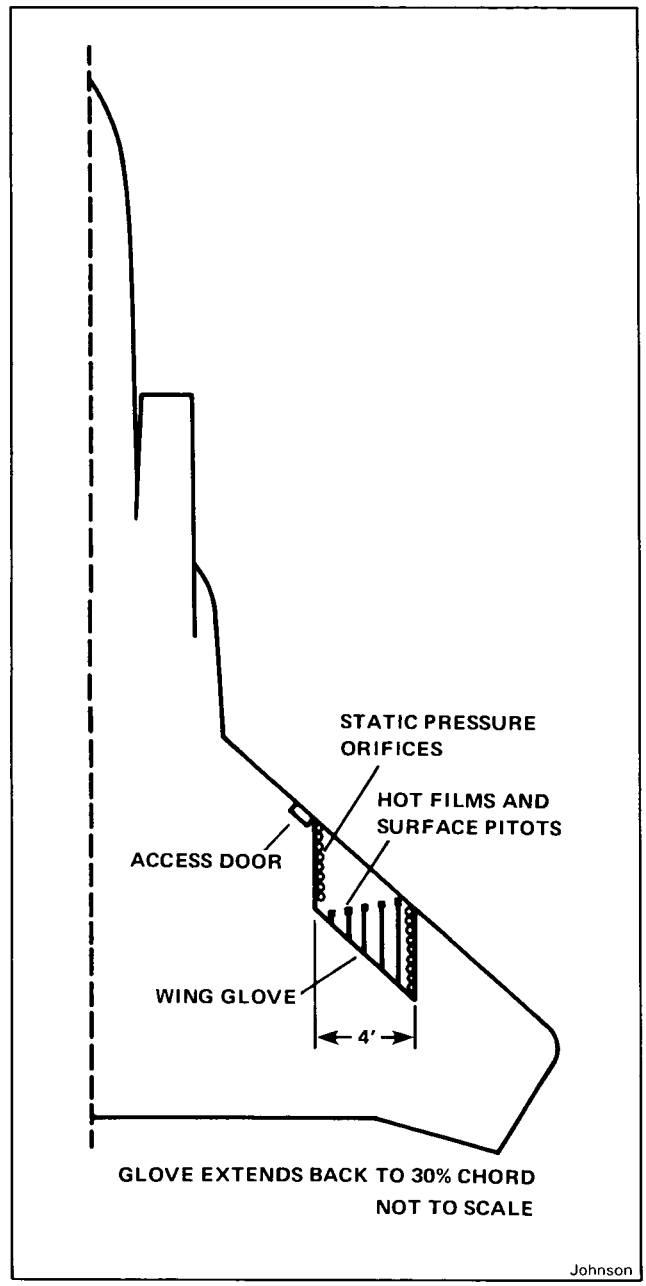

F-15 laminar flow experiment

In-Flight Thrust Calculation Accuracy

In a continuing effort to improve the accuracy of drag determination for new aircraft (i.e., the F-18, the F-20, and the X-29), the accurate determination of in-flight thrust is required. NASA Ames-Dryden recently conducted a study to determine the sensitivity of the net thrust calculation of an F404-GE-400 afterburning turbofan engine to variations in the input parameters. The

in-flight thrust (IFT) calculation program supplied by the engine manufacturer included two variations of the "gas generator method." One method is based on exhaust nozzle total pressure and area (the F/AP method), and the other is based on exhaust nozzle total temperature and weight flow (the F/W T method).

The influence of each parameter input into the IFT program on the calculation of net thrust was obtained by first making an IFT calculation using parameter values obtained from the "spec deck" to determine a baseline condition. The "spec deck" values for each parameter were then increased by 1% and reinserted into the IFT deck to calculate the new value of net thrust. The difference (or change) in the value of calculated net thrust (in percent) for a given parameter is the influence coefficient for that parameter.

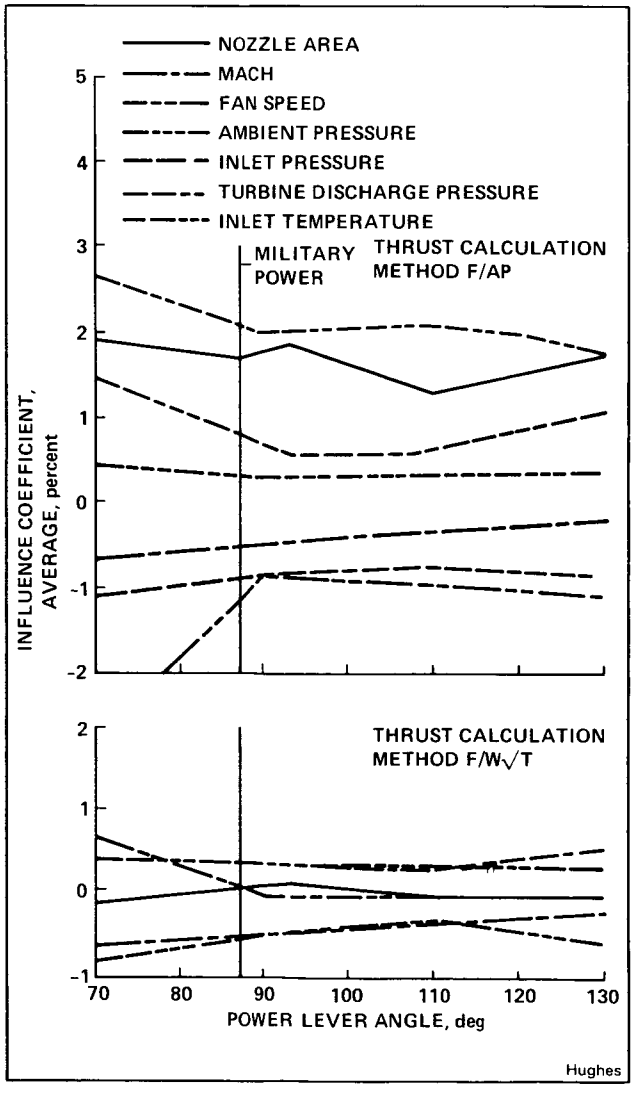

Summary of influence coefficients for each parameter

The plot shown in the first figure is a summary which consists of the average value of each parameter's influence coefficient for all five flight conditions evaluated over the range of power-lever angle for both thrust calculation methods. By comparing the relative values of average influence coefficients, those parameters having the largest influence on the calculation of IFT can be easily determined. As expected, the nozzle area and nozzle pressure have the most influence on the F/AP method, while nozzle total temperature and Mach number have the most influence on the F/W T method.

The influence coefficients and the estimated parameter accuracies are root-sum-squared to determine the overall estimated accuracy in calculated net thrust for both thrust calculation methods. The overall estimated accuracy was determined for all five flight conditions, and is presented in plot form (see the second figure) to compare the relative accuracy of the two net thrust calculation methods. The F/W T method

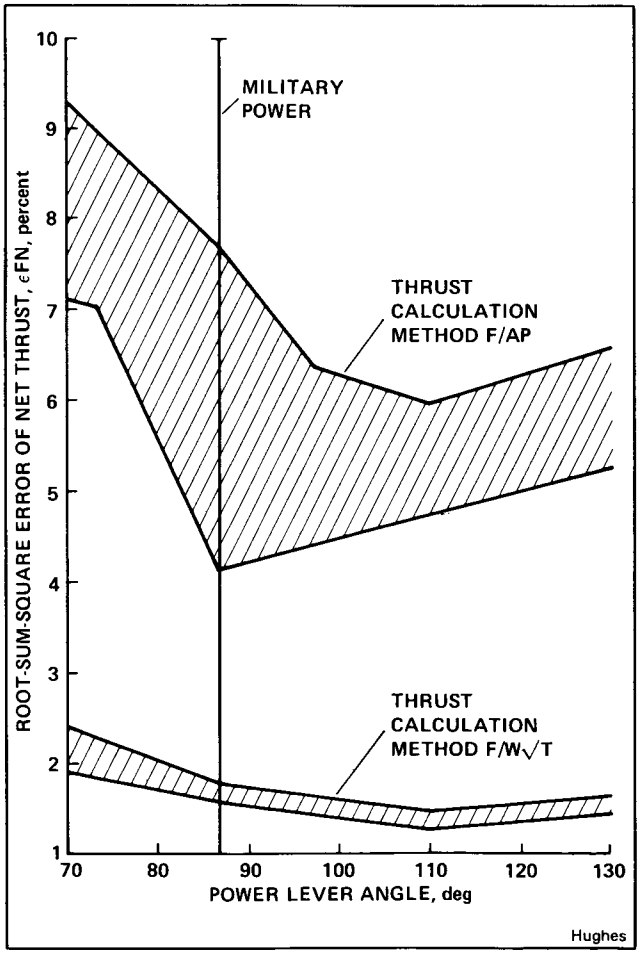

RSS error in calculated FN

shows an uninstalled engine thrust calculation accuracy of under 2% between military and maximum power, while the F/AP method shows a larger error in net thrust calculation ranging from approximately 4% to 7.75%.

The results of this study indicate that the thrust calculation using the F/W T method of thrust ca culation should be quite accurate, making it feasible to assess the advanced technology aerodynamics of vehicles such as the X-29 aircraft.

(D. Hughes, Dryden Ext. 3684)

HiMAT Wing Test

The left outboard wing panel of the HiMAT research vehicle was tested in the NASA Ames-Dryden Flight Loads Research Facility. The testing was conducted jointly under grant with the California Polytechnic State University at San Luis Obispo in response to industry inputs during the spring 1985 HiMAT Symposium.

Coupon tests were conducted to investigate the elemental anisotropic properties of the wing composite material. The coupon tests show that nonlinear theory is necessary in order to describe the material properties.

The wing was instrumented with strain gages and displacement transducers, and loaded near the outboard end. The photograph shows the large displacements observed just prior to failure. Strain measurements are compared with linear and nonlinear NASTRAN analysis. The comparison shows that the wing does not exhibit the nonlinearity predicted by analysis/sample tests.

(A. Vano, Dryden Ext. 3920)

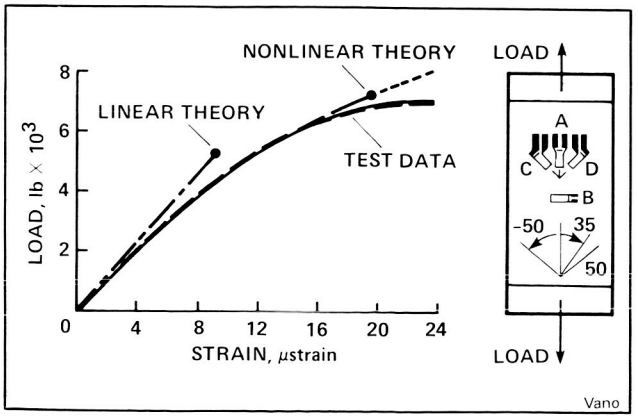

HiMAT coupon test results

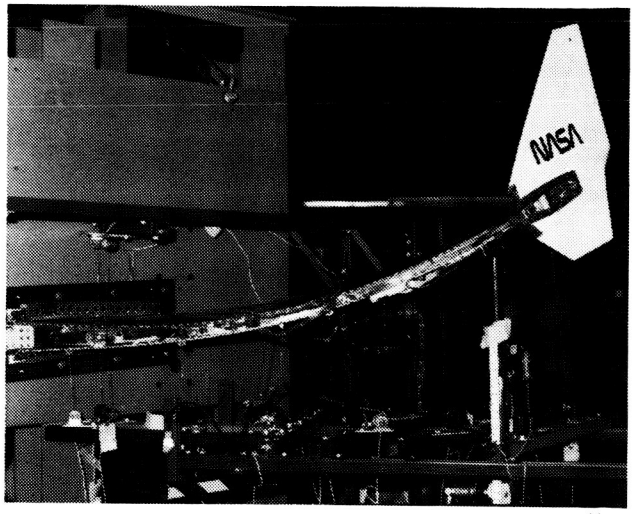

HiMAT wing with deformations just prior to failure

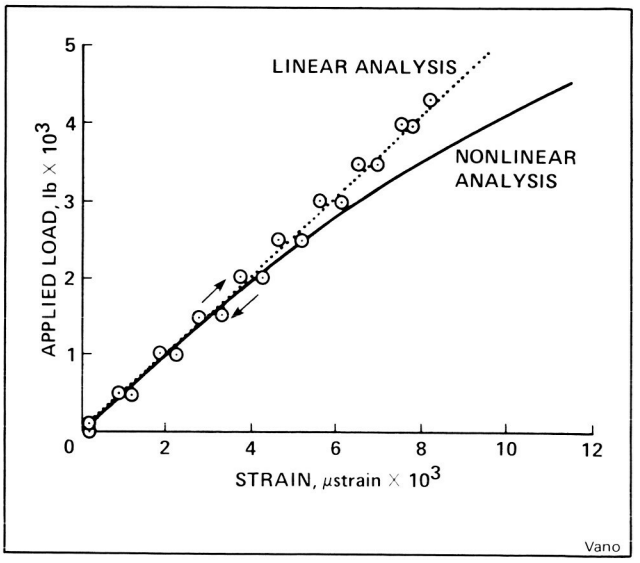

Comparison measured and predicted strains

Buckling Characterization of Hypersonic Aircraft, Wing Tubular Panels

When the speed of an aircraft reaches the hypersonic range, aerodynamic heating becomes significant. The hypersonic-flight vehicle concepts that have been advanced either use a thermal protection system (TPS) to prevent the vehicle from overheating, or allow an exposed vehicle surface to reach an equilibrium temperature with respect to the aerodynamic heating. For example, the Space Shuttle uses a TPS designed to limit the

structural temperature to 350°F (a warm structure). A different concept proposed for future hypersonic aircraft was an aerodynamically acceptable wavy heat shield made of heat resistant metal such as Rene' 41 to limit the structural temperature to about 1350°F (a hot structure). A major concern about hot structure is buckling which can be induced by the combined effects of thermal stresses and air loads.

Since curved shell sections exhibit high local-buckling strength, a tubular panel has been identified as one kind of efficient structural concepts which show promise of low structural-unit mass and high-buckling strength.

Thus, to characterize the buckling behavior of the tubular panels in a heated wing structure, five Rene' 41 noncircular tubular panels were attached to the wing-root region of the hypersonic wing-test structure (HWTS) for extensive nondestructive buckling tests under different combined load conditions (axial compression, bending under lateral pressure, and shear). The temperature environments were 70°F, 550°F, and 1000°F, respectively. The buckling loads were estimated by using the force/stiffness (F/S) method of plotting the test data. Predicted buckling-failure loads for the various load combinations, axial load (N_x) versus shear load (N_{xy}) were plotted and compared to predictions. In spite of some data scatterings owing to long-distance data point extrapolations, the overall test data correlate fairly well with theoretically predicted buckling interaction curves.

(W. Ko, Dryden Ext. 3581)

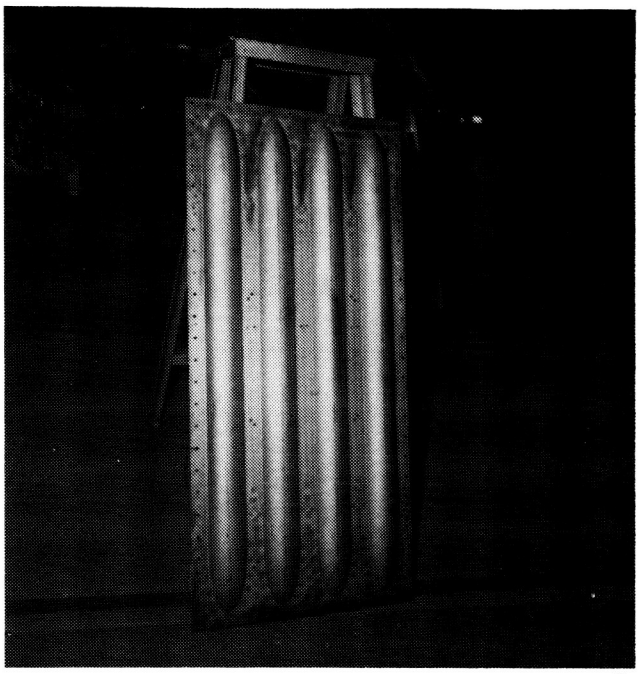

Ko

Rene' 41 tubular panel

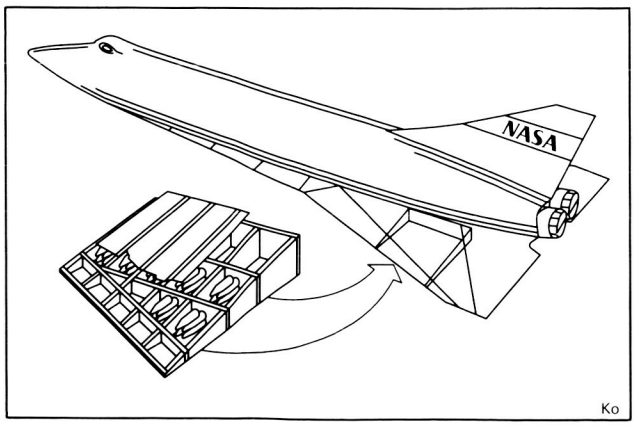

Ko

Hypersonic wing test structure

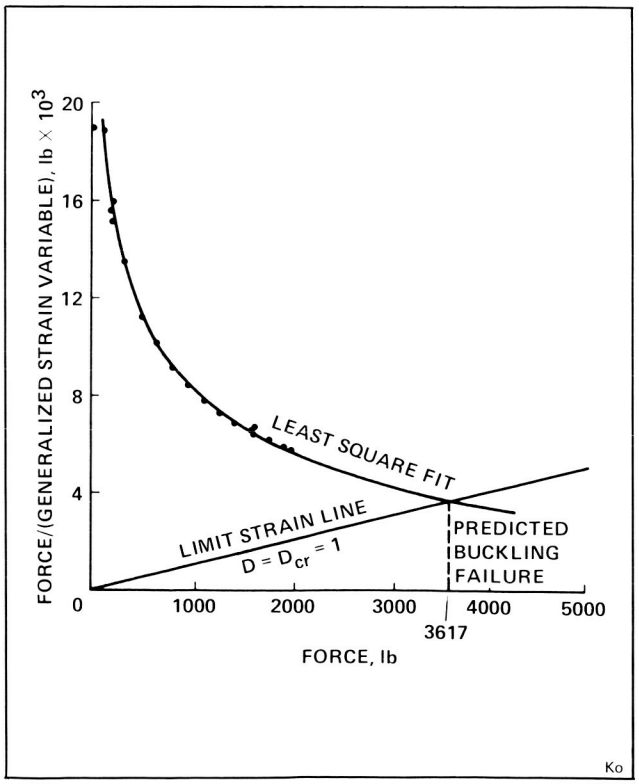

Ko

Force/stiffness plot

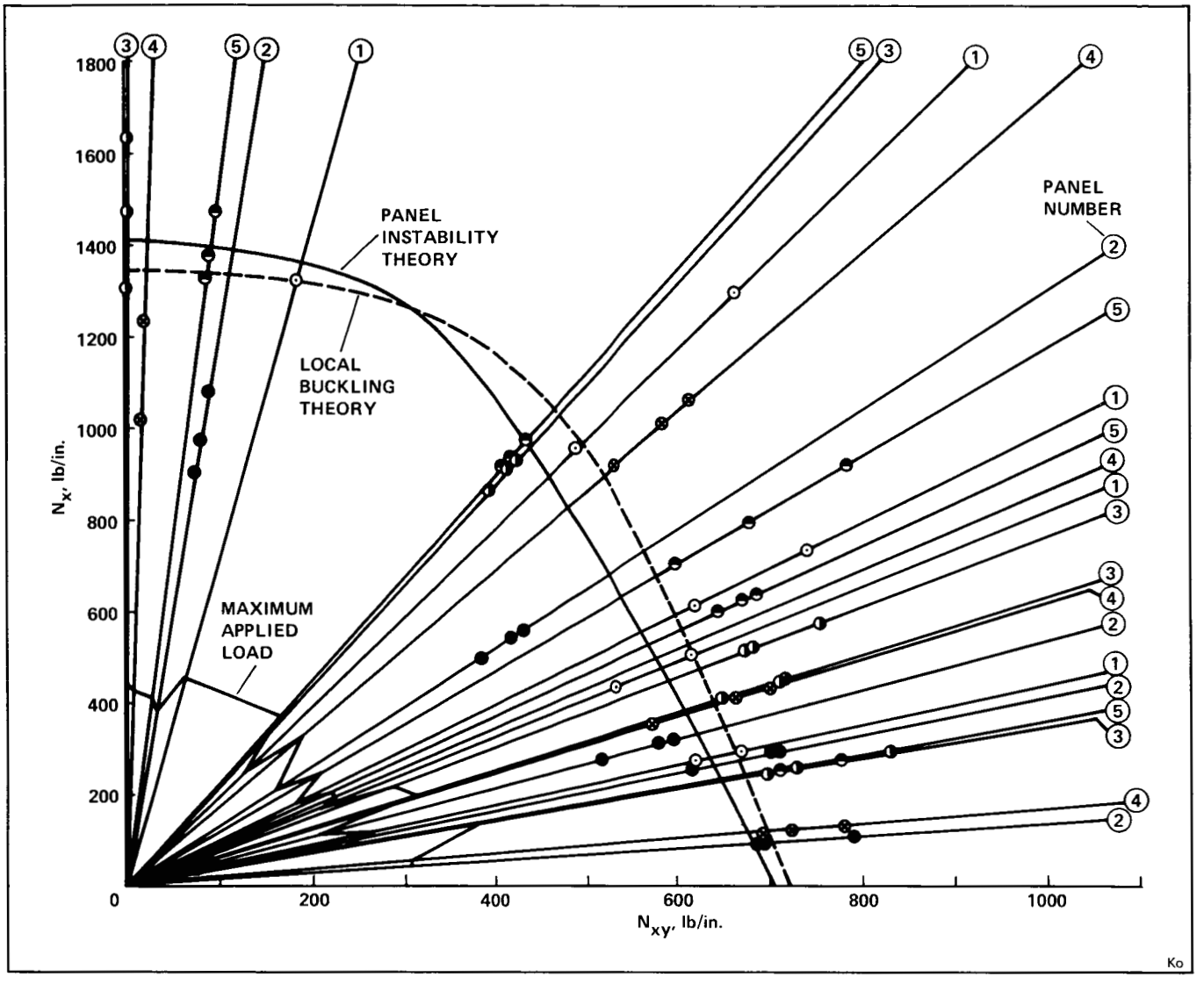

Buckling interaction plots for Rene' 41 tubular panels, T = 1000° F, P = 0

Hot Structures Research

In order to fully understand the thermal and structural performance of high-speed aerospace structures, heat-transfer and thermal-stress analyses are necessary. Before the thermal-stress analysis, the heat-transfer analysis must be performed. The structural temperature distribution obtained from the heat-transfer analysis will be used as input to the structural model for the calculations of the induced thermal stresses.

In the past the effects of internal free and forced convections were neglected in the heat-transfer analysis of the Space Shuttle orbiter subjected to reentry aerodynamic heating. Because of this, the structural temperature predictions were not highly satisfactory in some regions, i.e.,

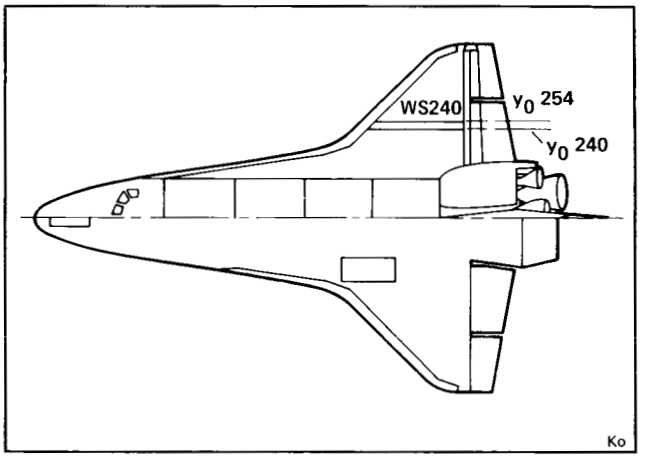

Locations of Space Shuttle wing segment that were analyzed

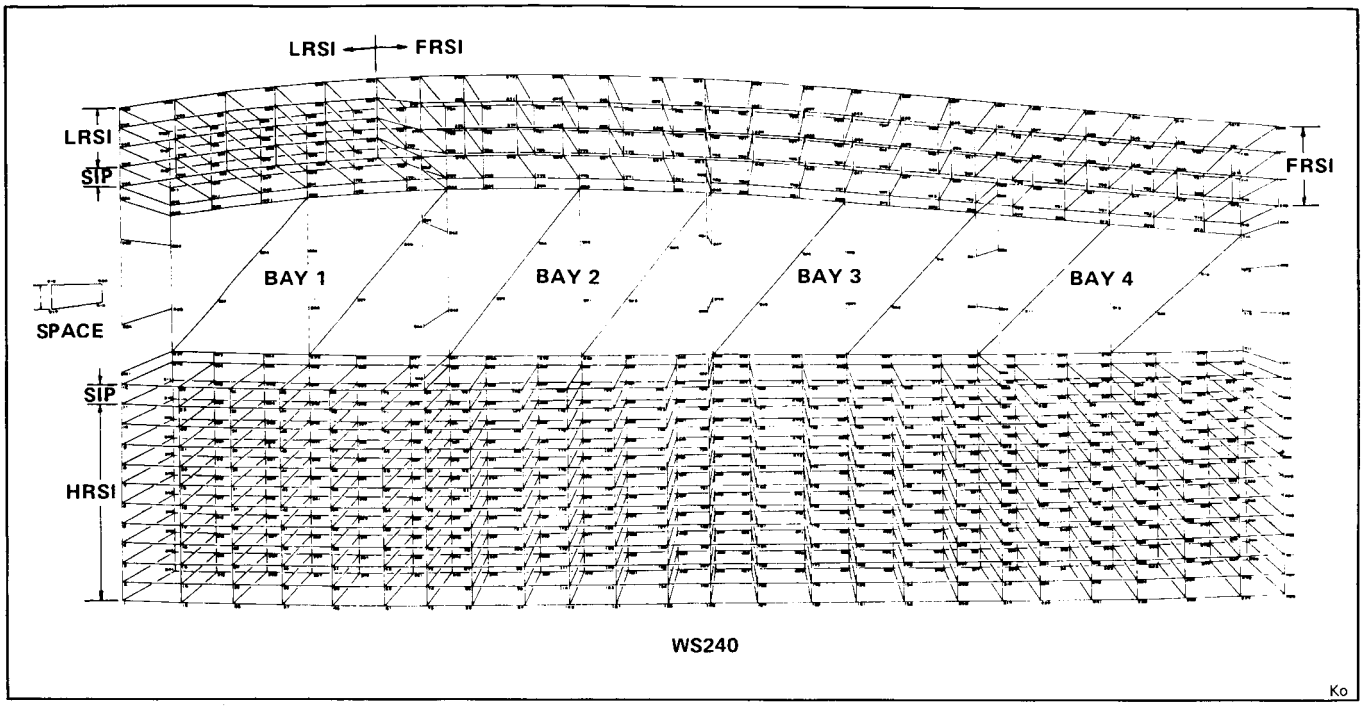

Three-dimensional spar finite element thermal model for WS240

the wing lower skins and the fuselage bottom skins. Since the outside cool air enters the interior of the Shuttle at 100,000 ft (30,480 m) altitude, there could be a certain degree of forced convection inside the Shuttle structure, and this forced convection will turn to free convection after the Shuttle orbiter lands and rolls out.

By introducing the effect of forced and free convections into the latest analysis, it was found that the predicted wing lower-skin temperatures could fit the flight data almost perfectly for the entire duration of the flight profile.

(W. Ko, Dryden Ext. 3581)

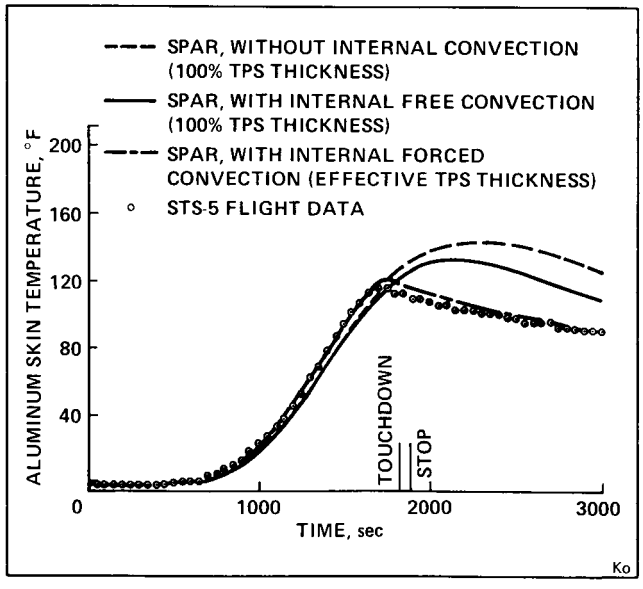

WS240 bay 4 lower skin temperature-time histories. STS-5

Fatigue Life Prediction of Airborne Launch System

The airborne launch system in the NASA Ames-Dryden B-52 aircraft has been used to carry various drop-test vehicles aloft to a high altitude and then release them. A simulated space shuttle solid rocket booster (SRB) drop test vehicle (DTV) which was launched from the B-52 airborne launch system is the heaviest store since the last X-15 flight test. In order to establish the structural integrity of the airborne launch system, fatigue life of critical components of the system had to be estimated. By using the fracture mechanics and the half-cycle theory, the random stress-spectrum for each critical part of the launch system was resolved into half-cycle groups of increasing and decreasing loads. Each half cycle was then considered as a half cycle of the constant amplitude cyclings under the same loading magnitude, and computed separately in time

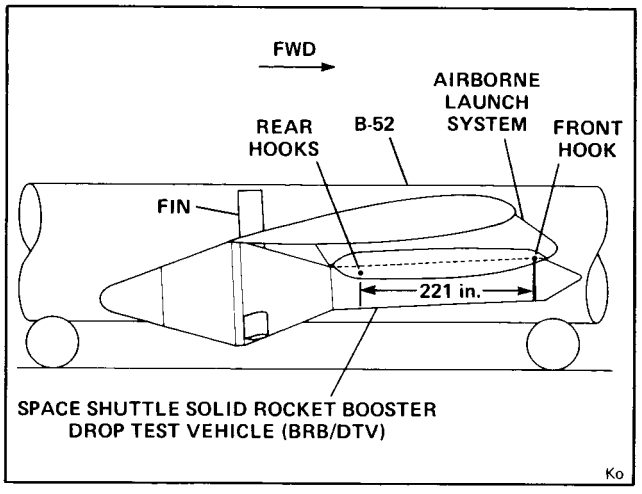

Geometry of Space Shuttle solid rocket booster drop test vehicle (DTV) attached to B-52 airborne launch system. View looking inboard at right side of B-52 and SRB/DTV

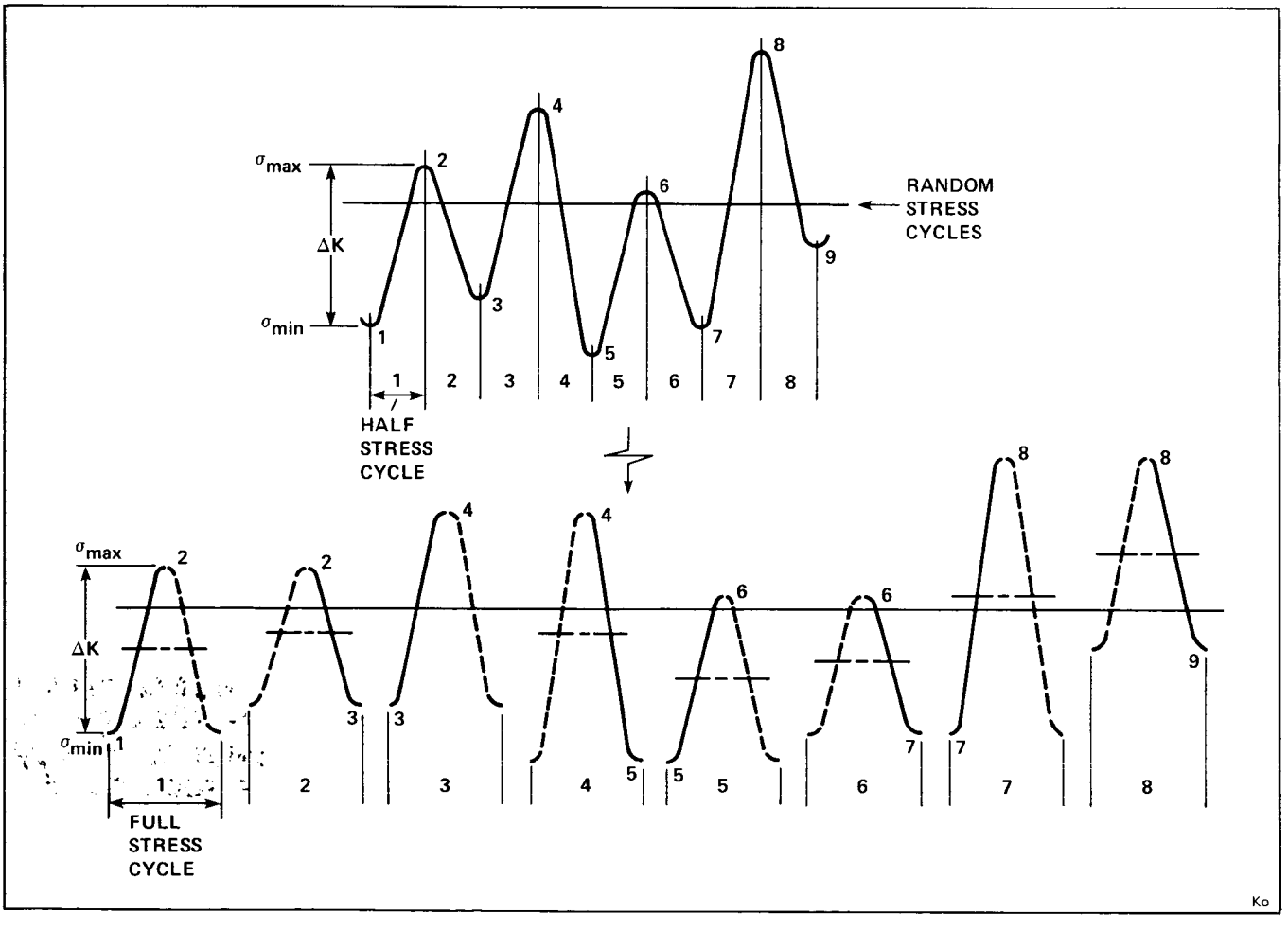

Resolution of random stress cycles into half stress cycles of different stress ranges

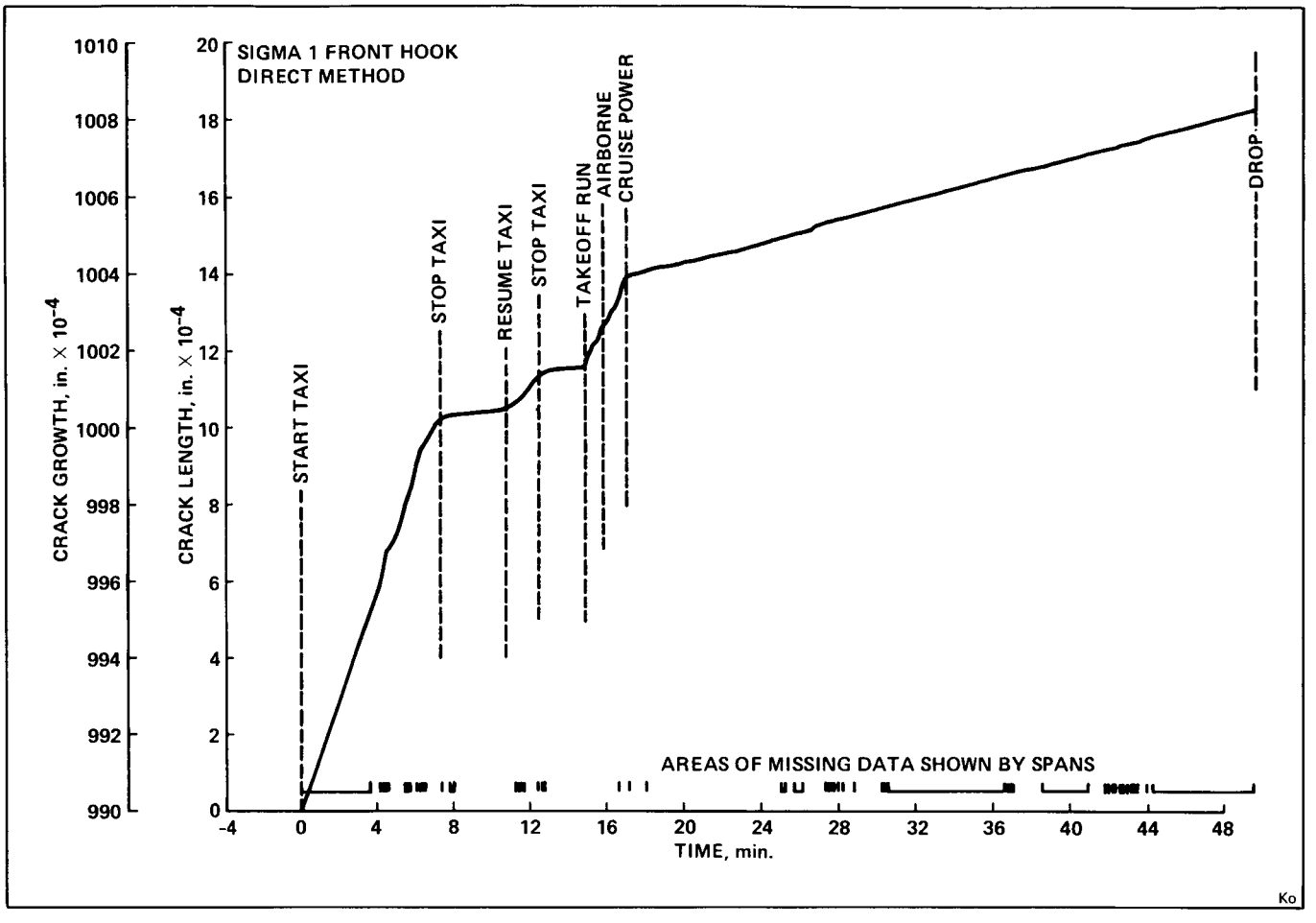

Crack growth curve for stress point 1 (σ_1), flight 1

sequence for estimating the corresponding damage. The results of the fatigue analysis gave the number of remaining flights for the SRB/DTV tests for each critical part, and therefore, a safety limit for flight-test number was established.

(W. Ko, Dryden Ext. 3581)

X-29A Flight Loads and Deflection Measurements

Measurements were made of flight loads on the X-29A using calibrated strain gages. Shear, bending moment, and torque were measured at four stations on the left wing, at the root of the right wing, at the root of both canards, and at the base of the vertical tail.

Flight-load and wing-deflection predictions were obtained using the FLEXSTAB static aeroelastic computer program which performs a direct-matrix solution of arbitrary configurations using linear theories. These include inviscid potential flow (Woodward) with wind-tunnel corrections, and a NASTRAN structural model. The solution includes: (a) stability and control derivatives; (b) airplane trim; (c) pressure distributions; (d) aerodynamic and structural loads; and (e) the airframe deflected shape. Known flap-deflection schedules allow predictions for a particular aircraft configuration and flight condition. Predictions were also made by Grumman using an in-house finite element computer program, and lifting-surface program.

Preliminary measured-and-predicted loads versus load factor are shown for the wing root at a typical flight-test condition. A comparison between these loads shows good correlation.

An electro-optical flight deflection measurement system was installed on the X-29 aircraft for the purpose of monitoring wing structural displacement owing to load. The measured deflection data are used to aid in the modeling of precise aerodynamic shapes for the study of key

maneuvers, and for the validation of computer aero-structural predictive tools. The system diagram is shown. The system consists of 12 infrared light-emitting diode targets, a target driver, two receivers, and a control unit which is also interfaced to the aircraft PCM system.

Preliminary measured-and-predicted deflections, expressed as wing twist versus semispan are shown for a typical flight-test condition. A comparison between the data shows reasonable correlation. The FLEXSTAB predictions are high due to the more flexible NASTRAN model which generated the FLEXSTAB structural influence coefficient matrix and because of certain trim effects.

(L. Schuster and W. Lokos, Dryden Ext 3919)

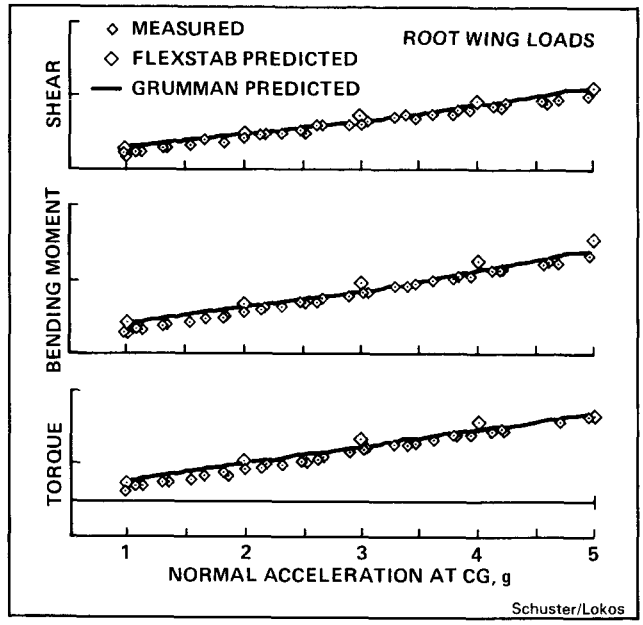

Flight loads and predictions, 5 G wind up turn

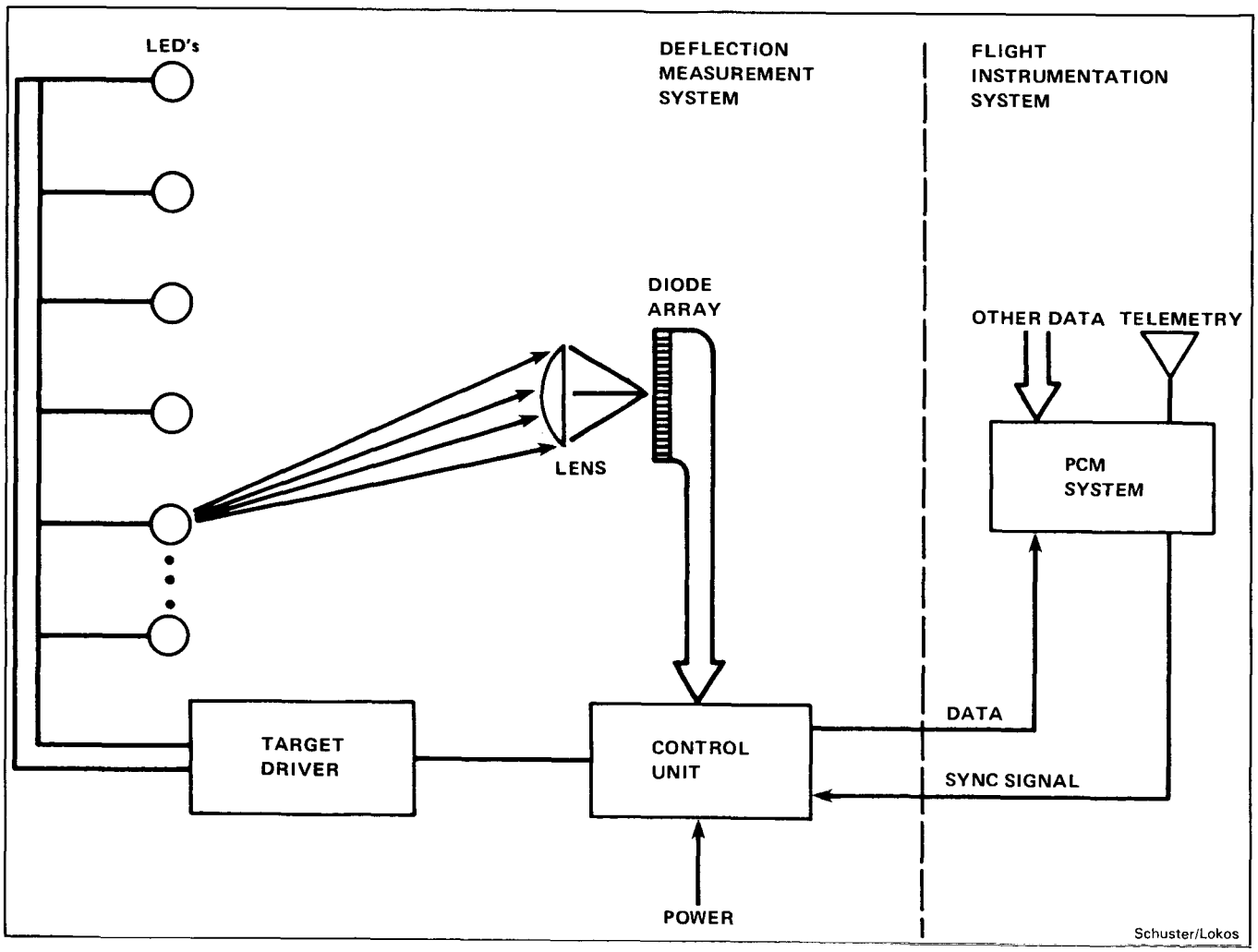

Flight deflection measuring system

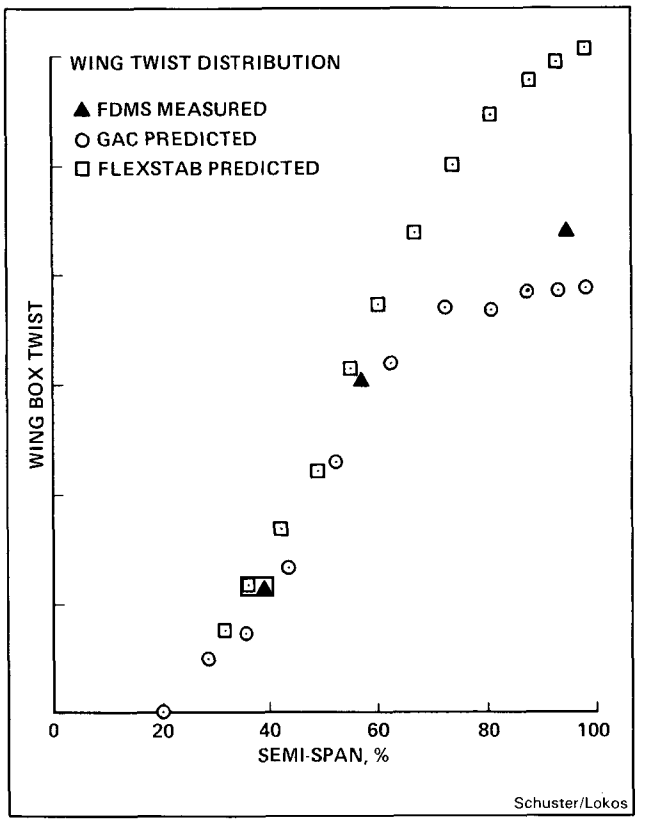

Wing twist distribution

Flow Separation in an Advanced Turbofan Engine

During flight tests of the F100 engine model derivative (EMD) engine in the NASA Ames-Dryden F-15 airplane during 1983, unexpected compressor stalls occurred in the high-altitude-low-speed part of the flight envelope. These stalls were not predicted by previous altitude facility tests, and could not be duplicated by tests specifically run on other F100 EMD engines. The stalls occurred only on throttle reductions from intermediate to idle power. As a result of the discrepancy between flight and ground test, a study of the stalls has been made in recently completed 1985 flights.

The F100 EMD is an advanced derivative of the F100 engine that powers the F-15 and F-16 airplanes. The F100 EMD engine features a redesigned fan and higher temperature capability combustor and turbine section. In contrast with the F100 EMD, the basic F100 engine does not have a compressor stall problem anywhere in the flight envelope.

In an attempt to define the compressor stall problem, high-frequency response-pressure probes were installed at the compressor inlet, and pressure data were recorded at 1000 samples per sec. During 1985 flights, these pressures showed dynamic pressure fluctuations during throttle reductions. The flow-dynamic characteristics were studied and appeared typical of separated flow, with no predominant frequencies present. The occurrence of the pressure dynamics was correlated as a function of the bypass ratio (the ratio of fan to core flow) and corrected compressor rpm, as shown in the first figure. In the 1983 tests, steady-state operation remained outside of the separated flow region; however, on throttle reductions, the engine control system allowed the engine to enter the separated flow region, and stalls occurred. This is shown in a cross-section of the engine, showing the three fan stages and the first compressor stage flow during a throttle reduction and for a throttle increase (see second figure). During a throttle reduction, the fan

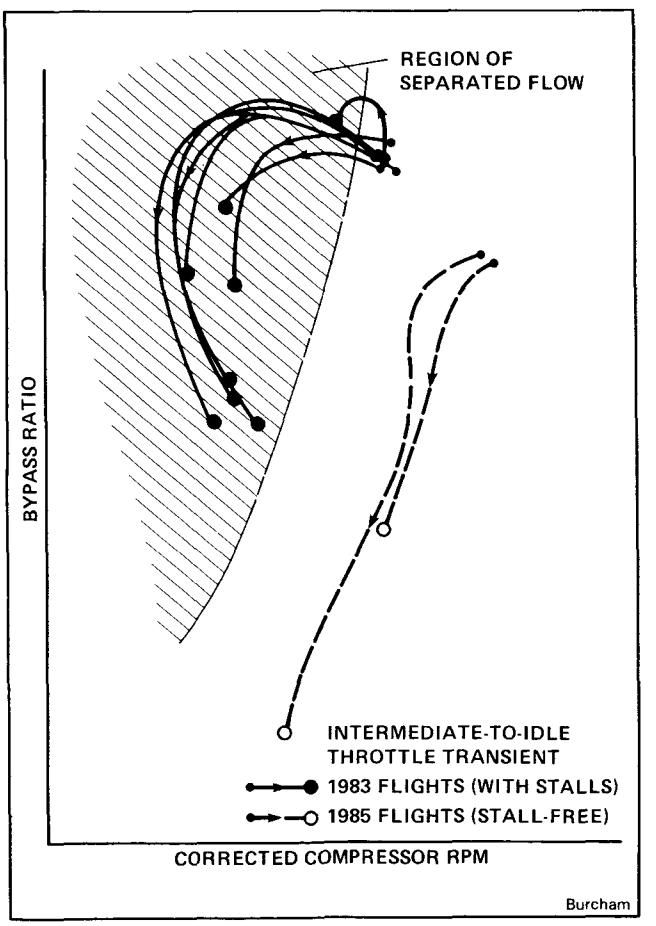

Comparison of 1983 and 1985 flight results for throttle reductions, F100 EMD engines in F-15

decelerates more slowly than the compressor, resulting in an increased bypass ratio and decreased compressor demand. This causes an adverse pressure gradient for the flow entering the compressor and increases the tendency toward flow separation.

Conversely, on a throttle increase, the compressor speed increases more rapidly than the fan, decreasing the bypass ratio. This results in a higher compressor airflow demand and a favorable pressure gradient which tends to reattach the flow. At the very low pressures encountered during flight at low speed and high altitude, the separated flow entering the compressor could be sufficient to cause stall. Changes to the control schedules have since been made and, in the 1985 flight tests as shown in the first figure, engine operation remains outside of the separated flow region and no stalls have occurred.

The reason why the flight results could not be duplicated in the altitude test facilities is being studied. Tests were conducted at the NASA-Lewis Research Center and at the USAF Arnold Engineering and Development Center. Further tests will attempt to define the compressor inlet flow dynamics in more detail. It may be that the ground facility flow dynamics are not quite the same as the dynamics occurring in flight. This question needs to be resolved so that future flight clearance engine test results will be valid.

(F. Burcham, Dryden Ext. 3126)

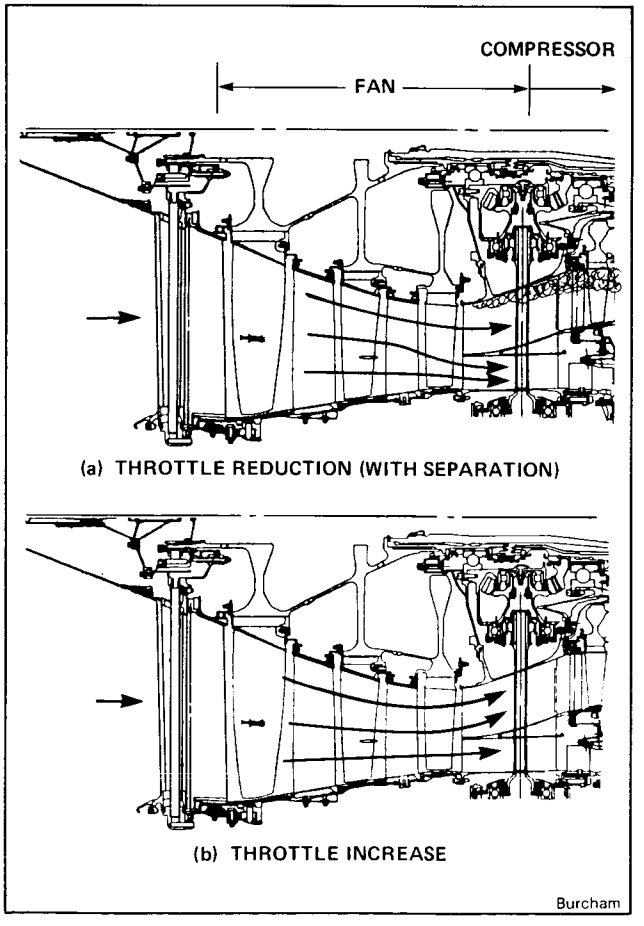

F100 EMD fan-compressor flow

Three-Dimensional Optimal Intercept Experiment

An optimal trajectory research experiment (OPTRE) has been flight tested at NASA Ames-Dryden. The OPTRE algorithm was developed at Drexel University under contract with NASA Langley. The algorithm provides a solution to a three-dimensional (3D) interception of a maneuvering target in real-time. This solution is displayed to the pilot to aid him to fly the optimal trajectory. The OPTRE was flown extensively on the six-degree-of-freedom real-time simulators at Ames-Dryden and Langley. This algorithm was flight tested using Dryden's F-8 digital fly-by-wire (DFBW) aircraft.

The OPTRE represents an advancement in the state-of-the-art in trajectory optimization. This minimum-time-to-intercept algorithm uses singular perturbation techniques to separate the systems dynamics into fast and slow modes by an order reduction procedure. These techniques allow problems involving many variables to be separated into a series of smaller sub-problems. The OPTRE provides a solution to both long- and short-range intercepts of both a stationary and a maneuvering target.

For checkout purposes, a synthetic target-generation algorithm was used. For this algorithm, the input is the relative position and velocities of the target.

The flight test was accomplished using the Remotely Augmented Vehicle Facility (see first figure) at Ames-Dryden. This facility uses a telemetry downlink of measured aircraft states and ground-based radar to obtain the aircraft position and velocity, and rates. This information is then used in the ground based computer which executed the OPTRE and the synthetic target algorithms. The display commands which were generated in the ground-based computer were uplinked to an attitude error indicator located in the cockpit of the F-8.

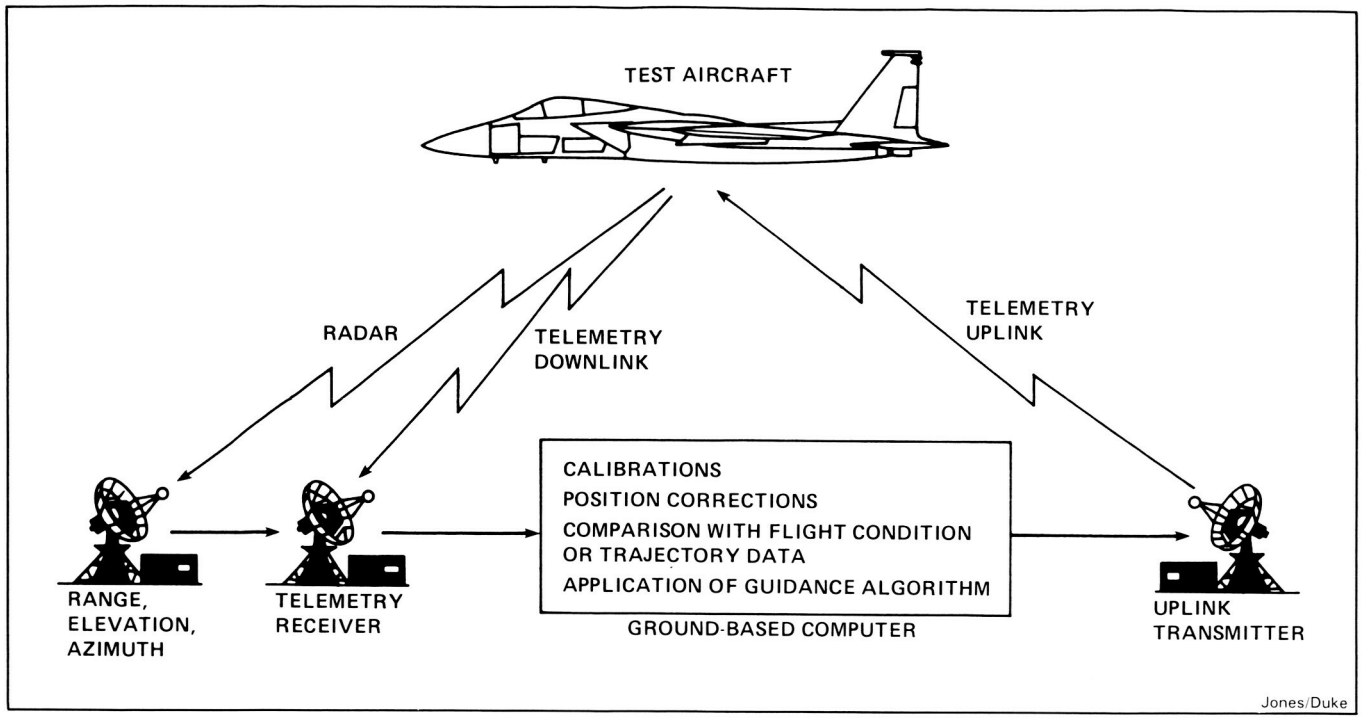

OPTRE flight test guidance system

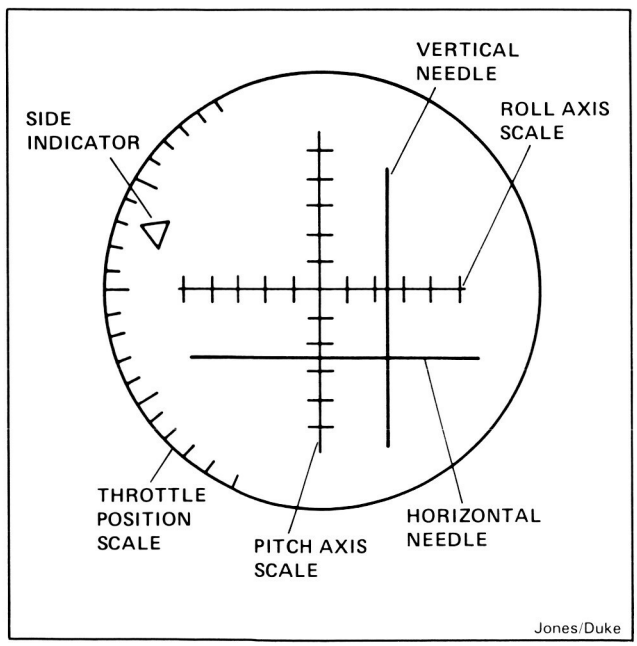

Generic pilot display device

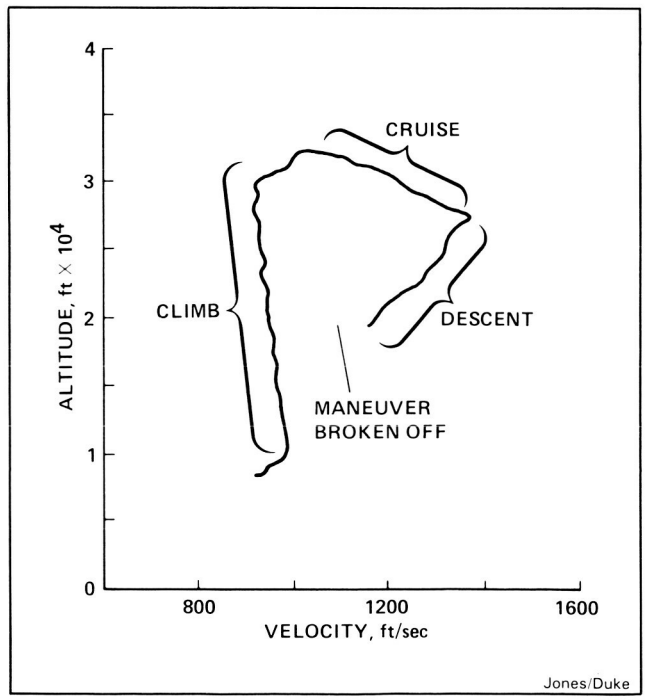

OPTRE altitude velocity profile for an intercept maneuver

The cockpit display unit (see second figure) consists of two flight-director needles and a throttle indicator. When the pilot has centered the needles and the indicator, the aircraft is on the optimal trajectory for minimum time to intercept.

Seven data flights were flown, including one functional check flight. Each flight consisted of one full maneuver and part of another. Three maneuvers with descent were flown. The altitude/

velocity profile for one of these maneuvers is illustrated in the third figure. Because of aircraft and time constraints, limited flight data were obtained. However, these data have proven valuable for future research.

(F. Jones and E. Duke, Dryden Ext. 3414/3802)

X-29 Flight Controls Testing

To facilitate a timely analysis of X-29 flight data, programs have been developed to do a variety of comparisons between flight data and analytical predictions in both the time and frequency domains. These comparisons are used both to study the validity of the prediction techniques, and to make an assessment of the safety of further envelope expansion.

In the time domain, flight-time histories may be overplotted with the time histories of the six-degree-of-freedom nonlinear simulation driven by the pilot control inputs recorded in flight. The linear model of the X-29 can also be driven by the pilot inputs recorded in flight in either the longitudinal or lateral axis, and overplotted with the actual flight time histories. These are valuable in assessing the total system performance. In the lateral axis the overall accuracy of the aero-model can be quickly checked by "driving" the linear model of the bare airframe with the actual surface positions as recorded in flight, and overplotting that with the flight-time histories.

In the frequency domain, both open- and closed-loop frequency responses are computed using fast Fourier transforms (FFTs) on flight time histories generated by pilot frequency sweeps (see figure). These flight-derived frequency responses may be overplotted with either analytically predicted frequency responses or those obtained from FFTs on a time history output of the nonlinear simulation. For some of the open-loop frequency responses, the appropriate input and output signals have been constructed by passing measured parameters through known control-system filters. The open-loop frequency responses are used to monitor the gain and phase margins actually occurring in flight, and to check

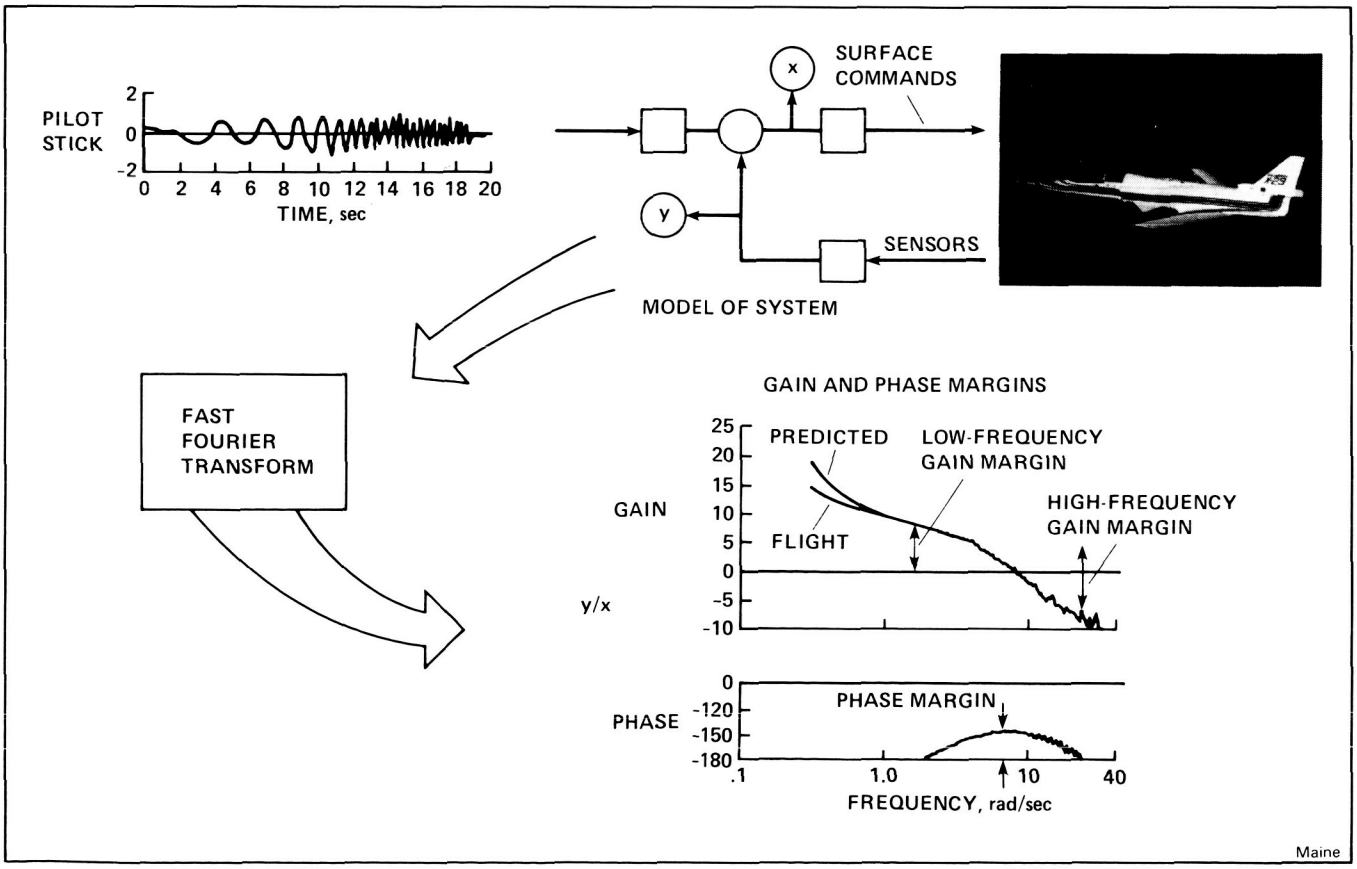

Flight-determined frequency response for unstable airframes

analytic predictions. This is particularly important on the X-29 longitudinal axis owing to the high level of instability. The closed-loop frequency responses have been primarily used in handling qualities research.

(T. Maine, Dryden Ext. 3794)

Expert System Flight Status Monitor

For the past year, systems engineers at NASA Ames-Dryden have been engaged in the development of an expert system flight-status monitor, and knowledge-acquisition tool. The complexity of the modern research aircraft flown at the Ames-Dryden facility has indicated a need for a tool that will augment the systems engineer monitoring of these research flights. Along with the augmentation of flight monitoring, the need for complete and systematic documentation of the aircraft systems has been noted. Therefore, the NASA Ames-Dryden engineers have been developing a knowledge-acquisition tool to systematically document the aircraft systems and provide the expert system with the necessary knowledge in a usable form.

The expert system flight status monitor is used in the control room to assist the systems engineers in monitoring complex systems. The expert system receives downlink data from the aircraft on its health and status, and processes this information in a real-time environment. The expert system then displays to the systems engineer the operability of the aircraft systems and the predetermined messages, along with cautions and warnings. The systems engineer is able to query the system for information such as the next worst failure. The pilot procedures, both normal and emergency, are included in the expert system. This system would be integrated to the simulation prior to its use in the control room to allow proper verification and validation. An extension of this project, once it has been proven in the control room environment, is to uplink a portion of the knowledge from the expert system to the pilot, thus allowing the pilot access to more complete knowledge of the aircraft systems.

In order to prove the feasibility of an expert system for flight systems monitoring, a demonstration system has been developed using a small subset of the total discrete information provided to the ground monitoring station from a typical digital flight-control system. The system was developed on a multi-user VAX 11/750 in

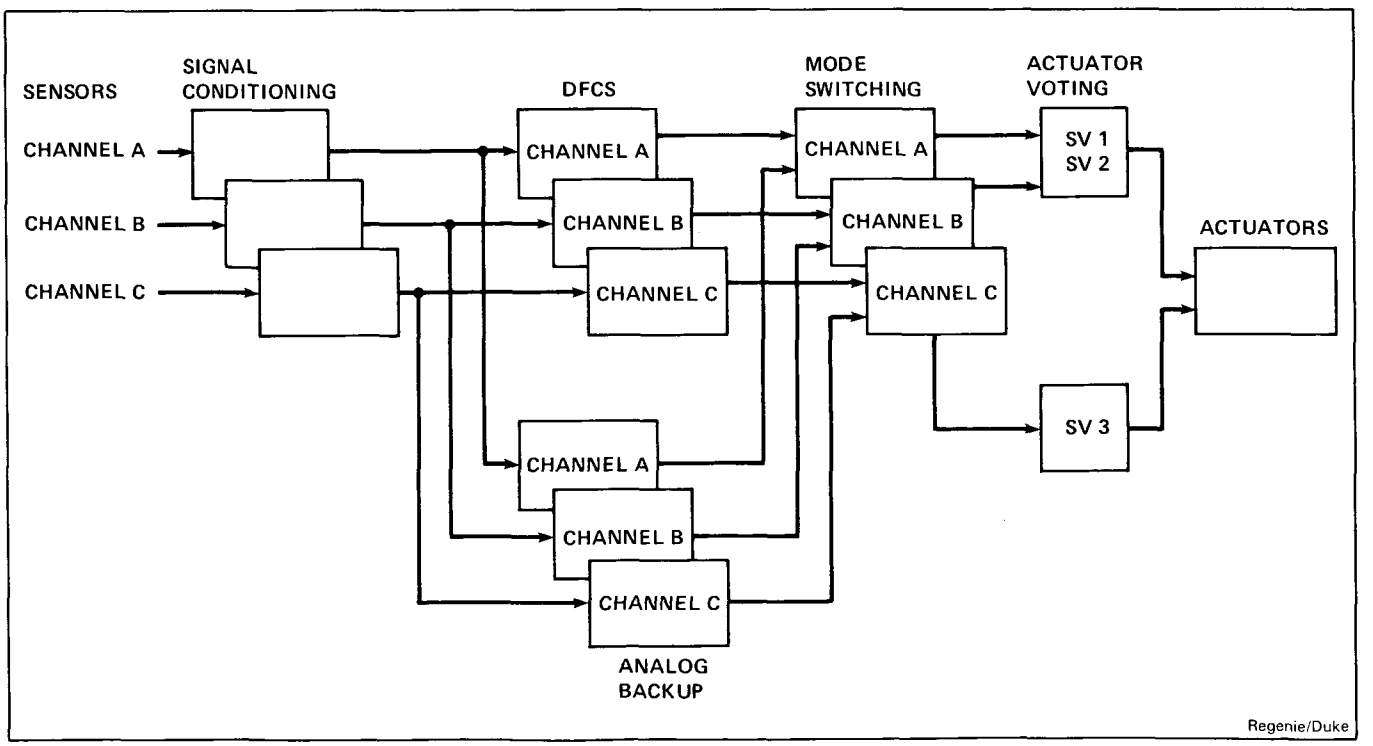

Overview of ditital flight control system

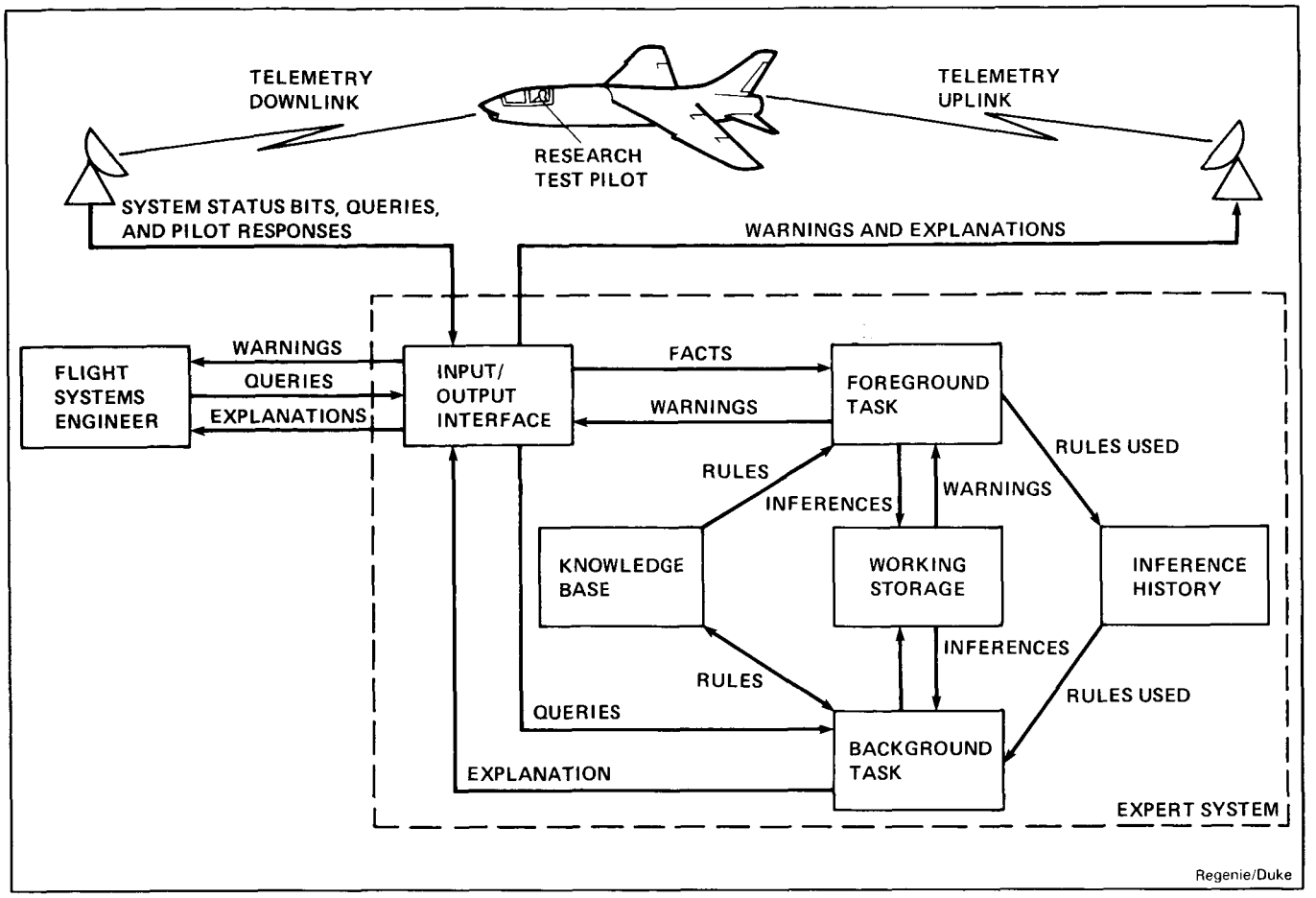

Overview of expert systems flight status monitor

Common LISP and has provided enough promise to justify continuing with a more complete and complicated system. Experience in developing the rules for this demonstration system indicated a need for a knowledge acquisition tool that would enable the domain expert to enter the rules in an orderly manner and to provide consistency. Therefore, a knowledge-acquisition tool is being developed to allow the engineers to enter the aircraft rules in a manner that coincides with their conception of the system.

(V. Regenie and E. Duke, Dryden Ext. 3430/3802)

Flying Qualities Study through In-Flight Simulation

Piloted investigations into the flying qualities of highly augmented aircraft in the landing approach task have been conducted at the NASA Ames-Dryden Flight Research Facility through the use of in-flight simulation. The test vehicle used in two recent in-flight simulation programs was the USAF/AFWAL Total In-Flight Simulator (TIFS) aircraft. TIFS is a highly modified C-131 aircraft configured as a six-degree-of-freedom

simulator that provides a high-fidelity reproduction of the motion and visual cues at the pilot position of the simulated aircraft.

One investigation recently conducted under NASA sponsorship on the TIFS aircraft was the pitch rate criteria program which was designed to generate flying-qualities data for the flared landing task to improve design criteria for highly augmented flight control systems. A general conclusion of the study was that existing criteria are based on pitch-attitude response, and that these characteristics do not adequately discriminate between the good and bad configurations of this study. However, recently devised frequency-and-time domain criteria have been developed and applied to this data base with promising results.

In March 1985, NASA sponsored an in-flight simulation of a shuttle on the TIFS aircraft. The primary objective of this program was to develop and evaluate a modification to the longitudinal shuttle-control system to improve the landing flying qualities of the Orbiter. In addition, the program evaluated factors that would influence these landing flying qualities to provide a data base for future design criteria. The evaluations were performed in the terminal phase of flight starting from a stabilized steep descent, and carried out through preflare, inner glideslope tracking, final flare, and simulated touchdown. Configurations investigated included the baseline Orbiter pitch-rate command/attitude-hold system, a shaped pitch-rate system developed at NASA Ames-Dryden, and Rockwell International's C* system which utilizes pitch rate and normal acceleration feedback. Time-delay effects were also evaluated with these configurations. The evaluations in the TIFS/Shuttle program included the development of the modified control systems to

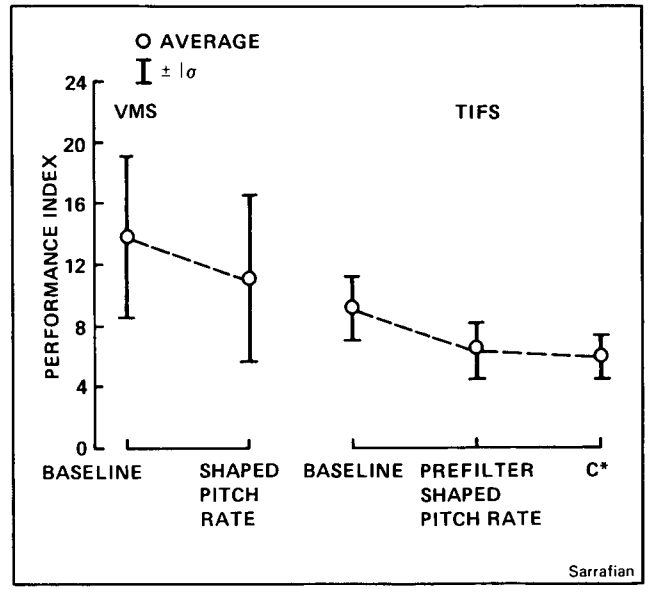

Landing performance statistics, high stress task

their final configurations, comparisons of these systems to the present Orbiter system, and astronaut evaluations to verify the significant findings.

The results from the TIFS/Shuttle in-flight simulation program verified previous work performed on the NASA-Ames vertical motion simulator (VMS) in that better landing performance (lower performance index) was attained with the shaped pitch rate and C* systems under a wide range of stress conditions. The present Orbiter system, though satisfactory for unstressed landings, showed some loss in touchdown performance under high stress. The astronaut evaluations resulted in a preference for reduced time delay with the present Orbiter system.

(S. Sarrafian, Dryden Ext. 3730)

Aerophysics

Optical Information Processing

A critical feature of automated space station subsystems is the capability of what can be termed "intelligent vision": the ability to recognize salient objects in an optical-input scene and make decisions for future actions based on understanding the image viewed. Examples of space-station components requiring rapid image understanding include maneuvering telepresence systems and data analyzing post-processors for space station scientific, commercial, and Earth observation experiments. The objective of the present research is the development of an optical processor/expert system hybrid device to perform the requisite rapid pattern recognition.

The figure below is a schematic diagram of an optical system which performs a two-dimensional correlation between the viewed scene stored on the input spatial light modulator, and a test scene directed to the electronically addressed programmable mask. At each position in the input scene where the desired object is located, an intensity peak appears on the detector array. By analyzing the strength and location of these peaks, the expert system then decides the next test scene required to facilitate object classification. By intelligently choosing the test-scene-programming sequence, the expert system allows for time-effective, multiobject distortion invariant (where distortion refers to physical deformation, defocus, rotation angle, and scale) pattern recognition. In addition, the expert system can "learn" by incorporating previously unclassifiable objects within the library of test scenes. Fast processing of the test scenes is possible owing to the use of a magneto-optic programmable mask with a potential time constant of 10,000 frames/sec.

At present, the overall system is in its early development stages. Feasibility testing of components and architecture is underway.

(D. Ennis, Ext. 6525)

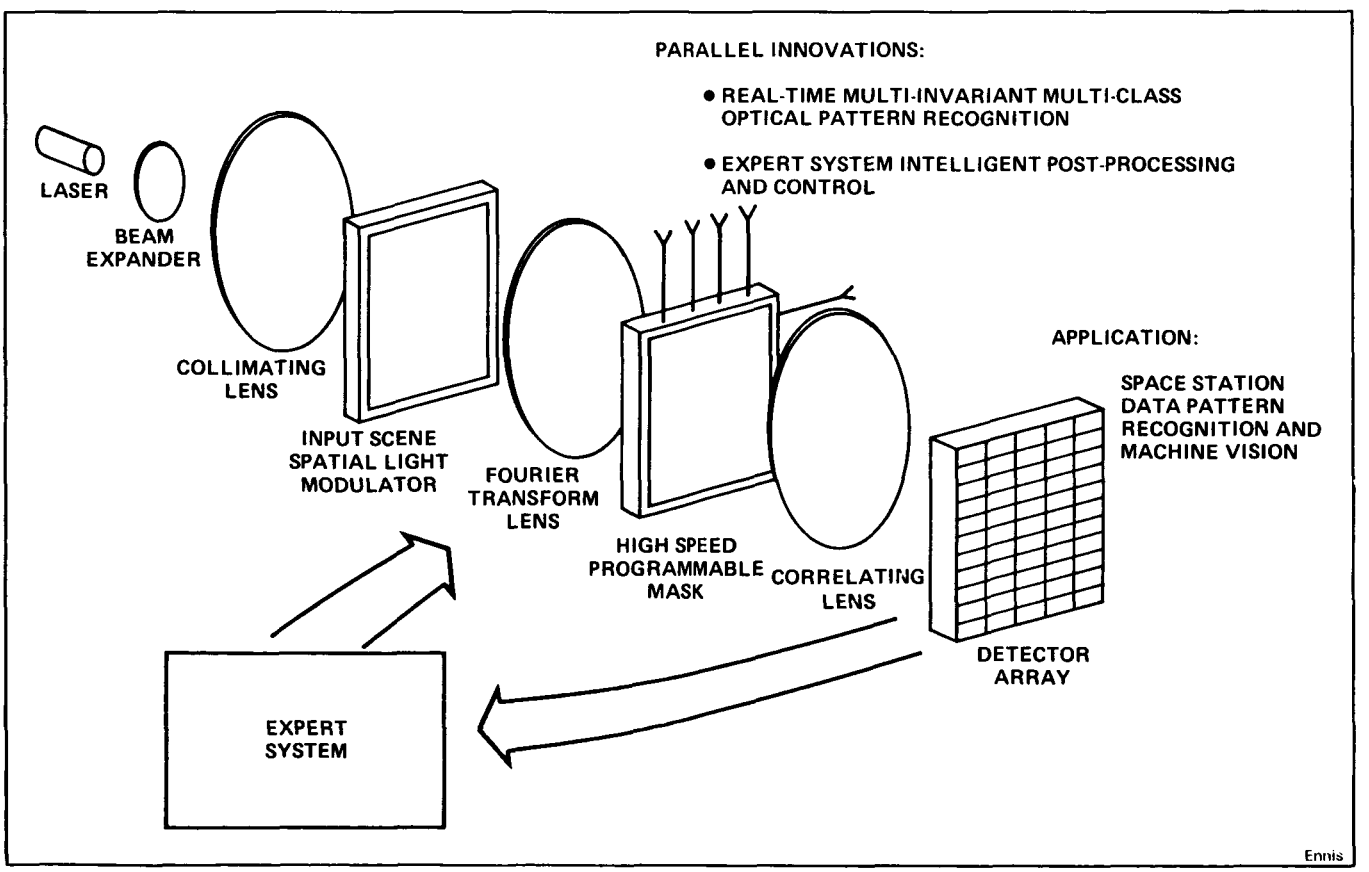

Schematic diagram of an optical processing system

Advanced Distributed System Networks

The focus is on the characterization of high-speed local area networks (LAN) for spaceborne use and particulary on the emphasis of capabilities which apply to the data-system requirements of the Space Station. The primary method to understand the concepts in detail has been to use discrete event simulation. This is being augmented and validated through analysis and emulation on commercial workstations and LAN. Detailed modeling of workloads (or scenarios of required services) is an important element in the studies. Building on last year's effort, two lower layer LAN models have been developed:

The initial model under the LAN extensible simulator (LANES I), has been released for studies of the star-coupled Fiber Optic Data System under development by GSFC. Documentation includes a requirement specification and user's manual. The computer simulations have been remotely activated and monitored at several sites around the U.S. through the use of the Telenet Wide Area Network.

The second model, LANES II, is in test in-house and is targeted for release by the end of September. It simulates the Fiber-Optic-Digital Data Interface (FDDI) under an ANSI draft specification for a high-speed fiber-optic token ring. The requirement specification is complete, and the user's manual is in review.

(T. Grant, Ext. 6526)

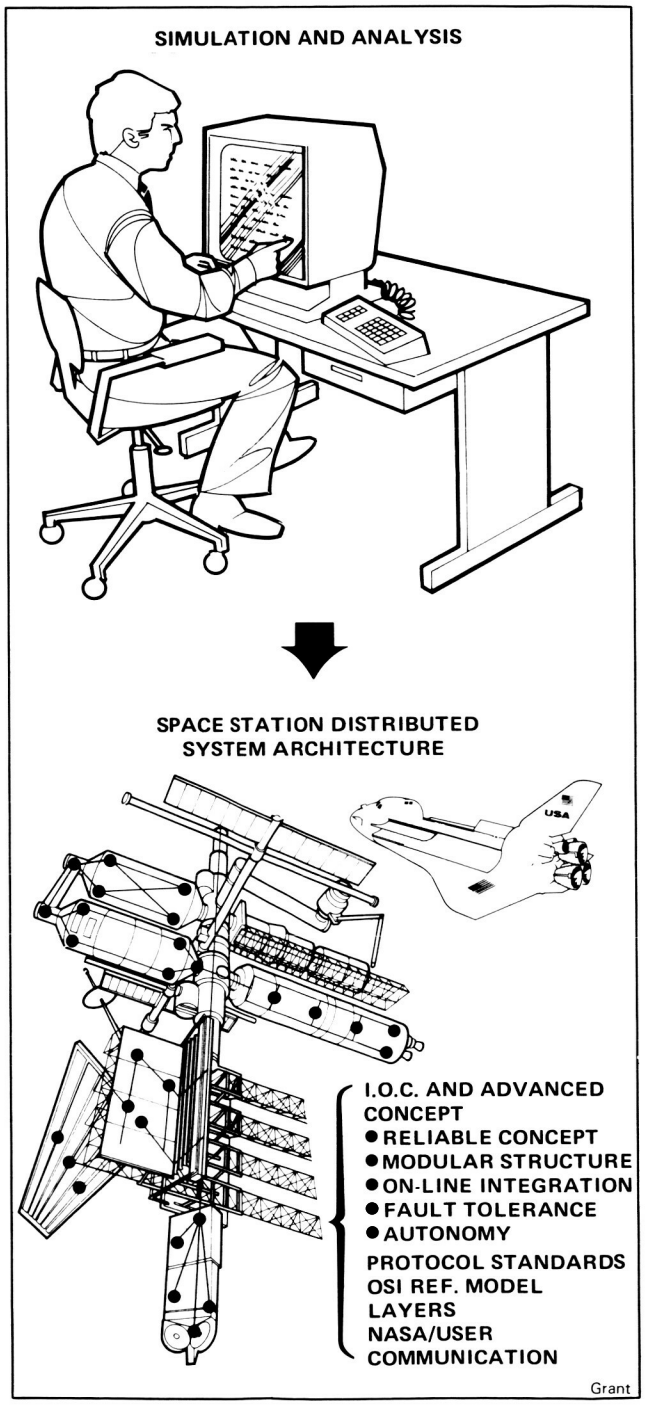

Commercial workstation and local area networks system

Automated Airborne Astronomical Flight Planning Tool

The 1985-86 appearance of Halley's Comet will provide the first precise observations at other than visible-light wavelengths. Two space probes and numerous Earth-based instruments will be used. Of the latter, the Ames Research Center's Kuiper Airborne Observatory (KAO) provides one of the best capabilities for infrared observations.

The KAO mounts a 1-m infrared telescope in a C-141 aircraft capable of flying at altitudes of up to 45,000 ft (13,500 m). This altitude eliminates much of the atmospheric attenuation and background radiation that hampers ground-based observation. The telescope looks out through an open port in the aircraft's left side. It has a range of elevation from 30° to 70° above the aircraft horizon, but only negligible motion along the aircraft axis. The telescope azimuth is, therefore, set by adjusting the aircraft heading. Once observation begins, the object's apparent position determines the aircraft's momentary heading, and thus its track. This is the primary limitation on KAO use.

The Kuiper Airborne Observatory Scheduler (KAOS) is an experimental knowledge-based system for scheduling KAO flights. The basic algorithm involves generation of possible flight legs and testing them against the operational constraints. Since KAOS was designed for rapid generation and testing of observation legs, it was suggested that it be used to search for near-circular observation tracks for observing the comet Halley. The method chosen was to generate sets of possible observation tracks at regular invervals over the time periods of interest.

Initial survey runs were made on the basis of round-trip flights from Sydney, Australia. KAOS was given a grid of nearby starting locations and ranges of starting times and observation times. The resulting search space proved too large for KAOS to deal with. It was decided to eliminate the time dimension by using the interchangeability of time and longitude. This gives a manageable search space at the expense of somewhat abstract results. It soon led to the concept of longitude free maps in which the actual starting longitude and time are parametrically related.

The longitude-free survey insert on the chart shows the results of the search for near-circular observation tracks. As can be seen, none of these tracks closes on itself; rather, the tracks appear more "U" shaped than circular or closed. The time cost for closing the "U" is about 3 to 4 hr even in these best cases, and is typically much more. Flights of about 10 hr would be needed to make efficient use of such tracks.

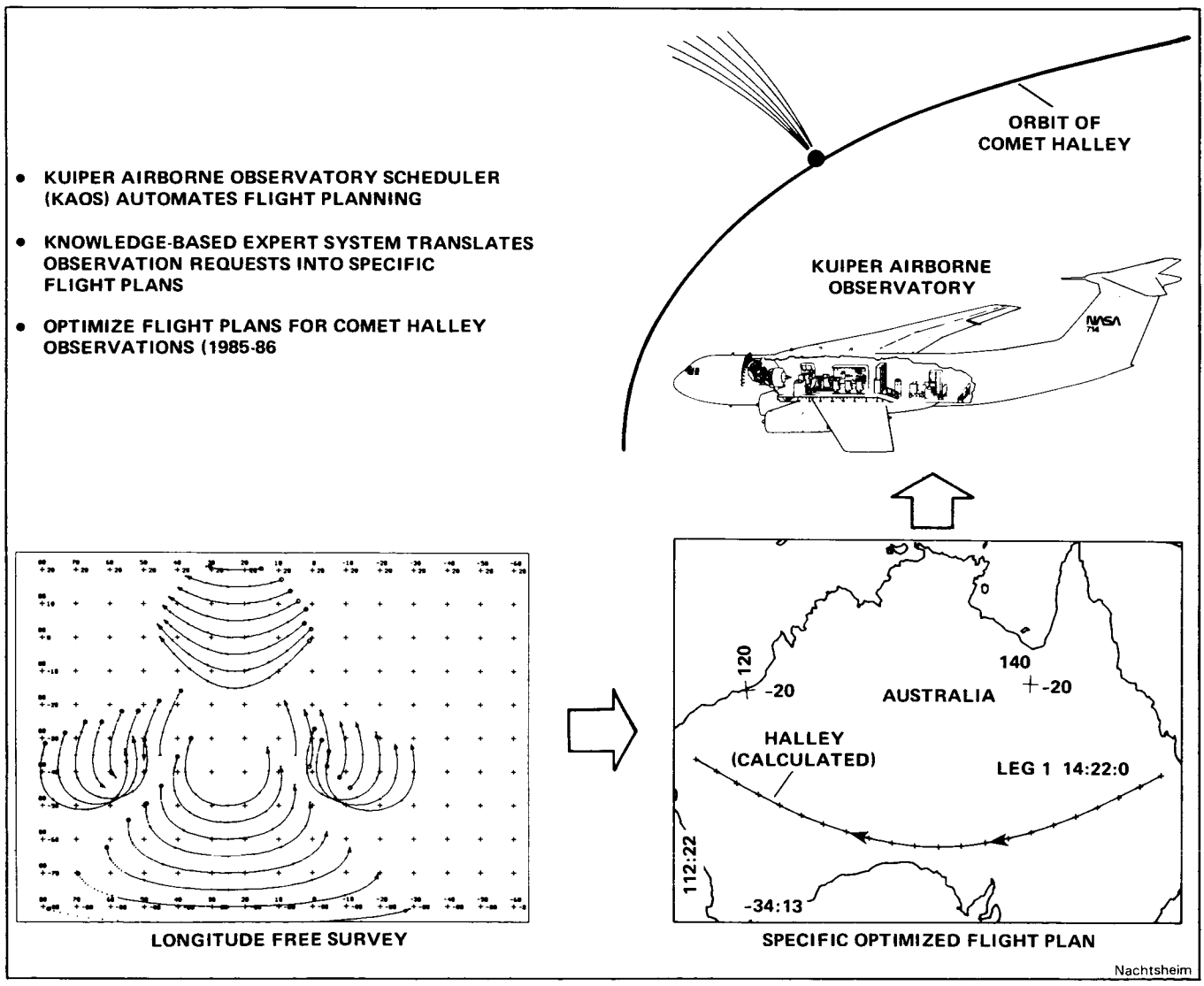

KAOS experimental knowledge-based system

The survey does point out some opportunities for long point-to-point observation legs for Comet Halley. In November 1985 there are possible flights from the northeast U.S. to Moffett Field. In April 1986 there are several possibilities for flights over Australia. During April 8-17, westward flights can be made across northern Australia at about latitude -20. A flight for April 10 is shown in the insert "Specific Optimized Flight Plan" on the chart. During April 18-31 there are eastward tracks south of Australia accessible on a Perth-Sydney or Perth-Melbourne basis.

(P. Nachtsheim, Ext. 6526)

Generalized Leading Edge Modifications for Increased Cl max of NACA 6-Series Airfoils

A simple method for altering the leading edge of any of the widely used NACA 6-series airfoils has been developed. This method requires only the use of a hand-held calculator and applies a mathematical function to the upper surface of a cambered airfoil or to both surfaces of an uncambered airfoil. The application of this function increases the bluntness of the leading edge, adds forward camber to the airfoil, and does not introduce any discontinuities in curvature, including the region where the original airfoil and modified airfoil blend into a single contour.

Increasing the forward thickness of the NACA 6-series airfoils will reduce the adverse pressure gradient near the leading edge on the upper surface at high angles of attack, and will result in an increased Cl(max). An increased Cl(max) will offer improved stalling characteristics, slower and shorter landings; and the reduced drag at higher lift coefficients will result in an improved rate of climb. This method can be used to modify any widely used existing NACA 6-series airfoil or as a design tool for developing airfoils which require a high Cl(max).

(S. Cliff, Ext. 5656)

V/STOL Fighter Configuration Aerodynamics

The aerodynamics of supersonic V/STOL fighter/attack aircraft are the subject of an ongoing research program in the Aerodynamics Division at NASA Ames Research Center. In this joint NASA, Navy, and industry program, resolution is sought of key aerodynamic uncertainties associated with contractor-defined concepts through the use of a variety of aerodynamic prediction methods, and extensive wind-tunnel testing. Both twin- and single-engine aircraft configurations are being investigated.

Three wind tunnel tests were conducted in FY85 on two single engine V/STOL fighter models. One model, a 1/9-scale representation of the General Dynamics E-7 concept, was tested in the Ames 9- by 7-Foot Supersonic Wind Tunnel at Mach numbers from 1.6 to 2.2. The other model, representative of the McDonnell Douglas 279-3 concept, was tested in the Ames 12-Foot Pressure Wind Tunnel and in the 9- by 7-Foot Tunnel, at a Mach number of 0.2 up to 90° angle of attack. All of the tests included investigations of the effects of Mach and Reynolds numbers on the longitudinal and lateral/directional aerodynamics, stability and control power about all three axes, effects of alternative configurations, and component buildup. Thorough analyses by both General Dynamics and NASA of the test data for the E-7 concept reveal that it is a viable design for a high-performance V/STOL fighter aircraft, considering the generally favorable agreement of the predictions with the test data. Analyses of the data for the 279-3 concept are focusing on the relative merits of canard-wing, wing-horizontal tail, and three-surface configurations.

The completion of the three tests this year marked a major milestone for this V/STOL fighter research program, in that tests of five models (three twin and two single engine) have now been completed in three Ames wind tunnels (the other tunnel is the 11- by 11-Foot Transonic Tunnel) covering a Mach number range from 0.2 to 2.5. The figure shows the installations of the models in the tunnels. These tests have resolved many aerodynamic uncertainties particular to each concept, and have established a large, comprehensive design base on realistic configurations.

(D. Durston, Ext. 6216)

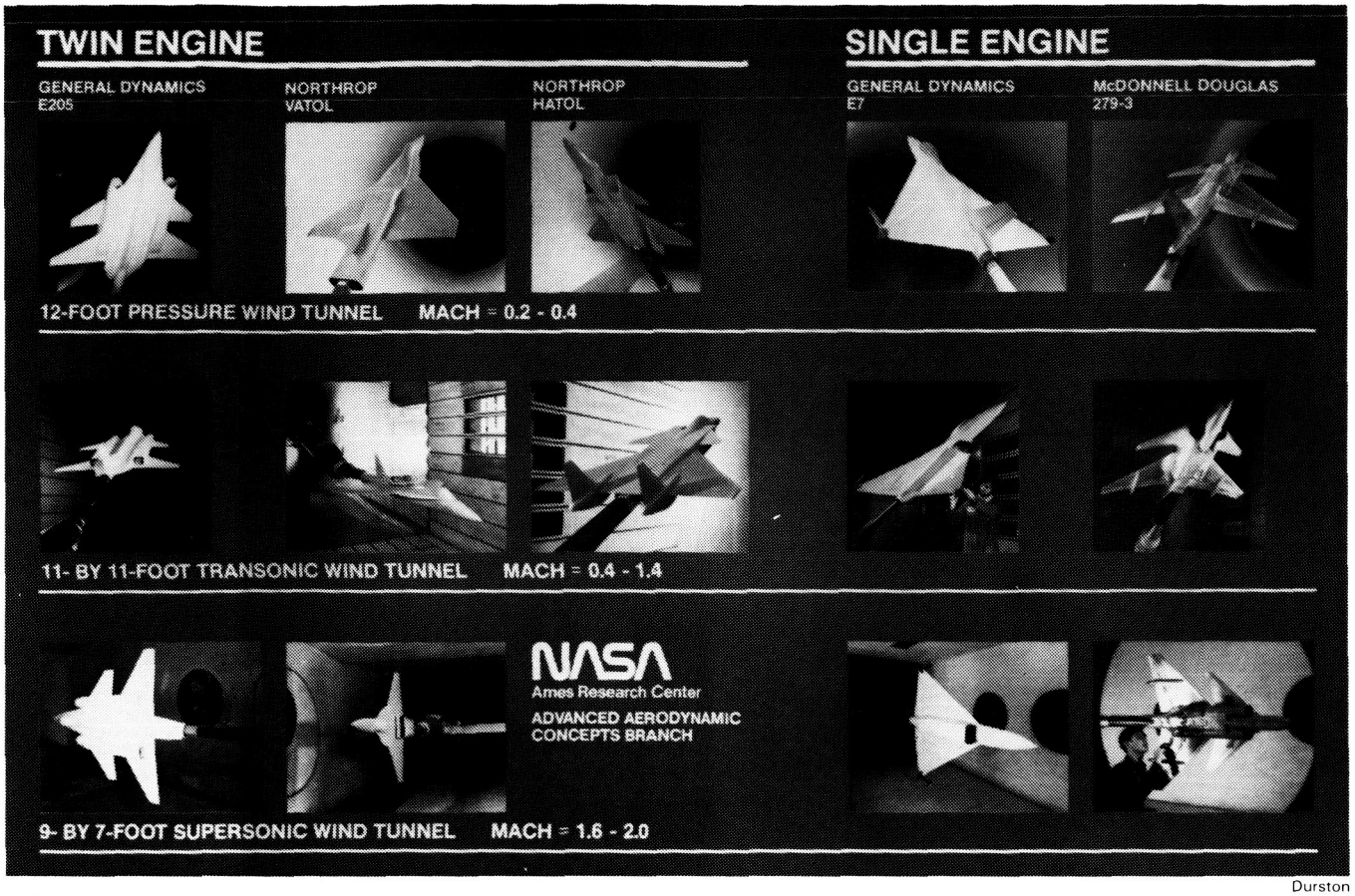

Durston

V/STOL fighter/attack aircraft aerodynamic research

Transonic PAN AIR Development

Linear PAN AIR currently solves the Prandtl-Glauert equation for subsonic or supersonic flow about complex aircraft configurations. Considerable experience and expertise has been developed in aerodynamic modeling with surface paneling methods. PAN AIR allows the aircraft designer much flexibility in creating his geometry, for instance, obtaining the surfaces from a CAD/CAM system. Because this ease of treating geometry, panel methods are a relatively fast and reliable method of analyzing new aerodynamic concepts.

By combining PAN AIR's higher-order source and doublet panels with a rectangular grid, transonic flow with shocks can be calculated. This has been previously demonstrated in two dimensions and three dimensions with linearized boundary conditions. The basic geometry scheme consists of a rectangular grid which penetrates the configuration and extends only to the linear region of the flow field as illustrated. This eliminates the

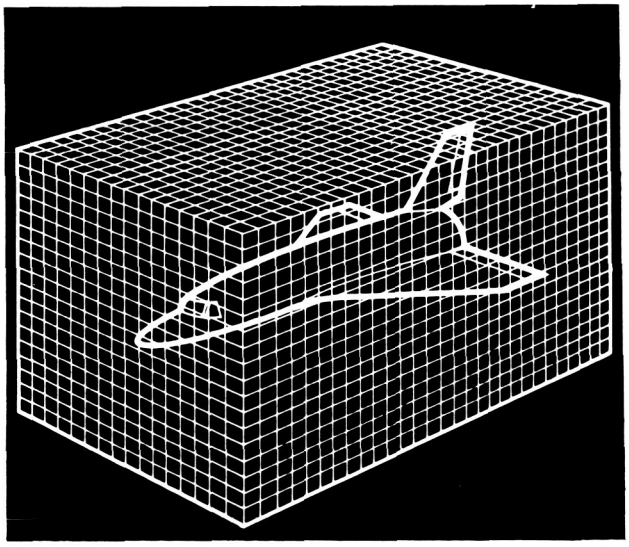

Woo

Schematic representation of an aircraft embedded within a rectangular grid. The grid penetrates the interior of the aircraft

problems of body-fitted grids and retains the ease of manipulating surface panels instead of volume meshes. The approach is now being developed through a contract with the Boeing Company. The goal is to demonstrate that a test-bed version of PAN AIR will solve the nonlinear full-potential equation for transonic flow about complete, realistic aircraft. (For instance, the first substantial test case will be the F-16A displayed. This test-bed code is now called TRAN AIR.)

(A. Woo, Ext. 6133)

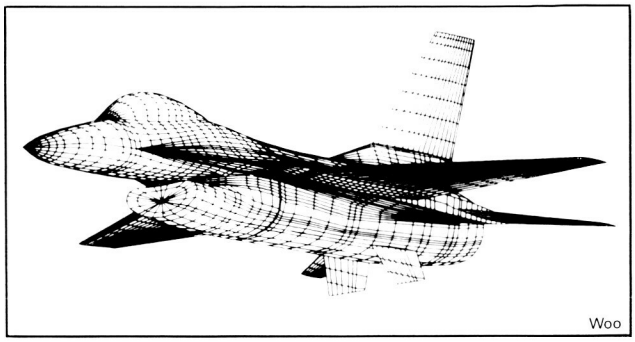

The first large test case is an F-16A geometry modeled with 3000 panels. Wing tip missiles and an external fuel tank will be added

Turbulence Model Improvements for Application to Transonic Airfoils

A focused, experimental research effort is under way at Ames to provide a basic understanding of the turbulence in flow fields of primary aerodynamic interest, and to use this information to guide the development of turbulence models required for accurate computations in computational fluid dynamics (CFD). The measurements employ the latest developments in instrumentation and computer-aided data handling and interpretation, e.g., three-dimensional laser velocimeters and hot-wires, holography for density and pressure measurements, and laser-oil film interferometers for skin-friction measurements.

Several of these experiments have led to turbulence-model improvements. An example of this is shown in the figure which represents the surface pressure coefficient over a portion of a model consisting of a cylinder with an axisymmetric convex bump. The axial region covered in the figure is the latter 60% of the chord of the bump and an equal distance on the downstream cylinder. At the two higher Mach numbers indicated, a shock wave develops at about X/C = 0.6, which is sufficiently strong to separate the flow. When these data were attempted to be calculated with a standard mixing length turbulence model, the dot-dashed curve on this figure resulted. The calculated shock wave was found to be much further downstream than was the actual shock wave. A careful analysis of the turbulence data suggested an improved model could result from introducing a lag in the development of the turbulence. Indeed, when this model is introduced in computations the results, shown by the solid line, reveal a marked improvement. It was also found that a popular higher-order model that also failed to predict the data, could also be modified through the use of wall functions to yield results

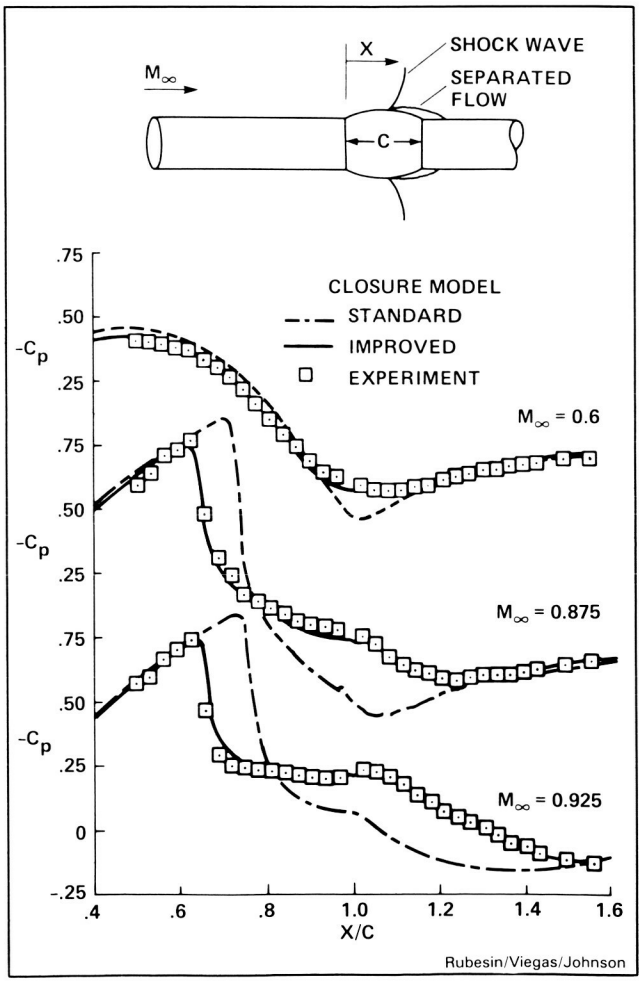

Comparison of measured and computed pressure distributions on an axisymmetric bump in transonic flow

in good agreement with the data. Similar improvement has been achieved in predicting the surface pressure on a NACA 64A010 airfoil in transonic flow at an angle of attack where shock induced separation occurs.

(M. Rubesin, J. Viegas, and D. Johnson, Ext. 6452/5950/5399)

Transonic Separated Solutions for the Augmentor Wing

The Augmentor-Wing has been described as having several aerodynamic advantages over a more conventional, single-foil, supercritical section of the same overall thickness-cord ratio. TAUG is a full-potential code developed to solve the multielement airfoil configurations of the augmentor-wing type. This code uses a fully implicit approximate factorization scheme (AF2) to solve the transformed full-potential equation in a general, nonorthogonal, body-conforming coordinate system. TAUG has been coupled with a boundary-layer and viscous-inviscid interaction algorithm. The viscous flow is modeled by solving the partial-differential boundary-layer equations using a predictor-corrector marching algorithm. To avoid singular behavior at the separation point, near- and in-reversed flow, the equations are solved in the inverse mode (i.e., either the wall-shear stress or the wake-centerline velocity is specified). Computational results are compared with experiment for a flow with a freestream Mach number of 0.7 and an angle of attack of 1.05°. Typical results obtained from the augmentor-wing viscous-inviscid code on a CRAY-Xmp computer required about 3 min of CPU time for a three-order-of-magnitude drop in the maximum initial residual on a 225X60 grid. The low cost of running the code makes it very economical in numerical optimization studies designed to obtain ideal aerodynamic surface shapes.

(J. Flores and W. Van Dalsem, Ext. 5369/6741)

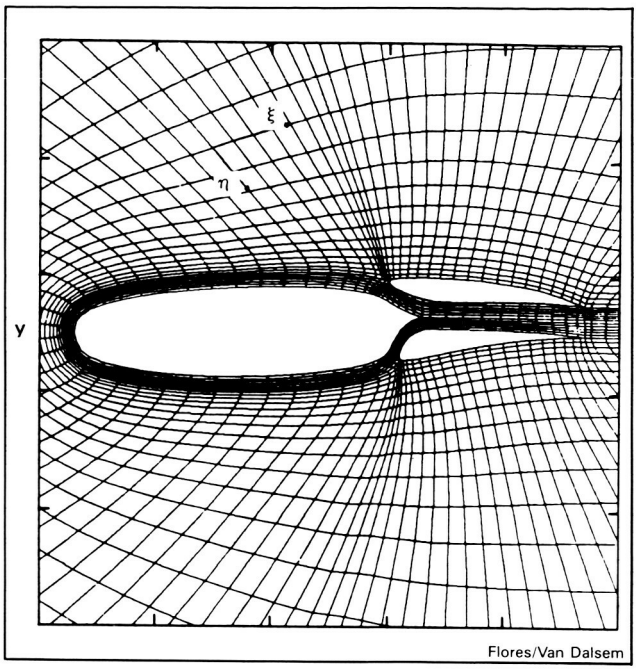

Augmentor-wing grid

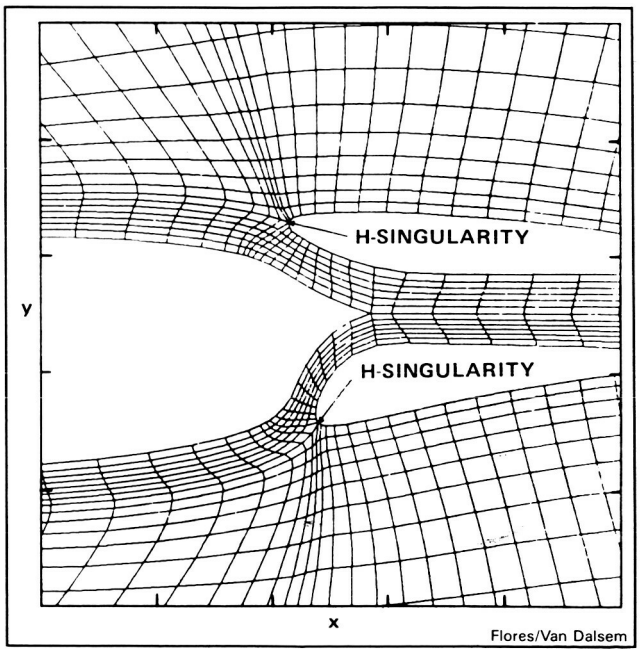

Expanded view of throat region

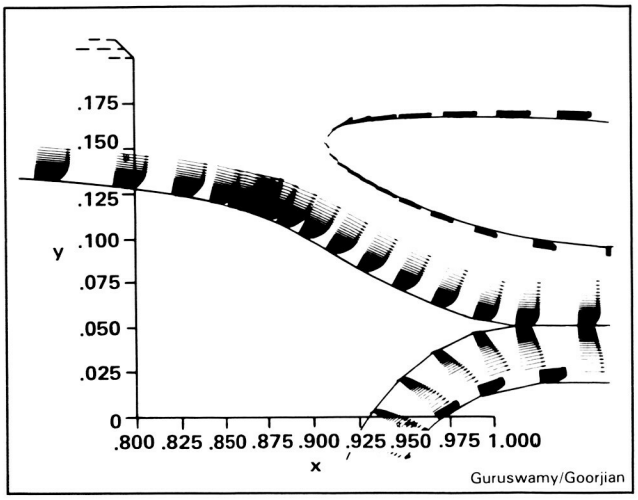

Velocity profiles in throat region

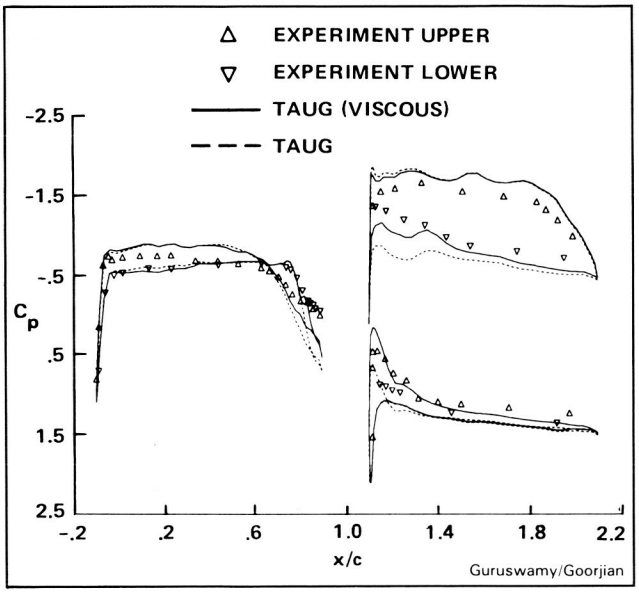

Pressure distribution MINF = 0.7, α = 1.05°, Re = 12.6 million

Transonic Aeroelastic Analysis of the B-1 Aircraft

Flight tests of the B-1 aircraft (which has a variable sweep wing), have indicated aeroelastic oscillations at transonic Mach numbers. Depending on the flight conditions, the B-1 aircraft flies at either 25.0° or 67.5° sweep angles. At both sweep angles, aeroelastic oscillations were observed at transonic Mach numbers at high angles of attack. Subsequent wind-tunnel tests conducted in the Ames 11- by 11-Foot Transonic Wind Tunnel also showed angle-of-attack-dependent aeroelastic oscillations at transonic Mach numbers. A theoretical analysis was conducted to complement both flight and wind-tunnel tests, with the goal of understanding the oscillatory phenomenon of the B-1 wing.

For the first time, a theoretical analysis was made by using the NASA Ames code, ATRAN3S, which has the unique capability of simultaneously integrating the transonic aerodynamic and structural modal equations of motion. Aerodynamic and aeroelastic analyses were conducted at 25.0° and 67.5° sweep angles for various Mach numbers and angles of attack. For both sweep angles, the wing was modelled close to the actual wing, both aerodynamically and structurally.

For the low-sweep case of 25.0°, aerodynamic results compared well with the wind-tunnel results, both at subsonic and supersonic Mach numbers. At this sweep angle, aeroelastic-response analysis was conducted for the transonic case at M = 0.72, angle of attack of 3.7°, and altitude of 33,000 ft. At these conditions, small oscillations were observed during the flight test of the B-1 aircraft. Response computations were initiated by giving an arbitrary modal displacement and simultaneously integrating aerodynamic and structural

equations of motion. Analysis indicated that the wing is stable at these conditions. However, the pressure distribution at the final stable aeroelastic position showed a transonic flow with a strong shock wave. The presence of the strong shock wave suggests that the wing may oscillate owing to a combined effect of the shock wave associated with the buffet phenomenon. The strong aeroelastic damping observed from the response analysis indicates that oscillations caused by buffet will be of small amplitude and will not affect the performance of the aircraft. This further verifies the observations made in both flight and wind-tunnel tests.

Flight and wind-tunnel tests had also showed aeroelastic oscillations of significant amplitude for the sweep angle of 67.5° at transonic Mach numbers at a high angle of attack. Both aerodynamic and aeroelastic computations were made for this sweep angle. Steady results from the code compared fairly well with the experiment at small angles of attack. At higher angles of attack, the results from the code deviated substantially from the experiment. The differences between the experiment and the code were due to the leading edge vortex formed in the experiment which was not modelled in ATRAN3S. A response analysis was conducted at the small angle of attack where the vortex had not formed and showed a low aeroelastic damping. The rate of damping for this case was a lot smaller than that observed for the 25.0° sweep. This small damping associated with the formation of a leading-edge vortex observed in the wind tunnel might have caused the aeroelastic oscillations of the B1 wing at higher angles of attack. Before this study, it was proposed that the observed oscillations in the flight tests were due solely to the presence of shock waves. But, at higher angles of attack, the calculations did not show shock waves as had been previously proposed. From this study, an alternative source for the oscillations observed at higher angles of attack has been proposed to be the leading edge separation vortices.

(G. Guruswamy and P. Goorjian,
Ext. 6329/5547)

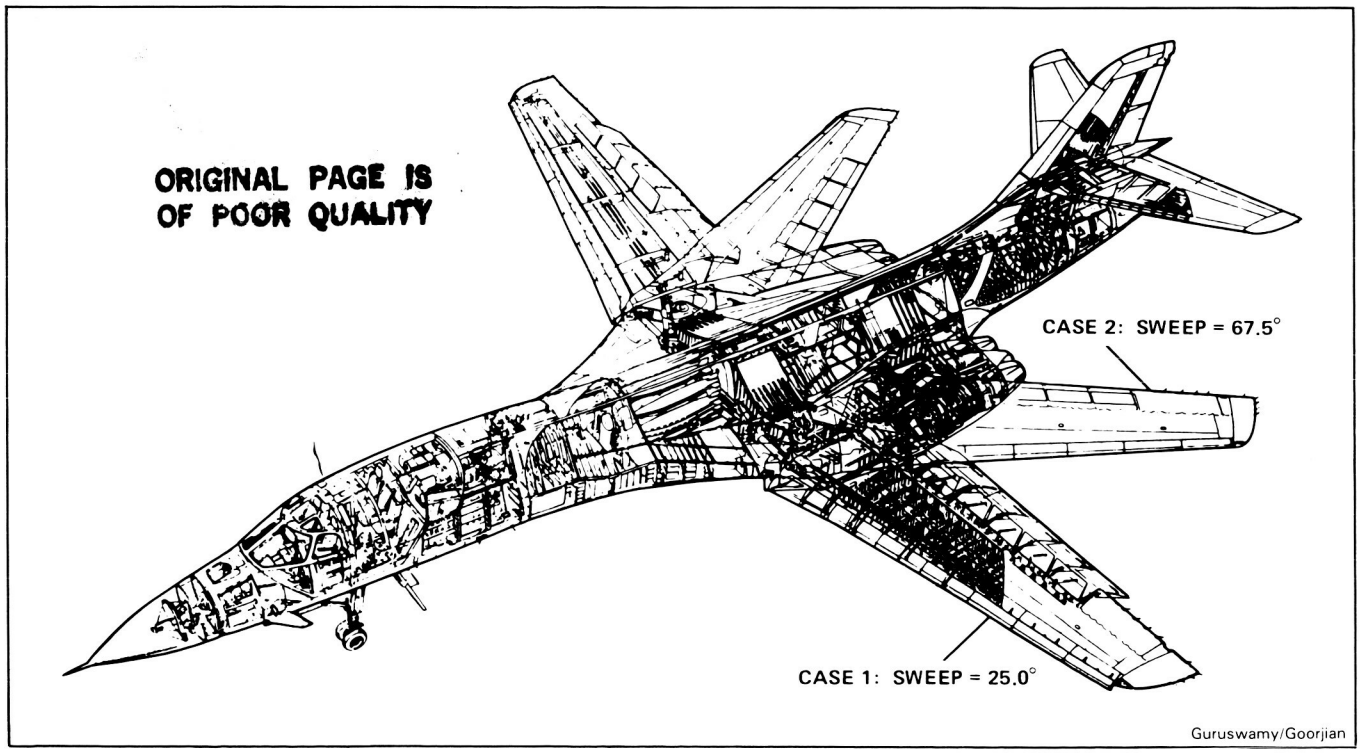

B-1 aircraft

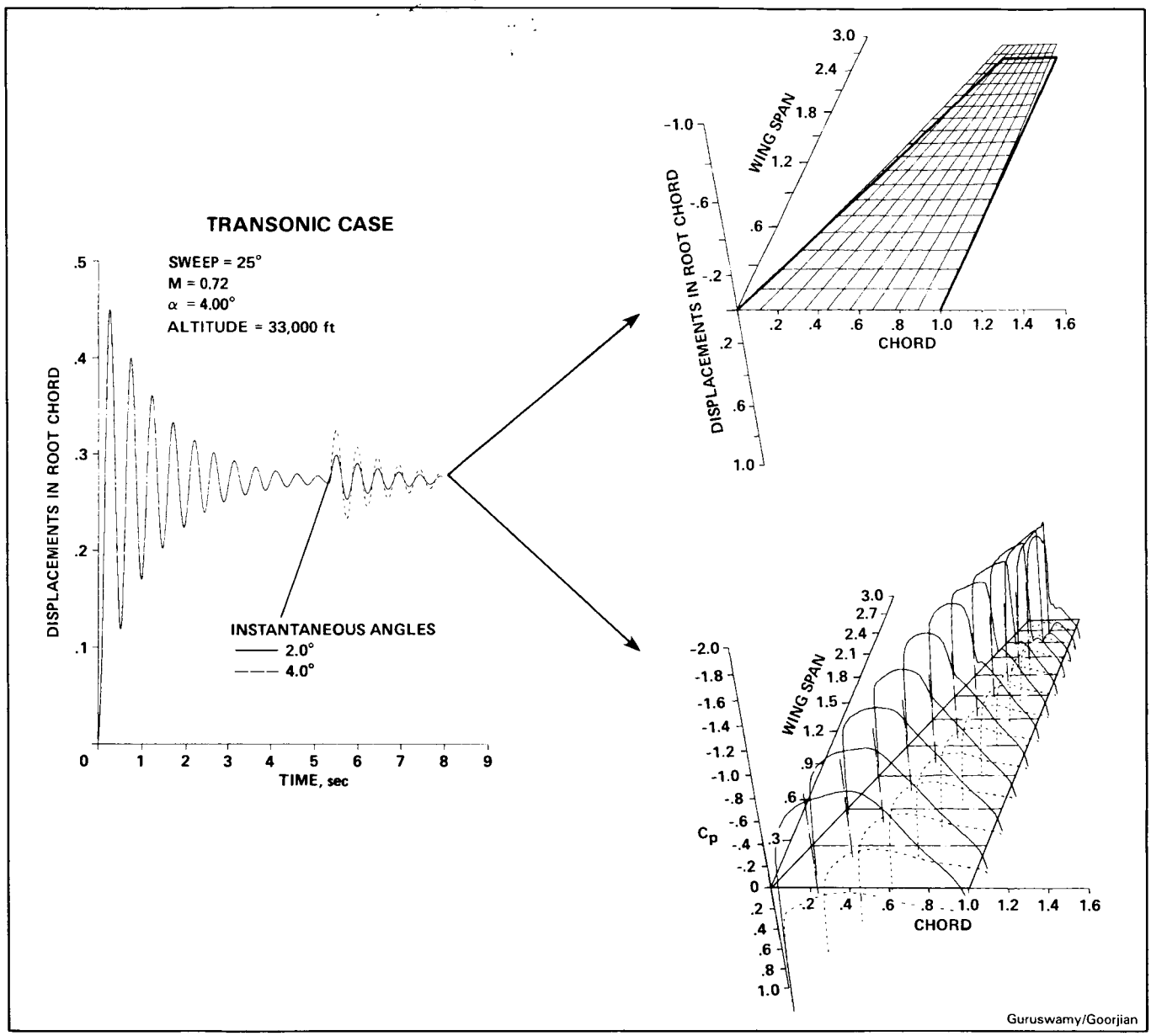

Aeroelastic response for 25° sweep

Computation of Transonic Separated Wing Flows Using an Euler/Navier-Stokes Zonal Approach

The accurate prediction of transonic, separated flows on wings is of prime importance to a designer. These flows are frequently encountered in high Reynolds-number regime, and/or during a high angle-of-attack maneuver of a fighter aircraft at transonic speeds. Presently, an understanding of separated flows mainly stems from the surface oil-flow techniques used in wind-tunnels. However, via supercomputers, the role of computational fluid dynamics (CFD) for simulating such flows has advanced quite significantly. Contributing to the CFD efforts, a computer code, Transonic Navier-Stokes (TNS), was developed in 1984-85. The TNS program solves the Euler/Navier-Stokes equations around aerodynamic bodies using a zonal method. In this method, the physical domain of interest is divided into zones, and the proper governing equations are solved interactively.

During 1985, impressive transonic, separated-flow solutions around wings were obtained by using the TNS program. The computations were in close agreement with experiment. An example simulation is shown in the accompanying figure. This figure displays an experimental surface oil-flow photograph and computed skin-friction lines (or computational oil-flow) for WING C. WING C is a generic, low-aspect-ratio wing designed by NASA Ames and Lockheed-Georgia under a cooperative program. The flow conditions were a free-stream Mach number of 0.85 at an angle of attack of 5° with a Reynolds number based on mean aerodynamic chord of 6.8 million. Note the close agreement between the experiment and computation for the separation zone. A separation front exists near the tip, parallel to the leading-edge at approximately 30% chord, both in the experiment and the computation. This simulation was achieved by using four grid zones with a total of 168,000 mesh points around the wing; the computation took about 3 hr on the Cray-XMP computer installed at NASA Ames.

(U. Kaynak and T. Holst, Ext. 6032)

Experimental oil flow

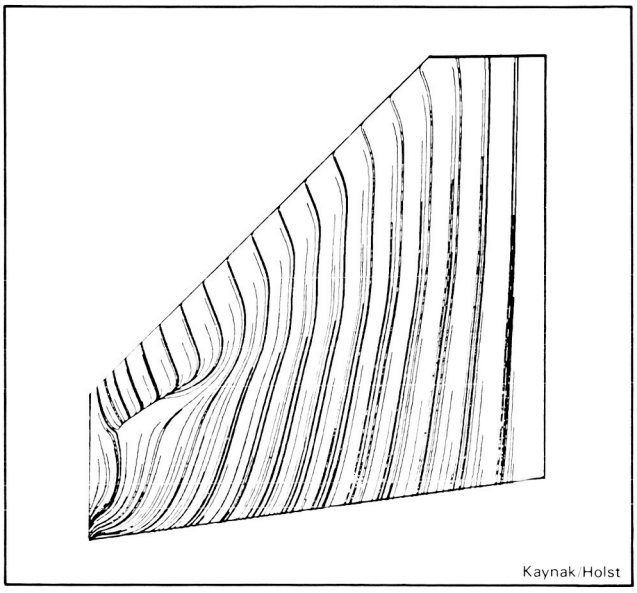

Computed oil flow

Space Shuttle Main Engine Power Head Flow Analysis

An upgrade of the Space Shuttle main engine (SSME) power head is under way to substantially increase the operating margin and the engine durability. The goal of the current engine redesign effort (Phase II+) is to increase the rated thrust of the SSME to 109% by 1989.

The incompressible Navier-Stokes code (INS3D) was utilized in the computational analysis of the hot gas manifold (HGM). As a result of the subsequent parametric studies, significant changes have been made to the HGM which allows additional margin at higher power level. All contemplated HGM changes have been validated with the code, and significant improvements were found. For example, in searching for an improved turn-around duct, over 20 configurations were investigated using the computational method with the outcome that one was chosen which produces the most favorable flow conditions. In addition to the reshaping of the turn-around duct, redesign includes changing fuel transfer from three circular ducts to two large area ducts. Later testing using cold air flow validated these computational results. This is the first time the computational fluid dynamics (CFD) has been used so extensively as a design and analysis tool in the SSME program, or perhaps throughout the rocket industry.

The flow through the main injector assembly, where the liquid oxygen (LOX) posts were modeled by a porous medium, was also simulated. This revealed the nature of the flow through this region of the SSME power head as well as the pressure drop through the rows of the LOX posts. To determine the loads on the LOX posts, details of the flow around single and multiple posts were simulated. These simulations exhibited very interesting vortex structure and would eventually help in designing the post assembly.

(D. Kwak, Ext. 6743)

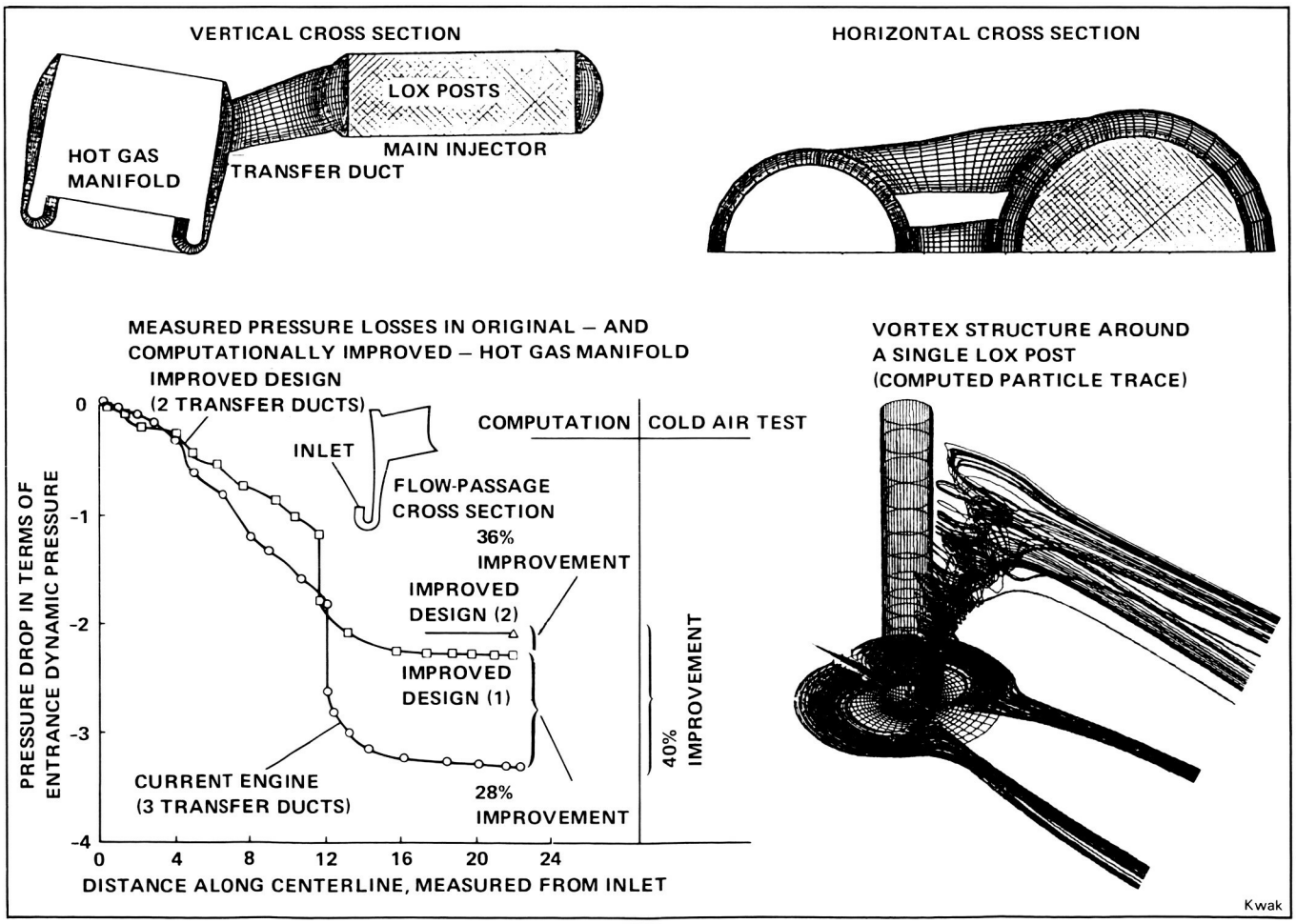

Computer model of SSME power head

A Simulation of Rotor-Stator Interaction Using Patched and Overlaid Grids

The aerodynamic processes associated with the flow of fluid through turbomachines pose one of the most difficult challenges for the computational fluid dynamicist. The unsteady nature of the flow, the complex geometries involved, the motion of some parts of the system relative to others, and the periodic transition of the flow from laminar to turbulent are some of the factors that contribute to the complexity of the problem. A clear understanding of these types of flows is essential for the optimization of the performance of turbomachinery.

Recent efforts in the use of multiple grids for solving geometrically complex problems indicate that performing calculations on multiple grids, which are either patched together or overlaid on top of each other, is a relatively straightforward task. The multiple-grid technology (both patched and overlaid multiple-grids) is now at a point where it can be routinely used to solve problems in two spatial dimensions. An obvious candidate for this new technology is the rotor-stator interaction problem. The motion of the rotor with respect to the stator makes it impractical to wrap a single grid around both the rotor and the stator airfoils. It is much simpler to use two grids, one around the stator and the other around the rotor, and to have these grids move relative to each other along a common boundary.

Two test problems have been successfully solved to date to demonstrate the feasibility of performing rotor-stator interaction studies with patched grids. The first test problem to which the patched-grid technology was applied consisted of two circular-arc airfoils moving relative to each other. The unsteady Euler equations were solved to simulate the flow through this system. The Mach number used for this calculation was supersonic (M = 1.5). The figure shows the geometry of the configuration and the pressure contours at a particular instant. The periodic-boundary conditions imposed on the upper and lower boundary results in a flow that is periodic in time. The calculation was time-accurate and reproduced the time-periodicity of the flow accurately. An important feature to be noticed in the figure is that the pressure contours are continuous across the patch-boundary along which the two H-grid used slip past each other (thus indicating a distortion-free transfer of information across the patch-boundary).

The second test problem consisted of low-speed turbulent flow (M = 0.07, Re = 100,000/in.) over a rotor-stator configuration of an axial-turbine. The calculation was performed using the unsteady, thin-layer Navier-Stokes equations. The second figure shows the geometry of the configuration and the unsteady shedding of vortices by the system (the unsteady component of the velocity-vector field is used to depict this phenomenon). The third figure shows the time-averaged pressure distribution on the stator airfoil (the flow is periodic in time). The comparison between the numerically simulated values and experimental results is good.

The moving-patch technique is not limited to rotor-stator interaction studies but has a multitude of applications in the general area of flows about bodies that move relative to each other. In particular, the capability should prove to be very useful in simulating propeller-nacelle interaction, helicopter rotor-fuselage interaction, and the flow

Rai

Pressure contours for the circular-arc airfoil rotor-stator configuration

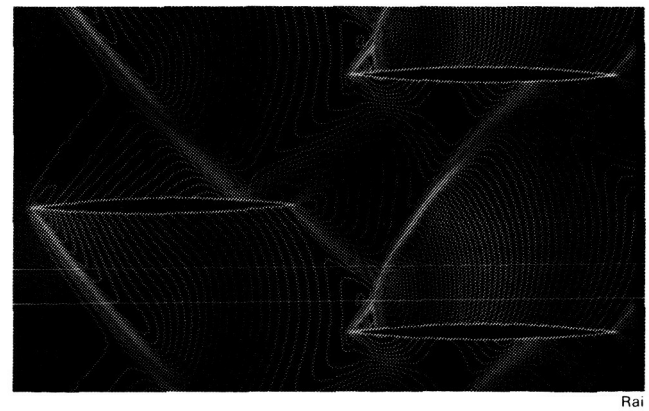

Rai

A Navier-Stokes simulation of rotor-stator interaction

about the counter-rotating propfan. Current research is focussed on performing a multiple blade calculation (several airfoils in each row) and extending the capability to three spatial dimensions.

(M. Rai, Ext. 6742)

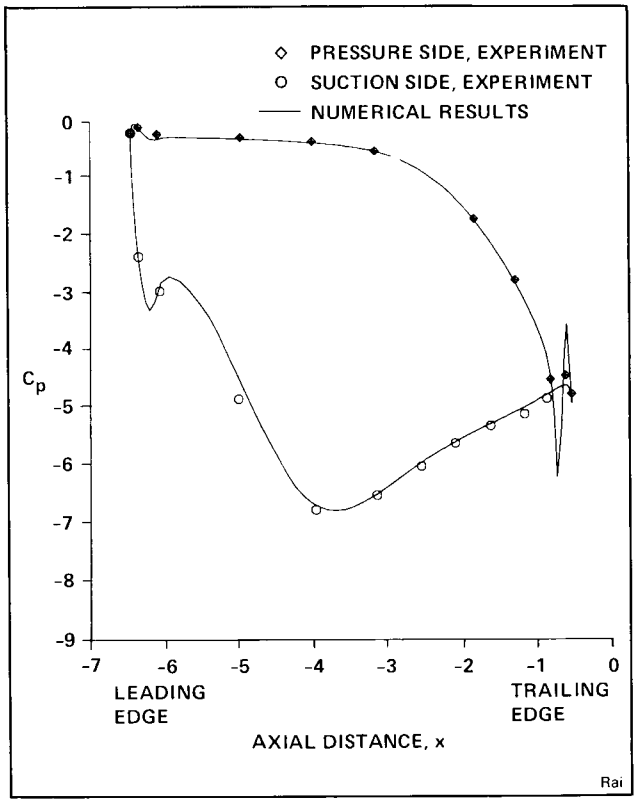

Time-averaged pressure distribution on the stator

Fast Simulation of Separated Three-Dimensional Flows

A computer code was developed which is capable of simulating unsteady separated three-dimensional shear layers using a minimum of computer time. The approach used is to solve the unsteady partial-differential boundary-layer equations in either the direct or inverse mode using a time-relaxation procedure. Both time-accurate and fast steady-state options are available. The code has been applied to a wide range of separated three-dimensional flows, two of which are shown below. Applications for the new code include computation of flows using a viscous-inviscid interaction scheme, acceleration and verification of Navier-Stokes algorithms, and the evaluation and improvement of turbulence models.

(W. Van Dalsem, Ext. 6741)

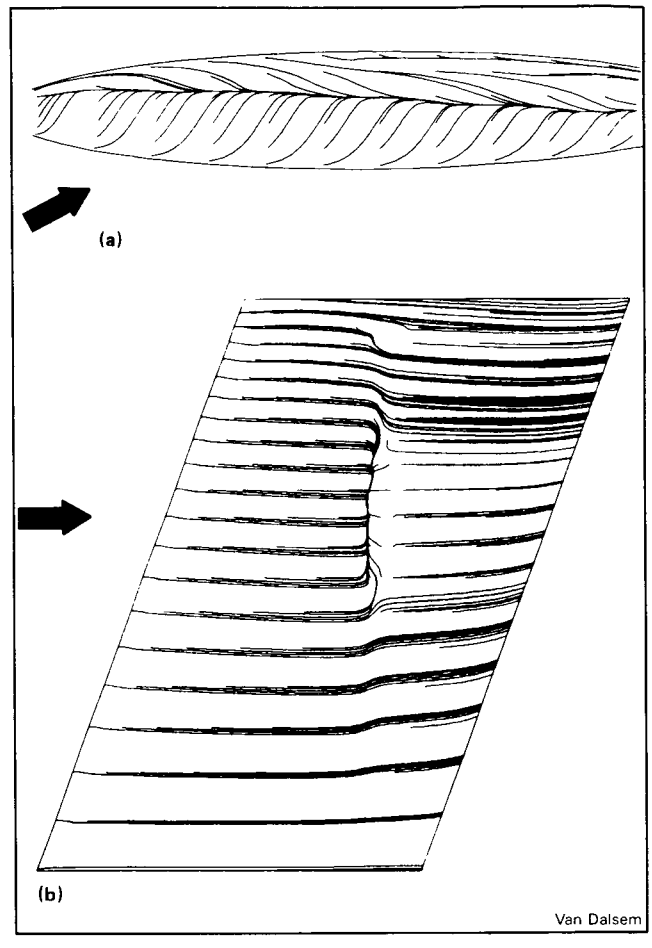

Computed near-surface particle paths for the flow over: (a) 6:1 prolate spheroid; (b) NACA 0012 wing in transonic flight

Large Eddies in a Supersonic Turbulent Boundary Layer

To date, virtually all research into the structure of turbulent boundary layers has been carried out in low-speed, incompressible flows. In an ongoing study, single and dual hot-wire probes have been used to accomplish a first look at the large-eddy structure of a supersonic turbulent-boundary layer. The investigation was performed in an axisymmetric turbulent-boundary layer in the Ames

High Reynolds Number Wind Tunnel. The free-stream Mach number was 2.9; the boundary layer was approximately 1.3 cm thick; and Re_δ = 194,000. The quantities measured were: streamwise turbulence intensity of mass-flow fluctuations; convection velocity of eddies of various length scales; space-time correlations of instantaneous streamwise velocity at two locations; and spectra, autocorrelations, and higher order statistics of the fluctuating hot-wire output signals. Conditional sampling of the hot-wire signals was performed to detect the passage and describe the character of the large turbulent eddies. Results indicate that the large scale structure in compressible turbulence is similar to that at low subsonic-flow speeds.

(S. Robinson, Ext. 6156)

Development of a New Laser Doppler Velocimeter System for the High Reynolds Number Facility (HRC-II)

A new two-channel laser Doppler velocimeter (LDV) has been successfully operated at the Ames HRC-II facility. A unique and innovative approach was required to overcome difficulties imposed by the design of this transonic blow-down tunnel. The plenum chamber, which enclosed the vented test section precluded direct optical viewing of the model. A dual optical assembly using computer-controlled scanning mirrors inside the plenum with fiber-optic transmission of the Doppler signal overcame this difficulty. Motion-tolerant mounting of the optical assemblies was used to permit expansion of the pressurized plenum while preserving alignment of the 10 meter-long laser beams.

Seegmiller

LDV system for Ames HRC-II

A new seeding system was devised to permit injection of 0.5-μ diam polystyrene latex particles in the settling chamber without depositing seed material on the test-section windows or porous side-wall suction panels. Initial measurements have been made of the velocity profiles in the turbulent wake of a supercritical airfoil.

(H. Seegmiller, Ext. 6211)

Swept Circulation-Control Research Wing

There are several ways to control the aerodynamic circulation on wings and, thus control the amount of lift. One type of circulation control that is currently under investigation is tangential blowing out of a slot located ahead of a rounded trailing edge. For some reason not entirely understood, the flow adheres to the trailing-edge surface, in what is known as the Coanda effect. The deflected flow can increase the lift of a wing section from two to five times that which is obtained by the conventional method of increasing the angle of attack. Recently, this pneumatic circulation-control method has been applied to the design of a helicopter rotor that can be stopped in flight in the X-configuration. In this configuration, it is hoped that the airspeed of the helicopter can be increased over the conventional speed, which is limited by the velocity of the rotor tips.

In support of the X-Wing project, a research wing model was built to study the effect of sweep angle on the concept of circulation control. The model was tested in the Ames 6- by 6-Foot Transonic/Supersonic Wind Tunnel over a range of sweep angles and Mach numbers. The figure shows an artist's view of the model in the tunnel with a rendition of the effect of the jet flow from the slot on the airflow around the model. The wing was mounted on the sidewall of the tunnel on a turntable that could be rotated, with a fairing to cover the mounting system. The wing section does not represent a specific shape from current X-Wing design concepts; instead, a simple 20%-thick, constant-chord ellipse was chosen that is representative of thick-wing technology. At sweep angles of 0 and 45°, surface pressures were measured at Mach numbers up to 0.75, at angles

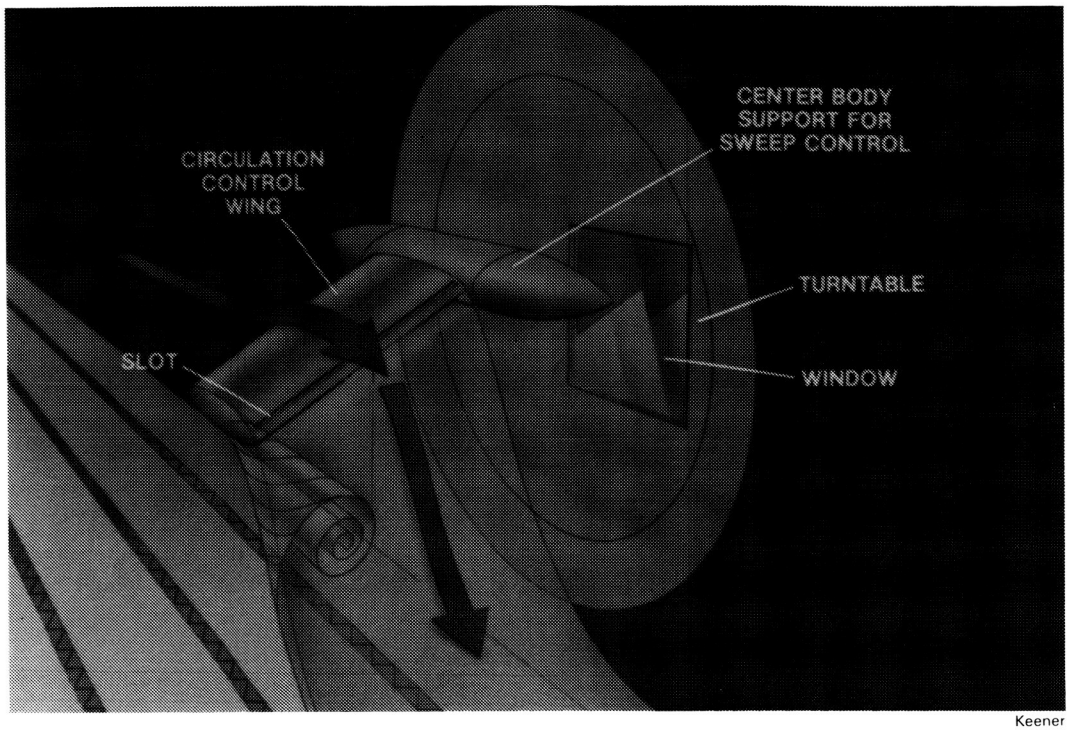

Keener

Artist's view of swept circulation-control model in Ames 6- by 6-Foot Transonic Wind Tunnel

of attack of -5° to 5°, and at blowing pressure ratios of up to three times the internal pressure. Dr. Norman Wood from the Stanford Institute for Aeronautics and Acoustics, a circulation control expert is analyzing the pressures from the standpoint of lift performance. At selected conditions, the oil-flow method was used to visualize the wing-surface and wing-tip flow pattern, and the location of Coanda-flow separation. In a cooperative effort with McDonnell Douglas Research Laboratory, Dr. Frank Spaid conducted boundary-layer velocity and flow-direction surveys from near the wing midspan to behind the trailing edge.

(L. Keener, Ext. 6260)

High-Speed Aerodynamic Prediction for Rotor Flow

A good aerodynamic-prediction method is a necessary tool in helicopter design. The present state of analytical prediction techniques used in the rotorcraft industry are limited to linear theory or are empirical in nature. There is an urgent need to develop better rotorcraft flow-prediction techniques to enable industry to design safe, quiet, and efficient rotorcraft. The goal of this study is to meet this need.

An unsteady transonic full-potential computer code, TFAR2, has been developed. This code can

provide the fundamental aerodynamic flow information for rotor-blades in prescribed unsteady motions. As an example, the delocalization phenomenon of rotor flow and onset of impulse noise can be calculated using the TFAR2 code. The phenomenon occurs for the operational-loads survey (OLS) two-bladed rotor at azimuthal angle 58° for the flight condition (advanced ratio 0.298, tip Mach number caused by rotation 0.665 and tilt forward shaft angle 5°).

(I-Chung Chang, Ext. 6396)

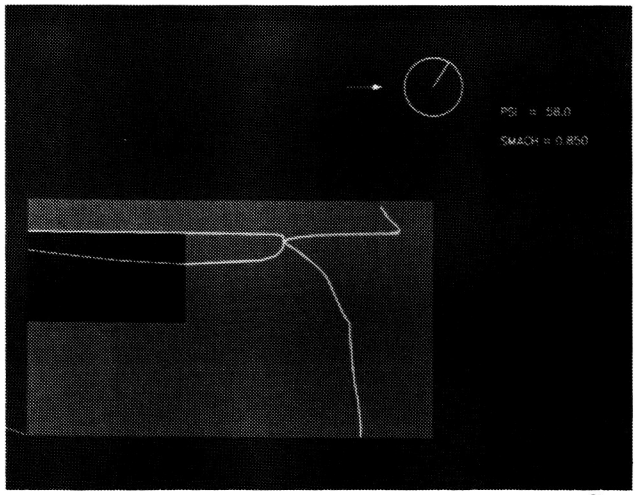

At delocalization, the inner and outer contours merge

Turbulent Boundary Layer Control for Drag Reduction

One proposed method for control of boundary-layer turbulence is the use of thin flat plates placed within the boundary layer, as depicted in the first figure. The ostensible purpose of the plates is to cause a sustained reduction in turbulent mixing within the boundary layer, thus resulting in a suppression of turbulent transport effectiveness downstream of the device. If successful, this would lead to reduced skin friction and a possibility of net drag reduction with potential application to reduction of fuselage drag on low-speed aircraft at cruise.

Research has been undertaken to experimentally study the alterations in boundary-layer properties caused by turbulence control using flat plates in the Reynolds number regime of 2000-5000 based on momentum thickness. The approach taken was to make direct, local measurements of skin friction and Reynolds

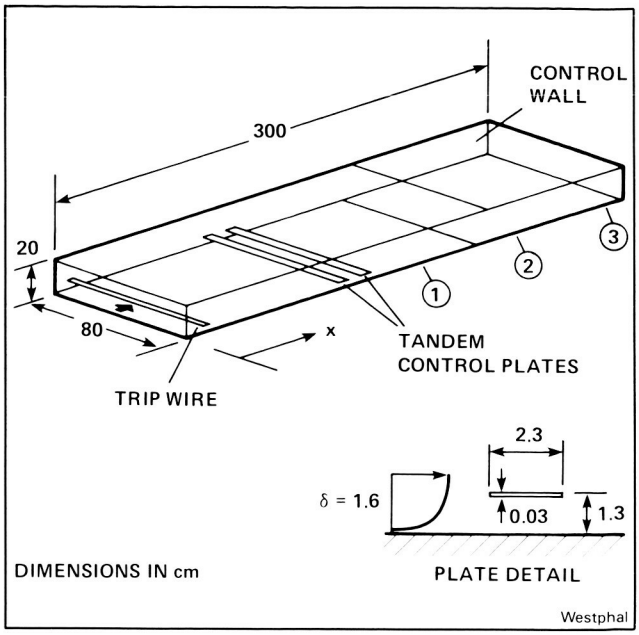

Turbulent boundary layer control for drag reduction experimental set-up

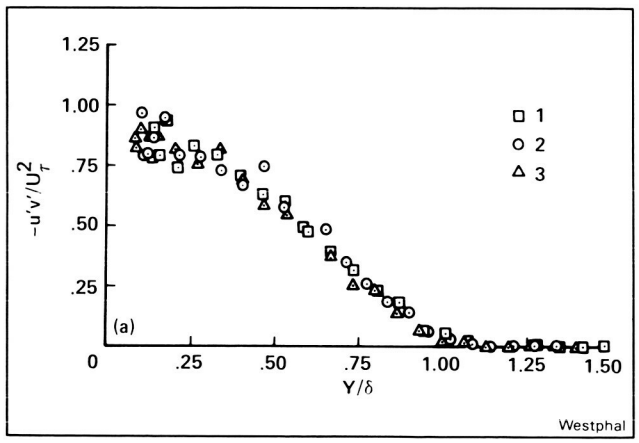

Reynolds shear stress natural boundary layer, U_o = 27.5 m/sec

stresses within the boundary-layer downstream of the control devices. Substantial effort was devoted to development of an interferometer based on the flow of a thin oil film for direct determination of the skin friction. Crossed hot-wires were employed for measurement of Reynolds stresses.

Results shown in the second figure indicate that the Reynolds shear stress was initially suppressed throughout the boundary layer by the use of control plates as compared to the natural boundary layer, for which the stress distributions are shown in the next figure. However, as the

flow developed downstream, the stress distribution recovered toward that of the natural boundary layer. The surface skin-friction data generally followed and lagged the recovery observed for the Reynolds stress distribution, as indicated by the results shown in the final figure. Thus far, it has not been possible to produce dramatic, sustained control of the boundary layer turbulence in the laboratory using flat-plate devices.

(R. Westphal, Ext. 5856)

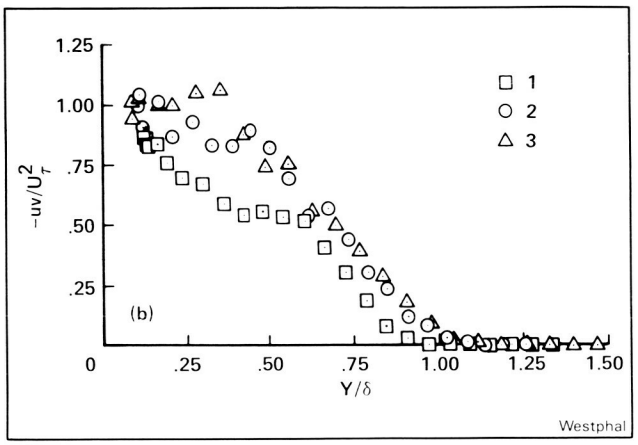

Reynolds shear stress tandem plate control, U_o = 27.5 m/sec

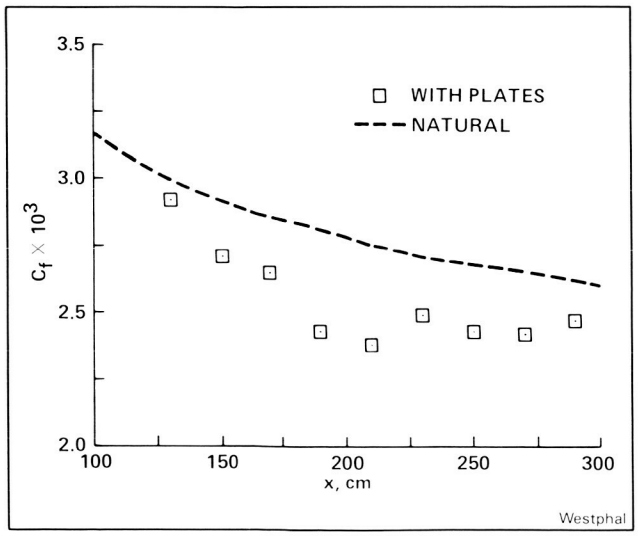

Effect of control on skin friction, U_o = 27.5 m/sec

Computer-Aided Visualization of Fluid Flow

Research was initiated on visualization of computational and experimental flow fields using the Silicon Graphics IRIS Workstations provided by the Numerical Aerodynamic Simulation Projects office. Programs have been developed to display computational fluid flow solutions (obtained from the Cray Computer) on the IRIS Workstations using a variety of techniques including the following:

(a) Dynamic 3D simulation of tracer particles released from various positions in the flow field. Color is used to flag the particles according to the release positions. (The displays are 3D perspective scenes and the viewer can dynamically change the viewing position while the particles are in motion. See first figure.)

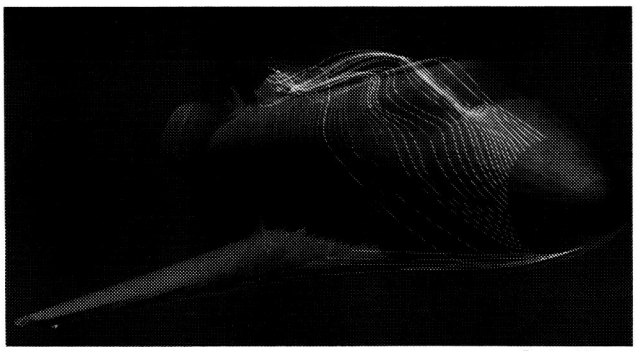

Buning/Watson

Computed stream lines about the Space Shuttle

(b) "See through" translucent surfaces representing surfaces of constant values (such as surfaces of constant Mach number or constant pressure. See second figure.)

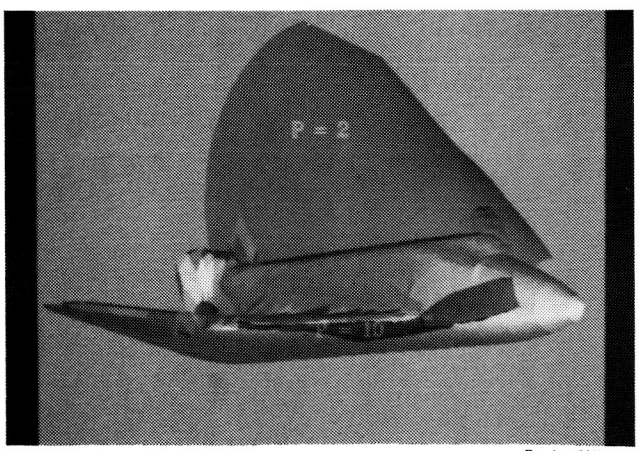

Buning/Watson

Transparent pressure contours

(c) Dynamic 3D velocity vectors distributed throughout the fluid with their origins either fixed in space or moving with the fluid. (See third figure.)

These displays are being combined with previously developed displays (such as the display of body surface pressure using colors to represent the magnitude of the pressure) to obtain a better "cause and effect" understanding of complex flow fields.

Over 25 organizations (companies, universities, or other government agencies) have requested and received the programs to create the displays listed above.

(P. Buning and V. Watson, Ext. 5194/6421)

Buning/Watson

Space Shuttle main engine flow visualization — current engine (3 duct)

Oblique Wing Aerodynamics Determined from the Navier-Stokes Equations

Future naval aircraft will require a substantial increase in range and endurance for fleet defense and strike missions. One of the most innovative concepts for providing an aircraft that would efficiently perform these missions is the oblique-wing concept. Under a memorandum of understanding between NASA and the Navy for flight testing a supersonic, research aircraft with a straight wing that can be set at different oblique or sweep angles to the direction of flight, an effort is initiated to compute the flow field around such an aircraft. An investigation of the flow phenomena associated with an oblique wing is accomplished for the first time by solving the thin-layer Navier-Stokes equations with an algebraic eddy-viscosity turbulence model.

Although the computed results are of a qualitative nature owing to the limited computer resources, they are very useful in understanding the flow phenomena generated by the oblique wing in a supersonic flow. When the angle of sweep is large, there is a significant difference between the upper-surface flow fields at low angles of attack and those at high angles of attack. Most of the lift force is produced on the trailing part of the wing at low angles of attack, and on the leading part of the wing at high angles of attack.

When the free stream is supersonic, the flow is supersonic almost everywhere around the wing. At high angles of attack, there are distinct pockets of high-speed supersonic flow away from the surface of the wing. These appear to be associated with spanwise vortex patterns. At low angles of attack, a vortex pattern along the wing span is not observed. But there is spanwise flow next to the surface, near the trailing edge of the wing. Simulated oil-flow patterns show regions of flow separation and reattachment. Insight into the nature and formation of spanwise vortex patterns is provided by particle paths. Computationally observed vortex patterns are similar to those visualized in water-tunnel experiments with a wing mounted on the body of an F8 aircraft. Water-tunnel experiments, therefore, are useful to study vortex patterns caused by an oblique wing in low supersonic flows.

The figure shows computed results for the following conditions. The free stream Reynolds

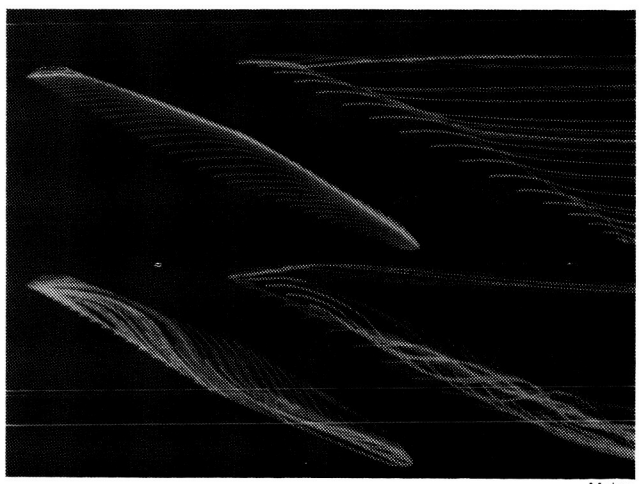

Mehta

Simulated oil-flow patterns (left) and particle traces (right) on the upper surface for $\alpha = 2^\circ$ (top) and 10° (bottom)

number, Mach number, and the angle of wing-sweep are 4.0×10^6 per foot, 1.4, and 65°, respectively. The wing has a 250 ft^2 plan area. It has a 14% thick airfoil section at the midspan (wing root) and a 12% thick airfoil section at the tips. The wing is not symmetric about the midspan.

(U. Mehta, Ext. 5548)

Circulation Control Airfoil Calculation

Two-dimensional Reynolds-averaged Navier-Stokes calculations for flow past an airfoil with a rearward exhausting jet have been completed. The airfoil section is elliptical with a slight amount of camber and the slotted chamber is integrated in the computation along with the rest of the flow field. The computations were performed using minor modifications to the airfoil code ARC2D and employed a spiral grid topology.

Under proper conditions the rearward jet remains attached to the curved trailing edge (Coanda effect), the momentum of the jet entrains the upper surface boundary layer and moves the stagnation streamline clockwise on the Coanda surface producing an augmentation in the total lift. High levels of lift can then be obtained over a wide range of Mach numbers and angles of attack. The computational capability is intended to augment experiments especially in the analysis of the complicated base flow region.

The computations were capable of predicting the lift-slope curves (increase in lift C_L versus increasing blowing rate C_μ) for varying Mach numbers (M) and Coanda geometry (in particular a rounded ellipse RE and a displaced ellipse DE). Other quantitative (e.g., pressure distributions) and qualitative (flow field structures such as separated regions and wake deflections) features of the flow were predicted quite well.

The computational capability will be used to enhance the understanding of the physical mechanisms of these flows and in the design of airfoil sections with larger operating envelopes.

(T. Pulliam, Ext 6417)

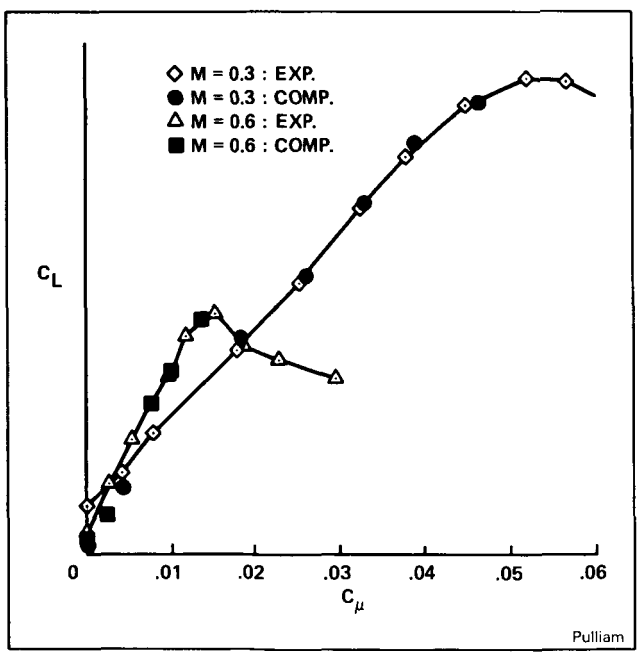

Pressure distribution for DE airfoil; $M_\infty = 0.3$, $\alpha_{geo} = 0°$, $P_r = 1.588$, $\alpha_{cor} = -1.79°$

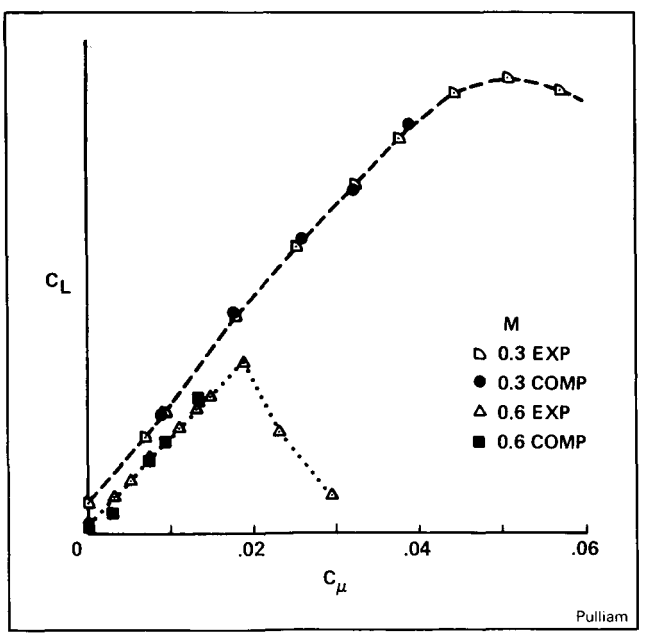

Lift slope curve for DE with slot HGT = 0.0025

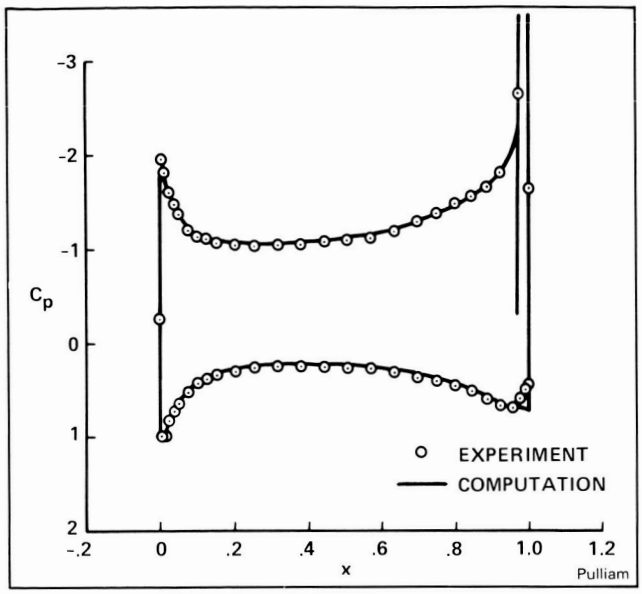

Lift-slope curves for RE with slot HGT = 0.0025

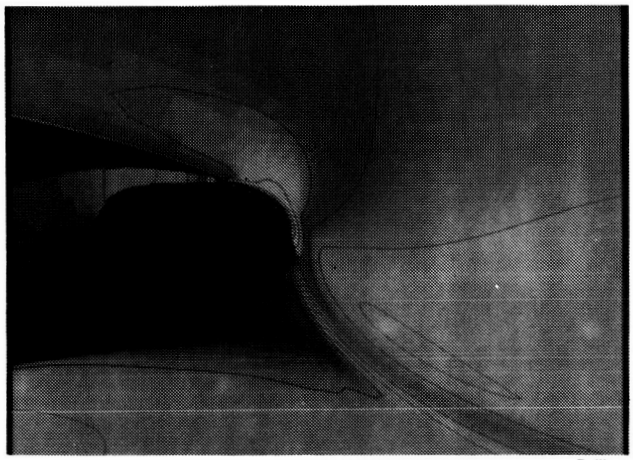

Mach contours in Coanda region for circulation control airfoil

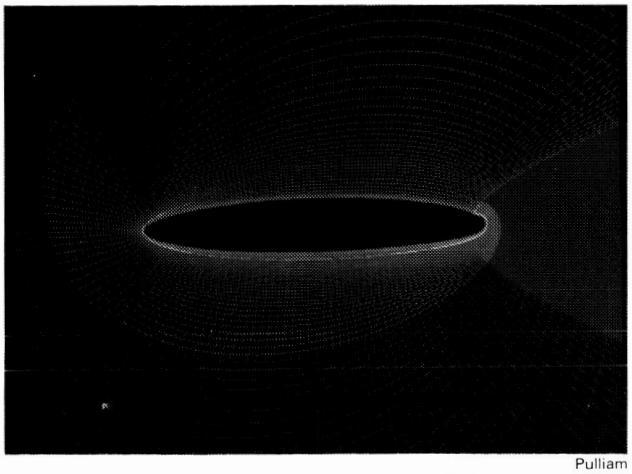

Spiral grid for circulation control airfoil showing chamber grid and spiral wrap boundaries

Properties of Molecules and Clusters

The determination of the properties of molecules and atomic clusters from calculations continues to produce important results for predicting and understanding the properties of matter. Studies have been completed on atoms and diatomic and triatomic molecules of transition metals (Cu, Ni, Fe, V, Ti, Sc, and Y), and gaseous species (H, O, F, and CO) which have led to a detailed understanding of the metal-metal and metal-gas chemical bonds for simple systems. More approximate, but comprehensive, calculations have been performed on large (up to 70 atoms) clusters of Fe, Ni, Al, Cu, and Be. Similar calculations on organometallic systems such as $Ni(CO)_4$, $Fe(CO)_5$, $Fe_2(CO)_9$, and $Cr(NO)_4$ have been completed and used to show that the generally accepted theory of site preference based on bulk metal may not be true for small clusters. Accurate spectroscopic parameters (dissociation energy, equilibrium separation, and vibrational constants) have been determined for most of the alkali and alkaline-Earth fluorides, chlorides, oxides, sulfides, hydroxides, and isocyanides.

An ongoing computational research program exists at Ames to probe details of polymer structure and to study the relationship between the molecular structure and observed properties of polymeric materials. The following molecular properties can be computed by using ab initio quantum mechanical methods: conformational geometries and energies, IR vibrational spectra (and vibrational force fields), energy barriers for internal rotation (activation energies for conversion between conformers) and optical anisotropies. The polymers are represented by small oligomeric models. During the last year, the conformation and preference for planarity of the imide nitrogen in polymides such as Kapton; the phenyl rotation in polystyrene models; and the phenylene rotation in dimeric and trimeric models of polyphenylene oxide, were studied.

(D. Cooper and R. Jaffe, Ext. 6213/6458)

Properties of Nonequilibrium Air in the Shock Layer Surrounding Aero-Assisted Orbital Transfer Vehicles

The shock layer formed in front of an aero-assisted orbital transfer vehicle (AOTV) during the aerobraking maneuver will be characterized by nonequilibrium distributions in the chemical composition and energy owing to the low gas density. Rotational and translational energy distributions will probably be in thermal equilibrium. However, there will not be sufficient collisions for vibrational energy and electronic excitation distributions to be equilibrated. In addition, the chemical composition will be governed by the finite rate chemistry rather than by chemical equilibrium. As a result of these nonequilibrium conditions, a large radiative heat load is expected.

The shock layer gases (initially 80% N_2 and 20% O_2) will be heated to extreme temperatures, dissociated and ionized. The location of the maximum in the nonequilibrium radiative heating load and the time required to reach equilibrium depend on the collisional excitation and dissociation rates which are not well known. Few experimental rate data exist for individual physical processes under the appropriate thermal nonequilibrium conditions. To remedy this situation, a computational chemistry research program has been started to provide needed rate constants, and cross sections for computer modeling of AOTV flow fields. In all cases, ab initio quantum mechanical methods are used to study the chemistry and physics of high-temperature nonequilibrium air.

Initial efforts have resulted in determination of N_2 excitation and dissociation due to collisions with electrons, charge exchange and other transport properties for $N + N^+$ collisions, charge exchange and other O_2^+ properties and the collisional dissociation of N_2 and O_2. In particular, the electron N_2 collision process was found to be the critical factor in determining the time required to reach equilibrium in the shock layer.

(R. Jaffe and D. Cooper, Ext. 6458/6213)

Use of Computer Modeling to Increase Performance of Arc-Jet Wind Tunnels

A computer code, ARCFLO II, has been developed to model the performance of constricted electric arc heaters. The computer code accounts for the transport phenomena occurring in the arc discharge by applying the basic conservation equations along the axis of the constrictor tube that confines and stabilizes the long arc column. At each station, a radial integration is performed that satisfies the mass, momentum, and energy conservation equations for a specified value of arc current and total mass flow rate. This axial marching process proceeds along the constrictor tube until the sonic condition is attained — which establishes the length of the constrictor tube. The computer solution yields the arc voltage, power, wall heating rate, pressure drop, efficiency, and the enthalpy level of the efflux.

Results of the computer study predicted the scaling law for the constricted arc heater enthalpy output, h, in terms of the current density, j, and the pressure, p. The computer-modeled scaling law is:

$$h = \text{const} \times j^{0.604} \times p^{-0.430}$$

This computer-generated scaling law was applied to the Interaction Heating Facility (IHF) to raise the enthalpy level from a shuttle value of 12,000 Btu/lb to 20,000 Btu/lb — corresponding to a more energetic entry associated with an aerodynamic orbit transfer vehicle. For the 8-cm diameter constrictor of IHF, this scaling law predicts that the current must be doubled to attain the higher limit. The electrode assembly was redesigned to accommodate the higher current operation; and verification tests were made to measure the increase in performance. The upper limit for IHF has been increased to 20,000 Btu/lb; and experimental measurements agreed with the derived scaling law with small differences in the exponents:

$$h = \text{const} \times j^{0.625} \times p^{-0.300}$$

The computer modeling technique applied to performance criteria for constricted arc heated flows provides an accurate and quick method for establishing requisite design parameters. Significant savings in time and resources result.

(W. Winovich, Ext. 5268)

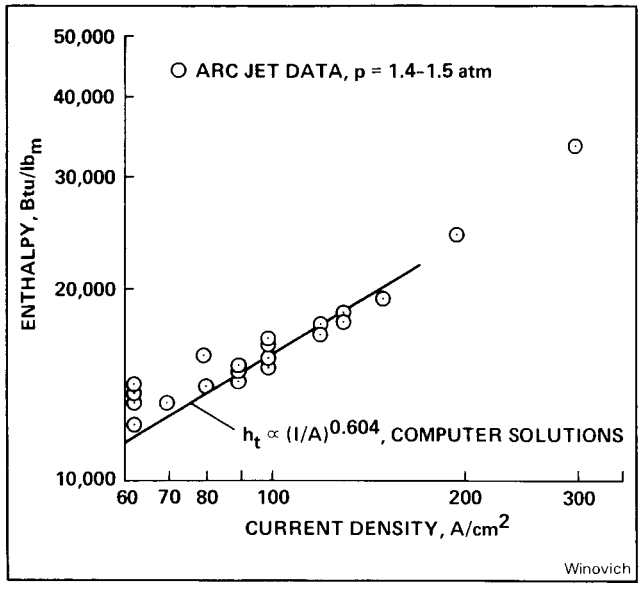

Enthalpy scaling law

Advanced Low-Density Heat-Shield Materials

Several new materials with enhanced homogeneity, improved mechanical properties or higher temperature capabilities than previously possible, have been developed for use in thermal protection systems for advanced reentry vehicles (i.e., aerobraking orbital transfer vehicle, transatmospheric vehicle, etc.). These materials incorporate new, smaller diameter (1-4 μm) aluminoborosilicate fibers rather than the previously used 11 μm fibers. (One composition of the 11 μm materials (FRCI-20-12) containing 20% aluminoborosilicate fiber at 12 lb/cu ft is currently used on the Space Shuttle Orbiters, Discovery and Atlantis). The presence of the smaller fibers at low concentrations increases the resultant material's tensile strength as much as 25% above the 11-μm material. At higher concentrations (>45%) enhanced dimensional stability compared to earlier materials was measured in isothermal tests at 1480°C (2700°F).

(D. Leiser and H. Goldstein, Ext. 6076/6103)

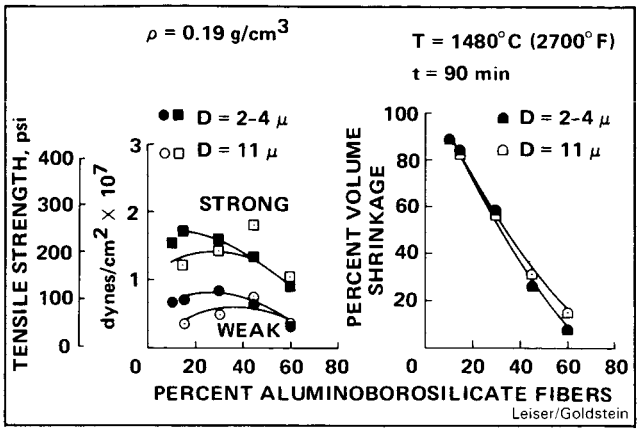

High temperature isothermal dimensional stability and tensile strength of FRCI as a function of aluminoborosilicate fiber size and content

Thermal Protection Materials Applications

Ames-developed ceramic thermal protection materials have been adopted for a number of major NASA programs. On the Space Shuttle, several materials have flown up to eight flights successfully. The Ames gap fillers, a ceramic cloth silicone rubber composite which was planned for single flight use, appears to be usable for many flights, certainly well in excess of the eight that they have already flown. The refurbishment rate for Shuttle tiles including the Lockheed Missiles & Space Company (LMSC)-developed LI-900 and Ames-developed FRCI-12 and LI-2200, all with the RCG coating, has been much lower than the original planned rate.

Advanced flexible reusable surface insulation (AFRSI), after initial problems on its first flight (Challenger STS-6) has now flown successfully with the Rockwell International (RI)-developed coating for five flights, on the Orbiter Discovery.

Initial studies of the next generation reentry vehicle, the aerobraking orbital transfer vehicle (AOTV), have resulted in Ames flexible ceramic heat shields being baselined on all phase A contractor vehicles. The AOTV flight experiment has also baselined the FRCI-12 material. The AOTV experiment is planned for 1991, and the operational AOTV in the latter part of the decade. In other related applications, FRCI-12 has been baselined for use as the antenna window on an advanced Navy tactical missile.

(H. Goldstein, Ext. 6103)

Lightweight and Heat Resistant Composite Panels

Two types of lightweight composite panels have been developed for application as sidewall, floor, and ceiling panels in aircraft interior and other aerospace vehicles. These panels are fabricated using a unidirectional graphite tape or a high-modulus graphite fabric. Both of these panels utilize as a matrix a resin blend of bismaleimide, vinylpolystyrylpyridine and a modifier to improve its adhesive properties. Graphite panels fabricated with this resin designated as 71775 are approximately 20% lighter than the baseline fiberglass epoxy panels currently used in aircraft interiors. As shown in the photograph, the graphite panels remain fairly intact and maintain their structural properties after exposure to a heat flux of 5 W/cm^2, while the baseline epoxy fiberglass fails catastrophically. Large graphite panels are being fabricated for a series of full-scale tests to be conducted by DOT-FAA.

(D. Kourtides, Ext. 6079)

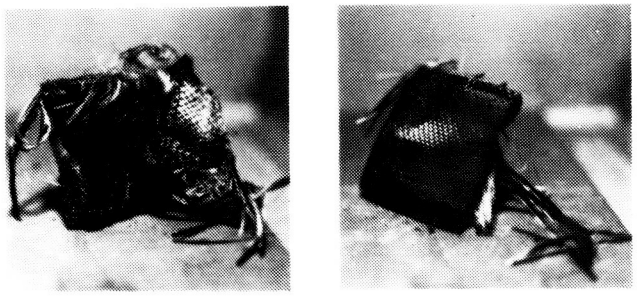

FRONT BACK

Fiberglass/epoxy panels (baseline)

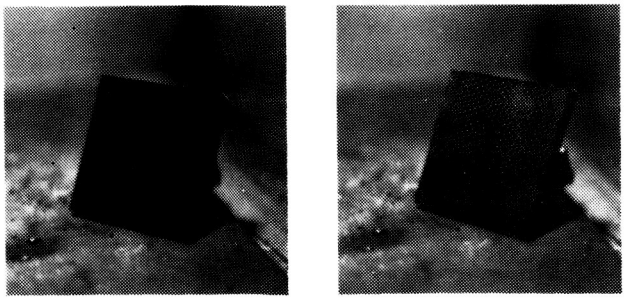

FRONT BACK

Kourtides

Graphite/71775 resin panels (advanced)

Tailorable Advanced Blanket Insulation (TABI)

Advanced versions of integrally woven core insulation structures suitable as thermal protection systems (TPS) for future space vehicles have evolved from the initial all-silica prototype construction. These flexible ceramic tailorable advanced blanket insulations (TABI) have been woven from silicon carbide yarn and aluminoborosilicate yarn with the core section filled with a silica batting. Gore-like test sections have been fabricated for high temperature characterization in Ames arc-jet facilities. These flexible ceramics should perform successfully in higher temperature environments than have previously developed sewn silica blankets. Preliminary arc-jet testing of TABI fabrics has shown a maximum heat flux capability for a silicon carbide fabric of 30 BTU/ft^2-sec greater than 7.5 BTU/ft^2-sec for an aluminoborosilicate fabric. This is compared to a heat flux capability of 4.4 BTU/ft^2-sec for an all silica sewn blanket such as advanced flexible reusable surface insulation (AFRSI). Future space vehicles under study such as aerobraking orbiter transfer vehicles (AOTV), transatmospheric vehicles (TAV), military aerospace vehicles (MAV), and hypersonic aircraft represent potential application of the TABI concept.

(P. Sawko and H. Goldstein, Ext. 6079/6103)

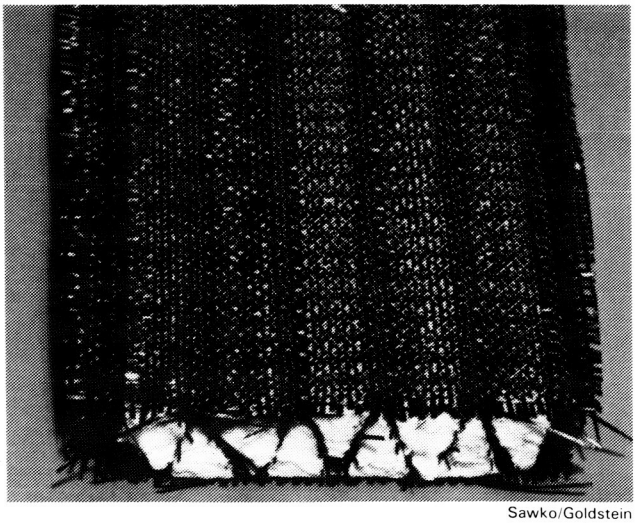

Sawko/Goldstein

Tailorable advanced blanket insulation (TABI) — single layer triangular silicon carbide fabric filled with silica batting

C-2

Space Research

Ames Research Center Life Sciences Payload on Spacelab Mission 3: A Spaceflight of 24 Rats and 2 Monkeys (UPN 805)

Research Animal Holding Facilities (RAHFs) have been developed to support rodents and squirrel monkey animal husbandry in the Spacelab environment. The Spacelab Mission 3 Payload was designed to validate this hardware for future Life Sciences dedicated missions. It consisted of an Ames single rack containing a RAHF supporting up to 4 squirrel monkeys; an Ames double rack containing a RAHF supporting 24 rats; a Biotelemetry System (BTS); a data processing microcomputer; and a Dynamic Environment Measurement System (DEMS).

The payload was flown on Spacelab 3 (April 29-May 6, 1985) as an engineering evaluation of the hardware, and contained 24 rats and 2 squirrel monkeys. The RAHF performed very well, with some minor exceptions which included a highly visible and unexpected particulate release. The problems seen in the particulate release involve a combination of more vigorous animal movement, unsealed gaps in cages, and an overly optimistic reliance on air flow to control particulate escape. These problems appear to be solvable.

The rats were recovered in excellent, healthy condition, and were microbiologically clean, as well. That the adrenals of the rats were normal and of a size identical to those of the preflight and control rats indicates that the rats did not experience significant or prolonged stress. Liver sizes (and the weights of the animals themselves) were identical to controls which indicates that the rats were adequately fed, watered and housed. Similar arguments can be made for the monkeys. This information allows us to state that the RAHF houses animals in space in a manner equivalent to vivarium-housed animals in laboratories, and allows us to support future animal research in space in an experimentally valid manner.

While the data is only partially reduced at this point, we are beginning to appreciate the vast, and hitherto unknown, wealth of information that we have obtained on the animals. Since one monkey demonstrated space-adaptation syndrome while the other did not, these monkeys, as a pair, are potentially valuable in evaluating models designed to diagnose, study, and prevent this syndrome.

These rats returned to Earth different animals. They showed the following changes:

(a) They were flaccid with an almost total absence of muscle tone.

(b) Marked loss of muscle in the six muscles studied (8 to 36% both antigravity and voluntary).

(c) A 50% loss in fiber diameter in the soleus muscle.

(d) An almost total absence of a Krebs cycle in the muscle.

(e) Hemorrhaging in one muscle (which had to be the result of readaptation to 1-g rather than a reaction to launch or reentry loads).

(f) A marked bone loss as measured in the third lumbar vertebra.

(g) A 25% decrease in elasticity and a 40% decrease in breaking strength as measured in the humerus.

(h) An increase in growth hormone-producing cells, and a decrease in prolactin producing cells.

(i) A decrease in thymus-gland size, which implies that little growth hormone was released.

(j) A surprising and unexplainable increase in the erythropoitic (red blood cell) system.

As data analyses are completed, we expect that this mission will yield the greatest amount of information ever obtained from a biological payload in space, and may well exceed the total amount of information on biological systems in space gained since the beginning of space investigation.

(J. Ferandin, Ext. 6602)

Joint US/USSR COSMOS Spaceflight Experiment

COSMOS 1667 (flown 10-17 July, 1985) was a reflight of the COSMOS 1514 mission which was flown in December 1983. The 1667 mission represented the second time that rhesus primates were flown by the Soviets in an extended orbital environment. The COSMOS mission is a continuation of joint US/USSR activities related to biological and biomedical aspects of spaceflight, which was conducted under the auspices of the cooperative efforts initiated under a 1971 agreement to create a joint working group on space biology and medicine.

As in the 1514 mission, cardiovascular measurements were made in one 4-6 kGm rhesus primate. Carotid-arterial pressure and blood-flow

velocity were measured using a combined pressure and flow (CPF) cuff. The pressure was measured using a semiconductor, strain-gage, pressure transducer contained in a cuff housing external to the vessel (applanation technique). The flow was measured using a continuous-wave Doppler measurement system. The implanted sensors were directly connected to external measurement, recording, and control instrumentation. Ground-based laboratory instruments were modified and reconfigured to meet Soviet flight requirements. The pressure sensors used were manufactured by Konigsberg Instruments and the cuff housing and Doppler sensors were constructed by L & M Electronics. Timing and control instruments and subsystems were developed in-house by Cosmos Project Staff and Ames support services personnel with assistance by L & M Electronics.

Both missions were flown aboard a modified "Vostok" USSR rocket in a specially configured Biosatellite capsule (BIOS). Animals were launched from the Soviet Launch Complex and recovered at a Siberian recovery site. The ground landing was accomplished using a soft-landing parachute system. Immediately after recovery of the BIOS capsule, post-flight evaluations were conducted prior to return to the Moscow Institute for Biomedical Problems. A series of pre- and post-flight physiological evaluations were performed on flight, back-up, and vivarium-control primate subjects. These evaluations included

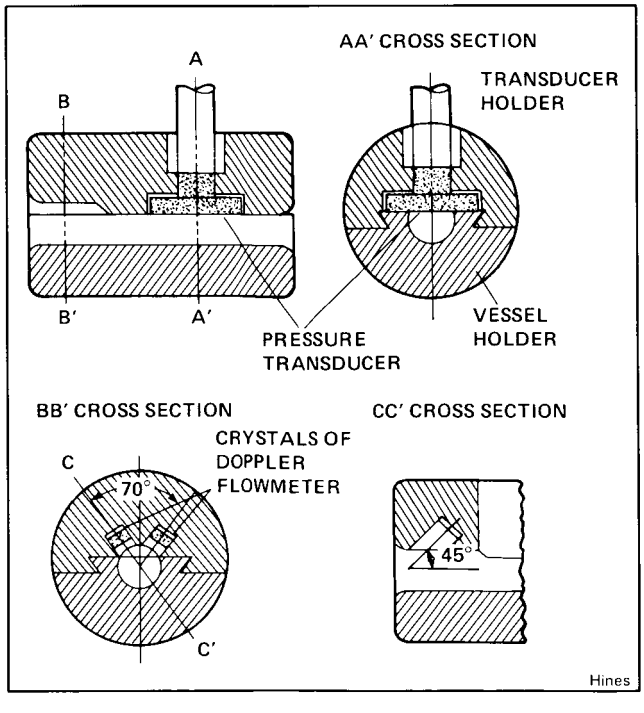

Arterial pressure and flow measuring cuff

orthostatic tilt, cross-calibration and bioengineering test procedures.

Initial analysis of the 1514 data showed an increase in blood velocity to the head during spaceflight, and lowered blood pressure and peripheral resistance in the vessels.

Analog flight data were recorded on a Soviet analog tape recorder. Post-flight, the analog data were transferred to a US analog tape recorder for return to the US for data processing. For the 1667 mission, a similar data-transfer activity is planned in early October 1985 for subsequent return to the US and data analysis. In support of these activities, US technical personnel will travel to the USSR with appropriate instrumentation to support the data transfer. At the completion of the transfer, the data will be returned to the US and analyzed in the NASA Ames Cardiovascular Research Laboratory. Following the data reduction, USSR specialists will travel to the US for joint US/USSR data analysis and interpretation.

(J. Hines, Ext. 6069)

Spacelab 3 Data Analysis

A total of 20 investigators participated in the postflight analysis of tissues obtained from rats flown on Spacelab 3. The scientific yield is the largest from any Life Sciences mission flown to date. Among the significant findings:

1. Muscle atrophy up to 31% was greater than anticipated for a seven-day mission.
2. Bone-breaking strength was reduced up to 28% (a reflection of changes in bone metabolism).
3. Interferon production by cultured spleen cells was dramatically reduced by flight, a possible reflection of impaired immunocompetence.
4. Growth hormone release by cultured pituitary cells was reduced. This could play a role in muscle atrophy.
5. Calcium-containing organs involved with vestibular function were not changed, suggesting that the general loss of body calcium observed during flight does not extend to the vestibular organs.
6. Cardiac muscle showed signs of atrophy which were biochemically characterized.

In addition to the scientific data, many of the investigators obtained operational experience in the flight program which will facilitate their participation in future flights.

(C. Schatte, Ext. 6748)

Large Primate Facility

A joint US-French project is scheduled to fly rhesus monkeys in the Spacelab in 1989-90. CNES, the French Space Agency, will build a module to house the animals. NASA will supply a modified version of its existing Research Animal Holding Facility (RAHF) to house the module and to provide the environmental-control system. Experiments to be flown will be joint endeavors by US and French investigators. The selection process is under way, with investigator teams to be established in early 1986. Prototype subsystems have been designed and are being tested by the French. A preliminary design review is scheduled for early 1986. Ames Research Center has begun development of training equipment and procedures preliminary to the establishment of a monkey colony from which to draw flight candidates.

(C. Schatte, Ext. 6748)

Evaluation of a Mounting System for a Silica Mirror

A system for mounting cryogenically cooled silica mirrors for infrared telescopes was developed for Ames Research Center (ARC) under a grant to the University of Arizona. Various tests of the mounting system are being conducted at ARC. Last year, tests were successfully completed to evaluate the component of mirror distortion that is induced by the mounting system during and after cooling to 7 K. It was found that the mirror figure change caused by the mounting system was less than 0.06 waves rms (at 0.633 m). Tests for the response of the system to vibrational loads are in progress; and a structural dynamic model of the system has also been developed at ARC in parallel. A sketch of the test configuration is given below. It can be seen that the mirror and supporting baseplate are coupled with double-blade flexures.

At this stage in the testing, the vibrational loading has been restricted to comparatively low-level sinusoidal inputs of the baseplate. Mirror motion resonances have been identified both analytically and experimentally at several frequencies in the range of interest (10 to 2000 Hz), and there is good agreement between analytical and experimental results. The ratio of mirror mass model to baseplate accelerations obtained experimentally at the first resonant mode of approximately 40 Hz is 140. This compares with the predicted ratio for a critical damping factor of 0.0036.

Tests will now be conducted at more severe loading levels, including the random vibrational loading associated with STS launch.

(J. Mansfield, Ext. 6520)

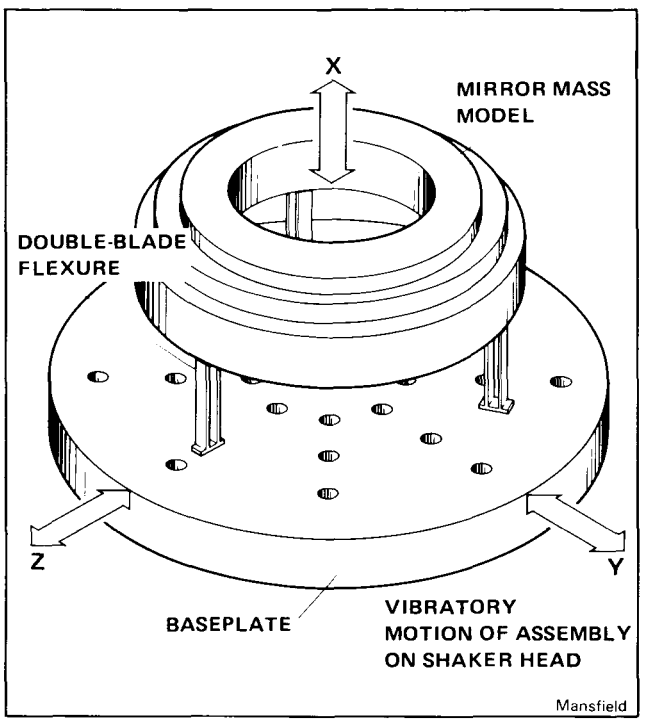

Vibration test fixture

Design Studies for a Life Science Research Facility on Space Station

Preliminary design studies have been completed for conducting life-science experiments in the science laboratory module (SLM) on a space station in the 1990s. With the SLM, life scientists for the first time can have a permanent facility in space to conduct truly comprehensive studies in all areas of biological inquiry. Such a national facility can permit life scientists: (1) to study the effects of the space environment on humans, (2) to understand the role of gravity on plant and animal species throughout their lifespan and multiple generations, (3) to study the flowering and fruiting of food crops for use in space, (4) to

understand the distribution and action of biologically important compounds in space, and (5) to develop and test the next generation of high-spectral resolution sensors for the study of biological processes on a global scale.

In conjunction with NASA's Office of Space Science and Applications, bioengineers at Ames Research Center have compiled high-priority experiment and equipment lists. Biologists throughout the U.S. participated in generating and reviewing this information, which was initially coordinated through the University of Texas. These descriptions were expanded by McDonnell Douglas in California whose technology development plan became the foundation for further design studies by Lockheed and Boeing for outfitting the SLM.

Some of the unique equipment that can be chosen for development for life science research includes the following: plant and animal habitats that could be operated automatically for up to 90 days, which would permit unattended upkeep and would conserve valuable scientist crew time; a research centrifuge could provide a 1-G environment for experimental controls (a simulation of lunar gravity 1/6 that of Earth's), as well as a variety of gradations for the study of those physiological functions that depend on some gravity stimulus.

Other high-priority, long-lead-time equipment includes bioinstrumentation, on-board analysis equipment, plant growth facilities, experiment management systems, a cryogenic freezer (-195°C), and a storage freezer (-70°C) to hold specimens (if onboard analysis of biological samples is limited). The accompanying artist's concept of the SLM is a cut-away view through the bioisolation wall and doors which separate the biological workstations (visible racks) from the noise and activity of the astrophysics, servic-

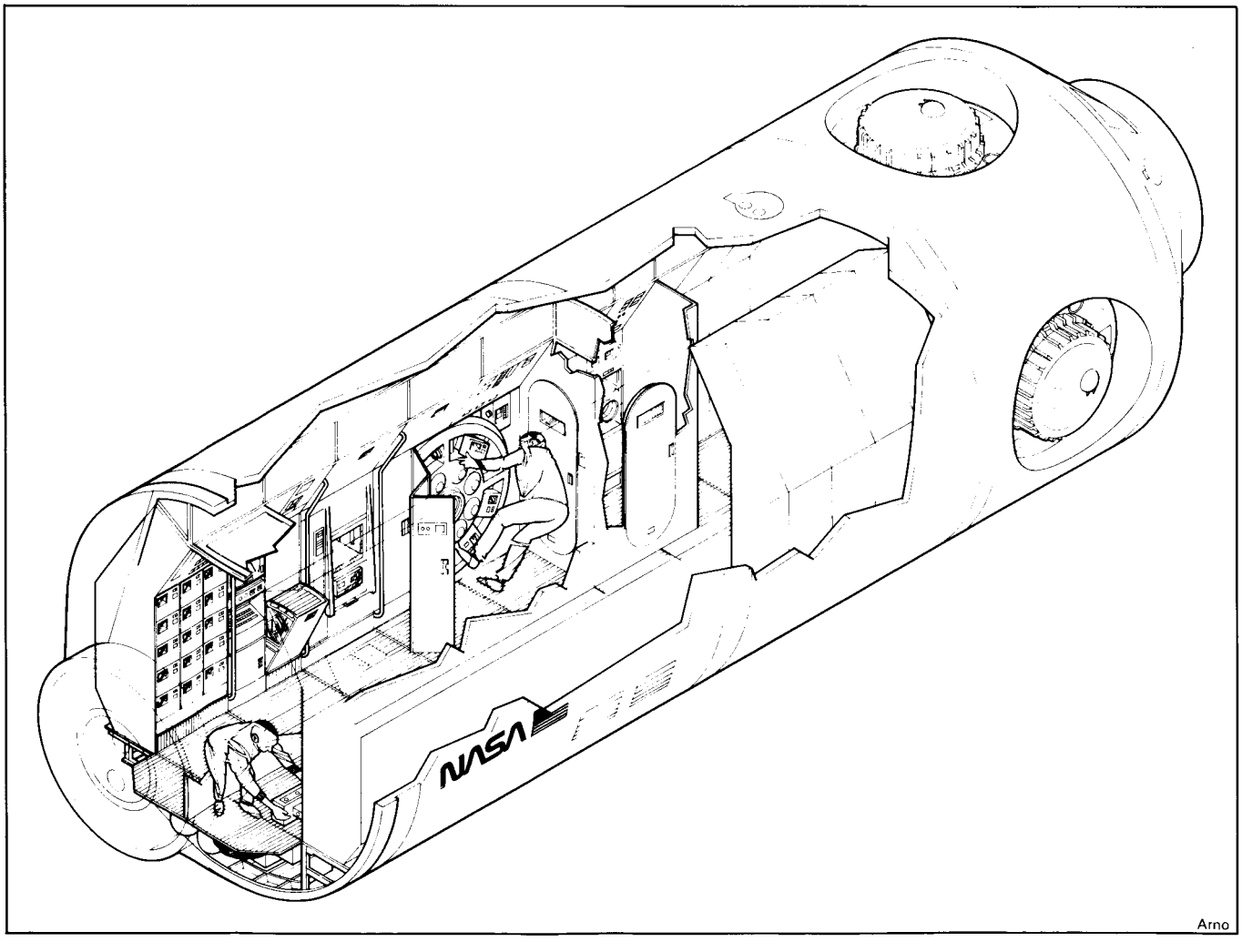

Space Station Life Sciences Research Facility Complex

ing, and human research equipment in the other half of the module. Some of the racks for space biology show habitats for small organisms (boxes on far left) and a circular research centrifuge. This scenario is one first-stage concept for a national laboratory for life science research in space.

As the space station expands and evolves, whole modules could be added for animal life science investigations. Another whole module has been suggested for the growing of crops to provide food and recycle air and water for the crew. Another "clean" module could contain special safe bioreactors for the development of space-borne biotechnology and the manufacturing of products.

(R. Arno, Ext. 6640)

Ground-Based Vestibular Research Facility (VRF)

The Vestibular Research Facility at Ames Research Center has been developed by NASA in conjunction with an outside advisory committee which is made up of members of the vestibular research community. This facility provides the community with unique, state-of-the-art equipment and techniques for: (a) sophisticated ground-based investigations of vestibular function in 1-g and hyper-g; (b) defining critical scientific questions for micro-g research, and providing a facility for obtaining baseline data for this research; and (c) defining equipment and methods required for conducting the research in space. The VRF consists of a multiaxis centrifuge, an air-bearing linear sled, and supporting neurophysiological laboratory equipment and personnel.

Accomplishments for the past year include development of user-friendly motion stimulus control software, conduct of precursor science experiments (University of Texas Medical Branch and University of Michigan scientists), design and checkout of hardware safety monitoring systems, and upgrade of hardware performance capabilities. Experiment-peculiar hardware was also developed for science investigations to be conducted by scientists from the University of Pittsburgh, Washington University, and Northwestern University. Engineering support for the VRF is provided by Johnson Engineering Corp. and Boeing Corp.

(R. Mah, Ext. 6538)

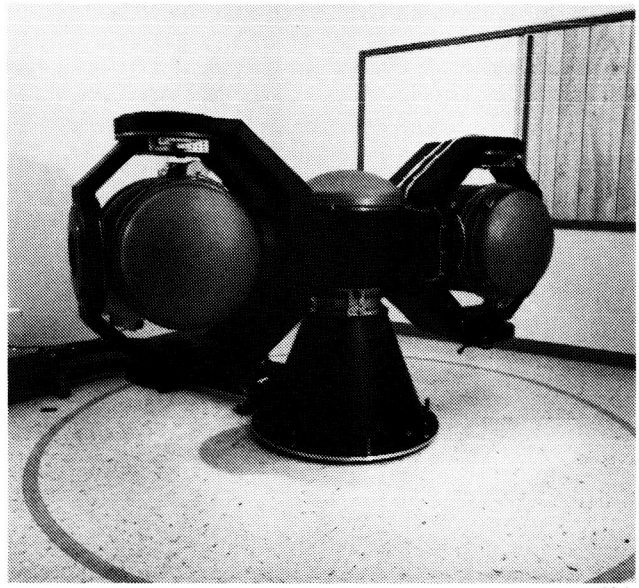

Mah

Ground-based Vestibular Research Facility

Multicrop Area Estimation and Mapping

Research on techniques to monitor agricultural land use via the Multi-Spectral Scanner (MSS) on the Landsat series of satellites is being conducted under a cooperative agreement among the Ecosystem Science and Technology Branch at NASA Ames, the Statistical Reporting Service of the U.S. Department of Agriculture, the California Department of Water Resources, and the University of California-Remote Sensing Research Program.

In 1985, Ames personnel contributed to the development of a procedure to perform multicrop area estimation and mapping in California. The procedure is based on the varying reflectance of plants in the near infrared and red portions of the electromagnetic spectrum. The pattern of change over the course of the growing season, as suggested by the reflectance in the two spectral bands and the timing and magnitude of peak reflectance values, is indicative of cover type. Both spectral bands can be easily monitored using the MSS scanner on Landsat.

The area estimation procedure is currently undergoing testing. Three acquisitions of data from the seven Landsat frames covering the Central Valley of California are being used to determine acreages for as many as twenty of the major commercial crops. Acreage estimates at the county and analysis district (Landsat frame) levels are being generated using a single variable

regression estimator. The digital data of the land use classification will be used to create land use maps at 1:24,000 scale.

The California project differs from previous large-scale agricultural inventories in several significant ways. First, the inventory includes a far greater range of crops than previous inventories. Second, when identifying cover types in an area as agriculturally complex as California, there are significant problems far in excess of those of other inventories using satellite or other forms of remote sensing data. Finally, the inventory will be conducted in virtual "real time" – data collected from March through August will be processed in September and October, and reported in December. The California project will also break ground by using a 16-bit, XENIX-based, microprocessing system developed at Ames to coordinate and perform the bulk of the data processing.

(J. Lawless and E. Sheffner, Ext. 5900/5149)

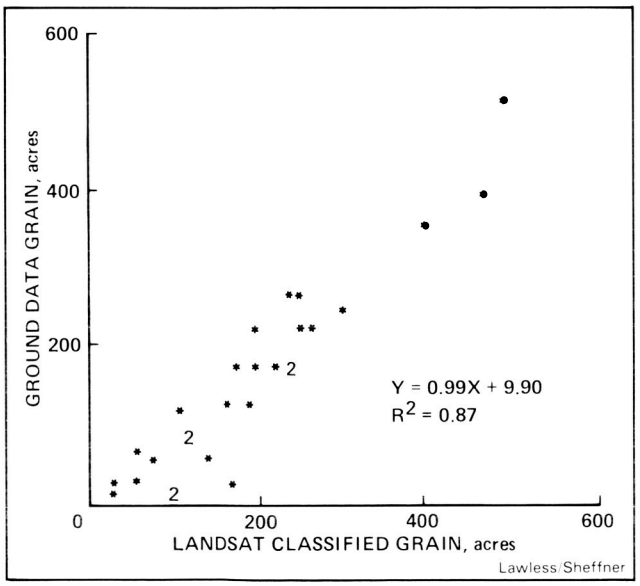

Acreage classified to grain from Landsat data versus ground data – Yolo County study site

Permafrost Modeling from Satellite Data

Permafrost, or perennially frozen ground, is the dominant controlling environmental factor in Arctic and Subarctic regions which cover approximately 25% of the land surface of the world. By maintaining low soil temperatures, permafrost restricts plant growth, increases surface water runoff, inhibits groundwater recharge, and limits nutrient cycling. Research to study the real distribution, thickness, and temperature regime of permafrost utilizing Thematic Mapper satellite data is under way at Ames Research Center.

Satellite-derived environmental data layers (such as tree canopy cover, species composition, surface temperature, and potential incoming solar radiation) are being incorporated within a logistic regression model to predict the areal distribution and physical characteristics of permafrost. This combination of remotely sensed data, together with geophysical borehole investigations and field observations, are providing the basis for development of new and improved nondestructive techniques for deriving physical and behavioral parameters of permafrost, both by correlation and by inference from existing conventional and satellite-derived data.

This research is being conducted in cooperation with T. Osterkamp, K. Dean, and G. Wendler, researchers at the University of Alaska; and J. Brown (National Science Foundation, formerly with the Army Corps of Engineers).

(J. Lawless and L. Morrissey, Ext. 5900/5149)

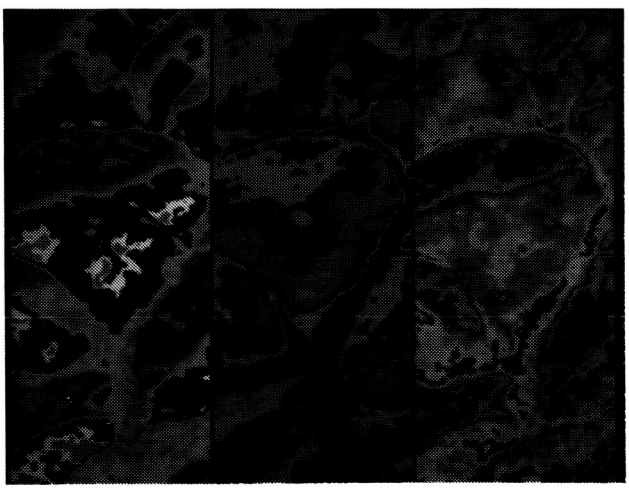

Acreage classified to grain from Landsat data versus ground data – Yolo County study site

Radiant temperatures, derived from the thermal band of the Thematic Mapper Scanner aboard Landsat 5, were calculated for a day scene (September 22, 1984) and a night scene (September 23, 1984). Temperatures in the daytime scene

reflect differential warming of various slopes, warmer south-facing slopes and cooler north-facing slopes, while nighttime temperatures correspond to differences in vegetation. A difference image, calculated by subtracting night from day temperature values, provides an additional information layer for vegetation discrimination.

Pilot Land Data System — System Access Capabilities

In recent years, there has been a growing recognition on the part of the land science community of the need for an advanced computer-based information system to support research and analysis. NASA's Office of Space Science and Applications determined that the best way to attain this goal was to establish a pilot data-system effort that will subsequently become an operational Land Data System.

To meet this need, the Pilot Land Data System (PLDS) Project was formed under the sponsorship of the Information Science Office (ISO). The project, undertaken by three NASA field centers including Ames, is an effort to build a prototype distributed data system linking existing NASA computing facilities currently utilized for analysis of remotely sensed and other land science data.

Pilot Land Data System activities over the next several years are intended to establish the basis

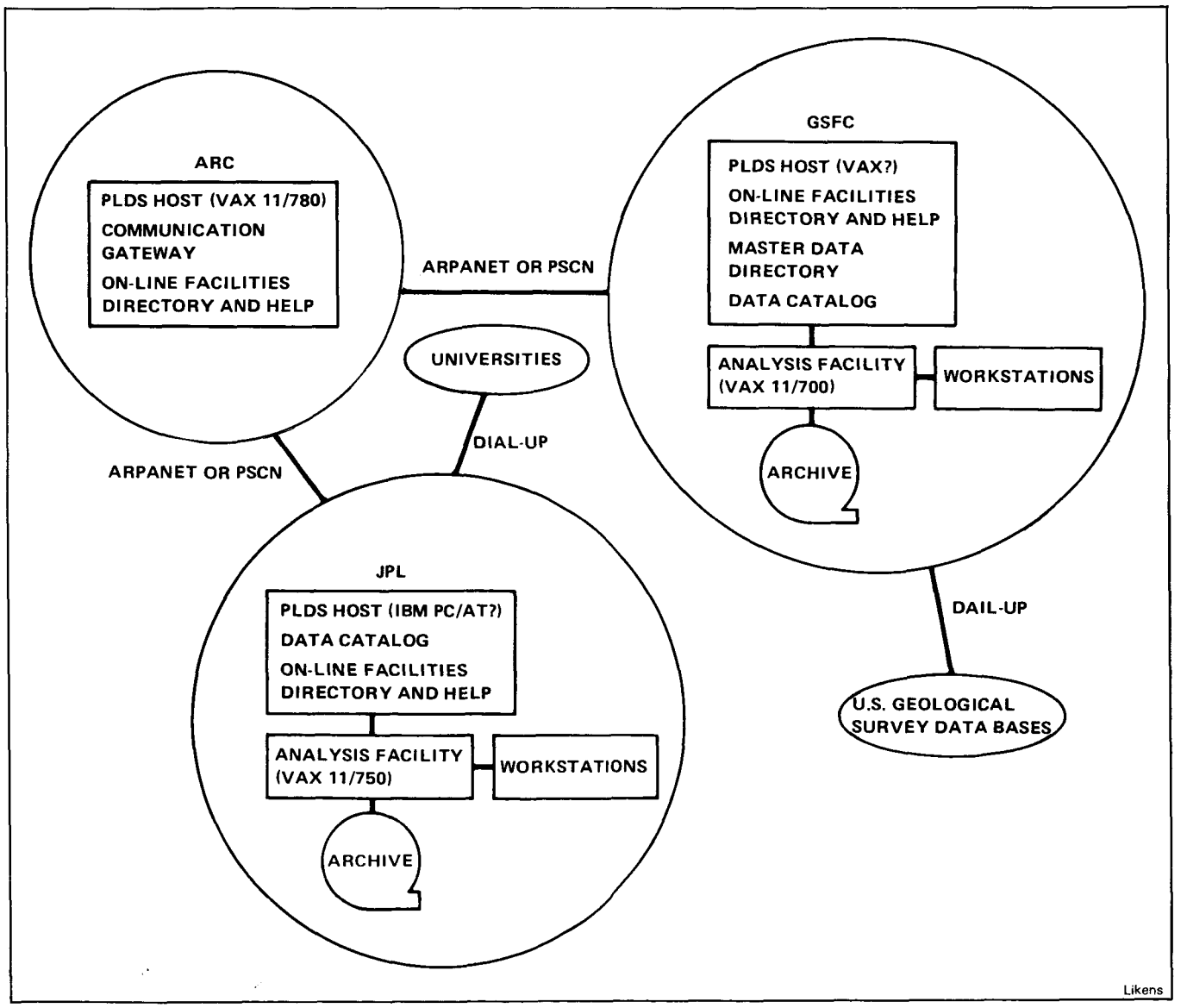

Planned configuration for system to be in place at the end of 1986

for the Earth Observation Information System (EOIS) and the Science Applications Information System (SAIS), which are proposed to support the EOS platform and Space Station, respectively.

Six PLDS engineering areas have been identified: (1) system engineering, (2) data management, (3) networking and communications, (4) system access capabilities, (5) land analysis software, and (6) special processes. Ames has the responsibility for networking and communications (Telecommunications Branch), and system access capabilities (Ecosystem Science and Technology Branch).

The system access capabilities task includes ensuring user access to supercomputers and hosts forming the PLDS system, workstation test and evaluation, graphics, and executive processes (e.g., on-line help, user interfaces). First-year system access capabilities activities were largely devoted to PLDS system engineering and preliminary work in the workstation area. This included a systems analysis comparing 53 currently marketed systems, and systems that can be readily assembled from commercial components. A major emphasis has been to coordinate Ames activities with other science data efforts funded by the ISO.

(W. Likens, Ext. 5596)

Nitrous Oxide Flux from Tropical Forest Ecosystems in the Amazon

Many tropospheric trace constituents are produced by biological and geochemical processes in terrestrial and aquatic ecosystems. As part of the Amazon Ground Experiment (AGE) study funded by NASA's Biospheric Research Program, a project has been initiated which addresses specific issues related to nitrous oxide (N_2O) flux from upland Amazonian soils. The quantitative significance of various processes of N_2O formation and destruction, and the spatial/temporal variations in atmospheric concentrations are fundamental issues. To date they remain poorly understood.

The rationale for studying N_2O fluxes from Amazonian soils is two-fold. First, a measurement program will attempt to enhance understanding of the global atmospheric N_2O budget. Current "known" sources do not account for observed atmospheric increases in N_2O concentrations. Based upon exploratory analyses, it is estimated that Amazonian forests alone could account for as much as 10% of the estimated global N_2O source. Second, an improved understanding of the spatial distribution of N_2O fluxes, and the mechanisms and factors controlling N_2O production is needed to evaluate nutrient budgeting in these systems, and to address the potential global impact of disturbance to these systems, e.g., through deforestation.

Measurements of N_2O fluxes in undisturbed terra firma forests over a range of major Amazonian soil types have been collected concurrently with estimates of nitrogen cycling. Results suggest that oxisol and ultisol soils, which account for approximately 70% of Amazonia soils, have higher rates of nitrogen mineralization, nitrate production, and nitrous oxide flux than do the more nutrient-poor white sand soils which cover less than 10% of the area. This type of stratification will enable scientists to make a more accurate estimate of the role of tropical forests in atmospheric processes.

(G. Livingston, P. Matson, and P. Vitousek, Ext. 6184/6884)

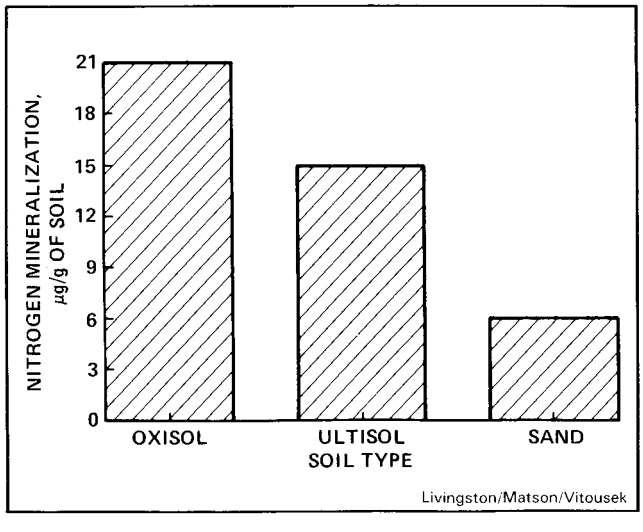

Nitrogen mineralization in soil over a 10-day incubation period. Each value is the mean of four sites each having three subsamples

Pathways of Nitrogen Loss Following Land Clearing in a Humid Tropical Forest in Central America

Tropical deforestation generally leads to large losses of carbon and nitrogen in the soil. The Premontane Wet-Forest-Life Zone is subject to the highest rate of deforestation in Central America, and carbon and nutrient losses from these fertile soils are extreme. Losses of 2000-3000 kilograms nitrogen per hectare have been reported. Losses of this magnitude could be extremely significant on a regional or global scale if even a small proportion of this nitrogen is lost as nitrous oxide to the atmosphere or is lost through leaching of nitrate to rivers.

Sponsored by NASA Headquarters' Life Science Division's Biospheric Research Program, this study measured the rates and regulation of nitrogen transformations and the pathways of nitrogen losses following land clearing and burning at a site in the Premontane Wet-Forest-Life Zone near Turrialba, Costa Rica.

Following clearing and burning, net nitrogen mineralization estimated by in situ incubations increased by 5-fold over the control forest, but dropped to baseline within six months. Nitrate pools in the soil increased by an order of magnitude following disturbance, but also were reduced to control levels within six to eight months. Potential denitrification rates estimated using an intact core method were generally lower in cleared plots than in forested plots. Nitrous oxide

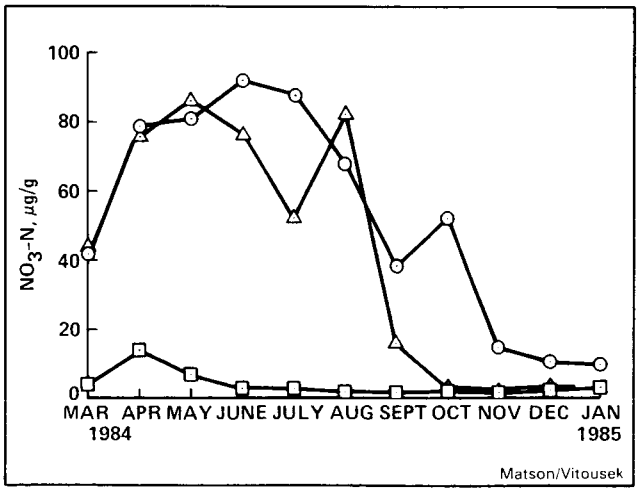

Average nitrate pools (ug/g dry soil) following clearing and burning. □ Control forest; + successional treatment; ○ vegetation-free treatment

production was not different between newly cleared plots and the control forest. Experimental studies suggest that soil wetness and carbon availability are major controls of denitrification and nitrous oxide production in these soils, and that clearing does not lead to increased losses of nitrogen to the atmosphere.

In an effort to identify the ecosystem components most responsible for preventing nitrogen loss to the atmosphere and to ground or surface water, a nitrogen tracer (N-15) was added to isolated plots in the field. Plots were harvested after seven months, and N-15 was analyzed in plant, litter, and soil components. The results of these analyses indicated that where vegetation was allowed to regrow, 20% of the N-15 was recovered in that component. Where vegetation regrowth was prevented, that nitrogen accumulated as nitrate on anion exchange sites deep in the soil profile. Anion exchange capabity is characteristic of many tropical soils, and acts to lower nitrogen losses, thus reducing the impact of clearing on river ecosystems.

(P. Matson and P. Vitousek, Ext. 6884)

Remote Sensing Prediction of Deciduous Forest Nutrient Condition

Transfers of energy, water, carbon, and nutrients in forest ecosystems occur largely in the forest canopy and the soil. The climate mainly determines the development of a canopy leaf mass. The soil fertility controls the efficiency of plant processes such as productivity, and nutrient utilization, and turnover. Using NASA remote sensing instruments, measurement of the nutrient condition of the canopy can help determine the role of forests in global biogeochemical cycling. The nutrient condition is a good predictor of ecosystem functioning, and is determined as the nitrogen, phosphorus, and lignin content of the leaves. Each of these biochemical contents is involved in photosynthesis, decomposition, and other processes.

All leaves are composed of many of the same organic molecules in different proportions. Nitrogen is mostly bound up in proteins and chlorophylls; carbon is in many forms but, most importantly, in structural compounds such as cellulose and lignin. Each of these compounds, plus water, absorbs a small amount of infrared and visible

radiation at highly specific wavelengths. An empirical investigation, sponsored by NASA Headquarters' Earth Science and Applications Division, is being undertaken by Ames and university colleagues to determine the predictive relationships between visible/infrared spectra and the biochemical contents of leaves and forest canopies. Leaves have been taken from canopies at field sites and their reflectance and biochemistry measured in the laboratory. Innovative statistical techniques have been applied to these data. Through careful selection of a subset of specific wavelengths, excellent predictive correlations have been found for each constituent as indicated by the coefficient of correlation (R^2). Nitrogen content is predicted with a value of 72% (of a possible 100%); chlorophyll content 98%, protein 77%, lignin 92%, cellulose 81%, and sugar 83%.

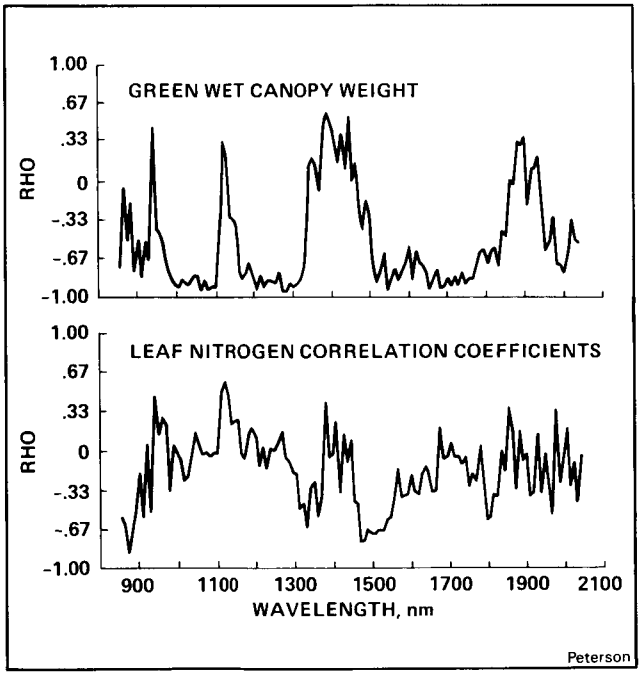

Correlation between the properties of a deciduous forest canopy and reflected solar radiation as measured by NASA's Airborne Imaging Spectrometer.

The investigation is also concerned with producing similar results from an airborne spectrometer for whole intact forest canopies. The high spectral resolution instrument developed by NASA (the Airborne Imaging Spectrometer) is being used. This device produces images with 128 different wavelength bands over forests. Data were acquired over mixed deciduous forests on Blackhawk Island in the Wisconsin River. From measuring these forest canopies, a range of canopy properties was established. These were combined with the spectral data, and the correlation between canopy properties and reflected solar radiation at each wavelength was calculated.

These correlations are shown in the figures attached. The top figure is for the total green mass of the canopy. This figure shows that strong inverse correlations (an inverse correlation is correct because more green mass absorbs radiation so that it is not reflected) occur at many wavelengths. This is due to the presence of water in the leaves. The bottom figure is for nitrogen content per unit leaf area of the canopy. Here, the strongest inverse relationship (more negative) occurs at about 1,500 nanometers. This is a region of the infrared spectrum where there is strong absorption by chemical bonds occurring in proteins. Proteins contain most of the leaf nitrogen. These results show great promise for a new technique to measure the general health or condition of plants.

(D. Peterson, Ext. 5899)

Building a Geographic Information System for Water Management in Oregon

Geographic information systems (GIS) are being used to manipulate geographic data in digital form to seek answers to scientific and management questions. Working with the State of Oregon, U.S. Geological Survey scientists on-site at the Ames Research Center have built a digital data base for the John Day River Basin and utilized it to address a variety of water management queries.

Two data bases have been created to date. Geographic data consisting of 20 layers were assembled using the interactive digital image manipulation system (IDIMS) by digitizing maps of several scales, converting additional existing digital map data, and registering all such data to uniform 100-m grid cells. Thirty files of geographically referenced tabular data were assembled using the ARC/INFO software package by reading existing files, converting formats, and entering new data.

Several applications were chosen by the Oregon State project team for analysis and were completed during a workshop using both the IDIMS and ARC/INFO software packages. These addressed typical problems that state agencies

face in deciding on whether to issue permits for various activities or in planning the best uses of water resources.

As called for in the agreement with Oregon State, all project work was completed on time, nine months after initiation. Presentations were made to members of the Oregon State Legislature with the result that a bill was passed authorizing continuation of the strategic water planning effort of the State using GIS as an important component. Work continues in an effort to incorporate additional data within the system and to investigate the translation of files between alternative hardware/software systems.

(J. Lawless and G. Thelin, Ext. 5900/6368)

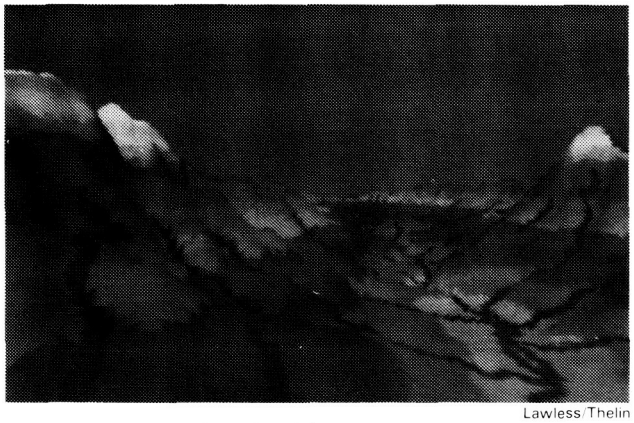

Lawless/Thelin

A perspective view looking up the valley of the Middle Fork of the John Day River. Streams originated from Digital Line Graph Data; terrain data are from Digital Elevation Models

Instrumentation Used in the Search for Extraterrestrial Intelligence (SETI)

The NASA SETI Program will utilize SETI-specific instrumentation to hunt for radio signals of extraterrestrial origin in the microwave window, from about 1 to 10 GHz. The signals may be narrowband carriers or pulses whose spectrum is as narrow as their duration permits. For this purpose, we need a high-resolution, wideband radio-frequency spectrometer — a receiver that looks at a large number of narrow channels simultaneously.

In February 1985, initial field tests of the prototype SETI MCSA (Multichannel Spectrum Analyzer — built at Stanford University with NASA grant support from the Office of Space Science and Applications' Life Science Division) began at NASA's Goldstone Deep Space Tracking Network facility. The prototype, at this stage of development, simultaneously monitors on a real-time basis 74,000 channels, each 1 Hz wide. The full system as planned will simultaneously monitor on a real-time basis 8-10 million channels, with variable resolution capability of 1, 2, 4, 8, 16, and 32 Hz.

During 1985, initial field tests of the pulse and drifting CW signal detection algorithms confirmed timings and noise statistics predicted by theory. As refinements to these algorithms continue, studies for the second phase of prototype instrumentation (the pattern detector), were initiated jointly by Stanford University and the SETI Institute. This postprocessor will realize in dedicated hardware the signal detection algorithms currently implemented in software. Such hardware realization will be necessary to maintain real-time analysis capability at the 8-10 million channel level.

(B. Oliver, Ext. 2298)

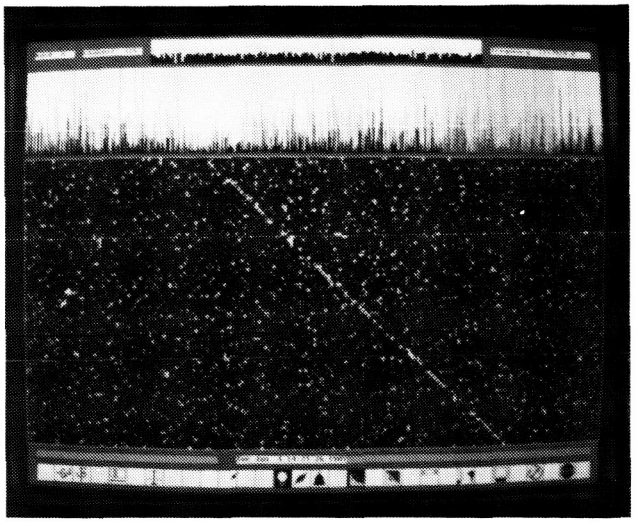

Oliver

Photograph of June 4, 1985, MCSA output of signal from Pioneer 10, utilizing Goldstone 26-m antenna. Utilizing NASA DSN equipment, this particular antenna cannot lock onto Pioneer 10's signal due to a combination of the great distance involved and the weakness of the carrier power (approximately 180 candlepower, including the Pioneer antenna gain). According to expectations, utilizing NASA's SETI Instrumentation on the 26-m antenna, the signal is clearly visible and easily detected.

Flight Trials on Space Shuttle of Autogenic Feedback Training as a Motion-sickness Countermeasure

Foremost among the medical problems identified by NASA's Office of Space Science and Applications is the nausea, vomiting, and malaise during the first few days of adaptation to weightless flight. Promising research toward an effective countermeasure has been conducted by psychologists in the Neurosciences Branch of Ames' Life Science Division, in collaboration with University of California and Rockefeller University.

In ground-based studies, motion sickness was reduced or prevented entirely in subjects who learned to voluntarily control their physiological activity by monitoring electronic biofeedback signals that informed them of real-time changes in their bodily functions, such as heart rate, respiration, skin resistance, and peripheral vasoconstriction. Autogenic Feedback Training (AFT), a self-training technique, was developed at Ames specifically to control the symptoms of motion sickness in the space environment.

Cowings

Biofeedback instrumentation, including data recorder, worn by astronauts on Spacelab 3 in an experimental test of a psychophysiological countermeasure to space motion sickness

The first in a series of experimental flight trials using AFT was conducted on both the STS-51C mission and on Spacelab 3 (STS-51B) in collaboration with the Astronaut Office at Johnson Space Center and the U.S. Air Force. There was a strong correlation between crewmembers' preflight proficiency in AFT and their success in controlling symptoms inflight. Other crewmembers, who acted as controls and who did not receive AFT on Earth, experienced symptoms inflight despite their use of antimotion sickness drugs. Adequate data were obtained for a preliminary assessment of AFT (although a final validation requires flight data from 8 treatment and 8 control subjects.

(P. Cowings, Ext. 5724)

Exercise Training and Orthostatic Intolerance

There is some evidence which indicates that highly trained endurance athletes have significantly lower tolerance when subjected to head-up tilt than do their sedentary counterparts. Astronauts exhibit varying degrees of orthostatic intolerance at the end of shuttle missions. Since most astronauts engage in regular endurance physical training, it is possible that such exercise may accentuate their orthostatic intolerance.

Results from an Ames Research Center study show that short-term (8–12 day) exposures to exercise and heat and long-term (6-month) exercise training programs indicate no significant effect upon acceleration or orthostatic tolerance, even though positive physiological responses to the training regimens were observed. The Ames findings suggest that the present type of physical training programs engaged in by the astronauts will probably not compromise $+G_z$ (head-to-foot) acceleration tolerance or tilt-table tolerance. The lower orthostatic tolerance observed in the trained athletes, therefore, may be due to a genetic predisposition. This should be considered when highly trained endurance athletes are considered for assignment as Shuttle pilots.

(J. Greenleaf, Ext. 6604)

Muscle Atrophy in Simulated Weightlessness on Earth and on Spacelab 3

Astronauts and animals lose muscle mass and strength during space flight; neither the exact causes nor the pattern of physiological changes responsible for the muscle loss have been established. In order to investigate muscle changes resulting from "weightlessness," rats, whose hind limbs are suspended, have been studies. The availability of samples from rats flown on Space Laboratory 3 (SL-3) allowed us to compare their muscles to those of suspended rats, and to evaluate suspension as a model of weightlessness.

Under suspension, different muscles showed different patterns of electrical activity, and muscle weight decreased to varying degrees. Also, muscle strength decreased earlier than did muscle weight. The electrical activity, which normally precedes contraction, was abolished in antigravity (hindlimb) muscles when the rats were suspended; but over the next two weeks of suspension, electrical activity of these muscles returned to normal. At the end of 28 days of suspension, the muscles had lost 10–45% of their mass. A hindlimb flexor muscle (which does not oppose gravity) showed a 75% increase in electrical activity, but still lost 10% of its weight. Rats suspended for 7 days lost the same amount of muscle as those suspended 28 days. The latter group showed further qualitative deterioration of the muscle, such as decreased enzyme content, and few muscle fibers remained intact.

Rats recovered from Space Laboratory 3 showed muscle weight losses similar to those of suspended rats; two extensors lost 23% and 35% of their weight, respectively, and the flexor lost 9%. (See figures.) The cross sectional areas of individual muscle fibers decreased in parallel with muscle weight. (See table.) Like the suspended animals, SL-3 rats also showed an increase in the number of fast (movement) fibers and decreased number of slow (antigravity support) fibers. Seven days of space flight on SL-3 resulted in muscle changes similar to those of suspension, thereby validating the suspension model. It is also of interest that the extent of the muscle loss on SL-3 was nearly identical to that in rats flown for 20 days on unmanned Soviet biosatellites, indicating that muscle loss occurs even earlier in flight. Finally, the disparity between muscle electrical activity and muscle weight of suspended rats on Earth suggests that in "weightlessness" electromyography may not provide an accurate index of muscle function. This space medicine research was sponsored by NASA's Office of Space Science and Applications, and performed in collaboration with Pennsylvania State University, UCLA, the University of Santa Clara, and the Biomedical Office at Kennedy Space Center.

(R. Grindeland, Ext. 5756)

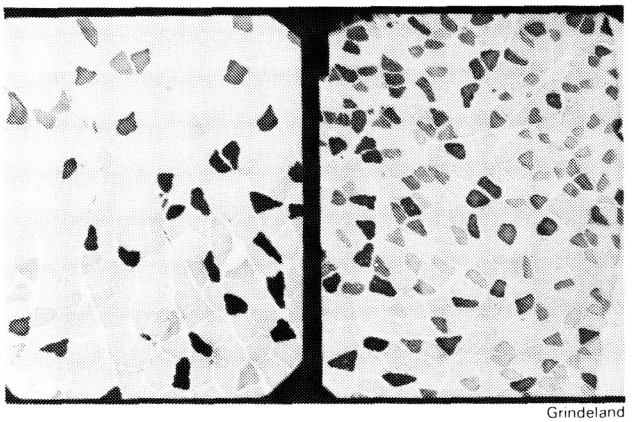

Grindeland

Two micrographs at the same magnification showing soleus muscle of the young rat: one control (larger cells) and one from Spacelab 3 (smaller cells). The dark-stained fast-twitch fibers are markedly increased in the flight muscle. The lighter slow-twitch fibers contract slower to maintain posture against the force of gravity

		FLIGHT ANIMAL	CONTROL ANIMAL
% FIBER TYPE	SLOW TWITCH	54	65
	FAST TWITCH	46	35
CROSS SECTIONAL AREA (μm^2)	SLOW TWITCH	963	2643
	FAST TWITCH	726	1555

Grindeland

Spacelab 3 rat soleus muscle

Mechanism of Rapid Bone Loss

During weightless spaceflight, significant bone mineral loss occurs in the lower extremities. Using a primate model, ground-based research on bone loss associated with immobilization allows investigators to examine the process of disuse osteoporosis, to document the time history of bone loss, and to evaluate the potential for recovery.

Neither high-calcium diets nor the use of pulsing electromagnetic coils to stimulate bone growth were effective in preventing bone mass loss in the lower extremities. Immobilization gives rise to uncontrolled bone resorption. The massive loss of bone results from the excessive number and depth of penetration of osteoclasts, the bone-resorbing cells. Bone loss continues throughout seven months of continuous immobilization (see figure). At this point, bone mineral content in the cross section is reduced approximately 30%, and bending stiffness is reduced 35%. Repair and reconstruction of the tibial cortex begins after one month of reambulation. Within 8-1/2 months, sufficient cortical bone has been restored to return bending stiffness to normal values (although histological remodelling changes continue for at least 40 months of recovery).

Young

Large resorption cavities in the tibial tuberosity after 7 months of immobilization. There is crumbling erosion on the outer surface of the anterior tibia

In the primate model, the extreme alterations in bone are obviously correlated with skeletal loading. The potential role of special exercises in the prevention of loss of control and regulation of osteoclast recruitment and activation will be the subject of future investigations.

(D. Young, Ext. 5549)

Trace Contaminant Gases in a Space Cabin

Research on trace contaminant gases in the atmosphere of an enclosed environment is applicable to both manned and unmanned extended duration space missions. Potential hazards to humans, experiments, and instrumentation can result from contaminants generated by materials off-gassing, human metabolic products, and experiments. Hazards can also be created by interaction of trace gases. These interactions include synergistic effects, breakdown products produced as chemicals degrade, or effects owing to chemical interaction stimulated by various spectral wavelengths. These dangers create a need for the identification, control, and removal of potentially hazardous trace contaminants.

A study was undertaken to investigate atmospheric trace contaminant origin, frequency, concentration, and duration of existence in a closed environment in space. The goal was to create a model gas mixture that could be used in the laboratory to simulate the atmosphere that might be found in a space cabin environment. A data base was obtained from previous Skylab and Shuttle missions. This data base included information from gas grab samples and desorbed charcoal canisters. The data base was then organized and evaluated. Substances were classified according to their chemical category, toxicological category, and frequency of occurrence and concentration (as a percentage of the Space Allowable Concentrations – SMACs).

A simple, dynamic program was utilized to choose 12 gases from approximately 100 chemicals identified in the charcoal data set, and 12 gases from the 100 chemicals identified in the

gas grab sample data set. In order of priority, the chemicals chosen were those that:

1. Had the highest concentration within each chemical category.
2. Had the highest frequency within each chemical category.
3. Represented each toxicological category.
4. Represented each chemical category.

An engineer might use these chemicals, loads, and frequency of occurrence information to evaluate and design a trace-contaminant-removal system. Chemicals chosen from the gas grab samples might be used to evaluate a monitoring and detection instrument for a closed environment in space.

(M. Schwartz, Ext. 5542)

Multiplex Gas Chromatography for Future Planetary Studies

Gas chromatography is a powerful technique for the analysis of gaseous mixtures. Besides being a major analytical technique with a great many applications, including atmospheric analysis on Earth, it has also been successfully employed on space missions such as the Viking Mars lander and the Pioneer Venus probe. Recent advances in gas chromatography suggest that conventional gas chromatography is still one of the most powerful methods available to conduct the desired analyses in future planetary missions, but limitations in the technique exist which can be alleviated with multiplex gas chromatography.

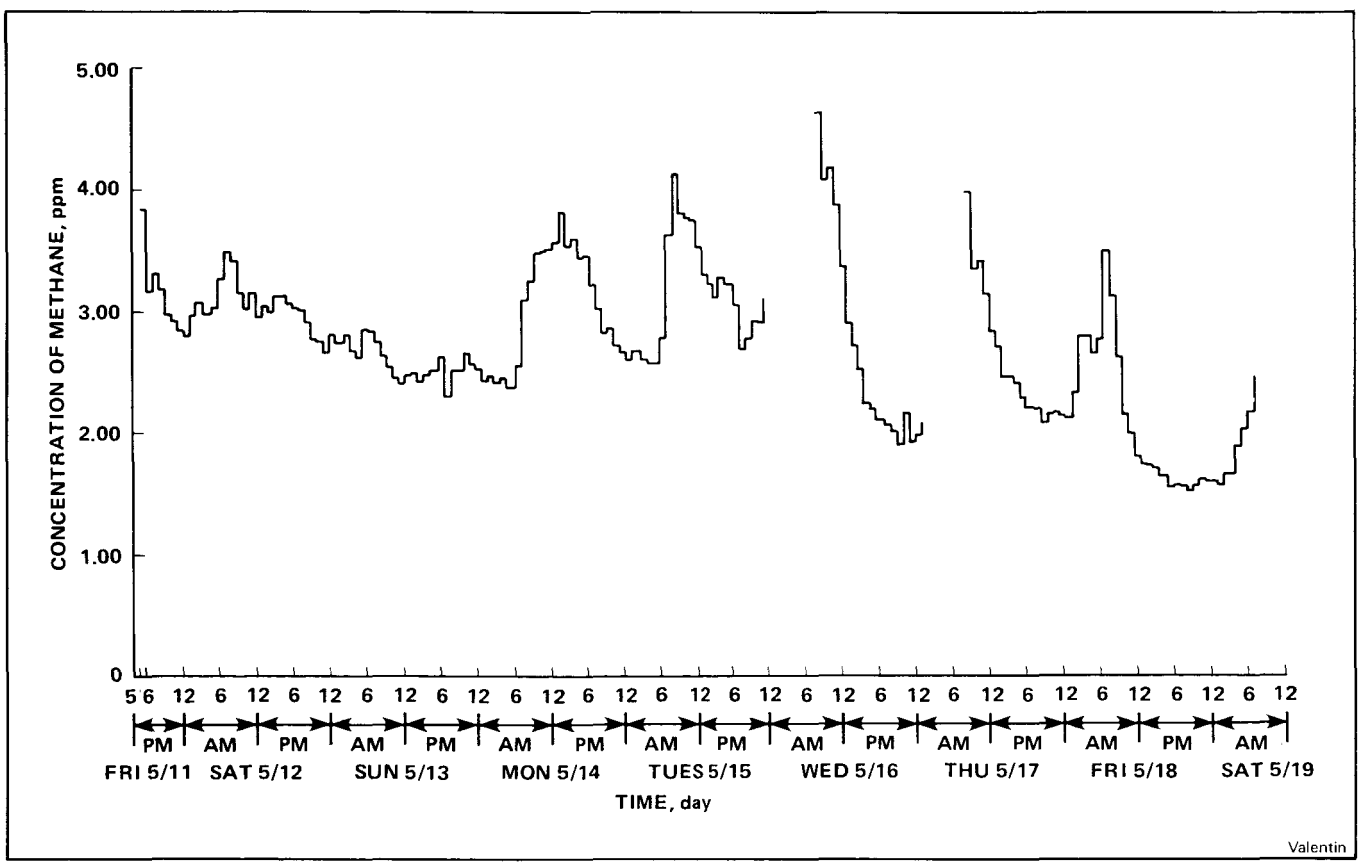

Profile of the concentration of methane in ambient air showing one-hour averages for an 8-day period

Multiplex gas chromatography pseudorandomly introduces many samples to the chromatogram without regard to elution of preceding components. The resulting data are then reduced using mathematical techniques such as cross-correlation.

Under the Planetary Biology Program sponsored by NASA's Office of Space Science and Applications, the basic technique of multiplex gas chromatography was demonstrated using chemical modulators with only one gas stream, which consisted of the carrier in combination with the components being analyzed. Several advantages came from using this technique in combination with these modulators: improvement of several orders of magnitude in detection limits, improvement in the analysis of complex mixtures by selectively modulating some of the components present in the sample, increase in the number of analyses that can be conducted in a given period of time, and reduction in the amount of expendables needed to run an analysis.

Multiplex gas chromatography was demonstrated for the first time in a practical application by quantitatively determining methane in ambient air. Further, the analysis was done over both long and unattended periods of time without using any expendables beyond power for the analysis.

(J. Valentin, Ext. 5766)

Superoxide Mixtures as Air Revitalization Chemicals

Superoxides are solid chemicals that, when reacted with water vapor, release oxygen and form a product that absorbs carbon dioxide. As a result of their ability to release oxygen and scrub carbon dioxide, superoxides (particularly potassium superoxide (KO_2)) are used extensively in life-support applications. Some applications include: portable, self-contained breathing apparatus for miners; emergency oxygen source for aircraft; and, more recently, as a potential emergency oxygen source/carbon dioxide absorbent for the Space Station safe haven.

The poor utilization efficiency of potassium superoxide (only 50–80%) prompted research into improved superoxide chemicals. It was discovered that granules fabricated from an intimate mixture of KO_2 and calcium superoxide ($Ca(O_2)_2$) showed improved utilization efficiency with respect to both oxygen release and carbon dioxide absorption over the commonly used commercial superoxide, KO_2. This superior utilization efficiency of the $KO_2/(Ca(O_2)_2$ mixtures is shown in the figures where the amounts of oxygen released and carbon dioxide absorbed by two $KO_2/Ca(O_2)_2$ mixture formulations are compared to KO_2. The lower utilization efficiency exhibited by the KO_2 is caused by the formation of a fused product layer which hinders the transfer of water vapor and carbon dioxide to the interior of the chemical granules. In the case of the mixtures, this fused product layer is minimized.

The superior reaction characteristics of the superoxide mixtures, combined with their high oxygen storage density, long shelf life (unlike high pressure bottled oxygen), and the fact that they require no power during use make them attractive for emergency life support applications in spacecraft such as the Space Station.

(T. Wydeven and P. Wood, Ext. 5738/5737)

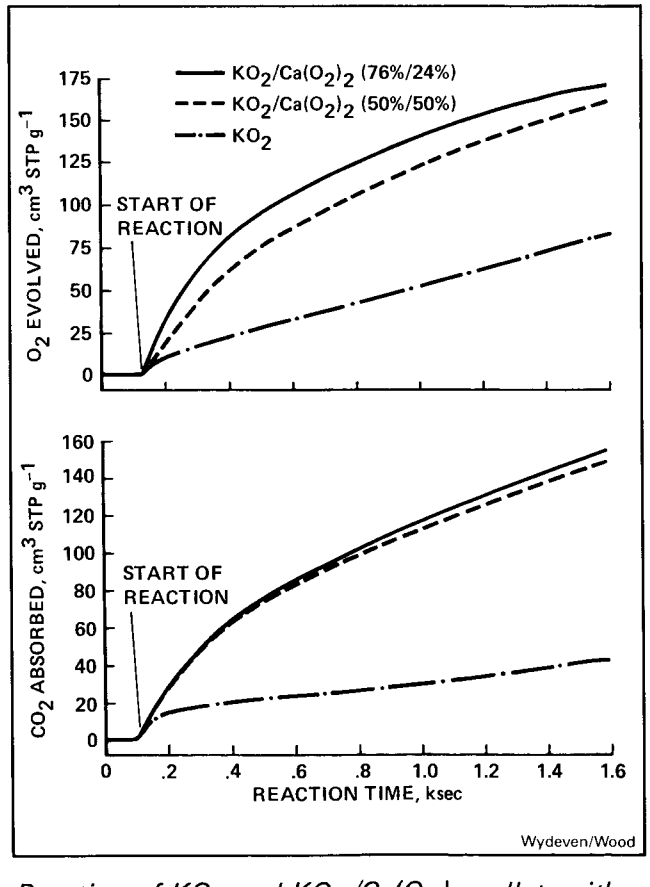

Reaction of KO_2 and $KO_2/Ca(O_2)_2$ pellets with humidified carbon dioxide/helium. Amounts of O_2 evolved and CO_2 absorbed as functions of the reaction time

Ion Mobility Drift Spectrometry (IMDS) as a Flight Analytical Instrument Technique

A detailed knowledge of the history and abundances of the biogenic elements and their compounds throughout the solar system can provide the exobiologist with a basis for understanding the conditions necessary for chemical evolution and the origin of life. Flight experiments conducting in situ analyses have already produced a wealth of information on the environments of Venus and Mars. Future missions will require instrumentation capable of providing identification and quantitation of a multitude of molecular species over a wide range of concentrations. In particular, analysis of the complex organics expected to be performed for a mission at Titan, may tax the limits of current analytical technology. A flight instrument utilizing IMDS technology can provide scientists with a powerful means of obtaining this information.

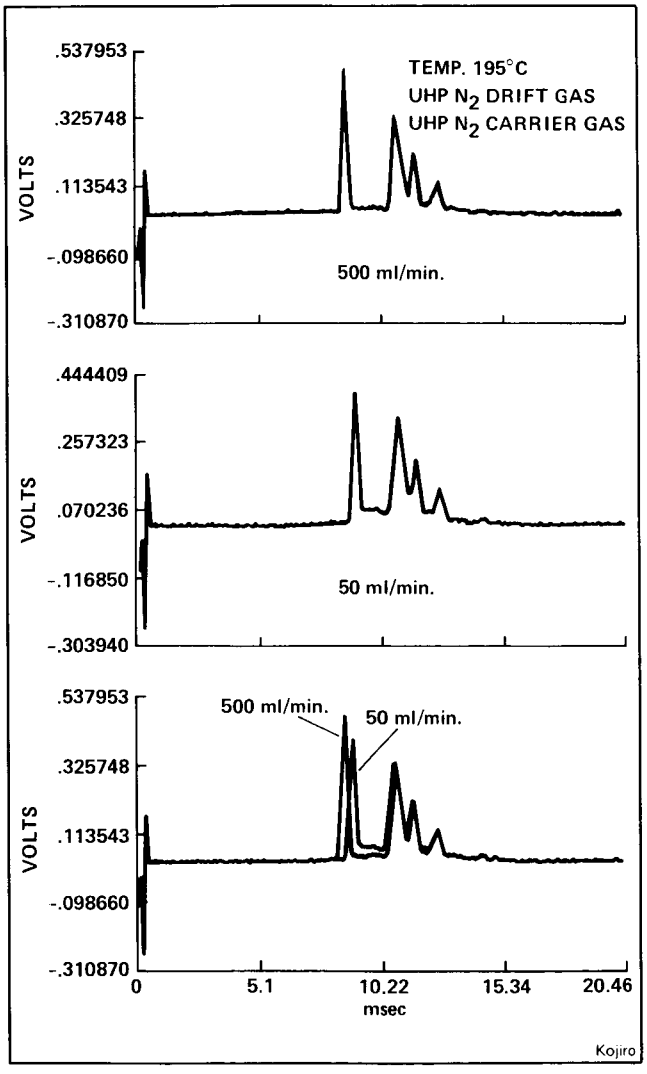

Pentane spectrum from Ion Mobility Drift Spectrometer (IMDS). Drift gas-flow rate is reduced by a factor of ten, yet pentane spectrum shows little change

The IMDS is an ion molecule reactor coupled with an ion drift spectrometer. Sample molecules are ionized to form product ions in the reactant region. An electric field moves the ions through a drift region against the flow of a drift gas, where they are separated according to their size and structure, thus producing an ion mobility spectrum. These spectra provide the IMDS with virtually universal sample-identification capability. To conform to the rigid limits of weight, volume, and consumables placed on flight instrumentation, several aspects of the IMDS must be studied and redesigned for flight use. In addition to miniaturization of the instrument, a reduction in the high-flow rates used for the drift gas is an obvious necessary consideration. The effect of drastically reduced drift-flow rates on IMDS spectra was investigated by lowering flow rates from 500 ml/min to 50 ml/min. Changes in peak shape, drift time, and total spectra were studied at each flow rate. Although changes did occur, IMDS analysis appears acceptable at the lower flow rates. Investigations into alternative drift gases and reactive carrier gases are also being pursued.

(D. Kojiro, Ext. 5364)

Modulated Voltage Metastable Ionization Detector (MVMID)

Gas chromatography has evolved into one of the most powerful analytical techniques currently available to scientists. The highly efficient, sensitive gas chromatographs (GC) used in today's laboratories accurately separate and measure complex mixtures of volatiles.

Hand-in-hand with the development of the GC, and responsible to a great extent for the improvements in sensitivity, has been the development of the gas chromatographic detector. Detection of parts per million (ppm) sample concentrations are easily within the capabilities of present day detectors, and parts per billion (ppb) analysis is now becoming routine. The Metastable Ionization

Detector (MID) (also called the Helium Ionization Detector) is the most sensitive, universal GC detector currently available. When operated at its most sensitive voltage range, however, it has a response range of only three orders of magnitude. This narrow response range makes the MID unsuitable for many areas of gas analyses.

Under sponsorship of the Planetary Biology Program, a voltage modulation system has been developed to expand the response range of the MID to over six orders of magnitude without losing any sensitivity. For large sample concentrations, the MVMID lowers the ionization efficiency of the MID by reducing the detector voltage. Large samples are quantitated by measuring changes in detector voltage. This prevents detector overload and increases the MID response range upward several orders of magnitude. Sample concentrations ranging from a few ppm down to a ppb are detected and quantitated by measuring detector current at maximum MID voltage. The MVMID is a sensitive, universal GC detector system which can be utilized for a wide range of gas analyses and future flight experiments.

(D. Kojiro and G. Carle, Ext. 5364/5765)

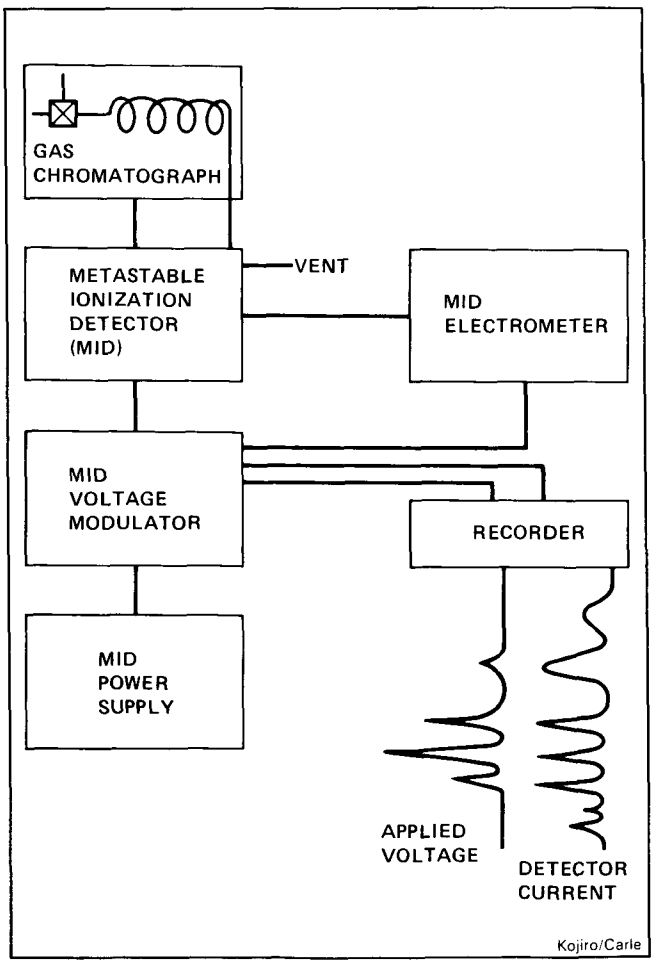

Diagram of a modulated voltage metastable ionization detector

Investigation of Porous Polymer Gas Chromatography Packings for Atmospheric Analysis of Extraterrestrial Bodies

For extraterrestrial probes, whether planetary, lunar, or cometary, atmospheric composition is an important analysis, and gas chromatography (GC) is the technique best suited to carry it out. The rationale for such analysis is that the data may provide important information on the origin and evolution of the solar system, chemical evolution, and life. Gas chromatographic instrumentation was used successfully aboard the Mars and Venus probes. However, for missions of much greater duration, weight, power and volume considerations require seeking ways to reduce significantly the size of the instrumentation and to increase its sensitivity. Column packings are the functional components of a GC system which cause the separation of multicomponent gas mixtures into individual elutable and measurable peaks for quantitation. The improvement of GC column packings is the subject of this study, which is sponsored by the Office of Space Science and Applications' Planetary Biology Program.

The column used on the Venus probe to measure the permanent gases in the atmosphere was Poropak N (16 m long), and a high carrier gas-flow rate was used. In order to reduce this dimension, commercial porous polymer types were surveyed which had some ability to resolve nitrogen, oxygen, argon, and carbon monoxide gases. Poropaks N and Q appeared superior. However, batch-to-batch variation was wide, so ARC learned how to synthesize porous polymers and to investigate some of the factors affecting the separations.

A polymer was synthesized which was superior to all commercial products and allowed at least a 50% reduction in length and flow rate of carrier gas. Similar studies were made concerning the separation of hydrocarbons, and new porous polymers have been synthesized which represent significant improvements in time of analysis,

column length, and carrier gas-flow rate. Further work will include column development for polar gases and water and investigation of capillary column usage to reduce further carrier gas requirements.

(G. Pollock, Ext. 6165)

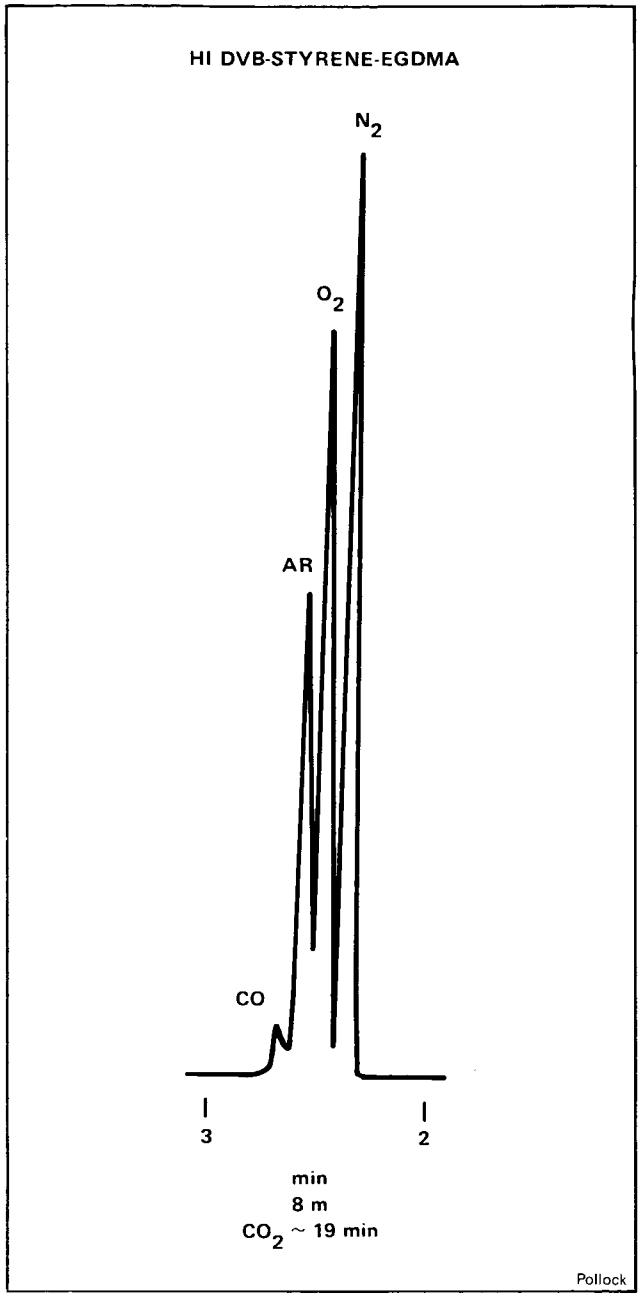

GC separation of the permanent gases on a column 50% shorter than the Pioneer Venus column

Production of Hydrocarbon Gases by Lightning in the Atmospheres of the Outer Planets

Lightning has been detected in at least three planetary atmospheres (Earth, Venus, and Jupiter) and is expected to occur in the atmospheres of the other outer planets as well. From observations made by ground-based telescopes and spacecraft instruments, the atmospheres of Jupiter, Saturn, and Titan (a moon of Saturn) have been found to contain many organic species, including hydrocarbons and simple nitriles. This was not expected if the planets were formed by simple thermodynamic condensation of a primordial solar nebula. The presence of species other than methane, ammonia, hydrogen, and helium indicates the occurrence, past or present, of active organic chemistry in outer planet atmospheres.

To study the production of compounds by lightning in planetary atmospheres, as part of the Planetary Biology Program, a research program has been initiated in collaboration with the State University of New York at Stony Brook. A facility has been built that enables various gas mixtures (representing different atmospheres of interest) to be subjected to high voltage/high amperage electrical discharges to simulate lightning-initiated chemistry in the atmosphere of Titan. Using a mixture of 90% nitrogen, 5% methane and 5% hydrogen, results showed that acetylene and hydrogen cyanide (HCN) are the dominant products, as expected from high-temperature shock models of lightning-initiated chemistry. Also, the yields of ethane and ethylene are within an order of magnitude of those of acetylene and HCN, which is not consistent with the equilibrium shock model. Smaller amounts of propane, propylene, allene, iso- and normal butane, and pentane have also been produced. Of these species, ethane, ethylene, acetylene, propane, and HCN have been found in outer planet atmospheres, but the others have not so far.

Work is continuing with gas mixtures more accurately modeling the various atmospheres to determine the compositions of planetary atmospheres, and hence, to provide guidelines for the design of analytical instruments to be carried aboard future spacecraft.

(C. McKay and T. Scattergood, Ext. 6864/6163)

Possible Evolution of RNA Polynucleotides in the Absence of Enzymes

DNA and RNA molecules are responsible for storing and transferring genetic information. This is a key step in the synthesis of enzymes which perform various functions in living organisms. DNA and RNA replication are based on the complementarity of the nucleic acid bases in the two strands of a double helical DNA molecule. The process of replication is highly complex; some nine different types of enzymes are necessary for DNA synthesis to occur. Even though DNA and enzyme syntheses are intertwined, it seems that storage and transfer of genetic information is the most basic function of a living organism. In the early stages of chemical evolution, the function of enzymes could have been performed by less effective catalysts, such as metals, clays or even small peptides. Therefore, most scientists working in the field of chemical evolution in the origin of life believe that on the prebiotic Earth, the replication of small RNA fragments (so-called polynucleotides) preceded the formation of specialized enzymes.

In this context, several attempts have been made to observe in vitro replication in the absence of enzymes. This turned out to be possible only when the mononucleotides (the building blocks of polynucleotides) are chemically activated. The type of chemical activation used is important because mononucleotides can undergo side reactions which compete with replication. One of the most important side reactions is hydrolysis of the activated mononucleotide to form a nonactivated (or free) mononucleotide that can no longer take part in the replication process.

In a series of studies modeling nonenzymatic replication, the hydrolysis reaction of an imidazolide-type activated 5′-phosphoguanosine was investigated. This compound has been shown to be a very effective and selective activated mononucleotide. It forms long oligoguanylates in the presence of polycytidylic acid acting as a template. The results showed that, in the absence of the template, after 47 days at 4°C there is still 50% of the activated nucleotide present in solution. Contrarily, in the presence of a relatively concentrated solution of template and activated monomer, the reaction results within seven days in consumption of the mononucleotide and formation of long oligoguanylates. These data show that hydrolysis is much slower than replication on the template.

This remarkable resistance towards hydrolysis may be one of the reasons this replication model is so effective in forming relatively long polynucleotides. It is, therefore, conceivable that on the primitive Earth where there were no enzymes and where template molecules were scarce, effective replication could only be achieved by molecules which were stable toward hydrolysis and reactive toward replication.

(S. Chang and A. Kanavarioti, Ext. 5733/6163)

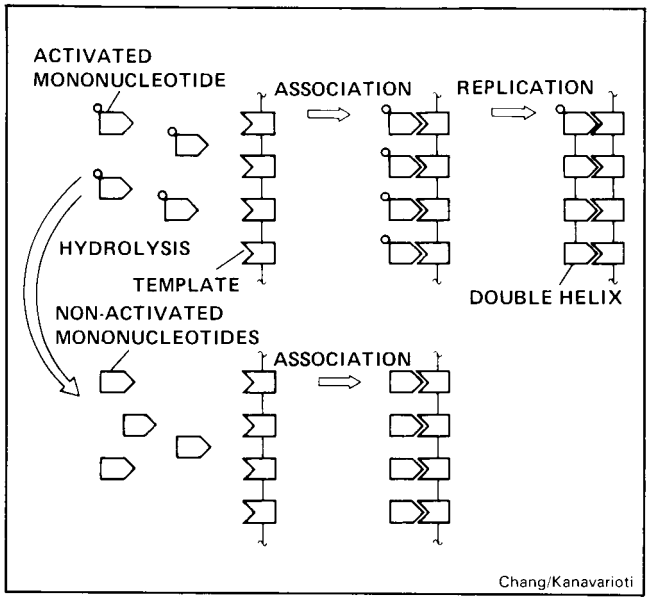

Nonenzymatic RNA-type replication

Mineral Energetics in Prebiotic Chemistry

Clay minerals have previously been implicated in the origin of planetary life in two contexts: as catalytic supports for the development of organic life forms, and as inorganic prototypic life forms from which organic life was templated. In either context, the energetic properties of clay minerals are central to their utility.

The Ames Planetary Biology Branch, in a program sponsored by the Office of Space Science and Applications' Life Sciences Division has been testing the hypothesis that electronic energy stored in clays in responsible for a variety of novel luminescent phenomena, and may also be of utility in driving clay surface chemistry.

Application of hydrazine, or substituted hydrazines to clay, results in the long-term emission of

ultraviolet light. Among the postulated triggers for this light release are chemiluminescent surface decomposition of hydrazine and intercalation (insertion) of hydrazine between the clay layers. Light release induced by hydrazine or unsymmetrically substituted dimethylhydrazine (UDMH) from a series of variably water-intercalated kaolins was studied in relationship to the ease of hydrazine intercalation by these liquids. Hydrazine and UDMH have different intercalating capacities and also different routes of decomposition. The profiles of light release observed from three hydrated forms of kaolin are consistent with the conclusion that intercalation is an important factor in light release. However, spectral studies will be required to establish this conclusion. Further research also is required to assess the contribution of decomposition to light release.

The influence of stored energy on mineral surface reactivity is of general interest to chemical evolution regardless of the particular reaction. However, this system is of particular significance. Hydrazine decomposition is the reverse of nitrogen fixation, a difficult and essential reaction that must have preceded the formation of living organisms. That decomposition occurs, in our system, concurrently with light emission gives hope that the reaction might be substantially reversed on an energized surface.

(L. Coyne, Ext. 5968)

Controlled Ecological Life Support Systems (CELSS)

The controlled ecological life support systems (CELSS) program, under NASA's Office of Space Science and Applications, supports a variety of inquiries directed at understanding how an integrated set of biological and physical-chemical processes can function in a stable state to provide the life-support and waste-removal requirements of a crew in extraterrestrial environments. A major component of a CELSS will be the plant growth module.

A science requirements workshop was conducted at Ames to address problems associated with the design, construction, and operation of a higher plant-growth facility. Topics covered ranged from the control of critical environmental parameters (e.g., irradiation, gas concentrations, nutrient solutions), to the definition of subsystem designs, to the monitoring and control of trace contaminants. The accompanying figure shows an artist's concept of a large plant growth chamber.

Scientists from Ames and the University of New Hampshire have constructed and operate several plant-growth chambers for the study of plant responses under stringently controlled conditions. As part of these studies, bacterial populations in the chamber's nutrient solution have been examined to identify species distribution, population sizes, and the effect of variations in the nutrient solution on microbial ecology and plant growth. Solution pH is maintained by a special electrochemical controller which obviates the need for external sources of acid or base.

In other work jointly conducted by Ames and the University of New Hampshire, research is directed at understanding gas exchange dynamics within simple plant-animal systems. The goal is to develop control techniques and management strategies for maintaining atmospheric levels of oxygen and carbon dioxide at physiologic levels. Manipulation of algal environmental conditions (i.e., light intensity, cell density, and nitrogen sources) has been shown to affect the relative rate of the algal assimilatory quotient, the balance of the uptake of CO_2, and the production of O_2.

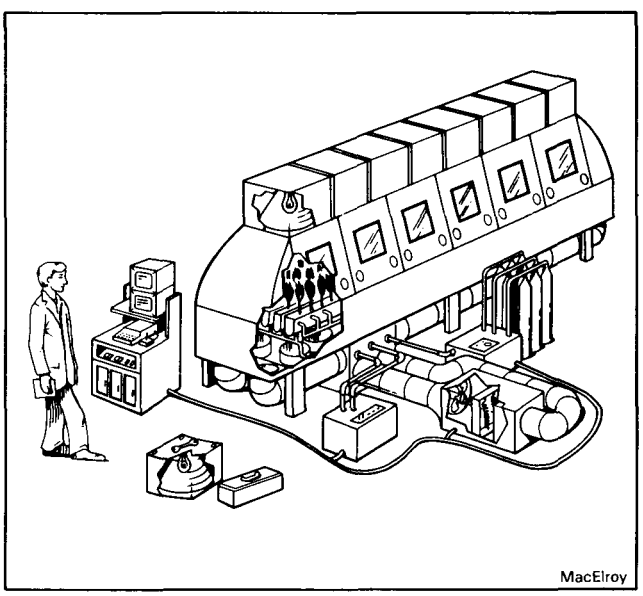

Artist's concept from NASA Ames design study for a large "closed" plant growth chamber for pre-spaceflight studies. Round glove parts and windows are along the sides, and mechanical devices are separated from the main chamber to reduce vibrational effects.

The results indicate that photosynthetic organisms can be used as effective control elements within a CELSS. To determine the mass balance of the system, the plant-animal system was indirectly coupled with a waste processor. Preliminary results indicate that the system, if properly integrated, could show mass closure of the important bio-elements, carbon, oxygen, nitrogen, and hydrogen.

Simultaneous development of a computer-simulation model of the plant-animal system is proceeding, and is using data from the experimental system for validation.

(R. MacElroy, Ext. 5573)

Cooperation of Primitive Genes

During the earliest stages of the origin of living cells, it is likely that the genetic material consisted of short RNA (ribonucleic acid) molecules rather than the extremely long DNA molecules of modern cells. In fact, the strands could have been so short that only a single gene (or at most, a few) occupied each strand. Therefore, in order to begin building up a significant genome, several separate strands would almost certainly have to have been involved at some stage (perhaps even before recognizable cells had formed).

However, this scenario presents a severe problem. In the absence of the tight controls on gene replication in a modern cell (causing exactly one copy of each gene per cell division), separate strands would not have the same rate of replication except by coincidence. This would lead to an unusual type of competition and Darwinian natural selection between separate genes, within the same genome, with the result that disadvantaged slower genes would be squeezed out by faster, "selfish genes."

Computer modeling was carried out at Santa Clara University under a NASA grant, and a solution to this problem was demonstrated. It is valid under a wide variety of conditions, provided that each gene contributes to the overall functioning of the collection (such as begin translated into a useful primitive enzyme). Even when one "selfish gene" produces more copies than its neighbors, as the products get distributed into daughter colonies, some colonies will be richer in the disadvantaged gene than others (see illustration). Colonies that are missing the disadvantaged gene will grow more slowly, or not at all, since they have lost some vital function. Thus, the faster "selfish gene" is continually edited out as its pure colonies are left behind.

The computer simulations show that even relatively large differences in replication rates (5:1) can be overcome by this mechanism. Furthermore, the fastest-growing colonies are those with slower "selfish genes." Thus, the pressure of natural selection at the level of collections of genes overcomes natural selection at the level of molecules, and actually favors the "selfish gene" which slows down and allows its partners to catch up. As soon as genes were able to produce any useful enzymes, however crude, that were of benefit to their neighboring genes as well as to themselves, natural selection would have forced them to cooperate and to maintain a stable genome. Thus "selfish genes" would not prevent the building of larger and more stable genomes.

(D. White and S. Chang, Ext. 5733)

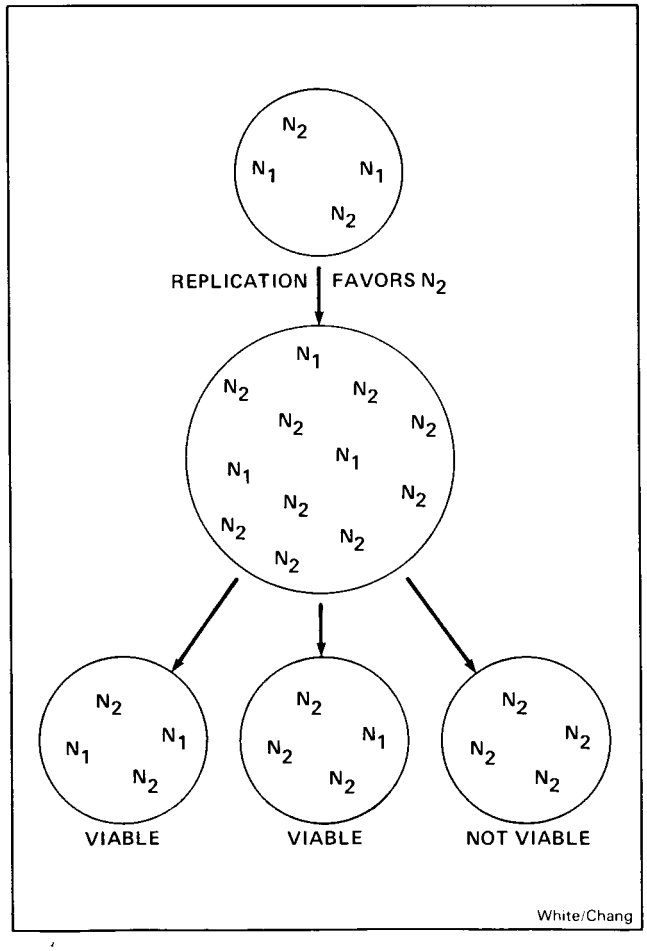

Natural selection promotes cooperation with a mechanism to retard "selfish genes"

Molecular Microenvironments and the Origin of Life

During and after the formation of simple biogenic organic molecules on the primitive Earth, the first processes of molecular organization occurred. The level of organization was probably quite simple. It involved interactions among organic molecules, ions, and the solvent (water), and resulted in the formation of molecular microsystems (structures) that were relatively stable. The driving force behind the organization of molecular microsystems is a decrease in the system free energy.

The structures and forces associated with noncovalent molecular organization are of interest because they would have directed the events and sequences in subsequent molecular evolution. They were also probably directly responsible for the reactions that formed specific polymer structures from which life functions evolved. And the forces were the same as those that determine the structures, dynamics and interactions of the large molecules that constitute present-day living systems, as well as the mechanisms of reactions that allow specific catalysis, and the storage and expression of biological information.

Sponsored by the Office of Space Science and Applications' Life Science Division, scientists at Ames Research Center and the University of California at Berkeley have been studying both fundamental organizational process of organic molecules in solution, and the forces that govern them. They have identified several mechanisms by which the ubiquitous solvent, water, influenced the interactions between prebiotic molecules. The effects are accompanied by changes in the structure of liquid water induced by the solute. An example of simple organization is the arrangement of water around the nucleic acid base pairs, adenine and uracil. Studying the modification of water structure simultaneously with the interactions among solute molecules led to an understanding of the unique organizational effect of water on prebiological molecules.

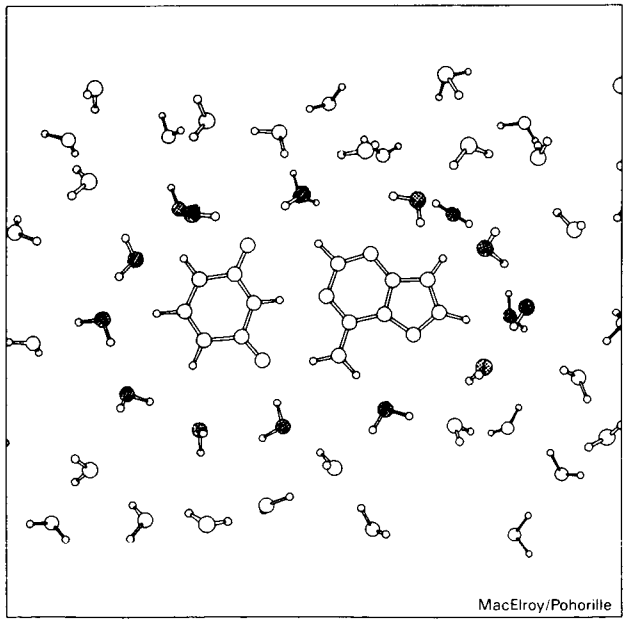

Arrangement of water around the nucleic acid base pair adenine and uracil. Water molecules in the first hydration shell are highlighted

Molecular interactions in solution have been studied with highly sophisticated techniques of molecular simulation, using the high-speed computer facilities available at Ames. To date, the research has explored a suite of small, organic molecules in water and other solvents. The data gathered are essential to understanding the behavior of larger molecules such as proteins and nucleic acids, the interactions among them, and the evolution of organization, recognition, and enzyme catalysis.

(R. MacElroy and A. Pohorille, Ext. 5573/6486)

A Model for Stray Radiation in Infrared Telescopes

Program STRAY is being developed at Ames Research Center to model the amount of stray radiation reaching the focal plane of a well-baffled infrared telescope. Unwanted radiation arises from both the scattering of the light of bright off-axis sources, such as the Sun, Earth, and Moon, and the thermal emission of the telescope itself. A series of specular reflections, scatters, and diffractions propagates this energy to the focal plane. The sum of the various paths yields the focal plane irradiance in watts/wavelength band/square arc minute.

In addition to the telescope geometry, the user selects the chopping amplitude, points in the focal plane, wavelengths, bandwidth, angles of incidence, incident irradiance, and temperature, emissivity and reflective properties of the blacks and optical surfaces. STRAY is written in FORTRAN 77 and runs on a VAX under the VMS operating system.

(A. Dinger, Ext. 6849)

Opaque Coatings Developed for the Submillimeter Region

A variety of materials have been studied spectrally in the 0.02-0.50 millimeter range of the electromagnetic spectrum to identify promising components for an opaque coating for SIRTF (Space Infrared Telescope Facility). Opaque coatings are commonly applied to the baffles of telescopes and other optical instruments to reduce internally reflected stray light. However, conventional optical-black coatings become quite reflective at the long wavelengths which SIRTF will employ. This survey produced more than 40 separate reflectance spectra of various coatings, binders, and additives. *Several specific combinations demonstrated a specular reflectance below 10% throughout the spectral range studied.* One particular combination, currently called Ames 24E, was further developed to improve its mechanical properties. This coating now withstands severe abrasion tests, and has been temperature "cycled down" to liquid helium temperatures at both Ames and U.C. Berkeley. Recent sensitive spectra indicate that the normal incidence specular reflectance of this coating is *less than* 10^{-3} at 0.2 mm.

(S. Smith, Est. 6264)

Antireflection Overcoat Found for the Submillimeter Region

A simple antireflection overcoat to be applied to infrared-opaque telescope coatings has been found which works in the far-infrared/submillimeter region of the electromagnetic spectrum. Opaque (black) coatings are commonly applied to the baffles and stops of telescopes and other optical instruments to cut down internally reflected stray light. Such coatings are often good absorbers, but because they are, their complex refractive index is large thus causing a strong first-surface reflectance. In the submillimeter region the first-surface reflectance interferes constructively with the very strong reflectance from the metal baffle surface below to produce a high total reflectance. A relatively thin overcoat of a low index, nonabsorbing material can strongly reduce the first surface reflectance and thus the total reflectance.

The figure below shows the specular reflectance of a typical absorbing coating (0.2 mm thick) measured both before and after being sprayed with an overcoat of Teflon (polytetrofluoroethylene). It is evident that the reflectance of the interference peak at the wavelength of 0.35 mm was reduced by a factor of 1.9, and that the location of the peak was shifted longward 0.017 mm. Similar reductions were observed in three other coatings at wavelengths between 0.1 and 0.5 mm. The complex index of the opaque coating was 3.5 ±1.1 i while that of Teflon was 1.4 with a negligible imaginary component. The thickness of the Teflon overcoat was about 0.025 mm.

(S. Smith, Ext. 6264)

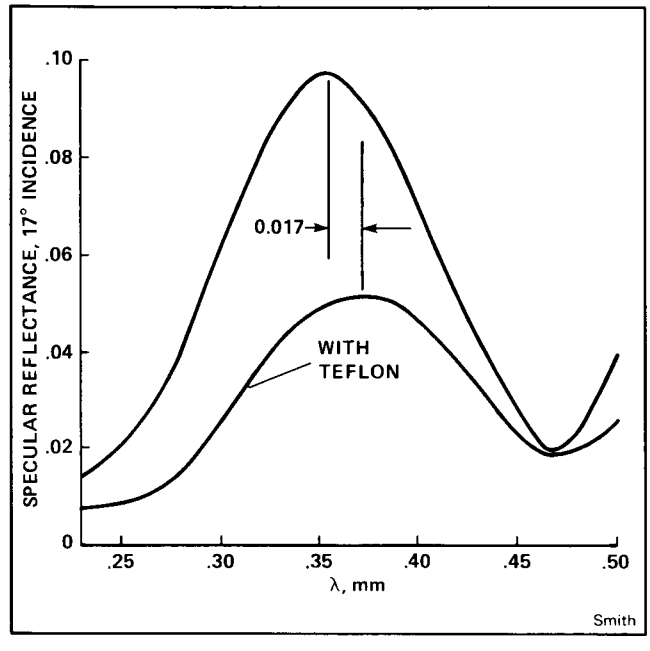

Specular reflectance of coating

Early Results from the Stratosphere-Troposphere Exchange Project

The Stratosphere-Troposphere Exchange Project (STEP) flew its first mission in April-May 1984. The goal was to document processes that irreversibly transport air between the troposphere and stratosphere, and also within the lower stratosphere, during the generation of large-scale mid-latitude storms. A knowledge of these processes is required to accurately predict how man-made chemicals affect the stratospheric ozone shield, and to explain the extreme dryness of the stratosphere.

The U-2 aircraft measured horizontal wind, temperature, pressure, water vapor, ozone, condensation nuclei, and cosmogenic radionuclides in the stratosphere. Instruments were provided and data analyzed by teams from NASA Ames Research Center, NOAA, University of Minnesota, and State University of New York. The stratospheric U-2 flights were coordinated with tropospheric flights made by NASA's Global Tropospheric Experiment using the CV-990 and the Electra aircraft. All three aircraft were directed to regions where the tropopause (boundary between the troposphere and stratosphere) was predicted to fold over itself. The predictions, developed especially for these experiments, proved extremely accurate, and all aircraft sampled the desired atmospheric structures.

The most striking result of the U-2 flights was the discovery in the stratosphere of highly laminated structures of ozone, water vapor, and condensation nuclei, with layers of maximum and minimum concentrations stacked atop one another, each about 1 km thick. These structures were located above the jet-stream core, which was, in turn, above an underlying tropopause fold. These stratospheric laminae raise two questions: (1) What causes them? and (2) What do they imply for irreversible transport?

The U-2 wind measurements shed light on both questions. Superimposed on the large-scale, mean winds are wave-induced velocities that rotate with height, turning through 360° every 2 km. Differential advections of the mixing ratios of ozone, water vapor, and condensation nuclei and of the potential vorticity by these wave-induced velocities fold the mixing ratio and potential vorticity surfaces, creating a laminar structure of alternating maxima and minima. Also, the folding process greatly increases the vertical gradients of the mixing ratios and the potentials for small-scale instabilities. The latter lead to irreversible mixing; thus a reversible, wave-generated transport is rendered irreversible by small-scale instabilities. The transfer is not from troposphere to stratosphere, but rather from the subtropical to the polar side of the jet.

Another striking result of the Spring 1984 U-2 flights was the positive correlations between water vapor and ozone observed in the dry stratosphere (i.e., above the hygropause, or water vapor minimum, at about 15 km in these experiments). These positive correlations, observed at large, medium, and small scales, are evidence of a stratospheric source of water vapor, presumably methane oxidation. Below the hygropause, the expected negative correlations between water vapor and ozone were observed.

(P. Russell and E. Danielsen, Ext. 5404/5527)

Cryogenic Testing of Secondary Mirror Chopping Mechanisms

Future cryogenically cooled spaceborne telescopes (such as SIRTF) will reach sensitivities in the IR limited only by the natural background from 2 to 200 microns. Optical modulation and image motion compensation require a secondary mirror deflection which can chop signals from 1 to 5 Hz with throws up to 30 arcmin. To maintain the sensitivity, the power introduced into the secondary mirror must be minimized.

A one-dimensional model simulating the expected mirror mass and moment of inertia using voice coil actuators, a flex pivot and proximity position sensing using both inductive and capacitive techniques has been tested for performance and heat dissipation.

Results revealed improved actuator performance from lower coil resistance and increased magnetic field, and improved sensitivity from the proximity sensors when operated at 8 K. Sources of power dissipation were found to be primarily owing to the resistance of the actuator coil, while hysteresis losses in the actuator and mechanical dissipation were a small fraction of the total heat dissipation. A laser interferometer was used to calibrate the proximity sensors at cryogenic temperature.

(M. Dix, Ext. 6525)

Development of a Sensitive Infrared Array Camera

The implementation of monolithic infrared detector arrays in imaging optical systems requires careful attention to the details of the system configuration of the analog signal, clock driving, and digital processing electronic circuitry. An infrared imaging camera with high sensitivity based upon a 16 X 16 format Si:Bi charge-injection device (CID) array. The optical system includes a circular variable filter wheel to define the radiation bandpass to 2% of the center wavelength, and a reimaging lens with a Lyot stop at the image of the secondary mirror. With careful

attention to the interplay of the various electronic subsystems, the instrument has been shown to achieve noise-limited performance imposed by the single pixel read-noise levels, the current value being 250 electrons per read. Hence, the instrument is capable of achieving background-limited noise performance near full well capacity. The limit on the instrumental sensitivity is then set by the single pixel quantum efficiency which for the array averages about 25%.

In August 1985 at Lick Observatory, images were obtained of the planetary nebula NGC 7027 at several wavelengths between 8 and 13 micrometers. The image presented here is at 11.3 micrometers wavelength. The spatial scale is 1.5 arcsec per pixel. The image displays the characteristic central minimum of planetary nebulae, as well as a lack of emission at one radial coordinate in the ring of emission.

(J. Goebel, Ext. 6525)

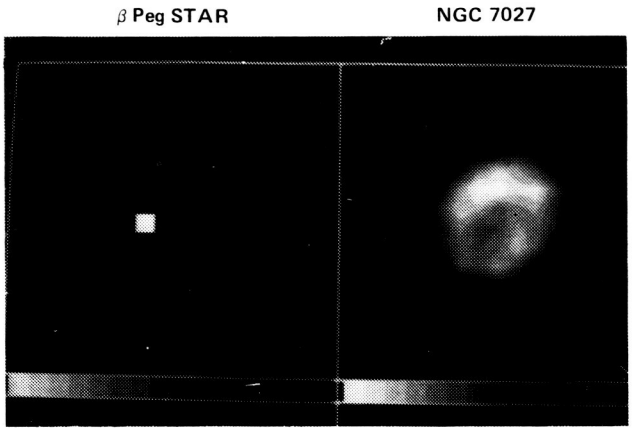

11.3 μm images of a point source (β Peg) (left), and the planetary nebula NGC 7027, obtained with 16 × 16 element IR array

Dewar Simulator for PODS Testing

A mechanical simulator has been built for the final testing of the Passive Orbital Disconnect Strut (PODS). These struts are an advanced type of Dewar support that has been developed in conjunction with the Lockheed Palo Alto Research Laboratory. They are a variable strength, variable thermal conductance device designed for high strength during launch and low conductance in orbit. The simulator was built to test a system of six PODS in the expected launch and orbital environments. (Previously, only a single PODS had been tested. Six is the number of PODS required for a statically determinant system.) The following tests have been performed in the simulator: (1) axial load required to short the struts – i.e., the load required to change the struts from the orbital configuration to the launch configuration; (2) simulate outer shell temperature gradient to see if such a gradient would short the struts; (3) side loads required to short the struts – i.e., simulate the loads of vapor-cooled shields; (4) modal vibration of the struts. The results of these tests were in good agreement with the predictions, and it is now considered that the PODS are space-flight qualified.

(P. Kittel, Ext. 6525)

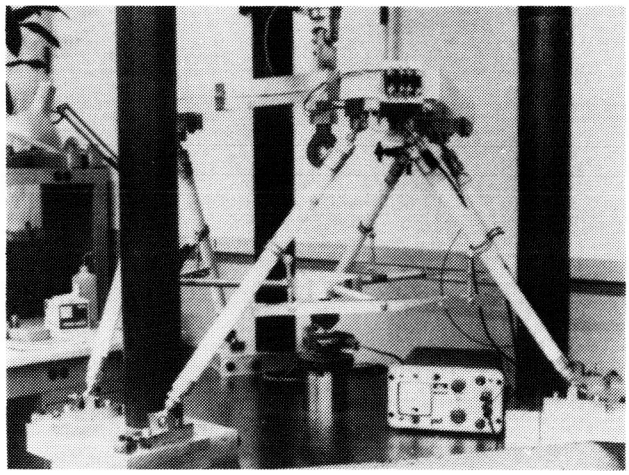
Kittel

Dewar simulator showing the six PODS in place. The upper end simulates the cryogen tank; the lower end simulates the outer shell

Aperture Shade Design Trade-Off Study for SIRTF in a Low Inclination Orbit

The 1-m aperture Space Infrared Telescope Facility (SIRTF) will operate with a sensitivity limited only by the zodiacal background. This sensitivity requirement places severe restrictions on the amount of stray light from sources such as the Sun and Earth which can reach the focal plane. In addition, radiation from these sources can degrade the lifetime of the telescope and instrument cryogenic system which is now planned to be two years before the first servicing. Since the aperture of the telescope represents a break in the telescope insulation system and is effectively the first element in the optical train,

the aperture shade is a key system component. The mass, length and temperature of the shade should be minimized to reduce system cost while maximizing the telescope lifetime and stray light performance. The independent geometric parameters that characterize an asymmetrical shade for a 600 km 28° orbit were identified, and the system sensitivity to three important shade parameters was explored. Despite the higher heat loads compared to previous missions, the analysis determined that passive radiators of a reasonable size are sufficient to meet the system requirements.

(J. Lee, W. Brooks, and S. Maa,
Ext. 6531/6547/6024)

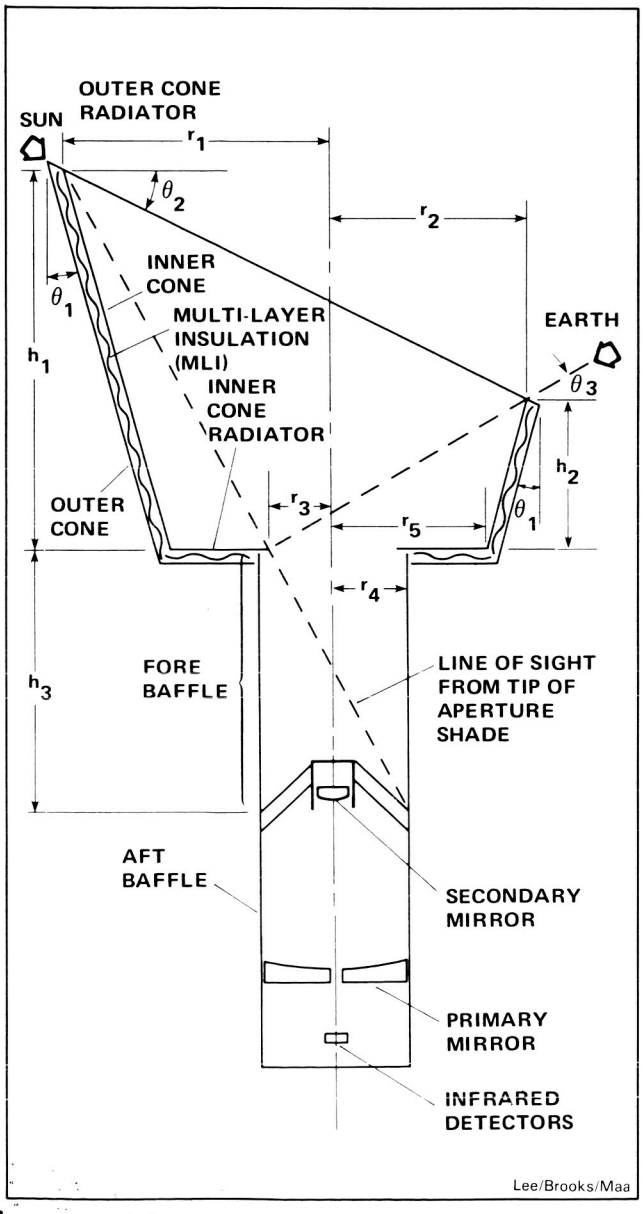

Aperture shade design — geometric parameters

Development of Antimony-Doped Silicon Integrated IR Arrays

The spectral response of integrated infrared (IR) array technology has been extended out to 30 μm with the development of antimony-doped silicon (Si:Sb) multiplexed arrays. Through a contract to Santa Barbara Research Center, hybrid Si:Sb arrays of 58 X 62 pixels have been produced. Each pixel in the array is 75 μm square, and the array frontal area is 100% optically active. The array is read out with the state-of-the-art CRC 228 direct readout (DRO) multiplexer. This device offers significant advantages for low-background space astronomy applications. Its readout noise is in the 50-100 rms electrons range, an order of magnitude lower than that of charge-coupled device (CCD) multiplexers. It will also allow operation of the array in two new modes (nondestructive read and random access) which are particularly well suited for space astronomy.

Both a low-background test dewar and microcomputer-based readout electronics were developed at Ames Research Center in FY 85 for the characterization of these new arrays. The devices will be tested under the low-flux conditions representative of the Space Infrared Telescope Facility (SIRTF). The results will be incorporated into the concept definition of the SIRTF Infrared Array Camera (IRAC), which has

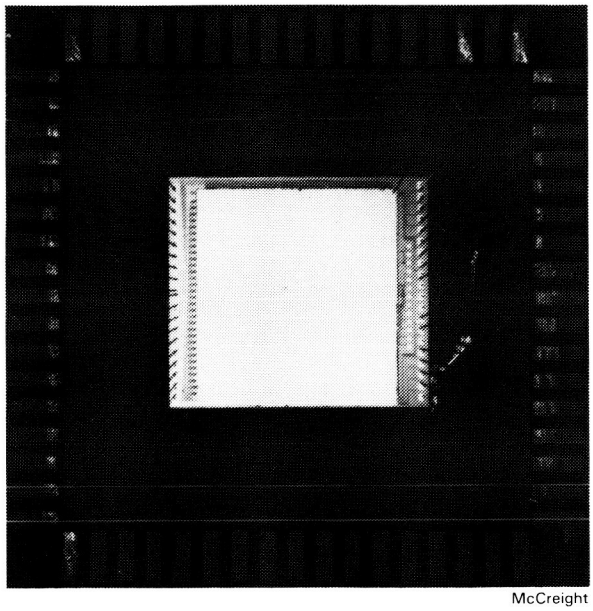

McCreight

Hybrid antimony-doped Silicon Infrared Detector Array, with Direct Readout Multiplexer

selected this Si:Sb DRO array for its baseline Band III focal plane. It will also be evaluated for potential application in the SIRTF Infrared Spectrometer (IRS), and it may have applicability in future astronomical applications such as the Large Deployable Reflector (LDR).

(C. McCreight, Ext. 6549)

Development of Beryllium Mirrors for Cryogenically-Cooled, Infrared Telescopes

Cryogenically cooled, infrared telescopes require mirrors with optical performance after being cooled to their extremely low operating temperatures. The operating temperature may be as low as 2 K. At this temperature, any lack of material uniformity in thermal linear expansion distorts the optical surface. Metals are attractive because of their high thermal conductivity and ease of mounting attachment (compared to the glassy materials). Beryllium is especially attractive from a structural standpoint with its superior stiffness to weight ratio. It can be made to achieve lower distortion than other lightweight metals such as titanium and aluminum.

A 50-cm diameter, lightweight beryllium mirror blank has been fabricated using the latest materials and processing technology under the sponsorship of the Information Sciences and Human Factors Division of NASA Headquarters. The finished mirror, figured and polished by the Perkin-Elmer Corporation, has been optically tested at 5 K. The blank for the mirror was made of high-purity beryllium powder that was consolidated to full density by a process known as hot isostatic pressing (HIP). The process combines high temperature and pressure to sinter the metal particles into a solid with uniform properties.

To test the optical performance of the mirror at the temperature required for the Space Infrared Telescope Facility (SIRTF), the mirror was installed in the Ames Cryogenic Optical Test Facility. In the Facility, which operates as a vacuum cryogenic Dewar, the mirror was cooled to 5 K. An interferometer mounted externally to the Dewar was used to take interferograms of the mirror through a small window. The interferograms will be used to establish the optical performance of the mirror at wavelength of the helium-neon laser source.

Data reduction has not been completed at the time of this report, but some surface distortion is evident. Analysis will be performed to determine the nature and cause of the distortion.

(R. Melugin, Ext. 6530)

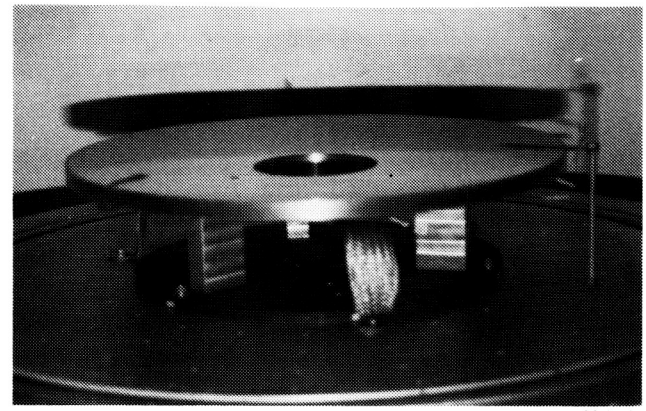

Melugin

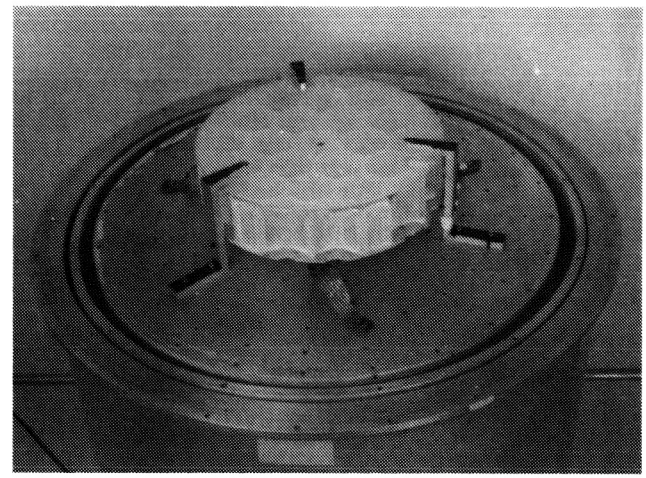

Melugin

Beryllium mirror in test configuration

Lightning in Planetary Atmospheres

Spacecraft observations have shown that lightning is a common feature of planetary atmospheres. Measurements of lightning activity in these atmospheres is expected to give insight into meteorological processes and to help elucidate the evolutionary processes that have produced the present atmospheric compositions. In particular, lightning produces significant amounts of trace gases and prebiological molecules. At Ames Research Center we are analyzing spacecraft

observations and doing laboratory studies to simulate lightning discharges in planetary atmospheres. Analysis of the gases and the spectra produced by the laboratory discharges is also under way.

(W. Borucki and C. McKay, Ext. 6492/6864)

Atmospheric Evolution Studies

A model of the CO_2 geochemical cycle was used to examine possible perturbations of the marine carbon cycle which might have resulted from the impact of an asteroid or comet at the Cretaceous/Tertiary boundary. The motivation for this study was to try to explain the prolonged (15,000-30,000 year) disappearance of calcium carbonate from boundary-layer sediments. It was concluded that a relatively short term (10-20 year) calcite dissolution event might have been initiated by rainout of HNO_3 synthesized by the impact, but that a long-term dissolution event caused by upward mixing of undersaturated deep water is unlikely to have occurred. A similar model was used to show that high CO_2 levels during the Eocene Period (~40 million years ago) could explain the relatively warm climate during that time.

Work is also in progress to understand the early climate of the Earth. Preliminary results of one-dimensional radiative/convective modeling indicate that a dense (10 bar) CO_2 atmosphere, predicted by some theories of atmospheric evolution, would have produced surface temperatures of about 80°C. High CO_2 partial pressures would apparently not lead to runaway greenhouse conditions, largely because of a strong albedo feedback caused by Rayleigh scattering. Further work is being performed to improve the model's parameterization of infrared absorption by CO_2 and water. This model will then be used to reexamine the question of whether a runaway greenhouse effect could have been responsible for the lack of water in Venus's atmosphere.

(J. Kasting, Ext. 5233)

Nonmethane Hydrocarbon Chemistry in the Troposphere

It was demonstrated earlier (1984), with the aid of a two-dimensional (2D) model of Venus plasma dynamics, that the temperature gradient across the Venus terminator is sufficient to produce the ion velocity field observed by the Pioneer Venus Orbiter.

Moreover, this gradient was found to be the probable cause of the large ion densities observed on the nightside of Venus. In a series of computer experiments performed in 1985 with the aid of a 2D model of ion and electron energetics, it was found that the observed ion temperature dip near the terminator was probably caused by expansion of the plasma as thermal energy is converted to the bulk kinetic energy of plasma flow. Further, the observed temperature rise antisunward of 120° was probably due in part to compression and in part to diabatic heating by the solar wind. The required nocturnal heat source for both the ions and the electrons is considerably smaller (by a factor of 4 or 5) than the dayside heat source (mainly solar ultraviolet radiation) because of saturation of the vertical heat flux resulting from inability of the ion and electron gases to conduct heat at velocities faster than the sonic velocity.

(R. Whitten, Ext. 5498)

Dynamics and Energetics of the Venus Monosphere

A one-dimensional photochemical model has been developed to examine the effects of nonmethane hydrocarbons (NMHCs) on the chemistry of the midlatitude troposphere. The model traces oxidation pathways for C_2H_6, C_3H_8, C_4H_{10}, C_2H_4, and C_3H_6, and predicts the abundances of various aldehyde and ketone intermediates. NMHC compounds have an important effect on odd nitrogen ($NO_x \equiv NO + NO_2$) chemistry because of the formation of peroxyacetyl nitrate (PAN), which can be a major NO_x reservoir. Model results indicate that PAN has only a small effect on summertime NO_x photochemistry, but that efficient downward transport of PAN during the wintertime can lower NO_x abundances in the upper troposphere by as much as a factor of 10. The same model predicts a factor of 4-5 increase in wintertime OH densities in the upper troposphere when NMHC chemistry is included. The model is being validated by comparing its predictions with measurements of PAN and hydrocarbons made by H. Singh.

(J. Kasting, Ext. 5233)

1. Report No. NASA TM-86852	2. Government Accession No.	3. Recipient's Catalog No.
4. Title and Subtitle RESEARCH AND TECHNOLOGY ANNUAL REPORT-1985		5. Report Date January 1986 6. Performing Organization Code
7. Author(s)		8. Performing Organization Report No. 85045 10. Work Unit No. G-1000
9. Performing Organization Name and Address NASA Ames Research Center Moffett Field, CA 94035		11. Contract or Grant No. 13. Type of Report and Period Covered Technical Memorandum
12. Sponsoring Agency Name and Address National Aeronautics and Space Administration Washington, DC 20546		14. Sponsoring Agency Code

15. Supplementary Notes

Point of contact: Dr. J. N. Nielsen, Chief Scientist, Ames Research Center
MS 200-1A, Moffett Field, CA 94035 (415) 694-5500 or FTS 464-5500.

16. Abstract

This report describes various research and technology activities at Ames Moffett and Ames Dryden. Highlights of these accomplishments indicate the Center's varied and highly productive research efforts for 1985.

17. Key Words (Suggested by Author(s))	18. Distribution Statement
Space science Life science Space and terrestrial applications Aeronautics Space technology	Unlimited Subject category: 99

19. Security Classif. (of this report)	20. Security Classif. (of this page)	21. No. of Pages	22. Price*
Unclassified	Unclassified	130	A05

*For sale by the National Technical Information Service, Springfield, Virginia 22161